SUPPORTING INFORMATION

The Synthesis of 12β-Methyl-18-*nor*-Bile Acids

Andreas Luxenburger,*[,†,⊥] Lawrence D. Harris,[†,⊥] Elizabeth M. Ure,[†] Roselis A. Landaeta Aponte,[†] Anthony D. Woolhouse,[†,∞] Scott A. Cameron,[†] Chris D. Ling,[‖] Ross O. Piltz,[Σ] Andrew R. Lewis,[§] Graeme J. Gainsford,[†] Alex Weymouth-Wilson,[‡] Richard H. Furneaux[†]

[†] Ferrier Research Institute, Victoria University of Wellington, 69 Gracefield Rd, Lower Hutt 5040, New Zealand
[‖] School of Chemistry, The University of Sydney, Sydney, New South Wales 2006, Australia
[Σ] Australian Centre for Neutron Scattering, New Illawarra Rd, Lucas Heights NSW 2234, Sydney, Australia
[§] Callaghan Innovation, PO Box 31 310, Lower Hutt 5040, New Zealand
[‡] New Zealand Pharmaceuticals Ltd, 68 Weld Street, RD2, Palmerston North 4472, New Zealand
[⊥] These authors contributed equally.
[∞] Deceased.
[*] Andreas.Luxenburger@vuw.ac.nz

Table of Contents

1. The synthesis of 25-*homo*-cholic acid (20)

Scheme S1. Synthesis of 25-*homo*-cholic acid 20[a]

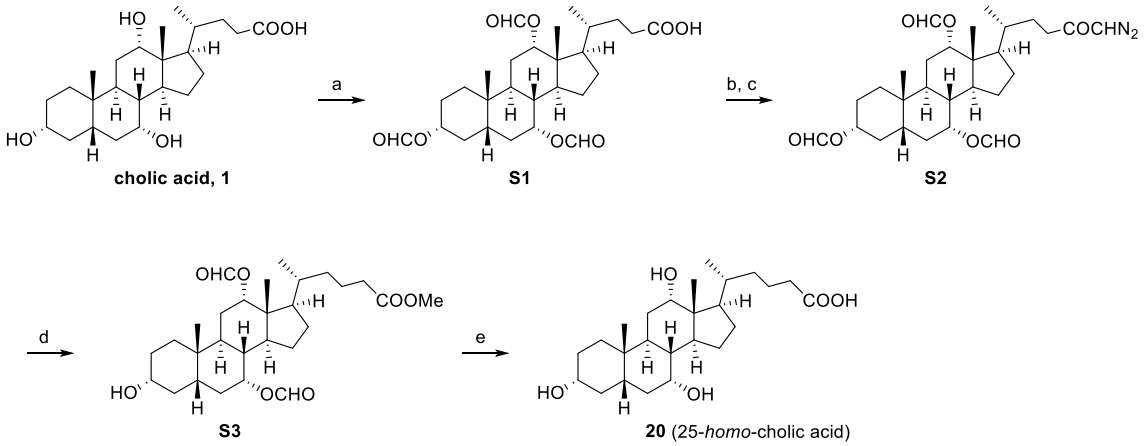

[a]Reagents and conditions: (a) Ref. 45,40b: HCOOH, $HClO_4$, Ac_2O; (b) (i) $(COCl)_2$, benzene, 5 °C-rt, 5 h; (ii) CH_2N_2, toluene/Et_2O, 0 °C-rt, o/n; (d) $AgNO_3$, H_2O/MeOH, Δ, 4 h; 62% (3 steps); (e) 2 M NaOHaq, MeOH, Δ, 3 h; 87%.

The required 25-*homo*-cholic acid starting material (**20**) was prepared from cholic acid (**1**, CA) in five steps, using an Arndt-Eistert homologation strategy.[40] The synthesis started with formyl protection of all three hydroxy groups.[45,40b] The resulting *tris*(formyl)-protected compound **S1** was then converted into the corresponding acid chloride which upon treatment with diazomethane gave the α-diazoketone **S2**.[40,46] A silver(I) nitrate-promoted Wolff rearrangement of **S2**, in the presence of methanol, furnished the 25-*homo*-methyl ester **S3**. Although these reaction conditions also caused cleavage of the 3-hydroxy protecting group, there was no disadvantage as all protecting groups were eventually cleaved by saponification to yield the desired 25-*homo*-cholic acid **20**.

2. The synthesis of 12β-methyl-25-*homo*-18-*nor*-chenodeoxycholic acids 27c and 28c from 12β-methyl-18-*nor*-chenodeoxycholic acids 27a and 28a

Scheme S2. Synthesis of 12β-methyl-25-*homo*-18-*nor*-chenodeoxycholic acids 27c and 28c.[a]

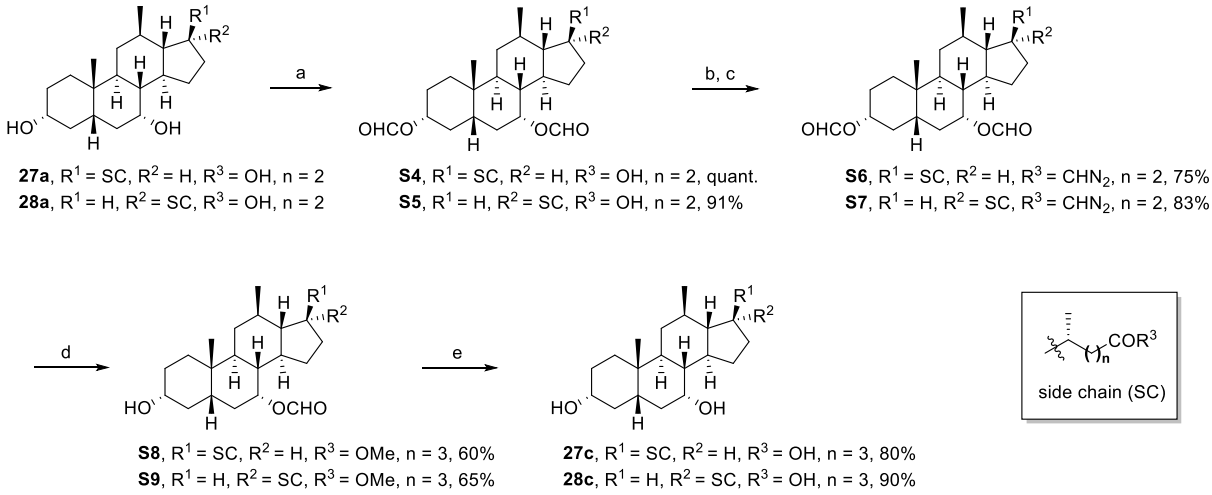

27a, R^1 = SC, R^2 = H, R^3 = OH, n = 2
28a, R^1 = H, R^2 = SC, R^3 = OH, n = 2

S4, R^1 = SC, R^2 = H, R^3 = OH, n = 2, quant.
S5, R^1 = H, R^2 = SC, R^3 = OH, n = 2, 91%

S6, R^1 = SC, R^2 = H, R^3 = CHN_2, n = 2, 75%
S7, R^1 = H, R^2 = SC, R^3 = CHN_2, n = 2, 83%

S8, R^1 = SC, R^2 = H, R^3 = OMe, n = 3, 60%
S9, R^1 = H, R^2 = SC, R^3 = OMe, n = 3, 65%

27c, R^1 = SC, R^2 = H, R^3 = OH, n = 3, 80%
28c, R^1 = H, R^2 = SC, R^3 = OH, n = 3, 90%

[a]Reagents and conditions: (a) HCOOH, $HClO_4$, 40-50 °C, 2.5-3 h; Ac_2O, 40°C-rt, 1 h; (b) $(COCl)_2$, toluene, 10 °C-rt, 2.5 h; (c) CH_2N_2 (prepared from MNU, 50% KOH_{aq}, Et_2O, -5 to -10 °C), toluene/Et_2O, 0 °C-rt, o/n; (d) $AgNO_3$, MeOH/H_2O, 2.5-4 h, Δ; (e) 2 M $NaOH_{aq}$, MeOH, 3 h, Δ. Abbreviations: MNU: *N*-methyl-*N*-nitrosourea

The synthesis of the two 12β-methyl-25-*homo*-18-*nor*-chenodeoxycholic acids **27c** and **28c** from the 12β-methyl-18-*nor*-bile acids **27a** and **28a** was accomplished by employing the same Arndt-Eistert homologation strategy[40] as for the preparation of the 25-*homo*-cholic acid (**20**) before (Scheme S1). Accordingly, **27a** and **28a** were formyl protected to give **S4** and **S5**, which, upon conversion to the corresponding acid chlorides and subsequent reaction with diazomethane, afforded the diazoketones **S6** and **S7**. These were then reacted with methanol, in the presence of catalytic amounts of silver(I) nitrate to give the respective 25-*homo*-methyl esters **S8** and **S9**. As before these reaction conditions caused cleavage of the 3-hydroxy protecting group. Final deprotection of the remaining protecting groups by saponification furnished the desired 12β-methyl-25-*homo*-18-*nor*-bile acid **27c** and its C17-epimer **28c** in good yield.

3. The synthesis of 12β-methyl-18,24-*bisnor*-chenodeoxycholic acid 27b from 12β-methyl-18-*nor*-chenodeoxycholic acid 27a

Scheme S3. Synthesis of 12β-methyl-18,24-*bisnor*-chenodeoxycholic acid 27b.[a]

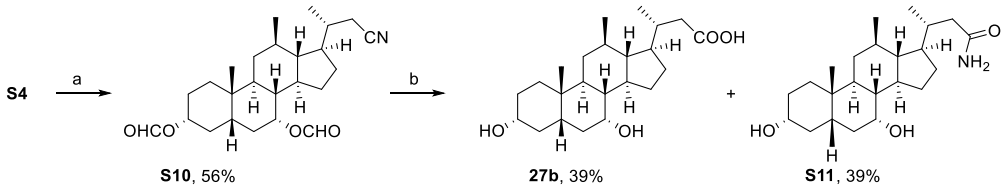

[a]Reagents and conditions: (a) TFAA, TFA, $NaNO_2$, 0 °C, 3 h then 40 °C, 1.5 h; (b) KOH, EtOH, H_2O, 90 °C, 3 days. Abbreviations: TFA: trifluoroacetic acid; TFAA: trifluoroacetic anhydride

4. NMR Spectra

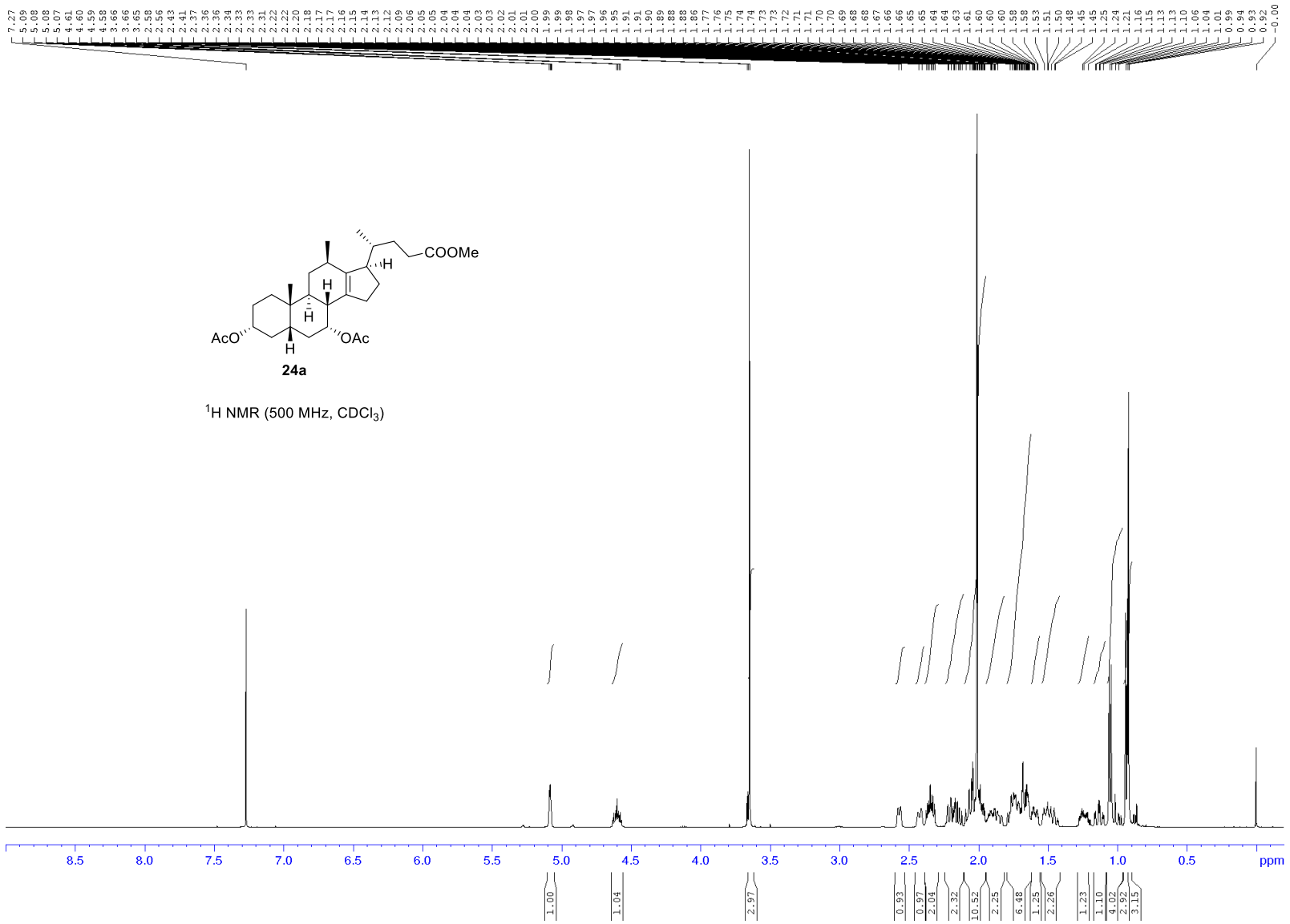

Figure S1a. ^{1}H NMR spectrum of **24a**.

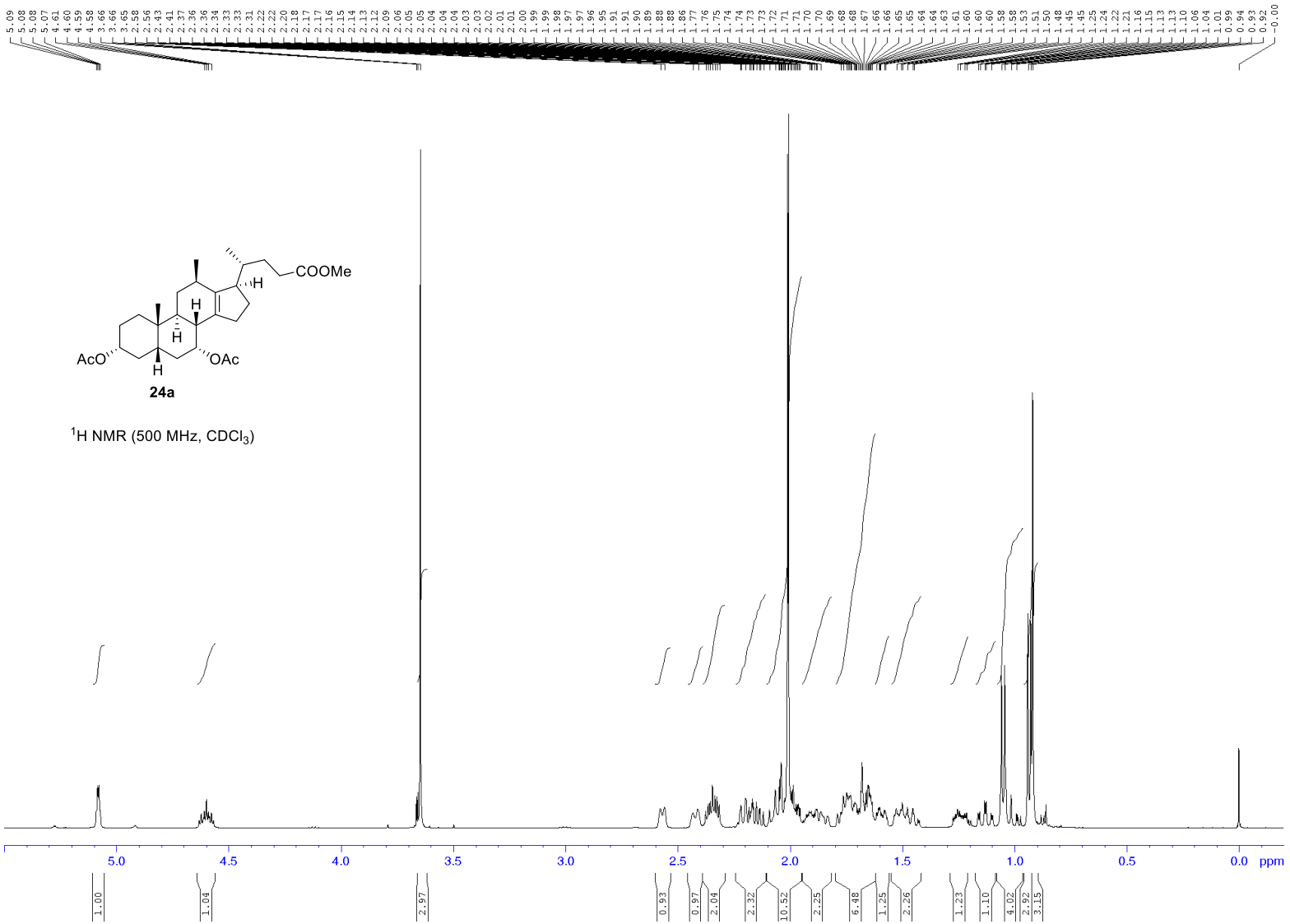

Figure S1b. ^{1}H NMR spectrum of **24a**.

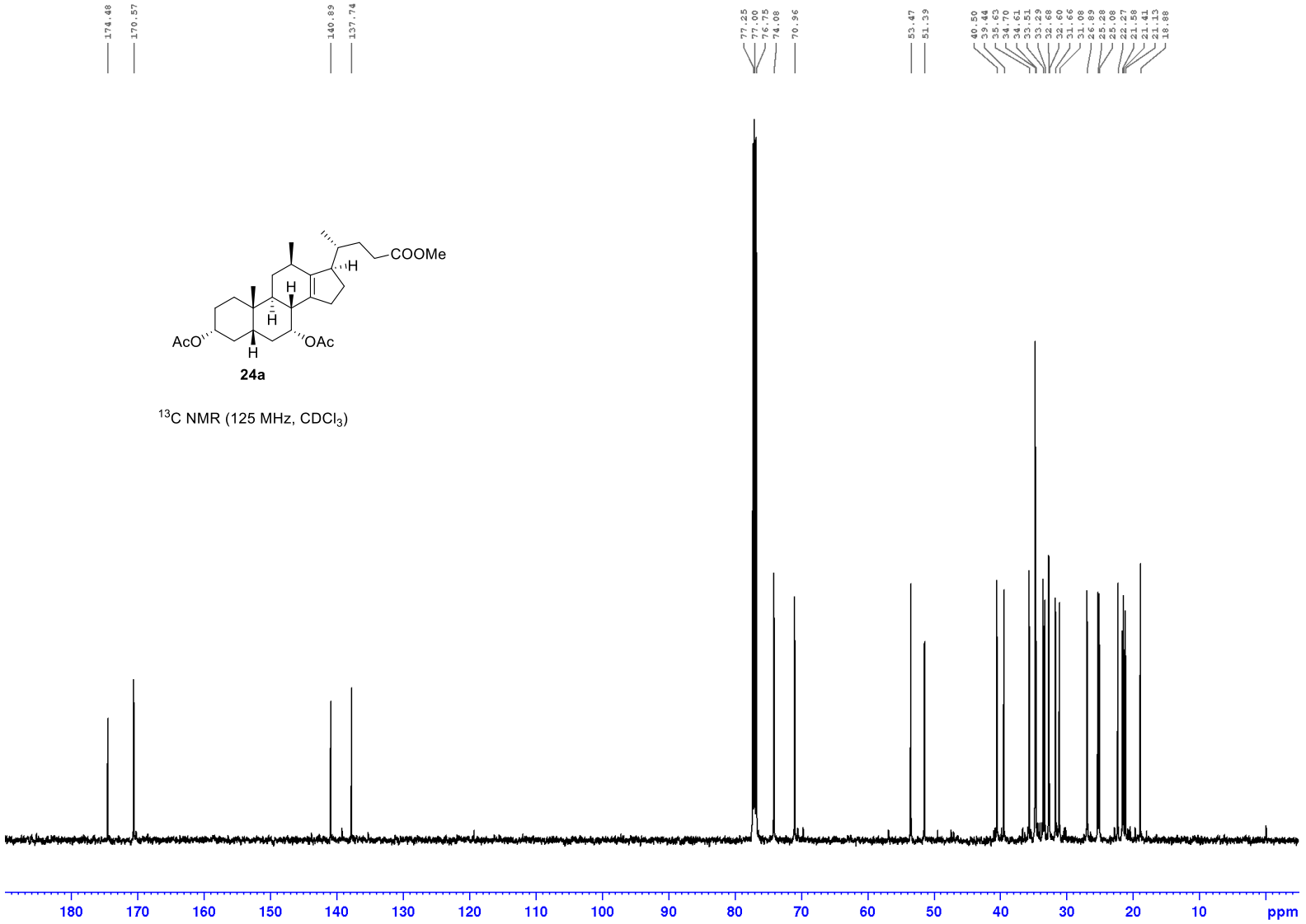

Figure S2. ^{13}C NMR spectrum of **24a**.

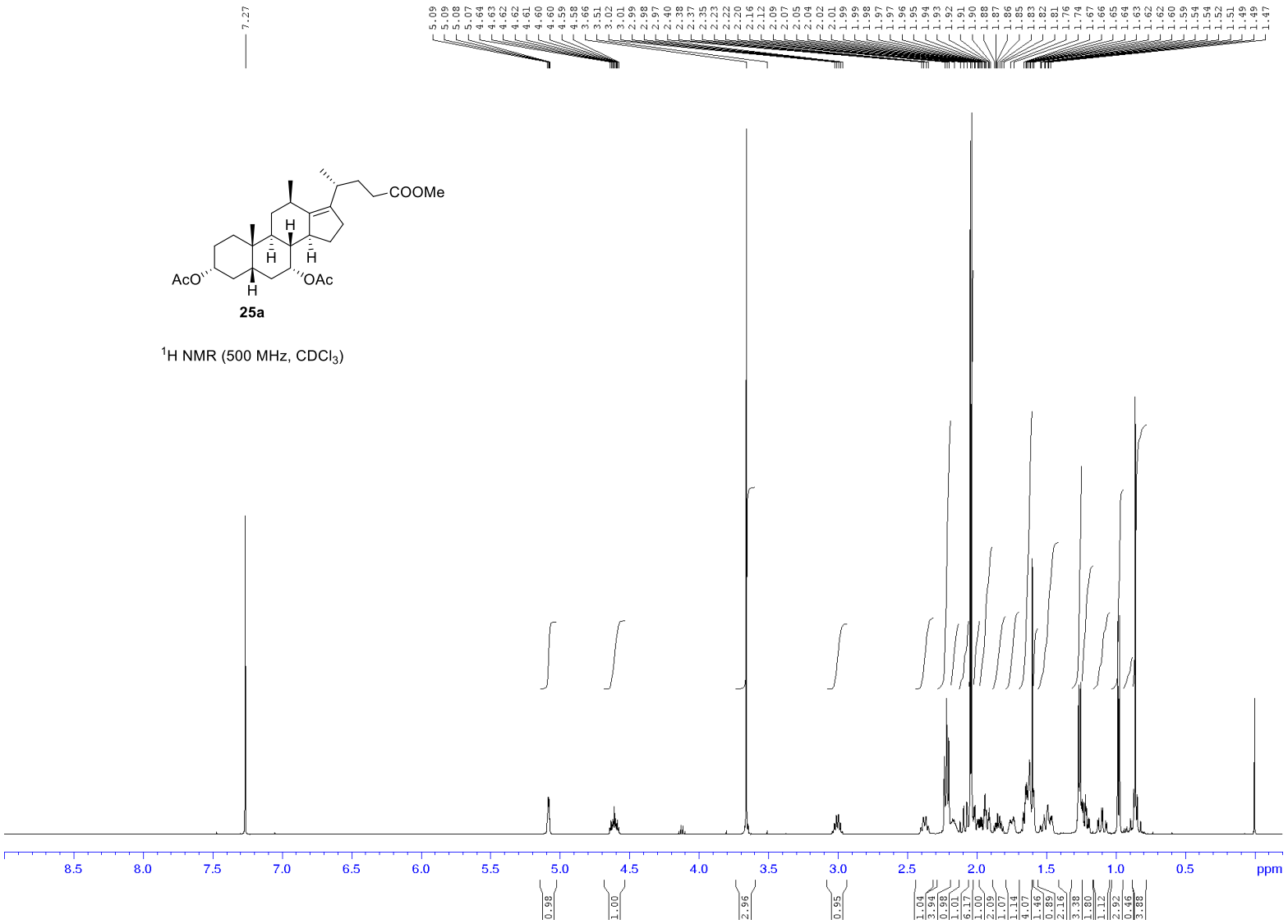

Figure S3a. ^{1}H NMR spectrum of **25a**.

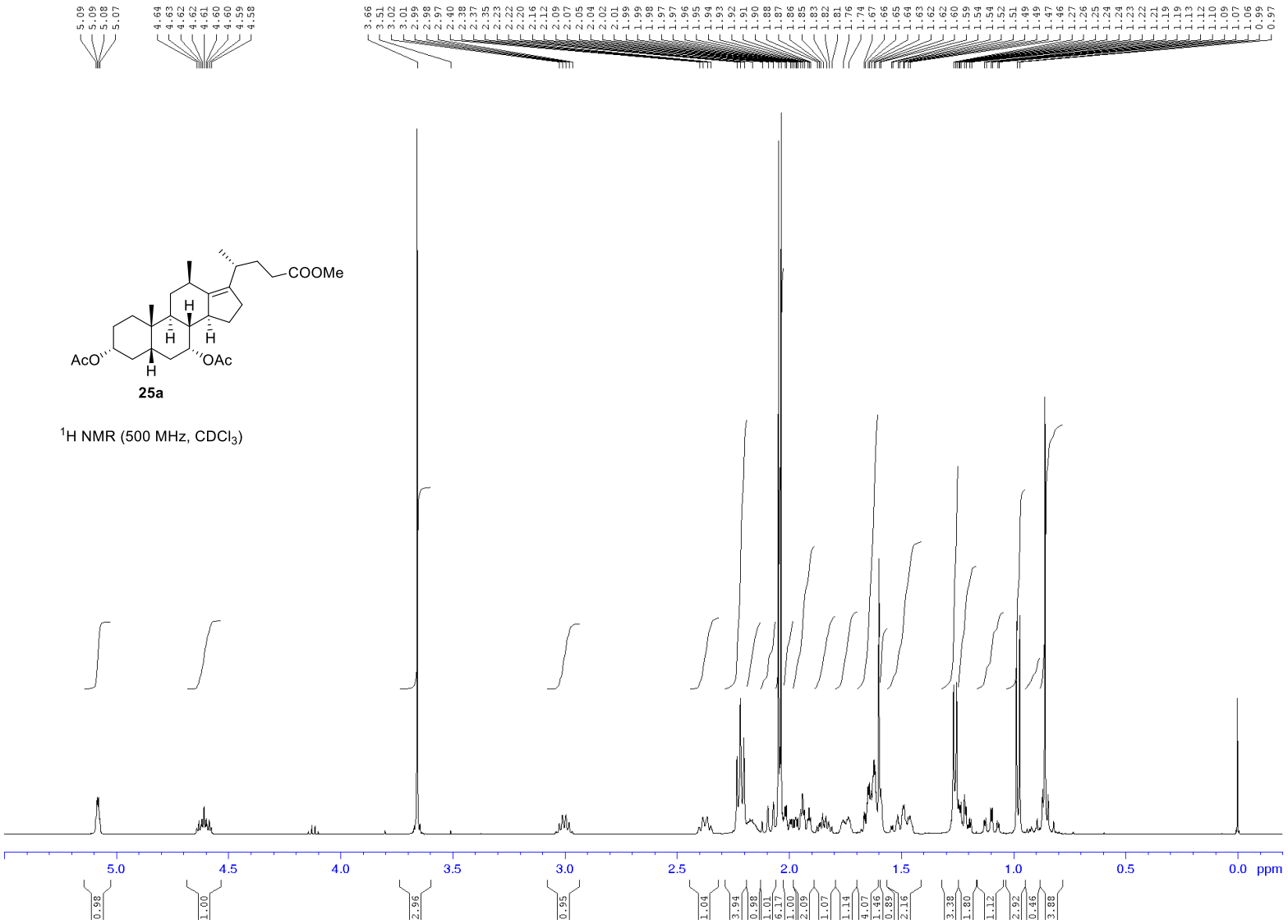

Figure S3b. ^{1}H NMR spectrum of **25a**.

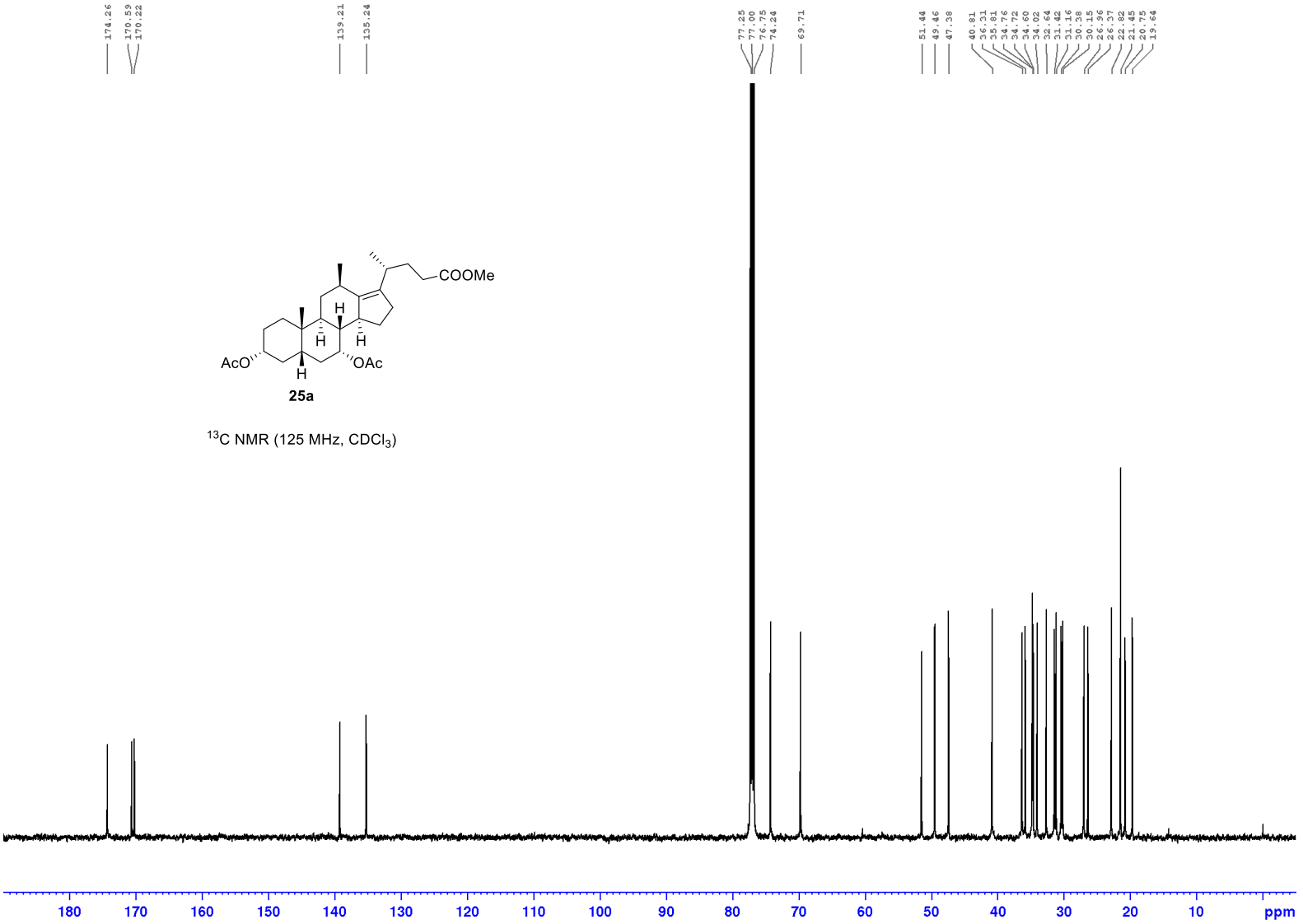

Figure S4. ^{13}C NMR spectrum of **25a**.

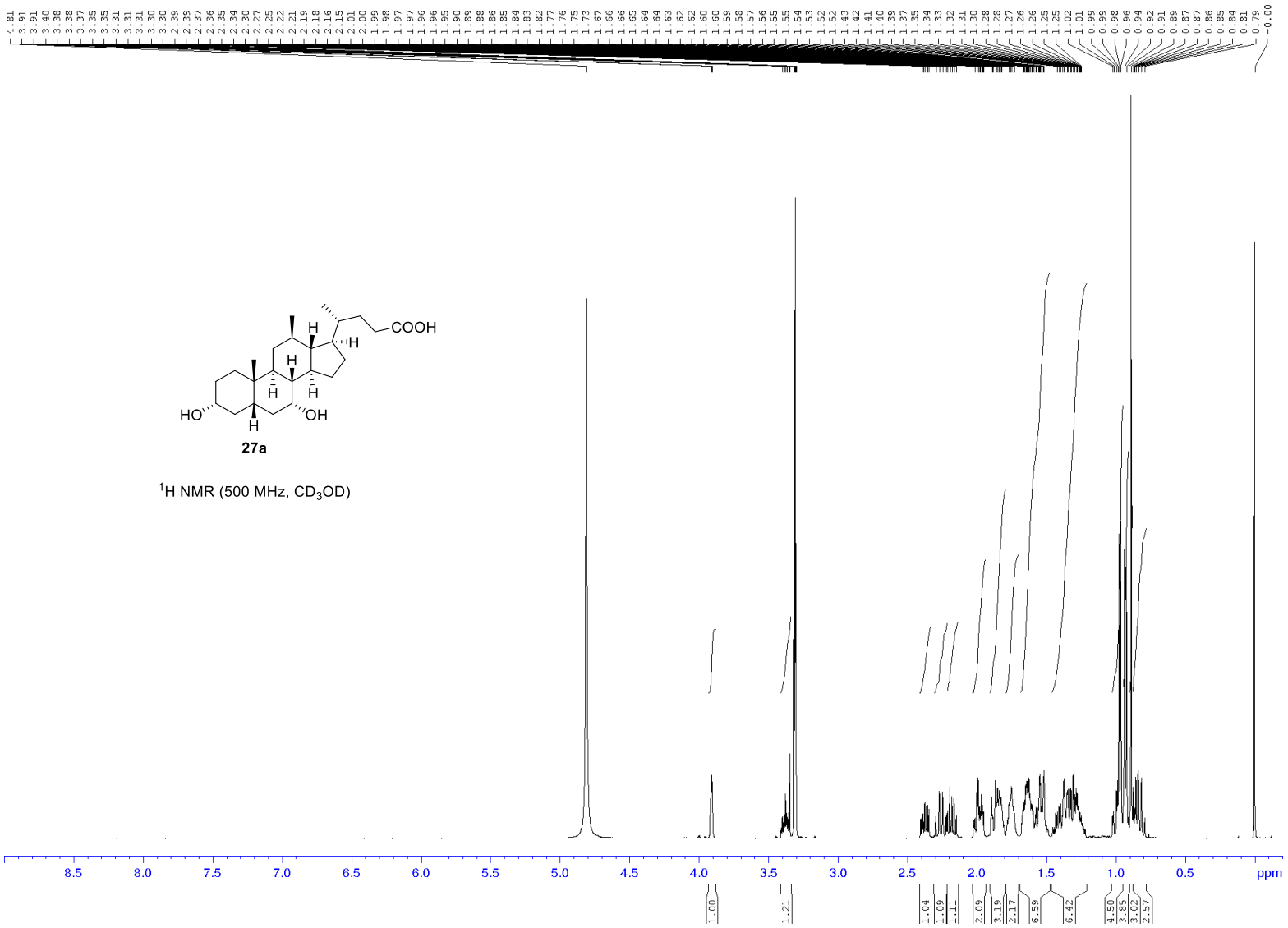

Figure S5a. ^{1}H NMR spectrum of **27a**.

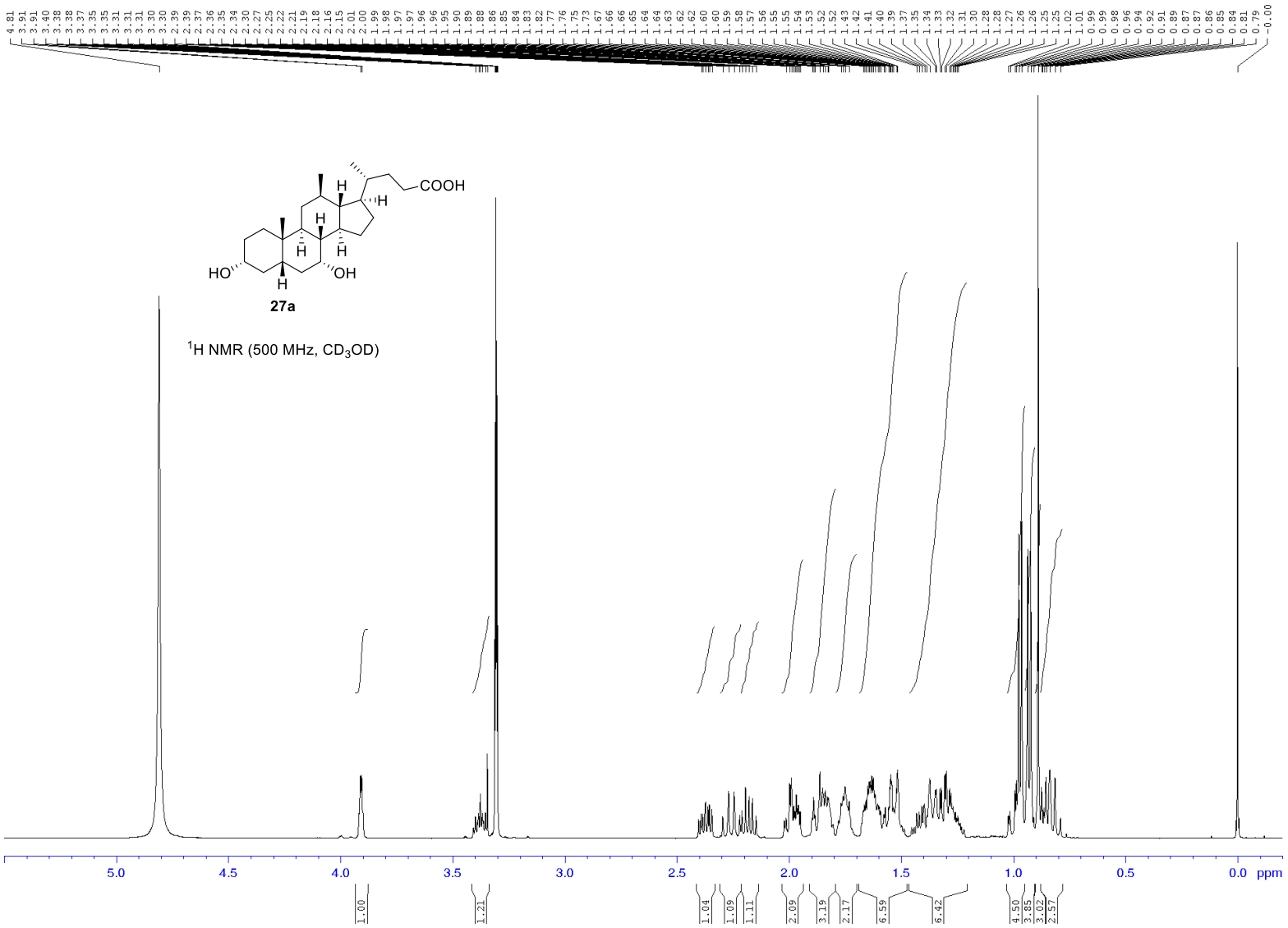

Figure S5b. ^{1}H NMR spectrum of **27a**.

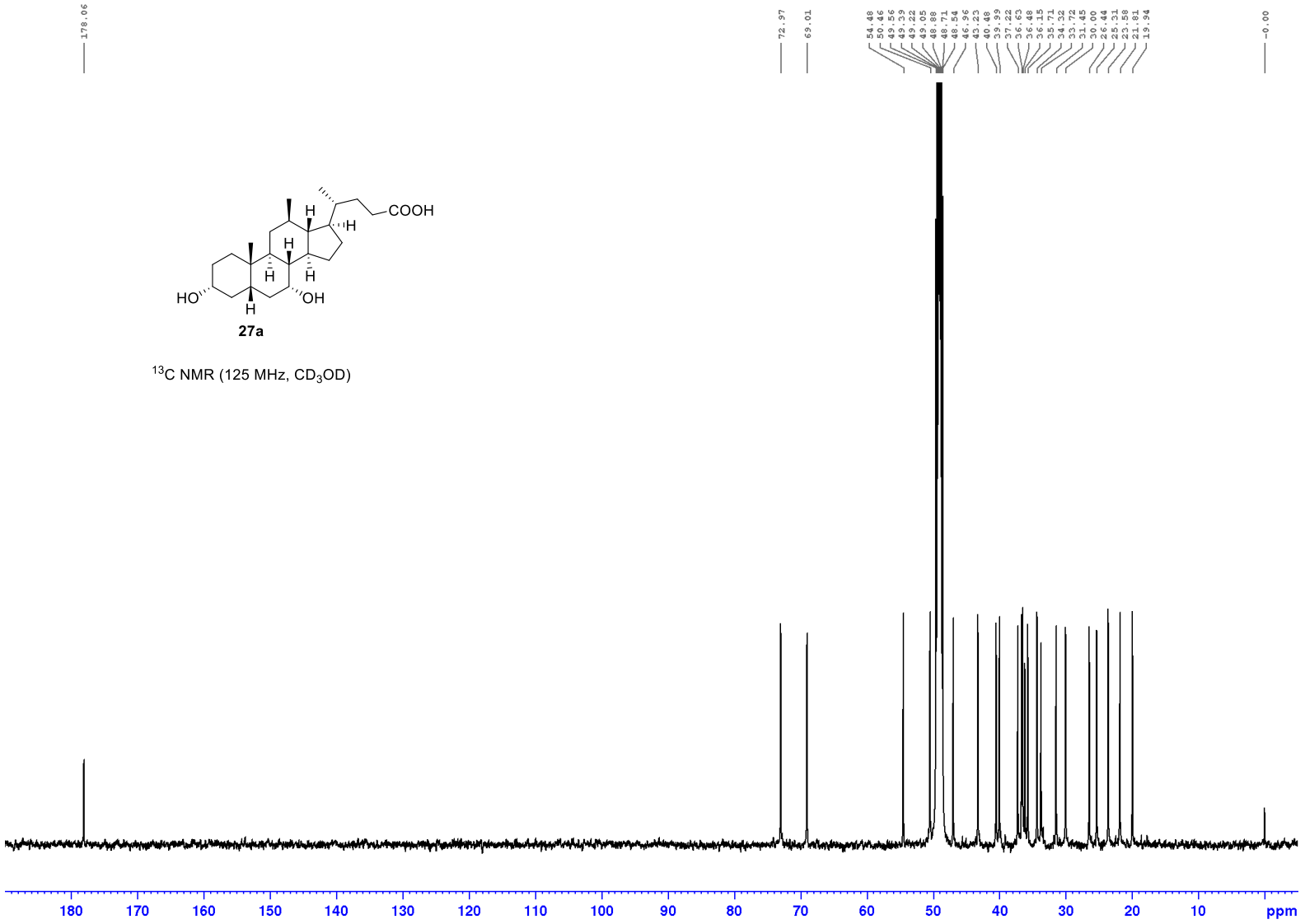

Figure S6. ^{13}C NMR spectrum of **27a**.

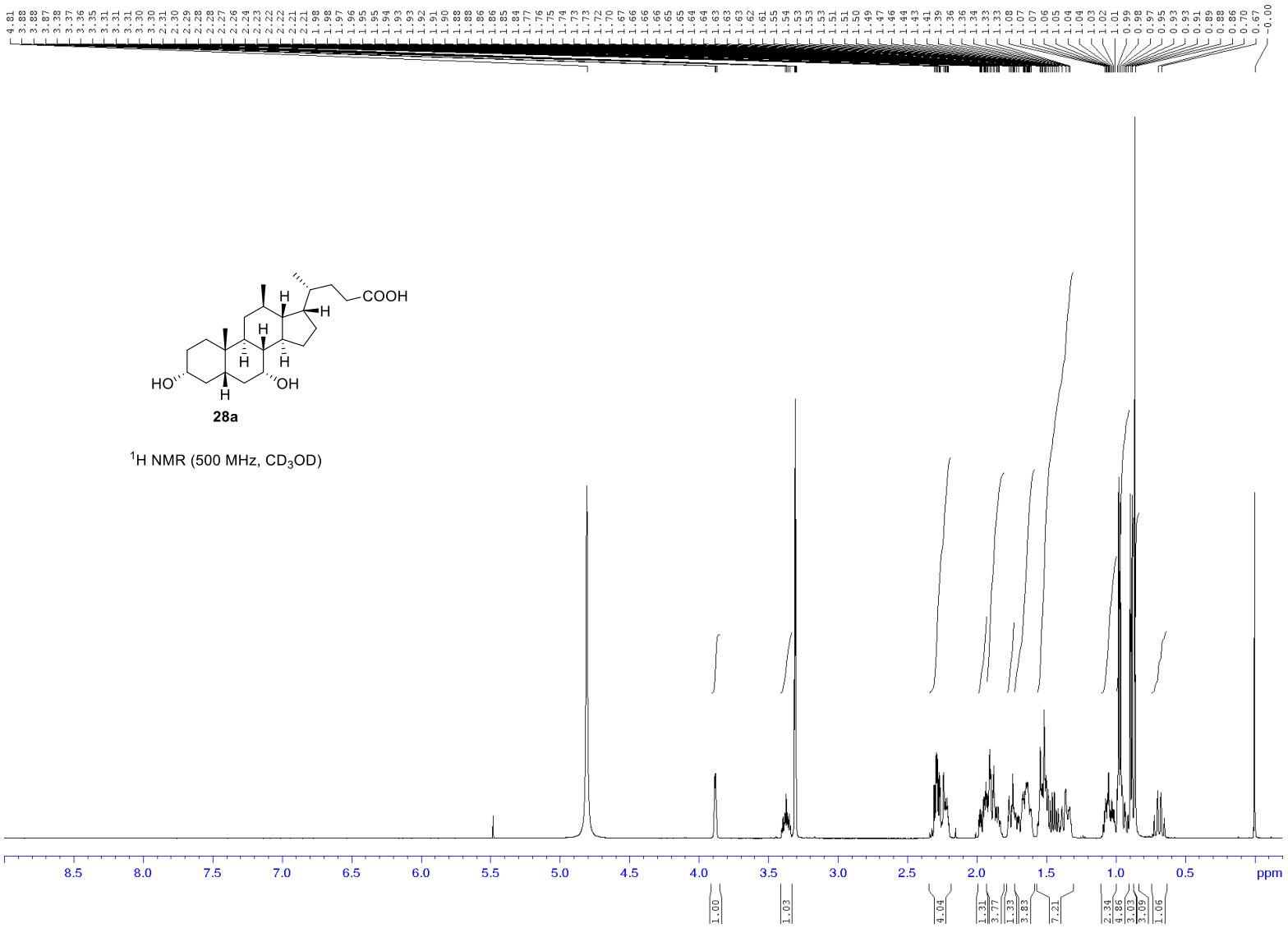

Figure S7a. ^{1}H NMR spectrum of **28a**.

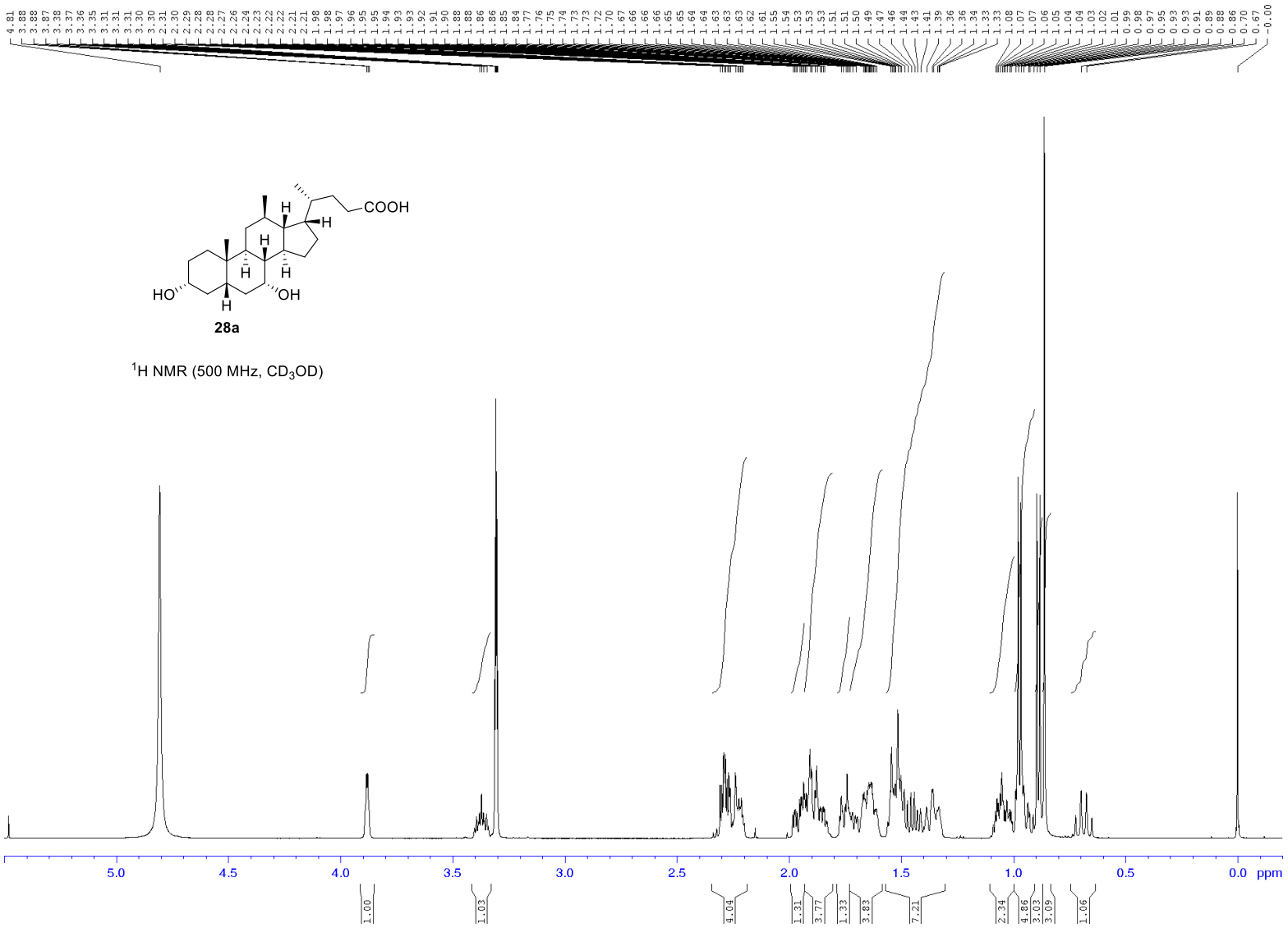

Figure S7b. ^{1}H NMR spectrum of **28a**.

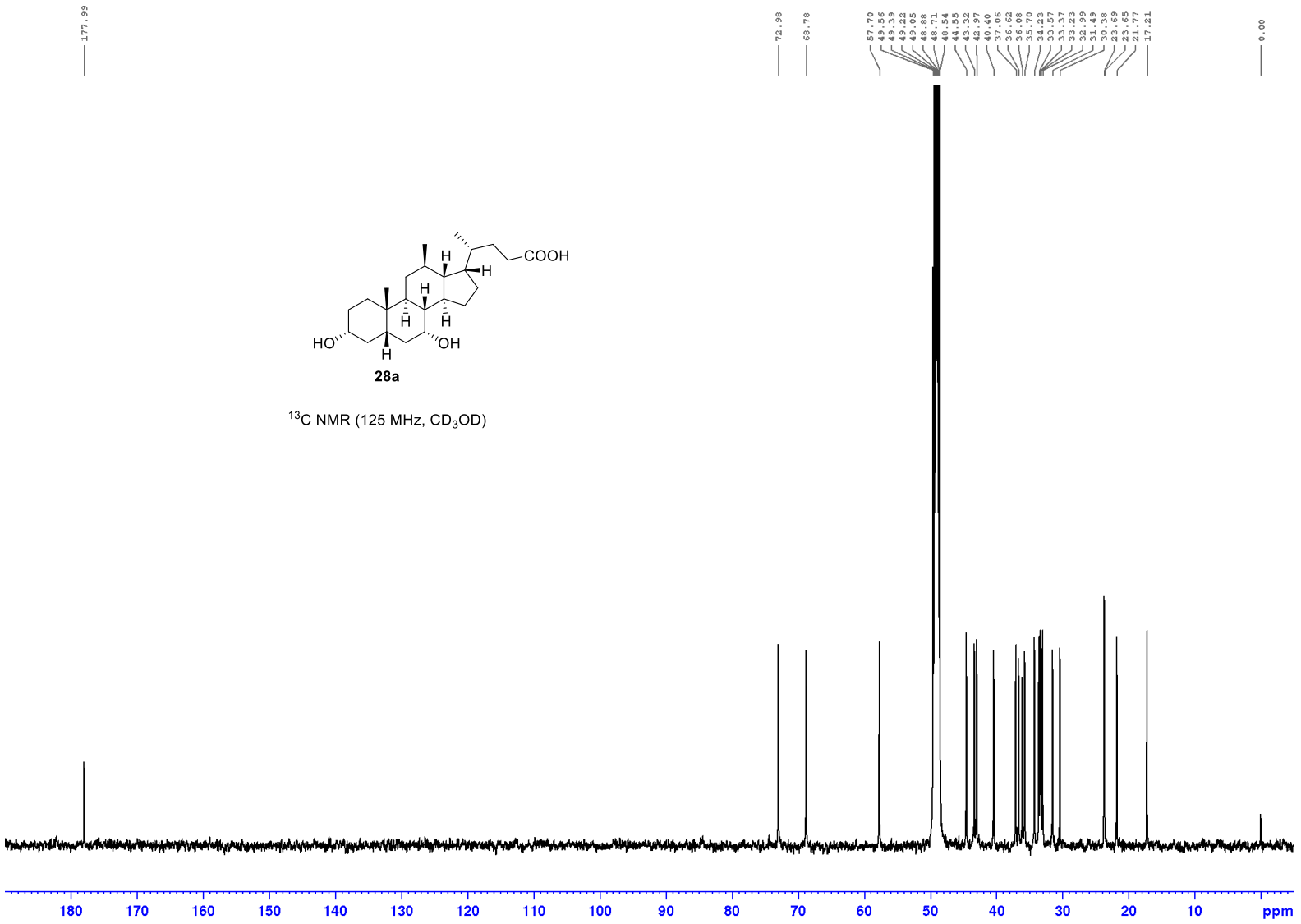

Figure S8. ^{13}C NMR spectrum of **28a**.

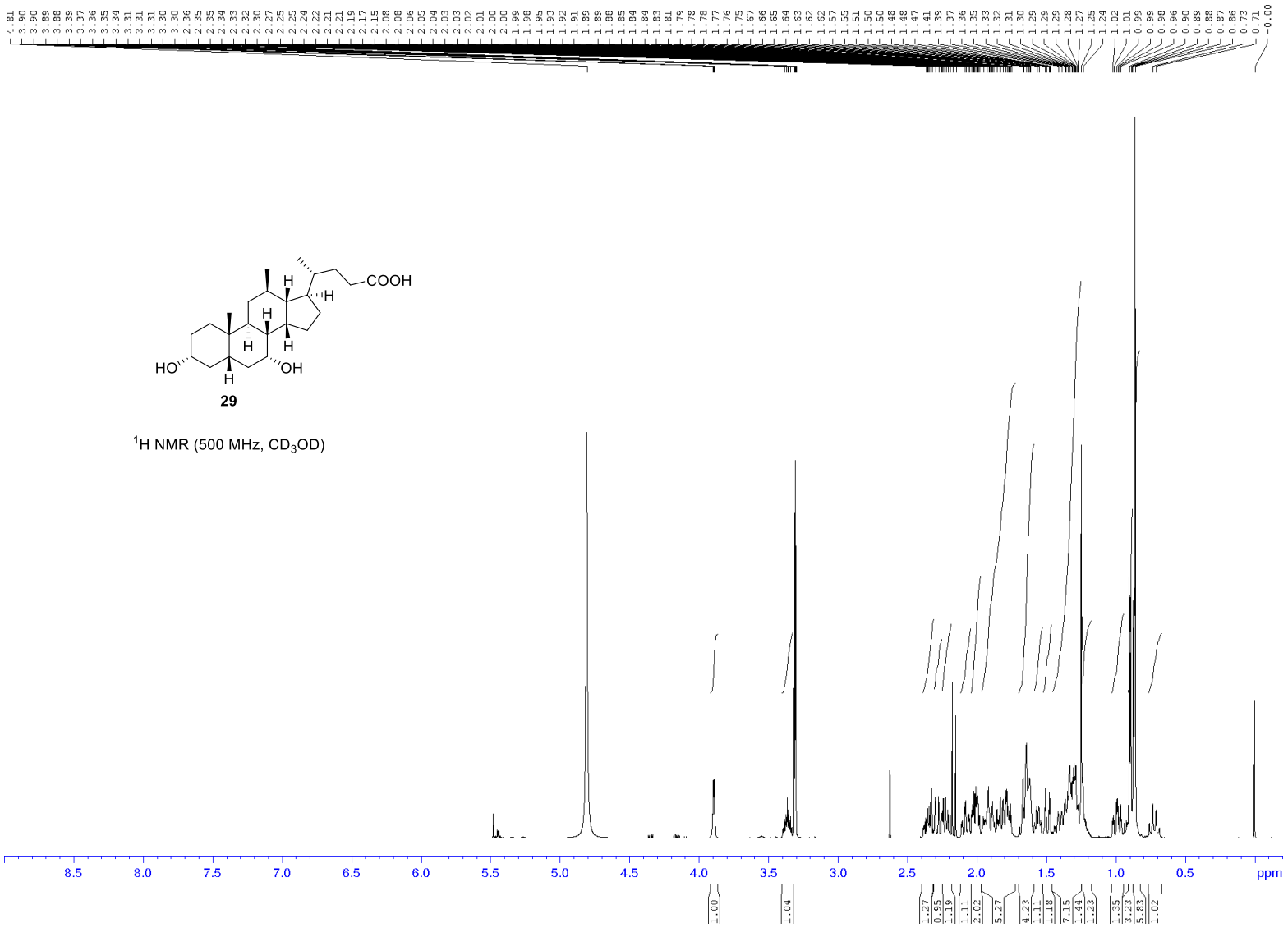

Figure S9a. ^{1}H NMR spectrum of **29**.

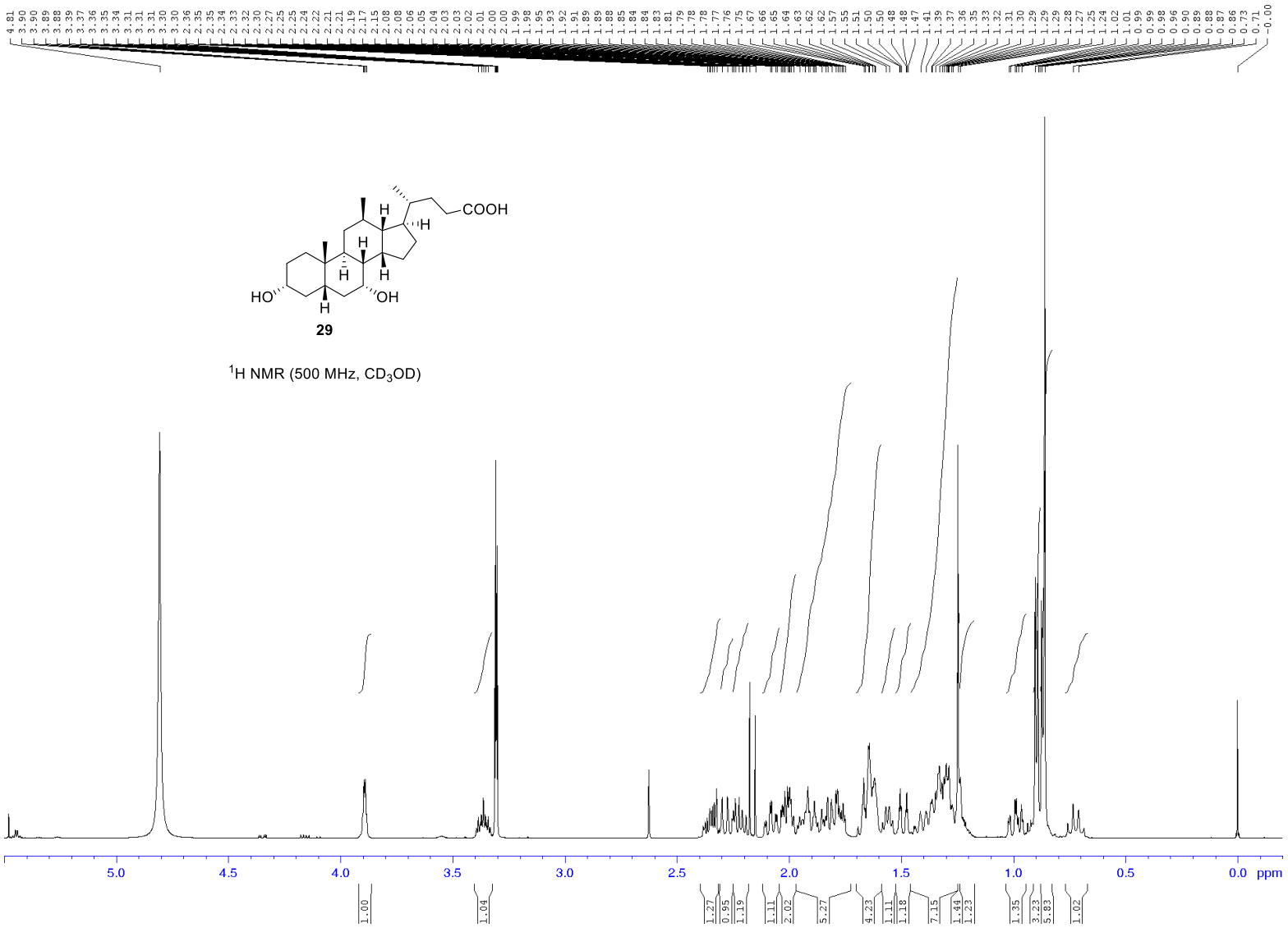

Figure S9b. ^{1}H NMR spectrum of **29**.

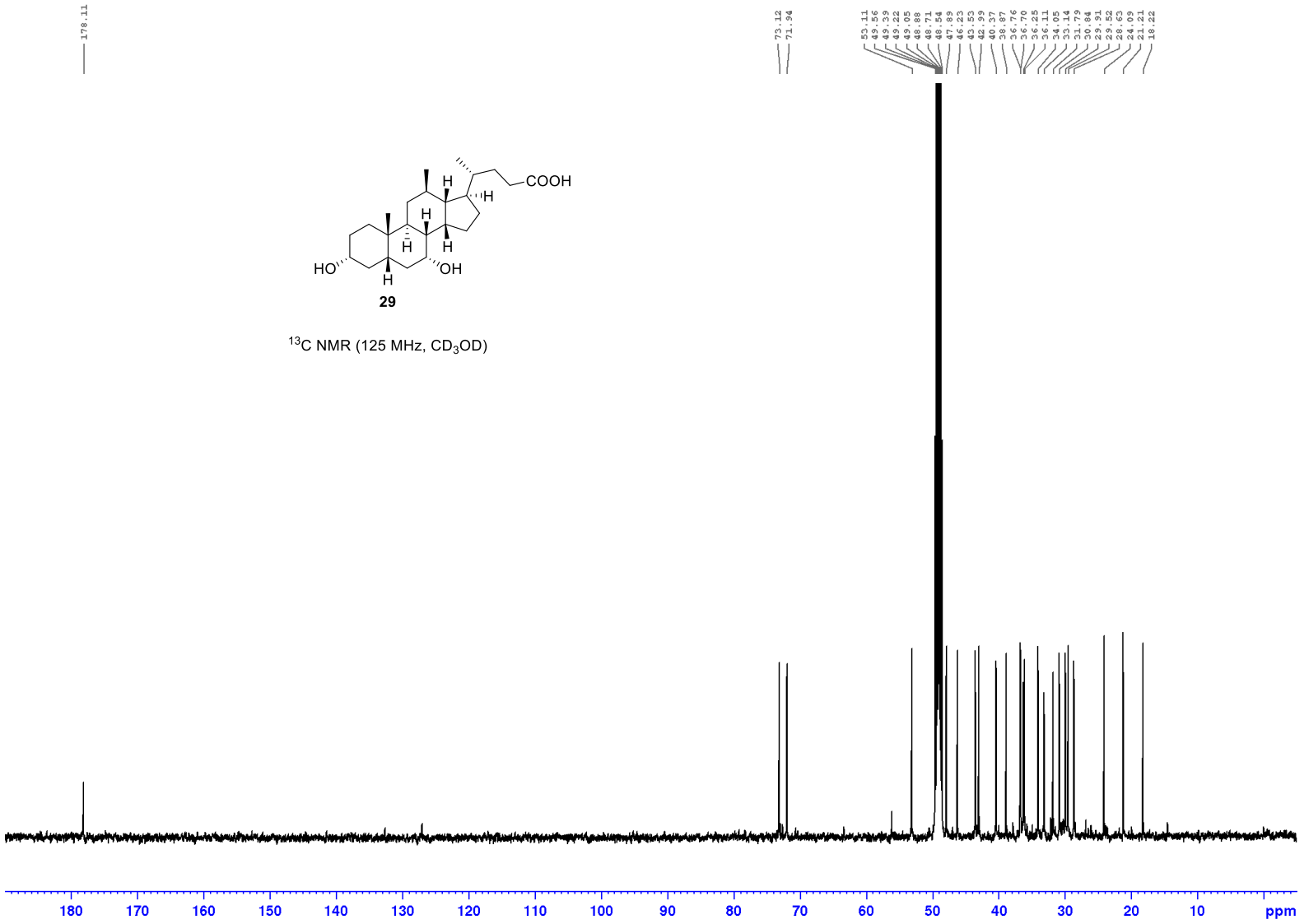

Figure S10. ^{13}C NMR spectrum of **29**.

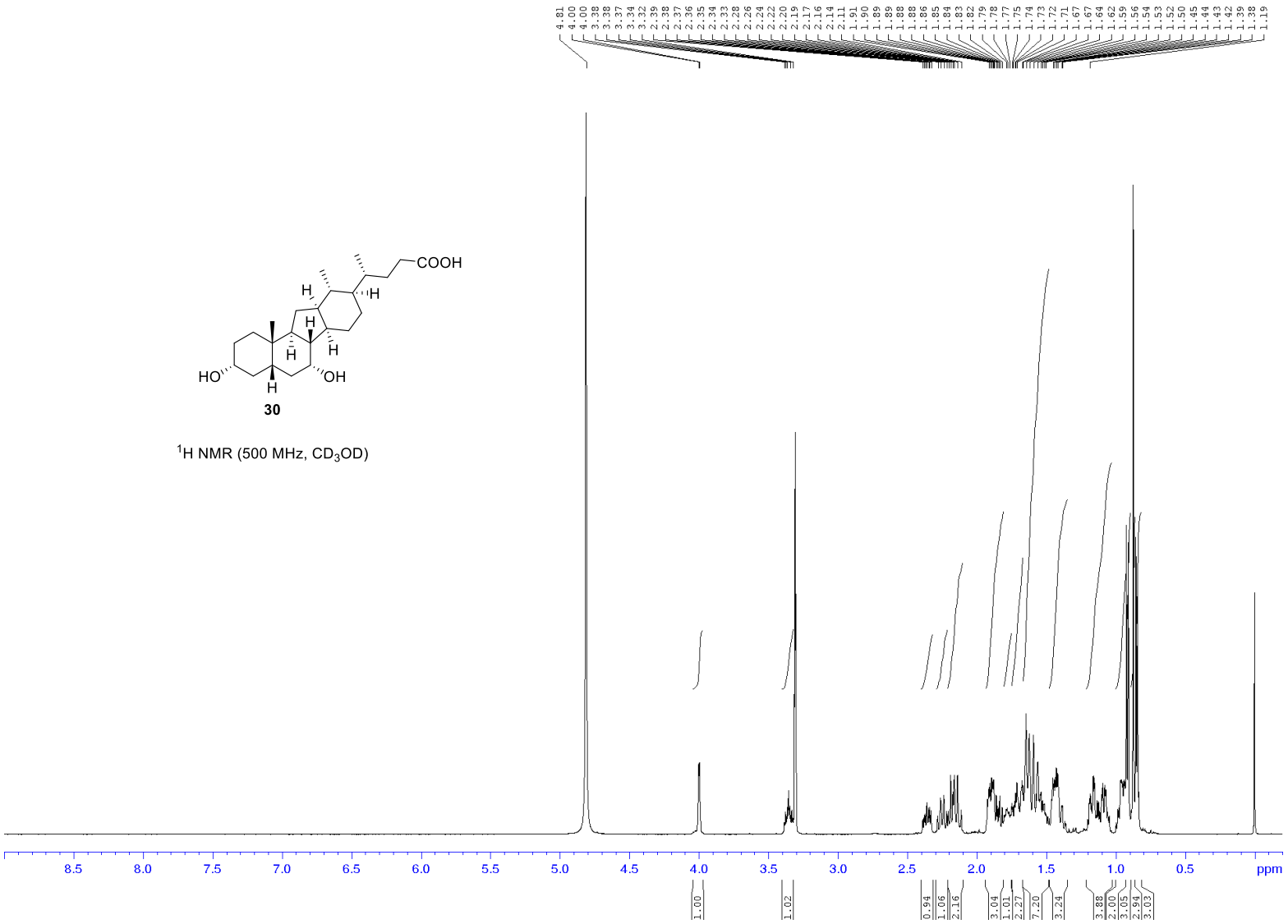

Figure S11a. ^{1}H NMR spectrum of **30**.

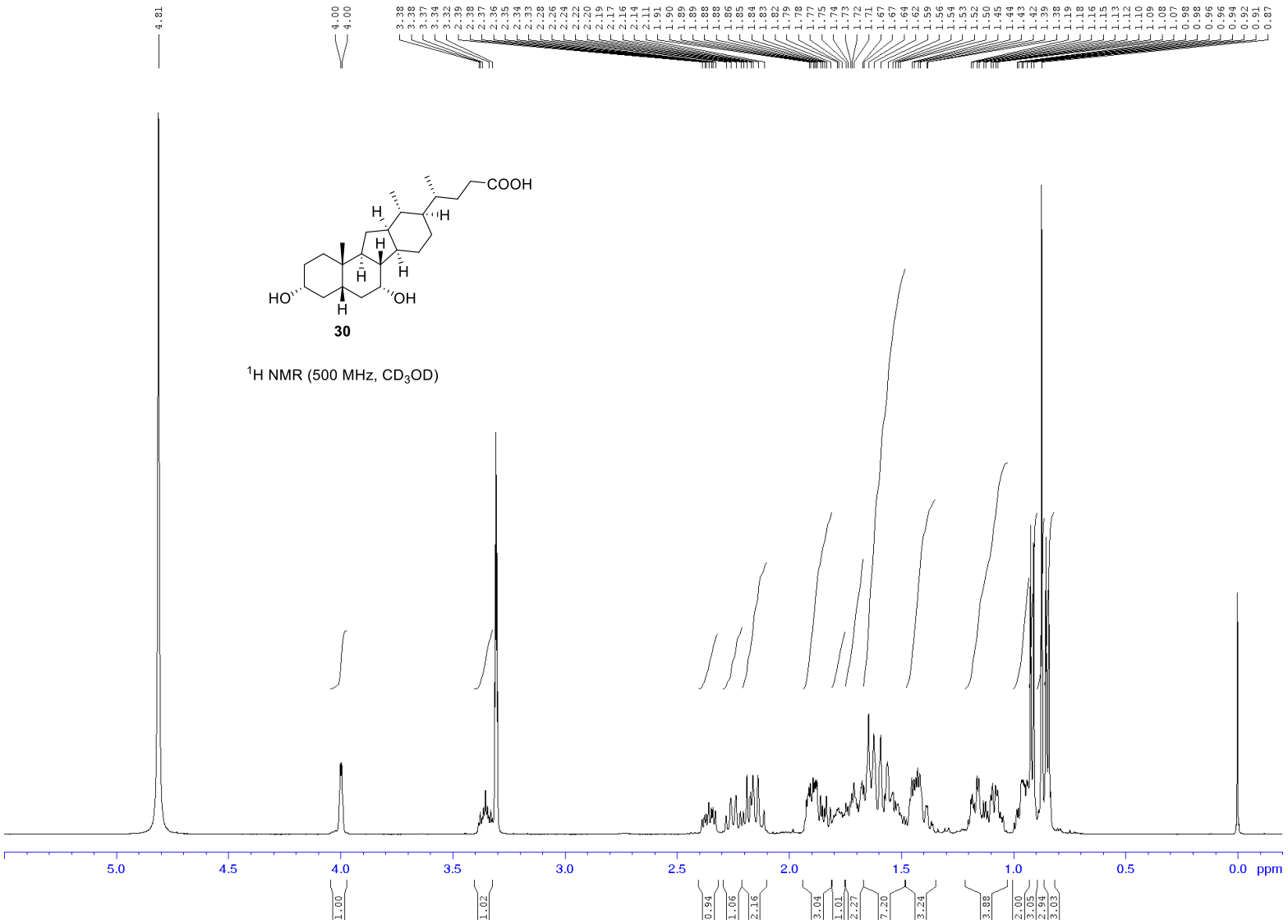

Figure S11b. ^{1}H NMR spectrum of **30**.

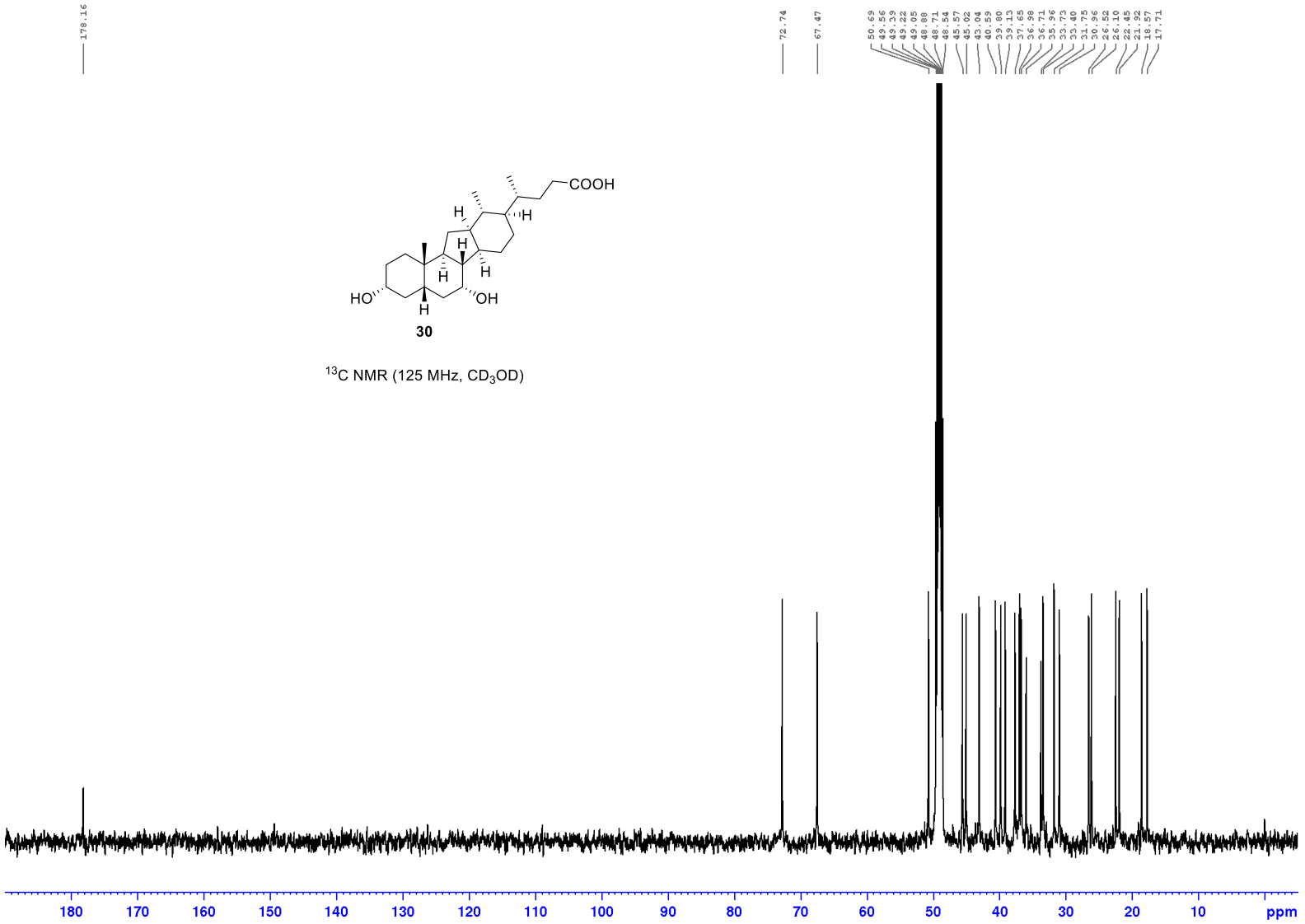

Figure S12. ^{13}C NMR spectrum of **30**.

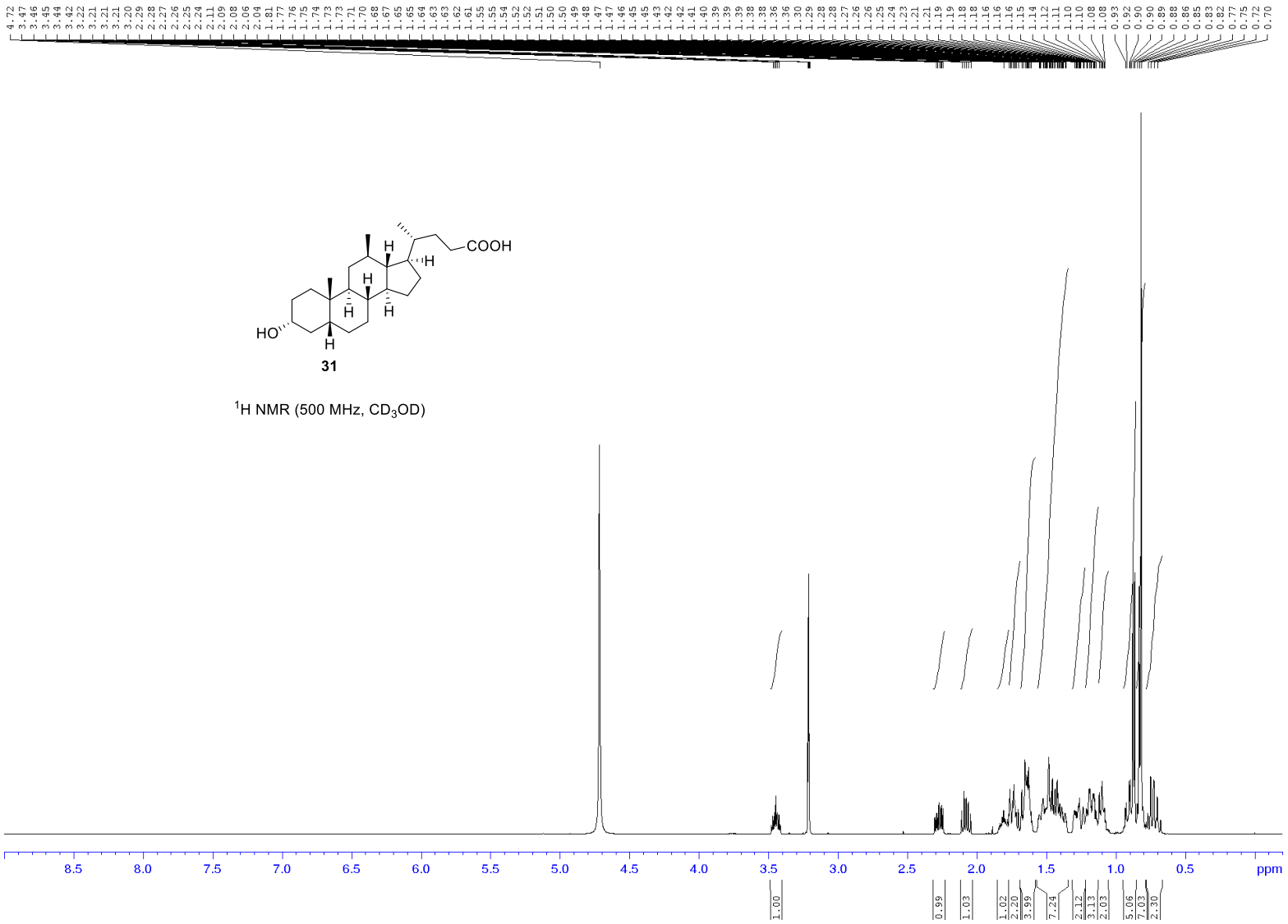

Figure S13a. ^{1}H NMR spectrum of **31**.

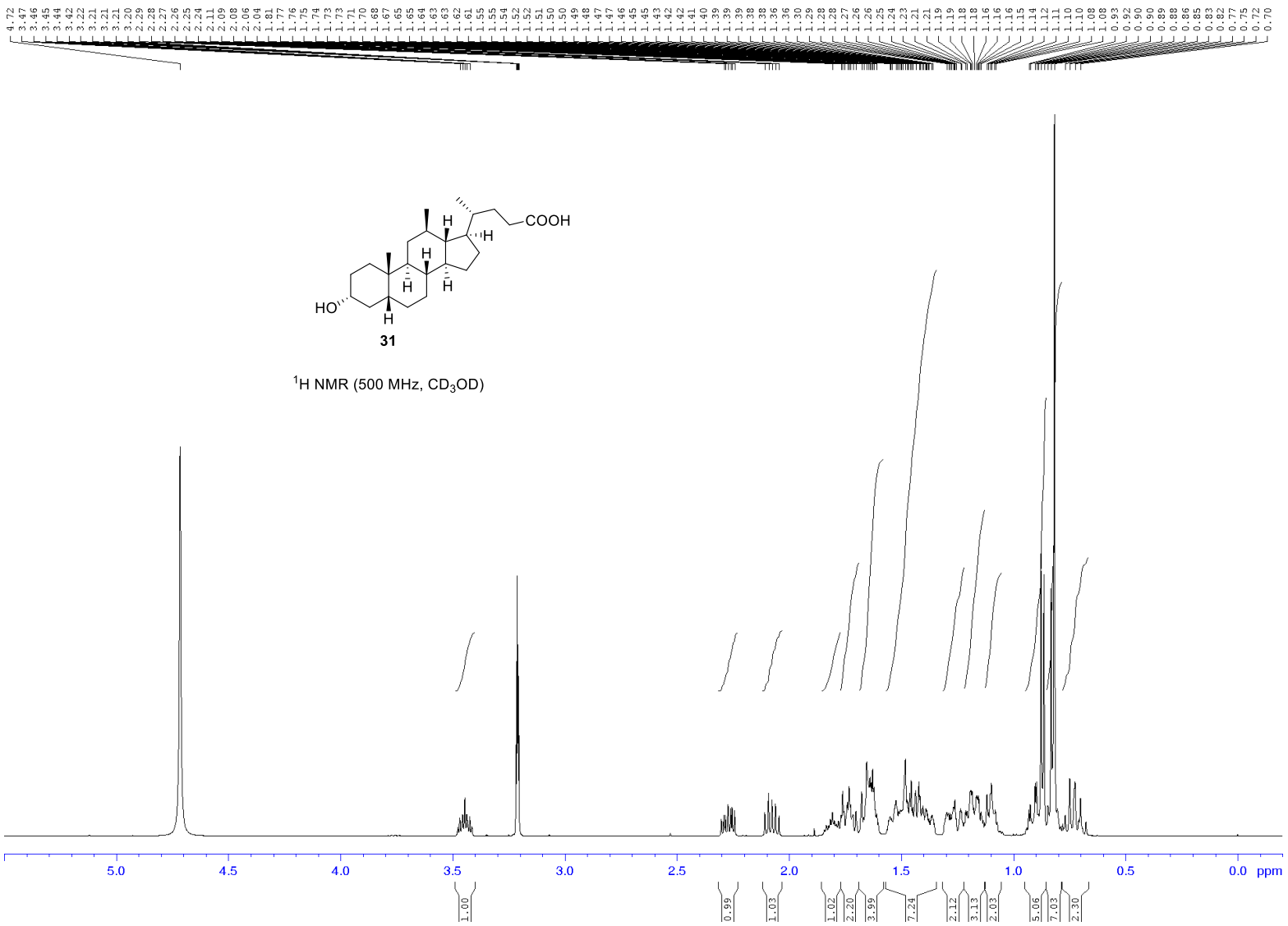

Figure S13b. ^{1}H NMR spectrum of **31**.

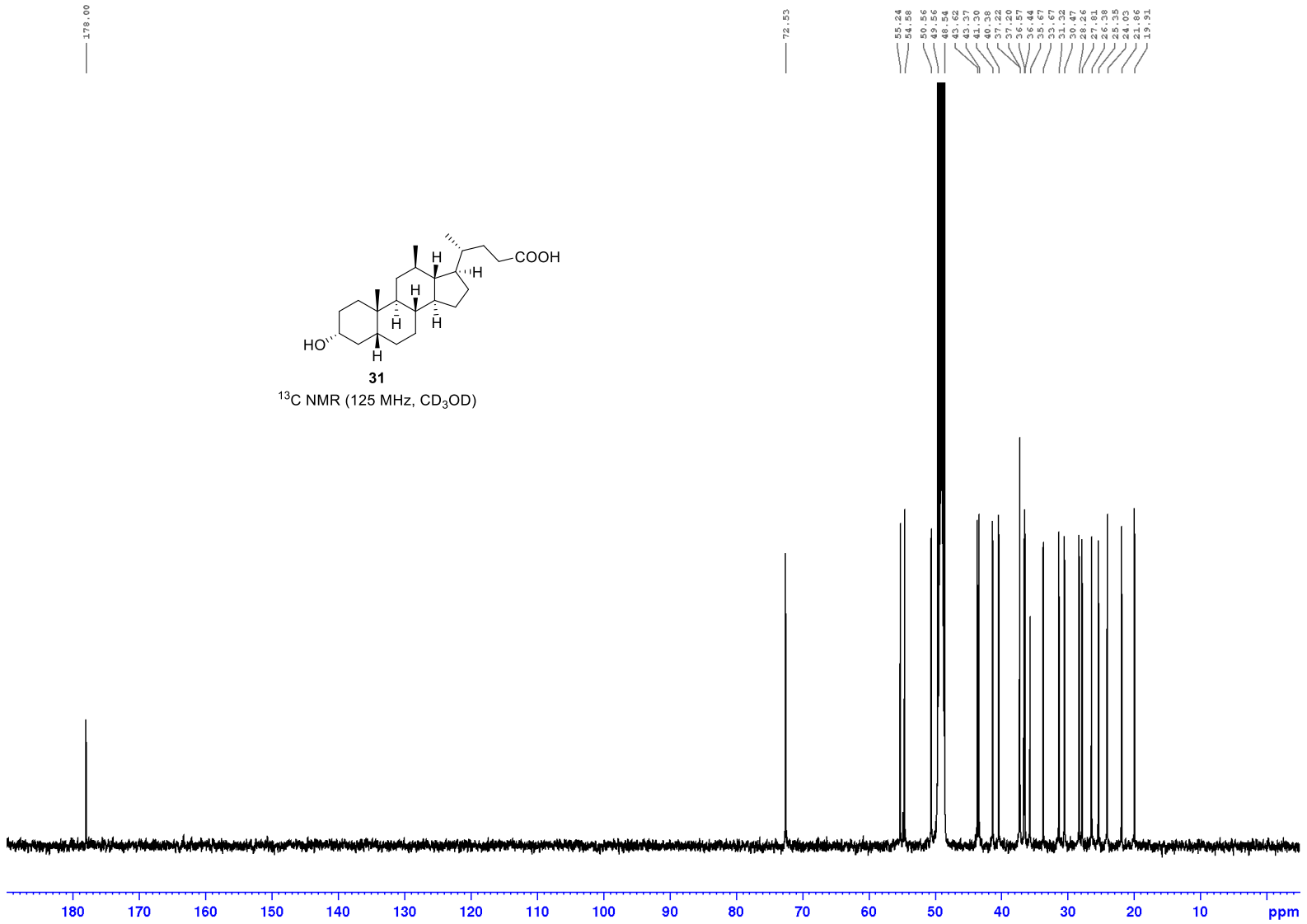

Figure S14. ^{13}C NMR spectrum of **31**.

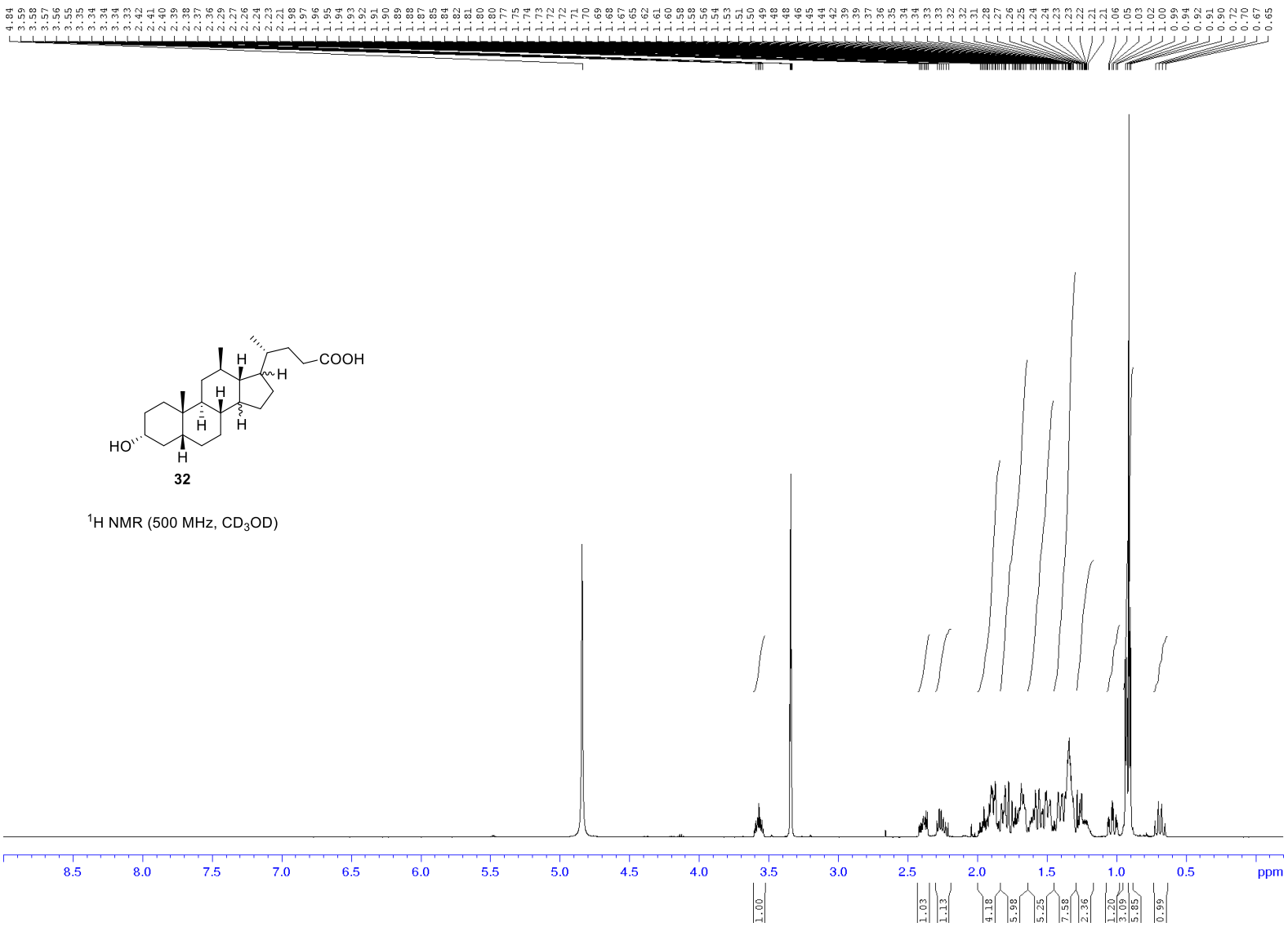

Figure S15a. ^{1}H NMR spectrum of **32**.

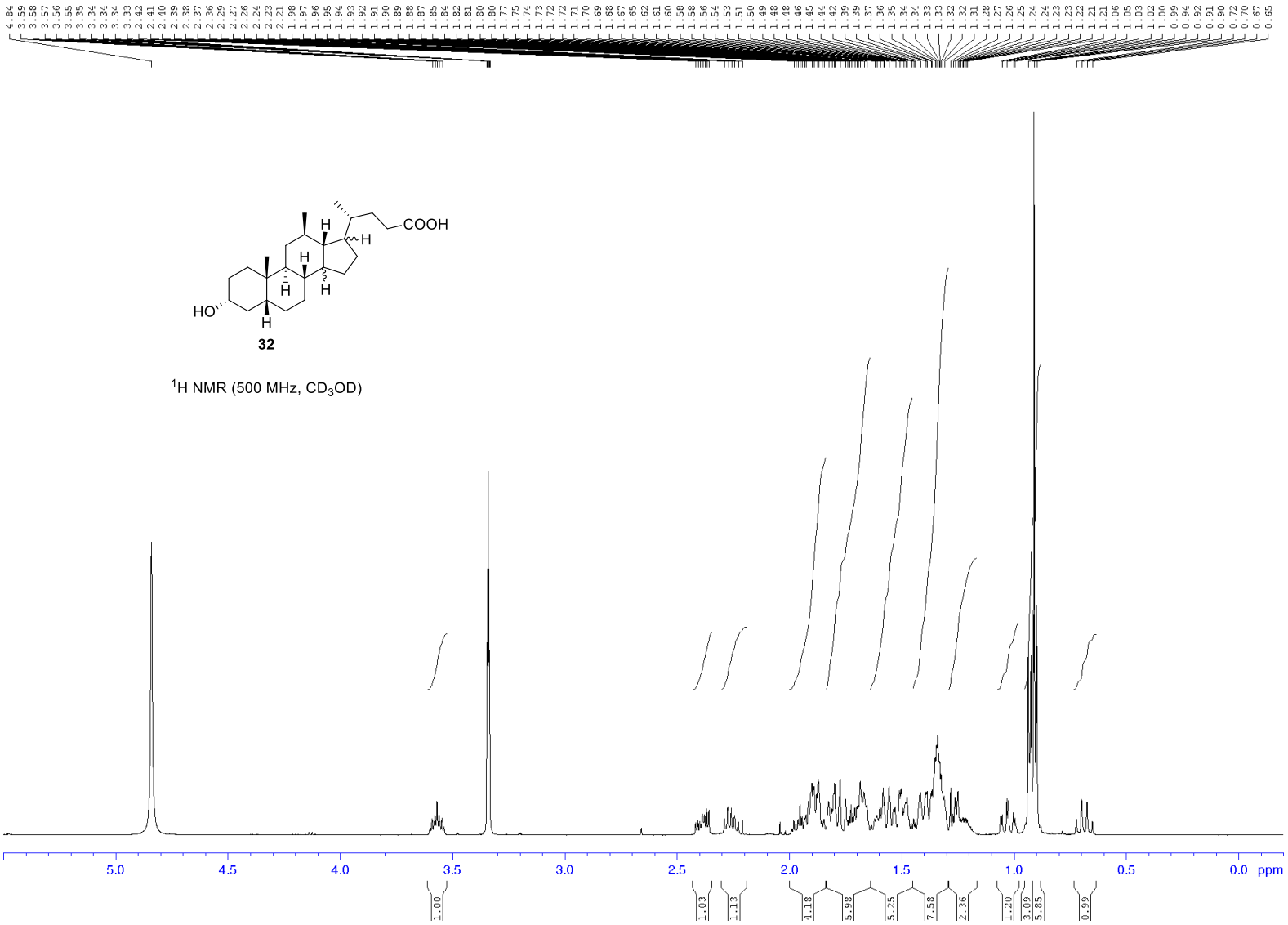

Figure S15b. ^{1}H NMR spectrum of **32**.

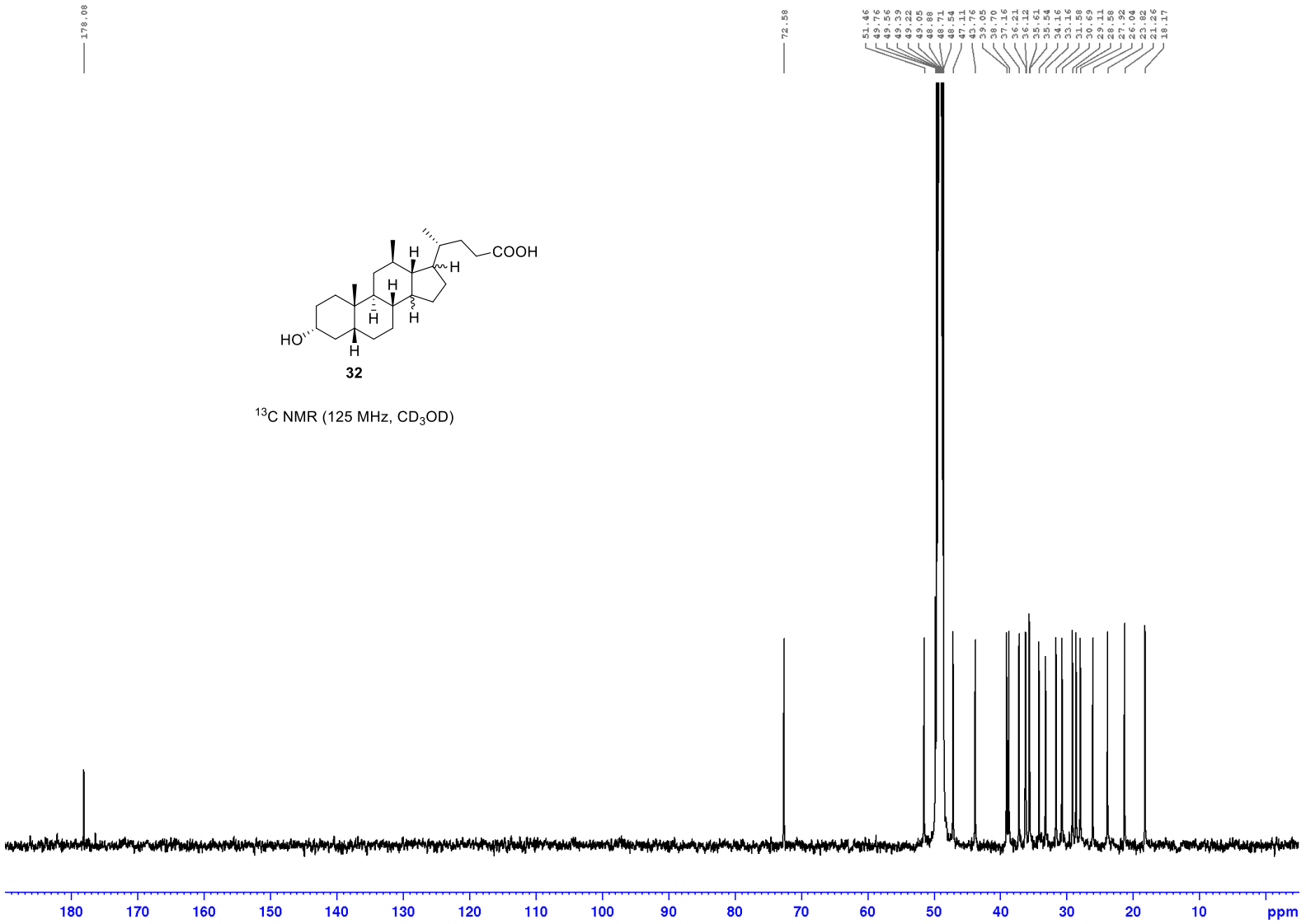

Figure S16. ^{13}C NMR spectrum of **32**.

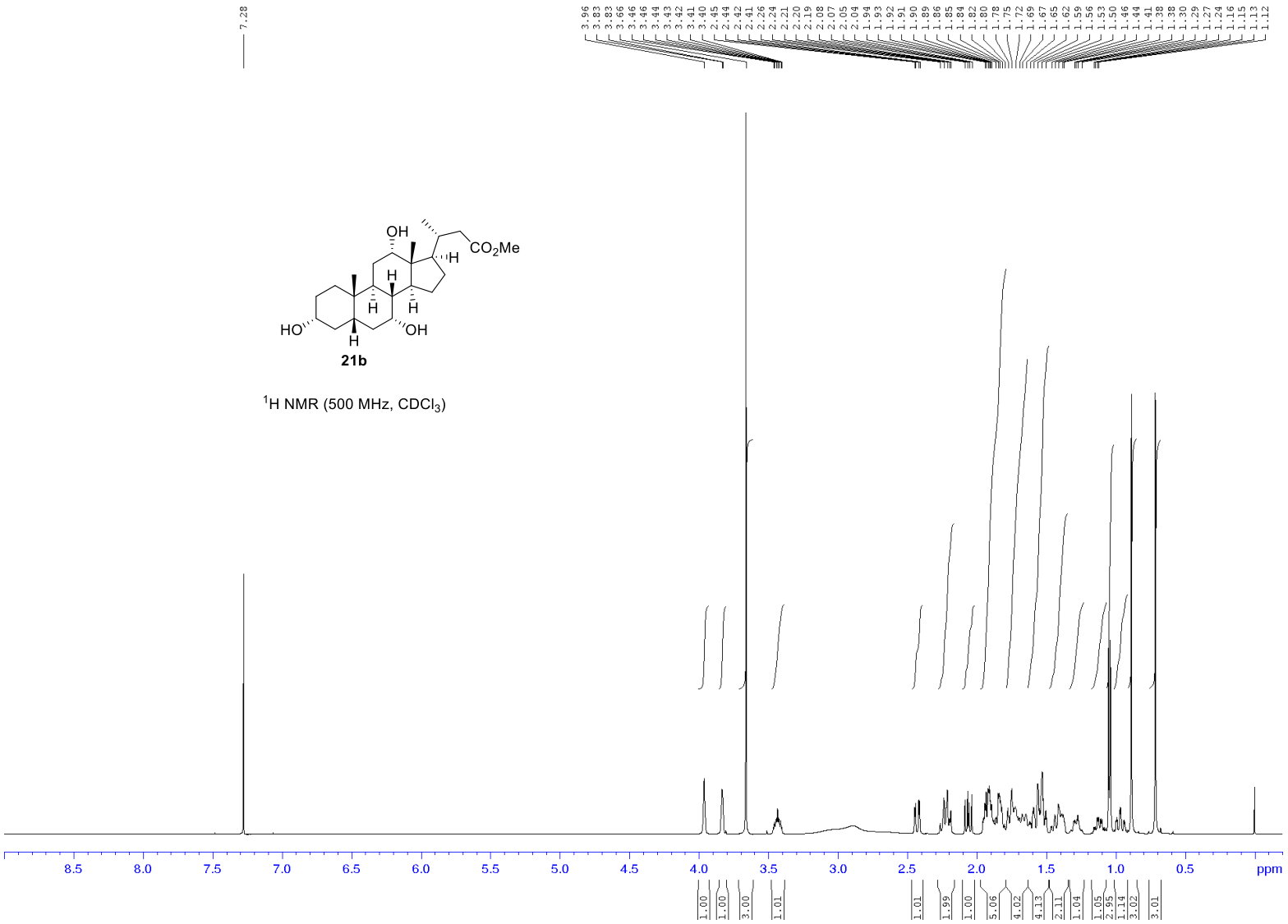

Figure S17a. ^{1}H NMR spectrum of **21b**.

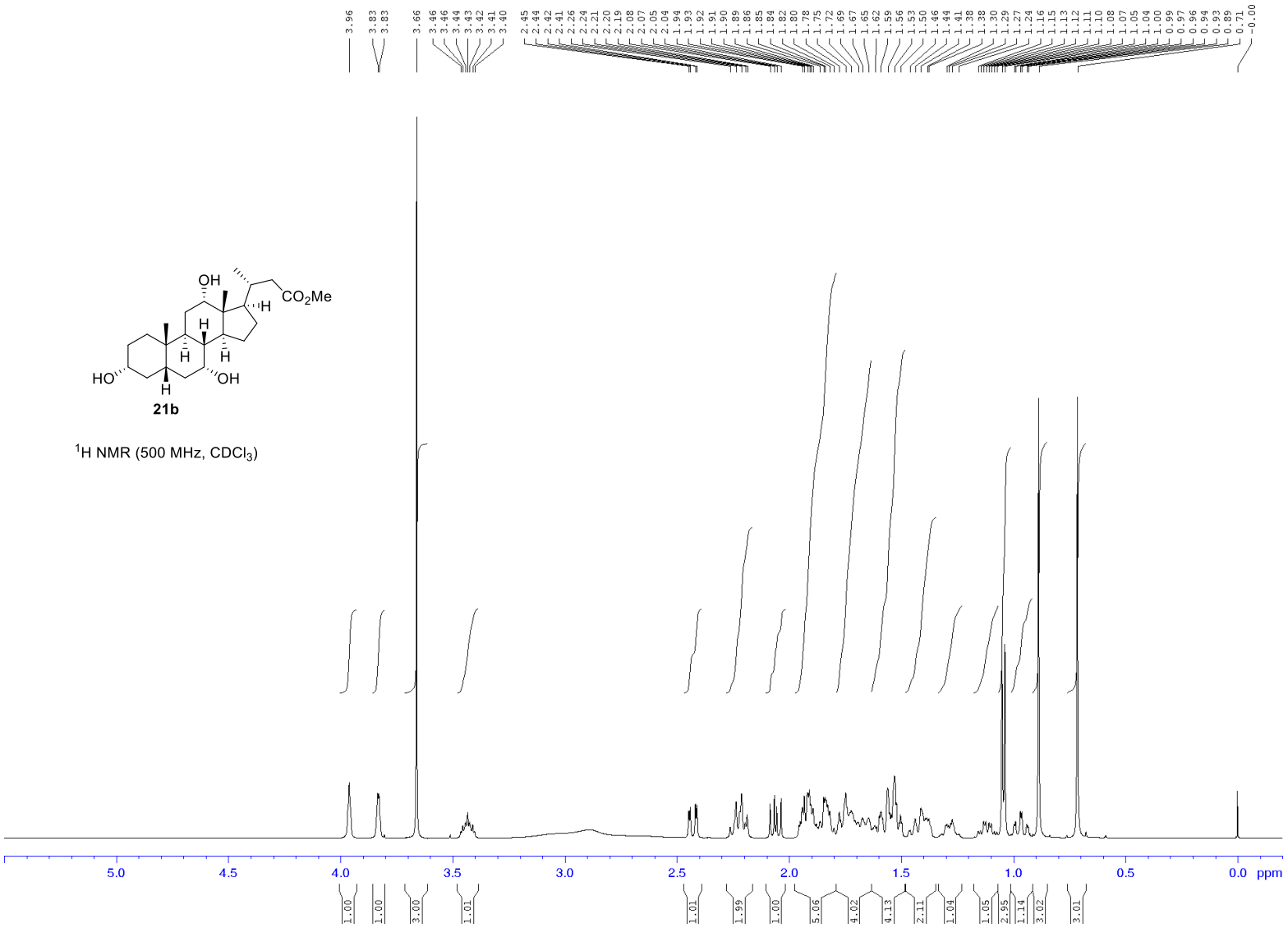

Figure S17b. ^{1}H NMR spectrum of **21b**.

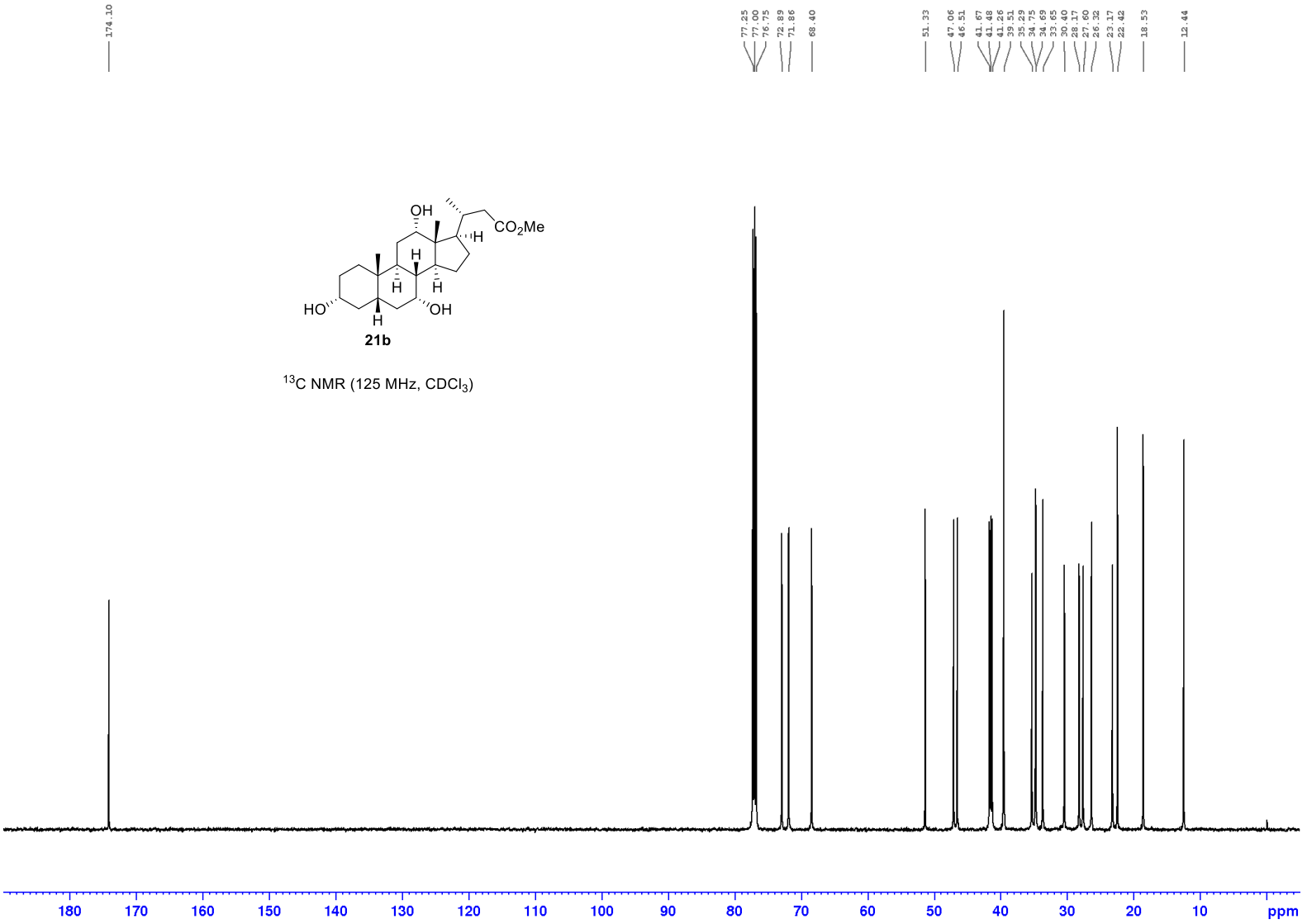

Figure S18. ^{13}C NMR spectrum of **21b**.

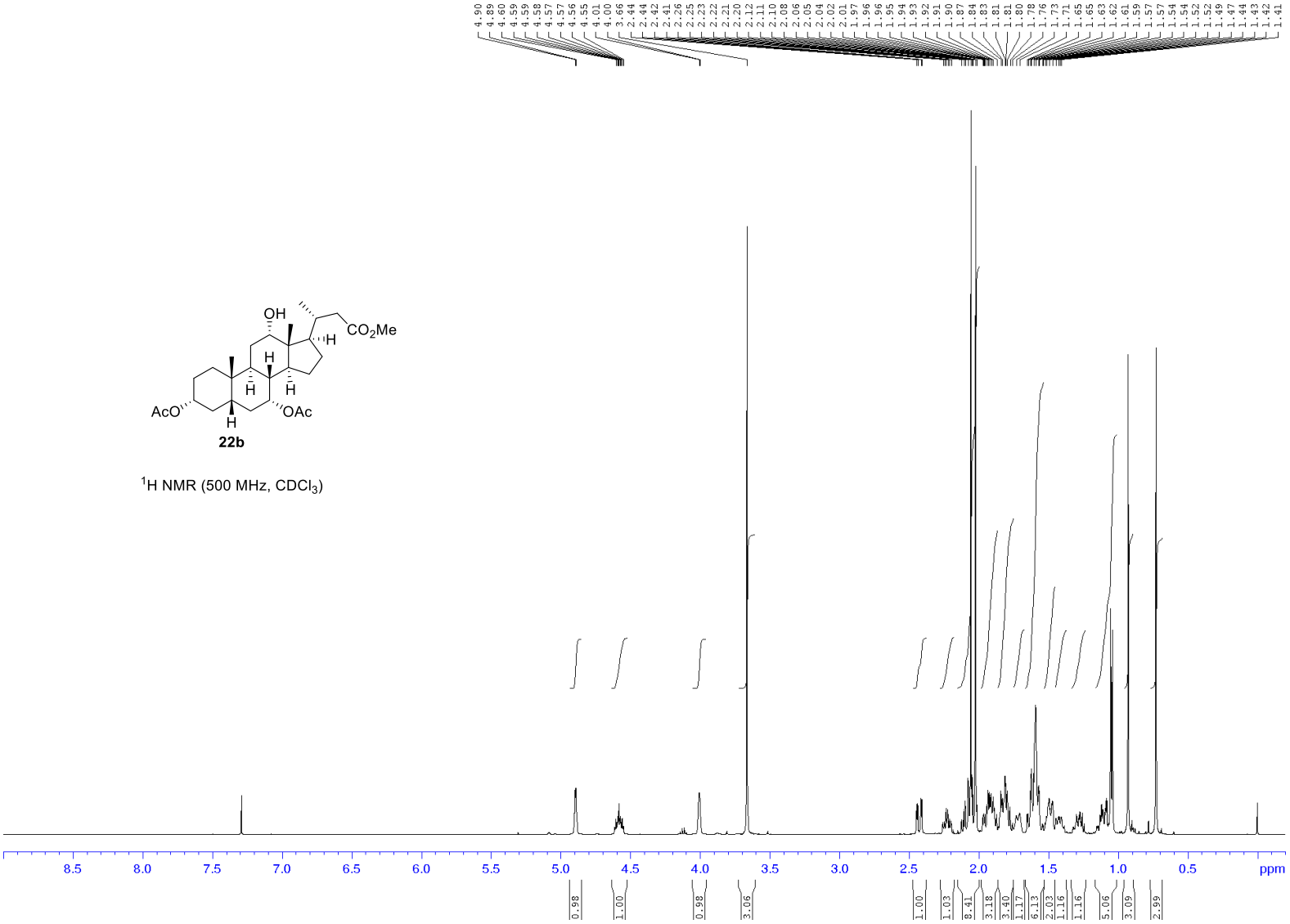

Figure S19a. ^{1}H NMR spectrum of **22b**.

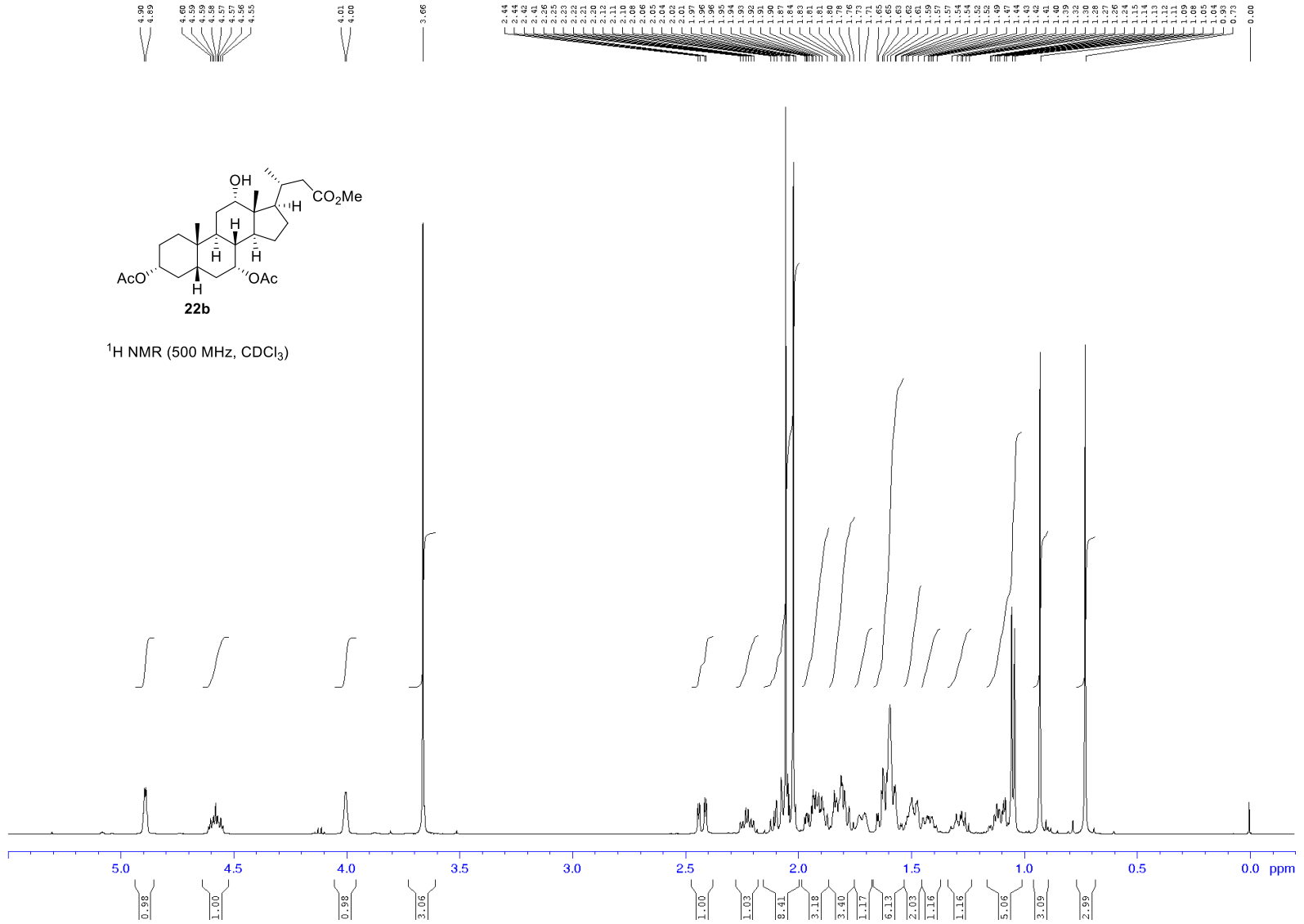

Figure S19b. ^{1}H NMR spectrum of **22b**.

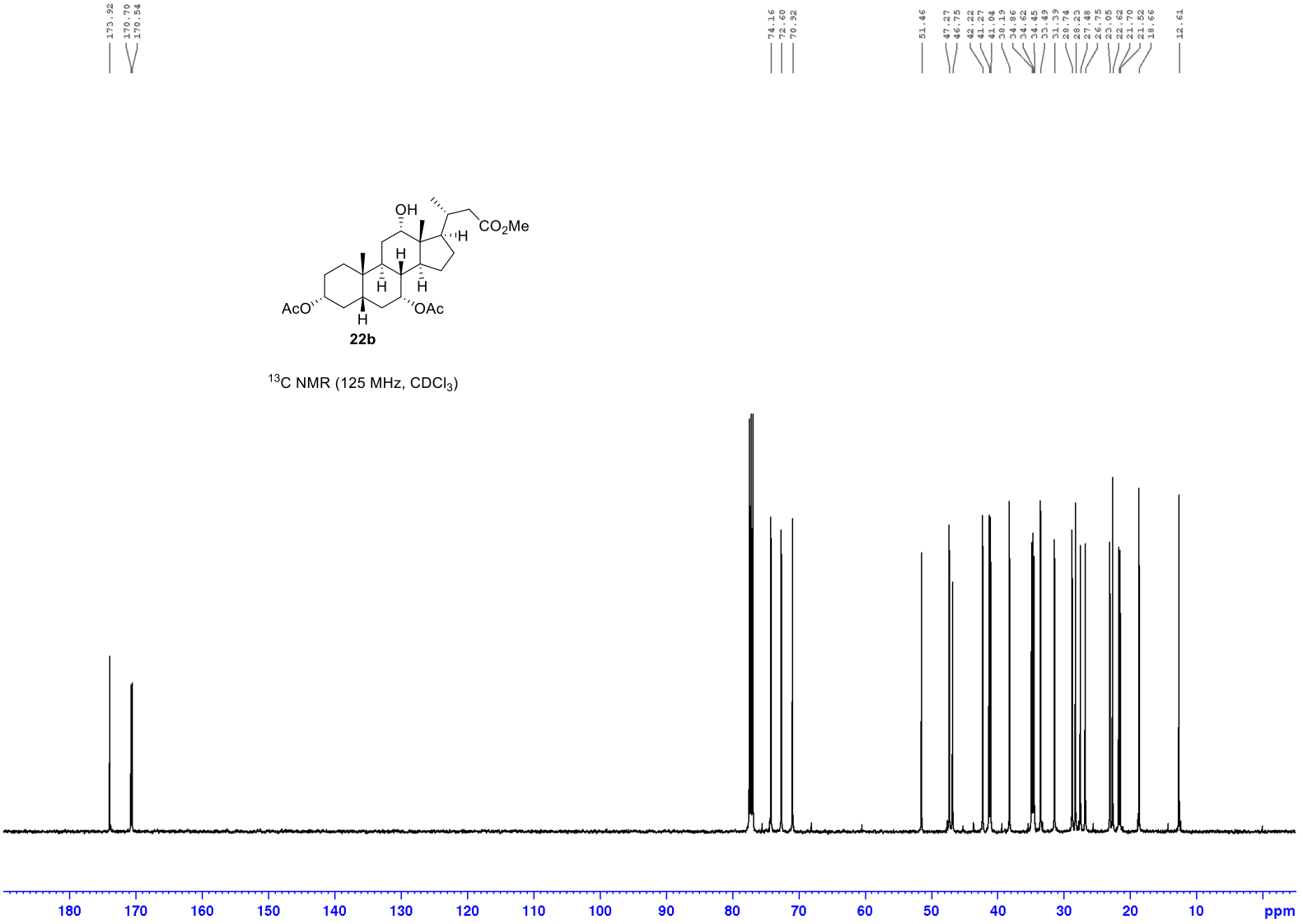

Figure S20. ^{13}C NMR spectrum of **22b**.

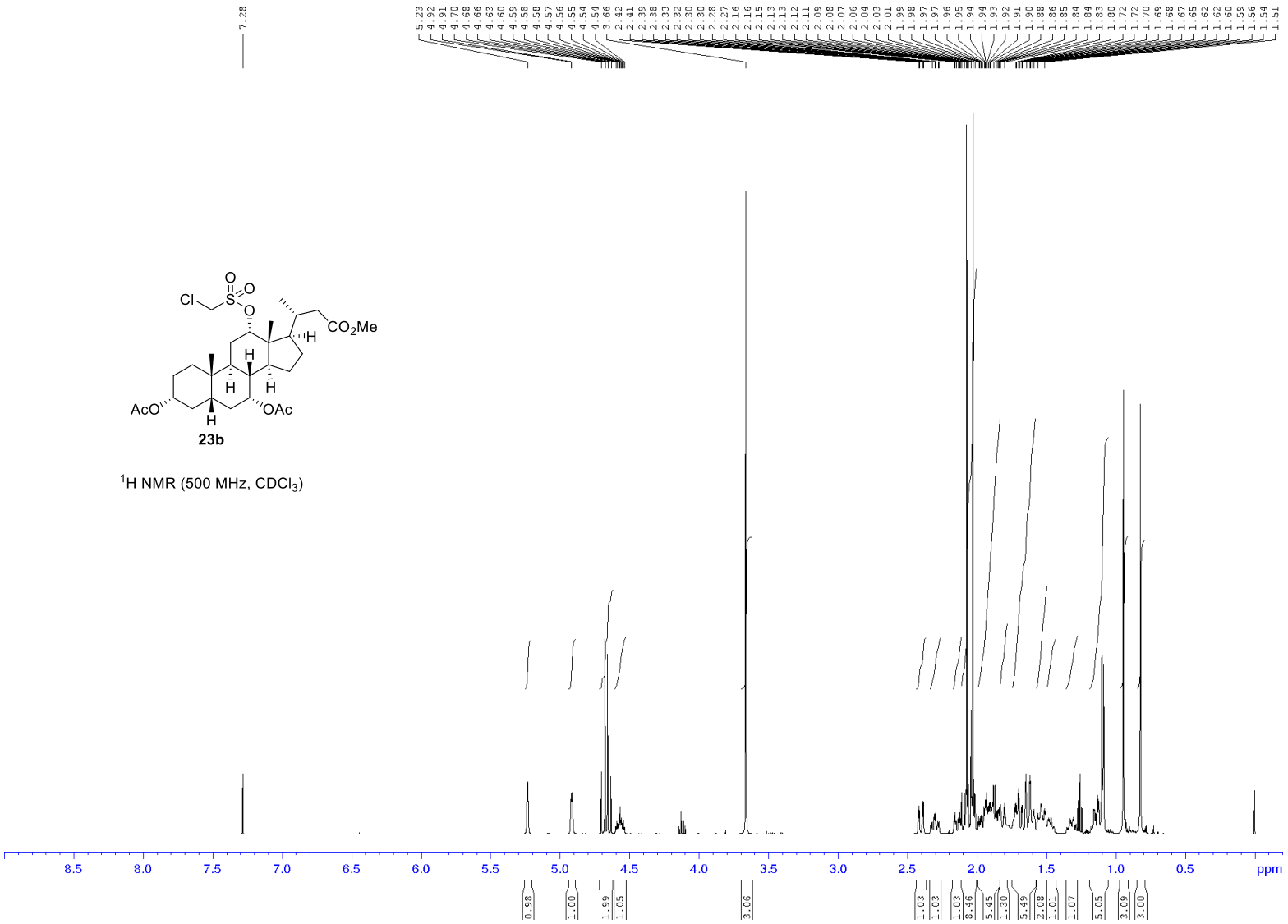

Figure S21a. ^{1}H NMR spectrum of **23b**.

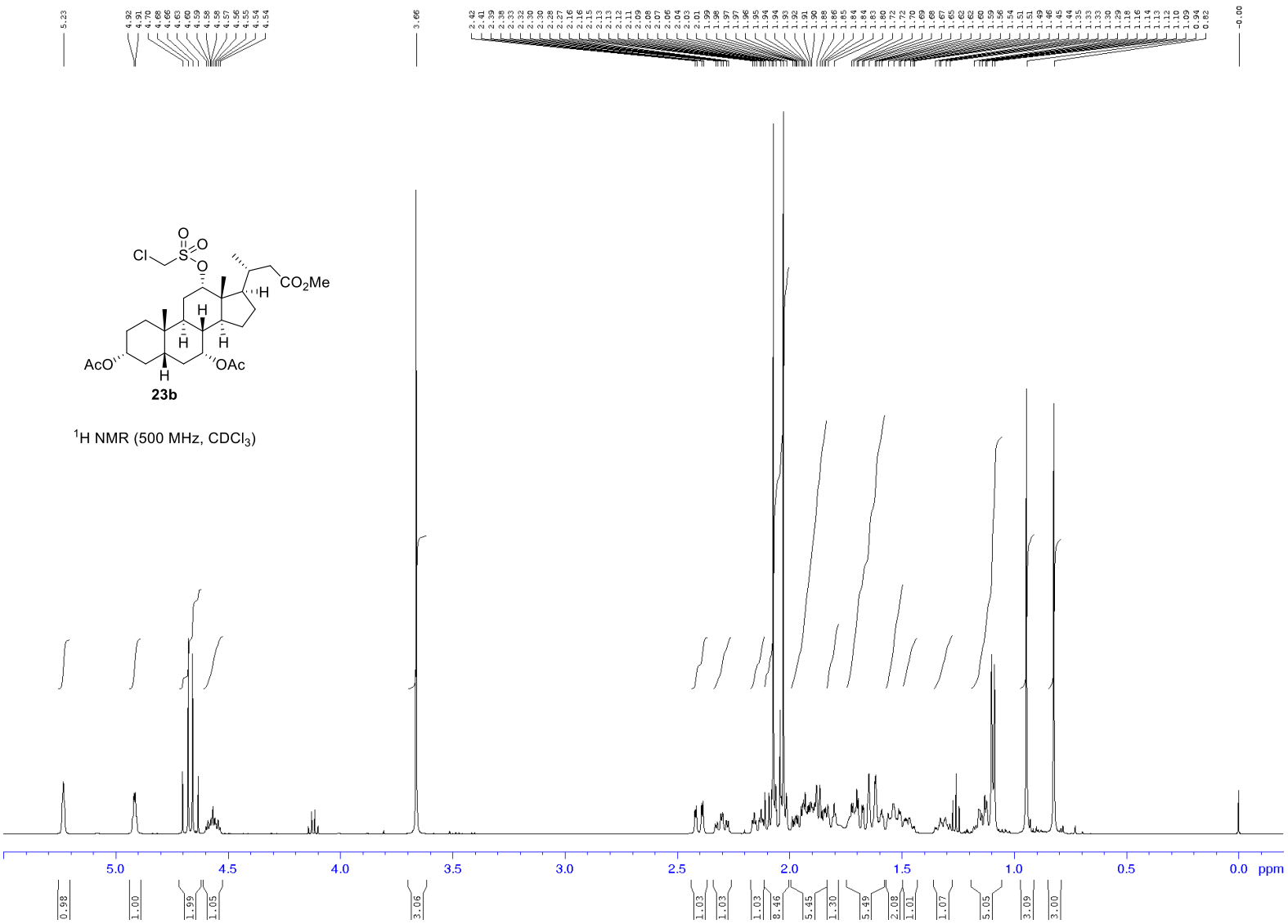

Figure S21b. ^{1}H NMR spectrum of **23b**.

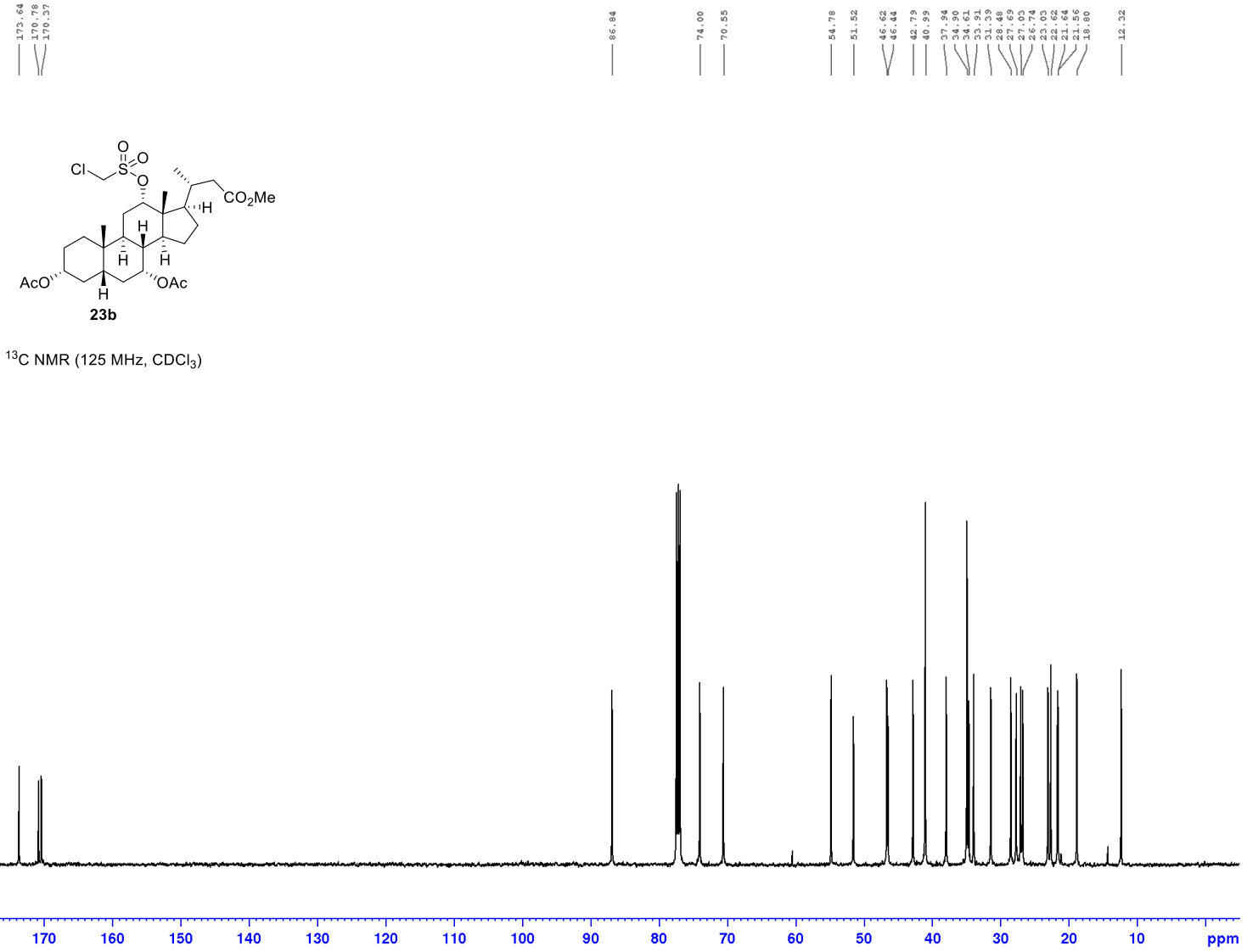

Figure S22. ^{13}C NMR spectrum of **23b**.

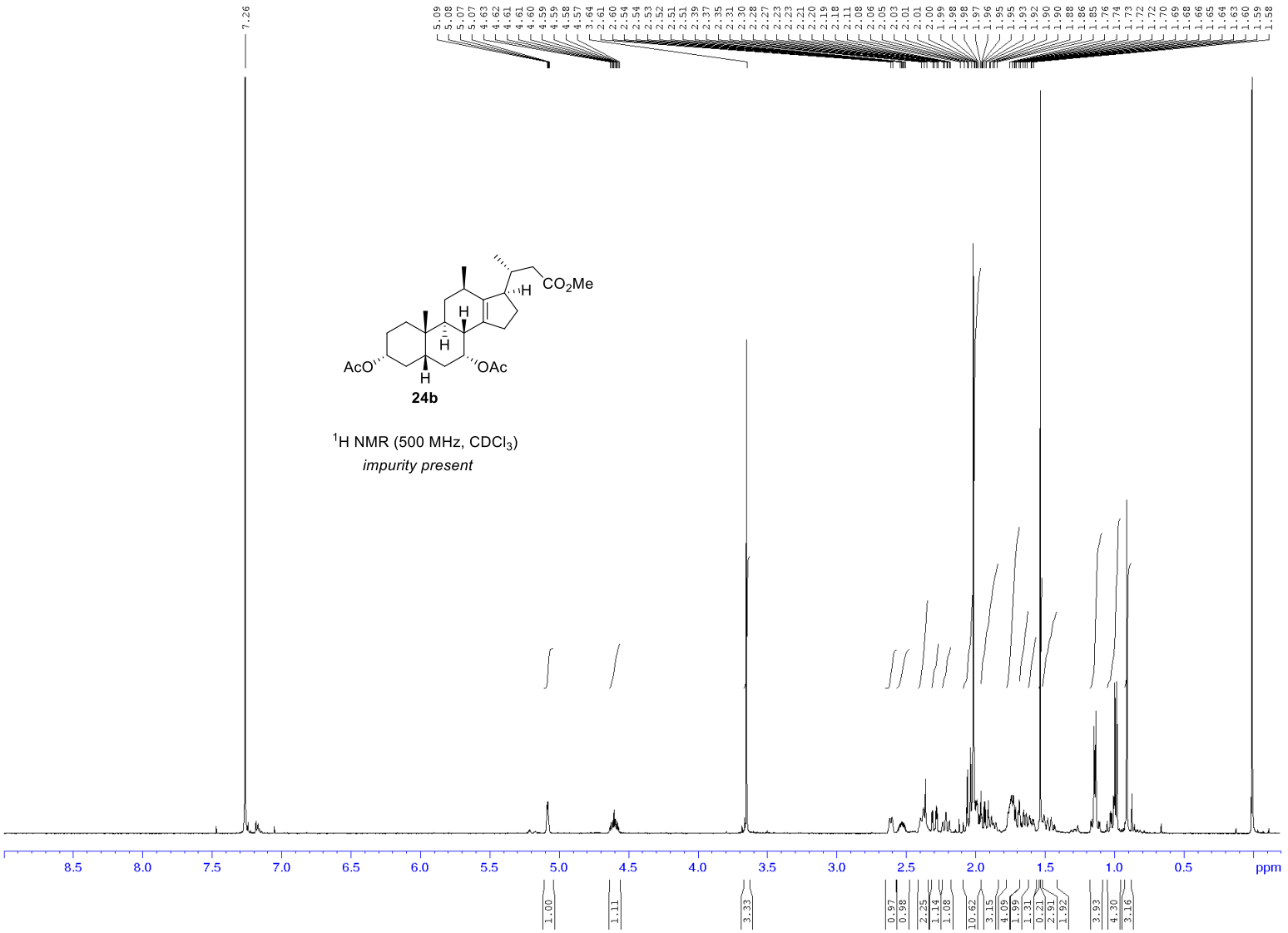

Figure S23a. ^{1}H NMR spectrum of **24b**.

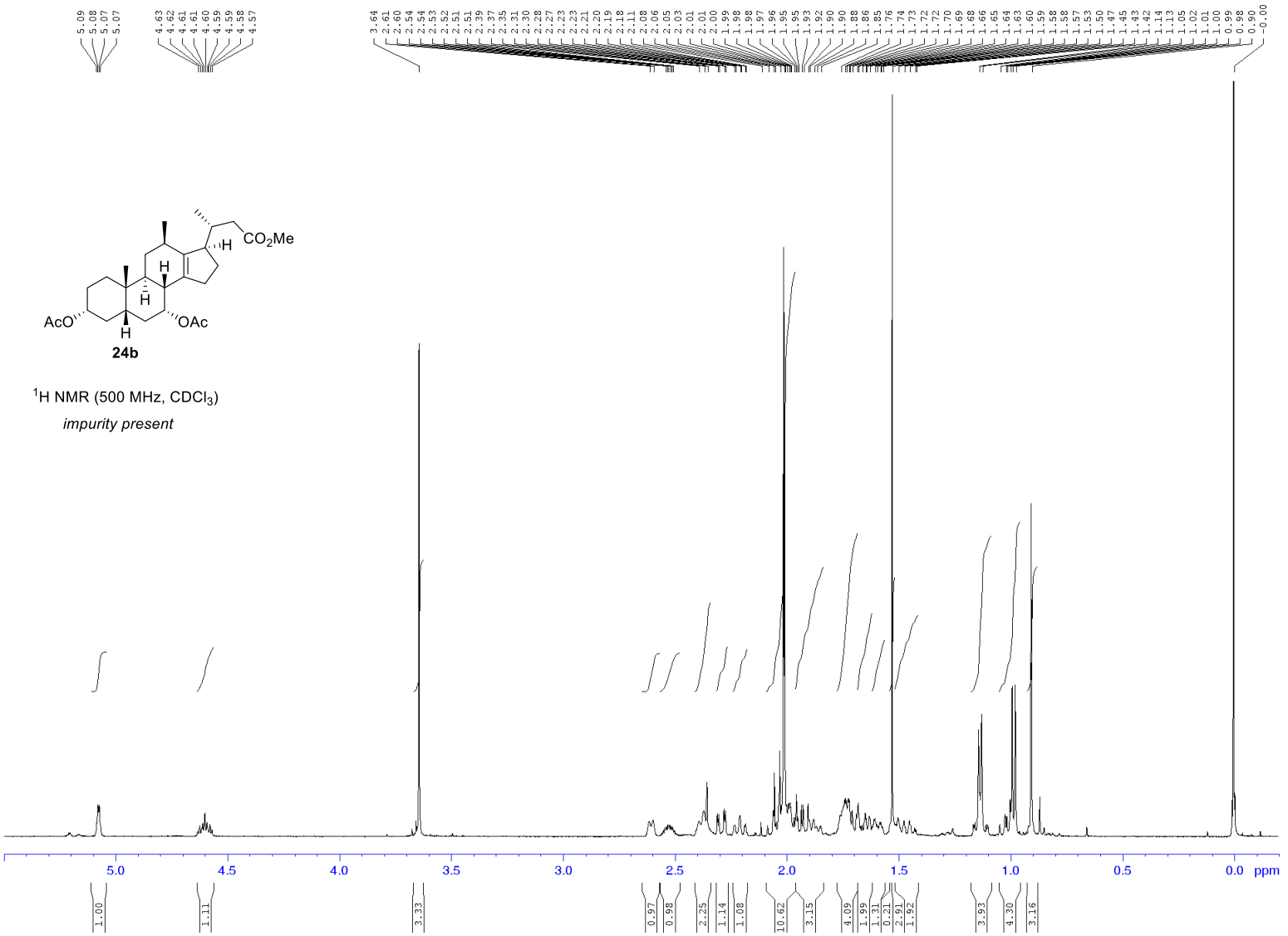

Figure S23b. ^{1}H NMR spectrum of **24b**.

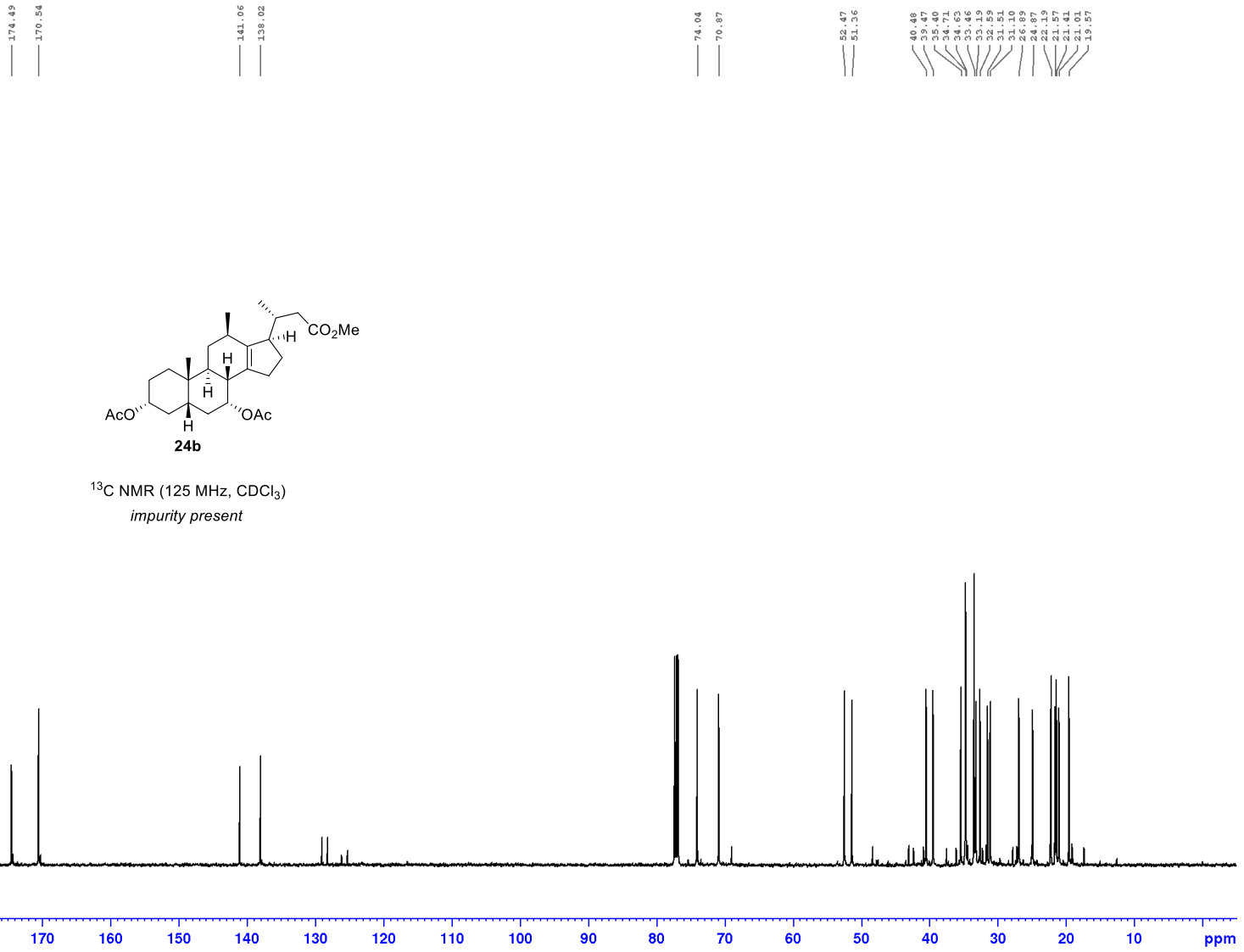

Figure S24. ^{13}C NMR spectrum of **24b**.

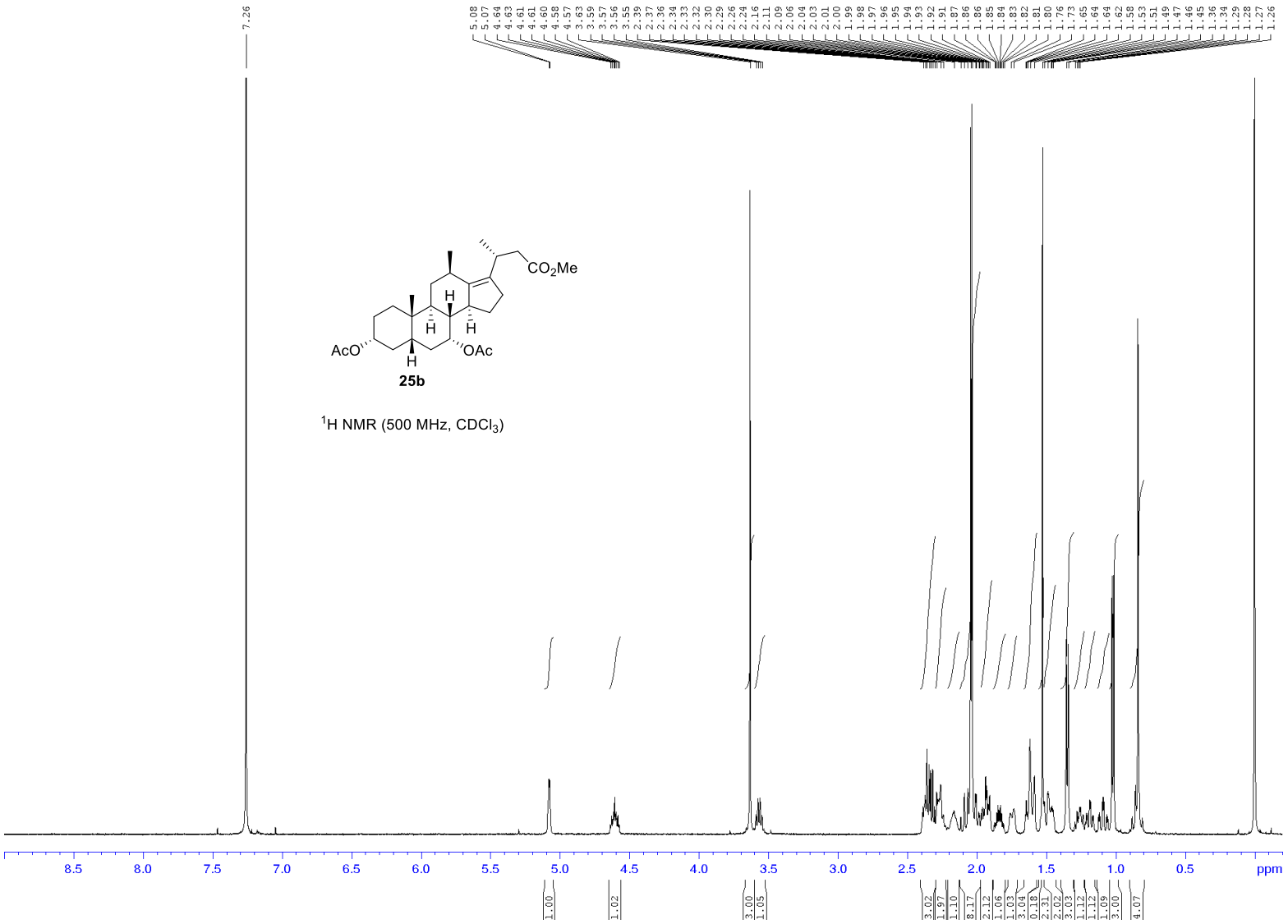

Figure S25a. ^{1}H NMR spectrum of **25b**.

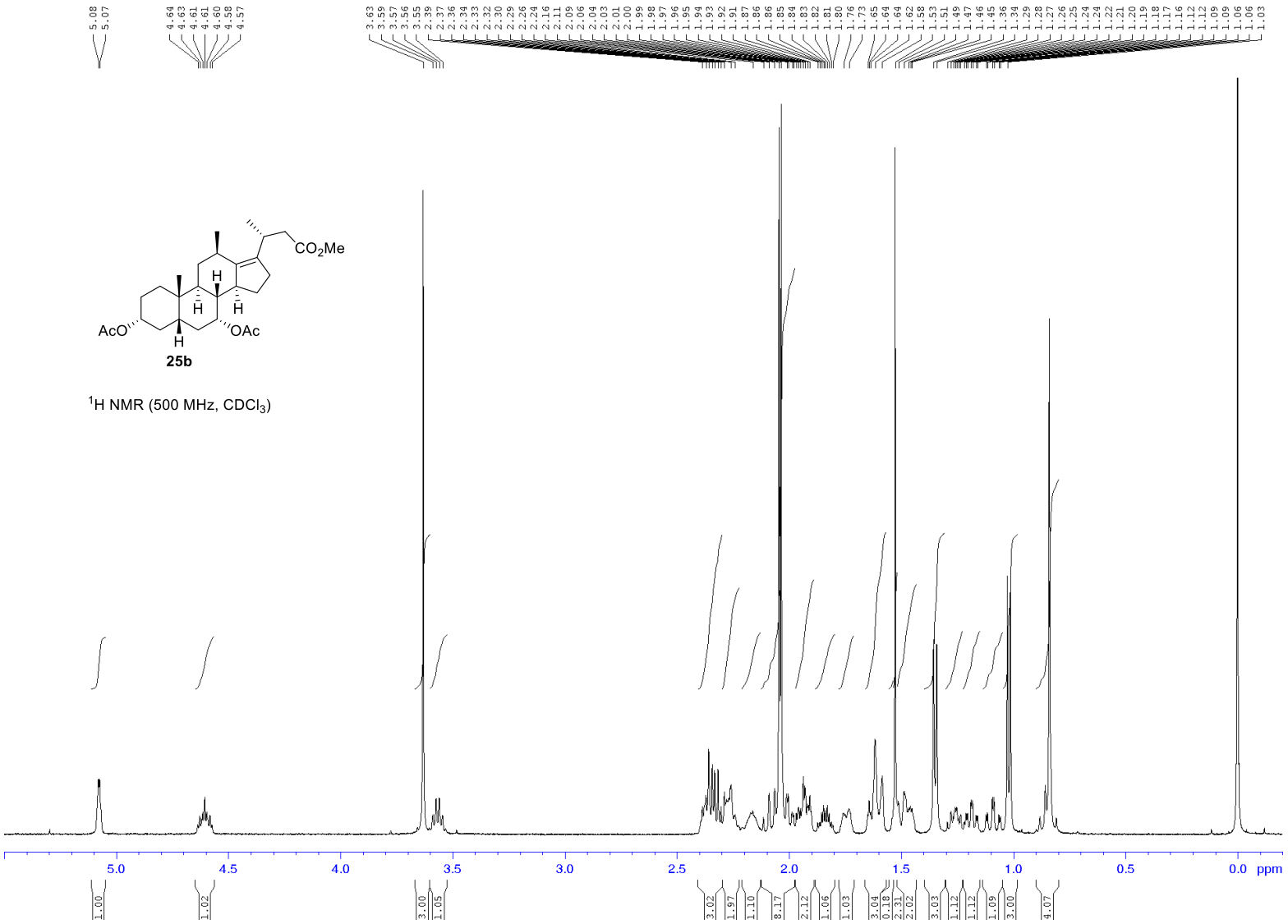

Figure S25b. ^{1}H NMR spectrum of **25b**.

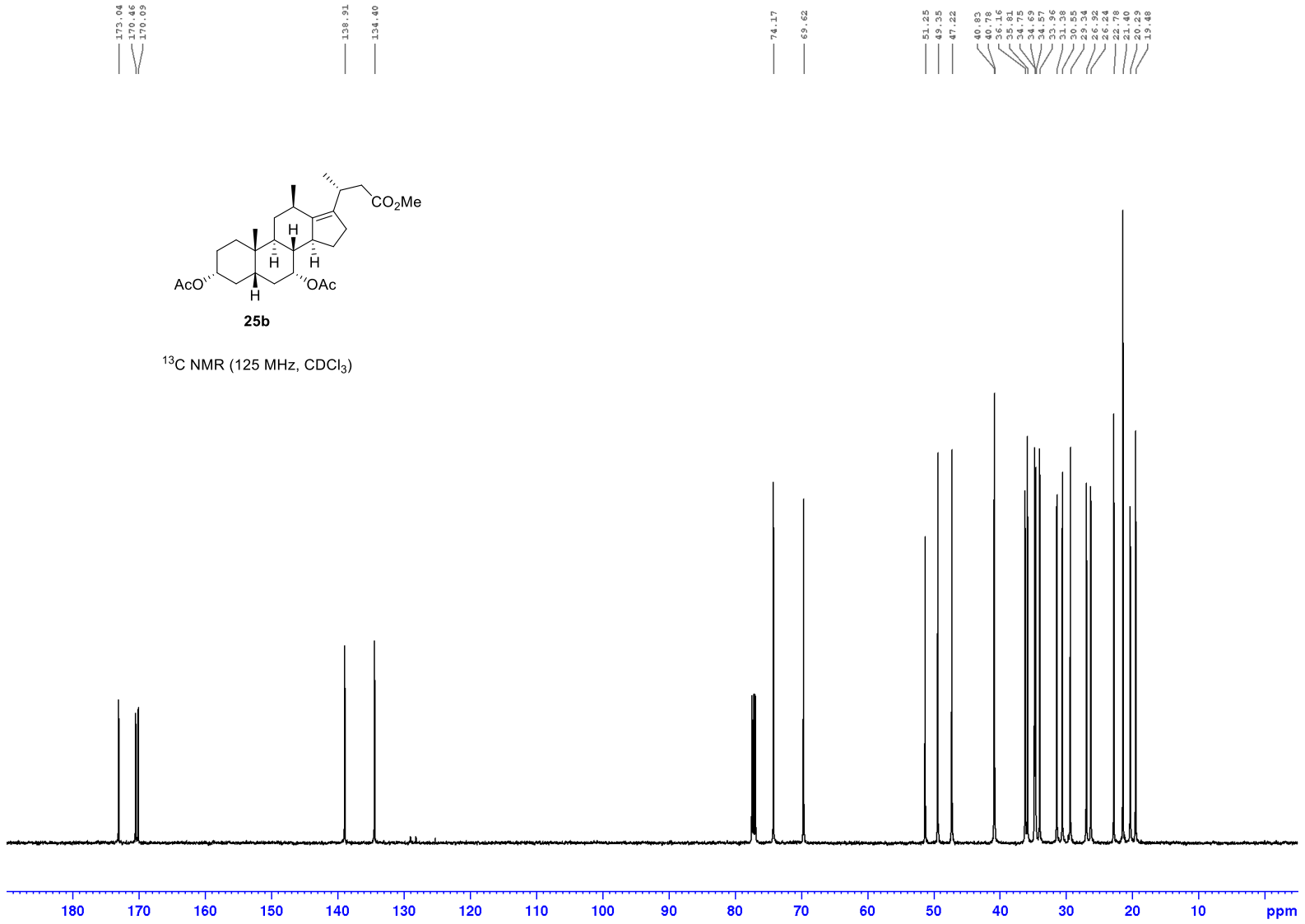

Figure S26. ^{13}C NMR spectrum of **25b**.

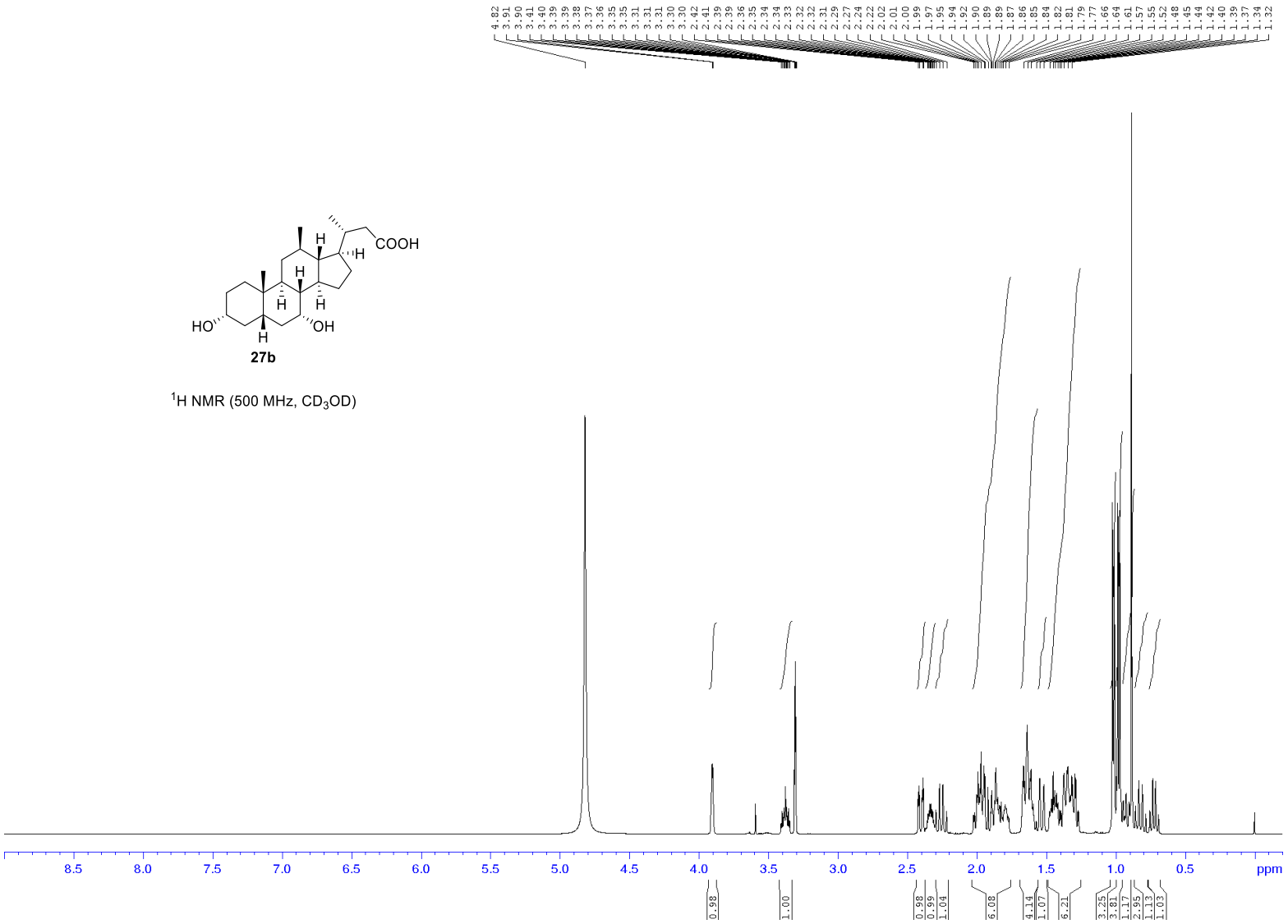

Figure S27a. ^{1}H NMR spectrum of **27b**.

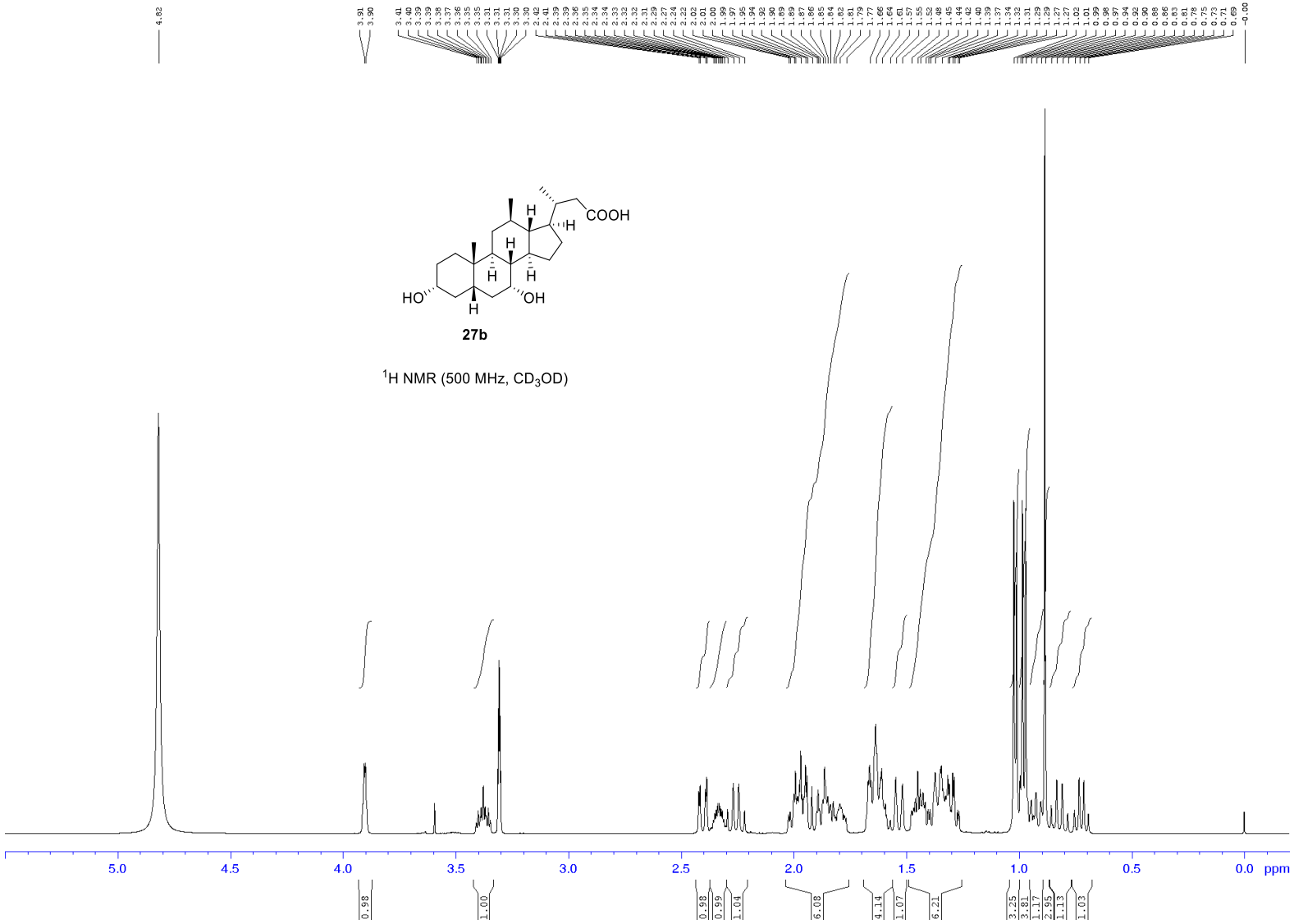

Figure S27b. ^{1}H NMR spectrum of **27b**.

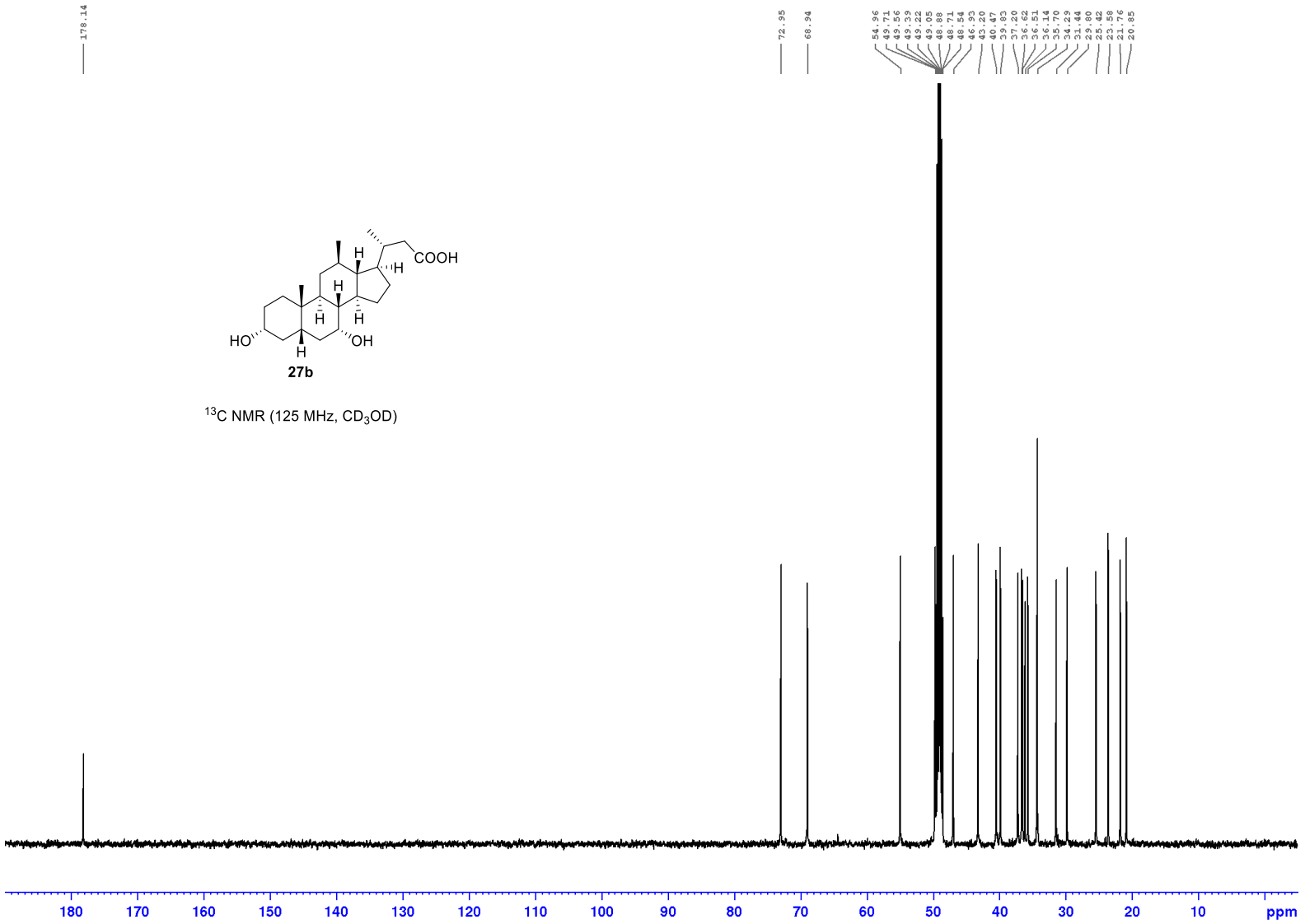

Figure S28. ^{13}C NMR spectrum of **27b**.

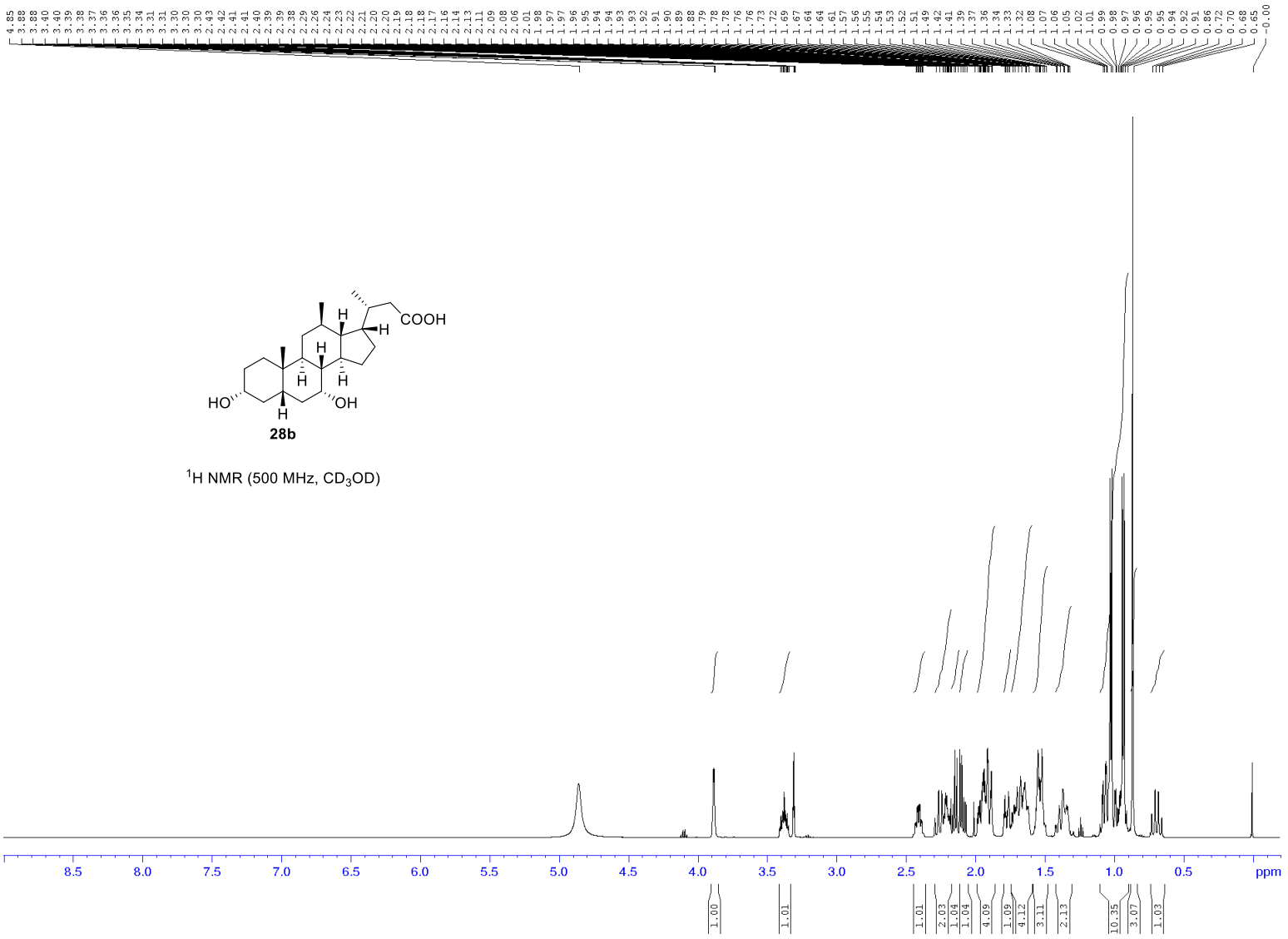

Figure S29a. ^{1}H NMR spectrum of **28b**.

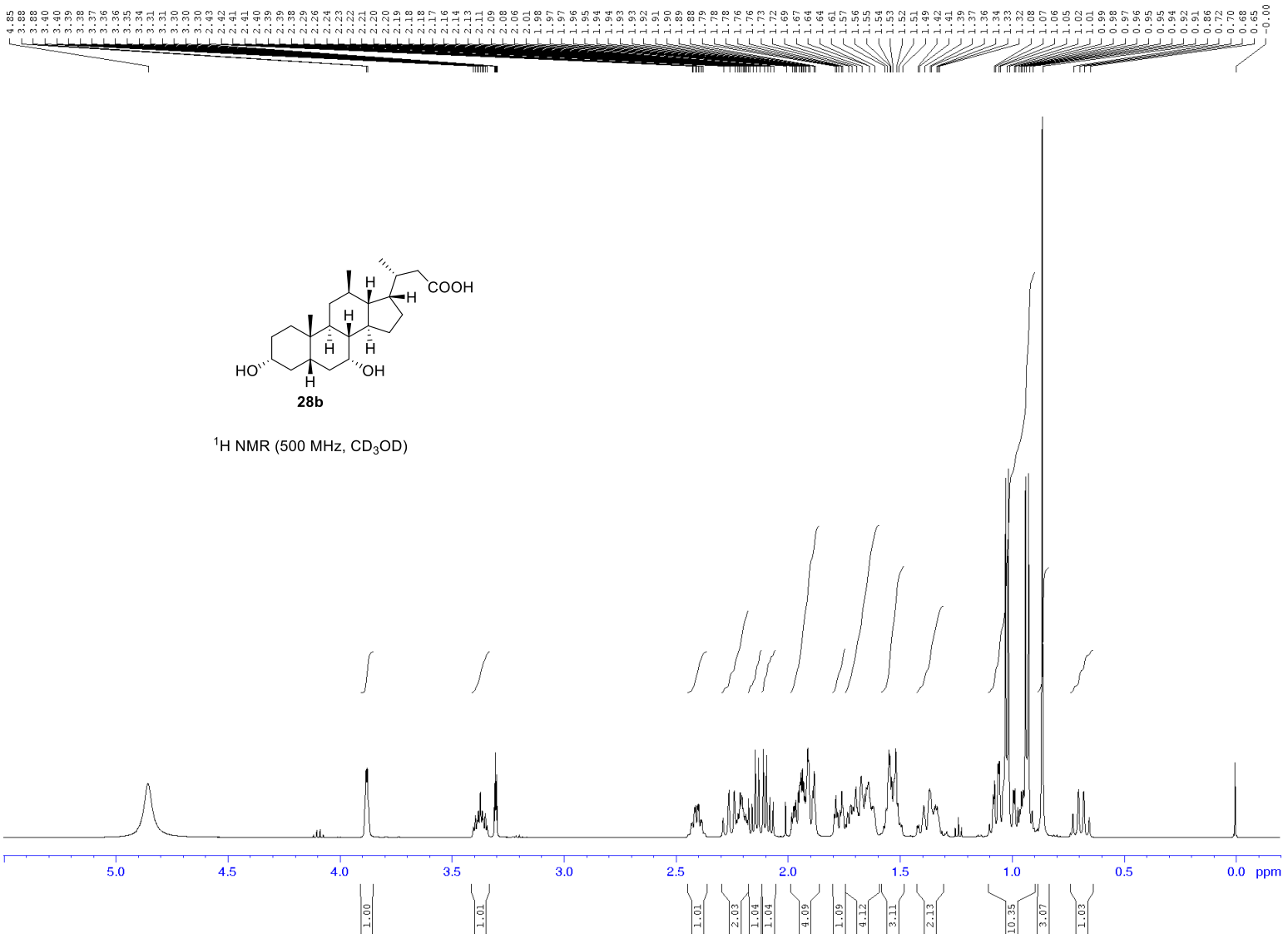

Figure S29b. ^{1}H NMR spectrum of **28b**.

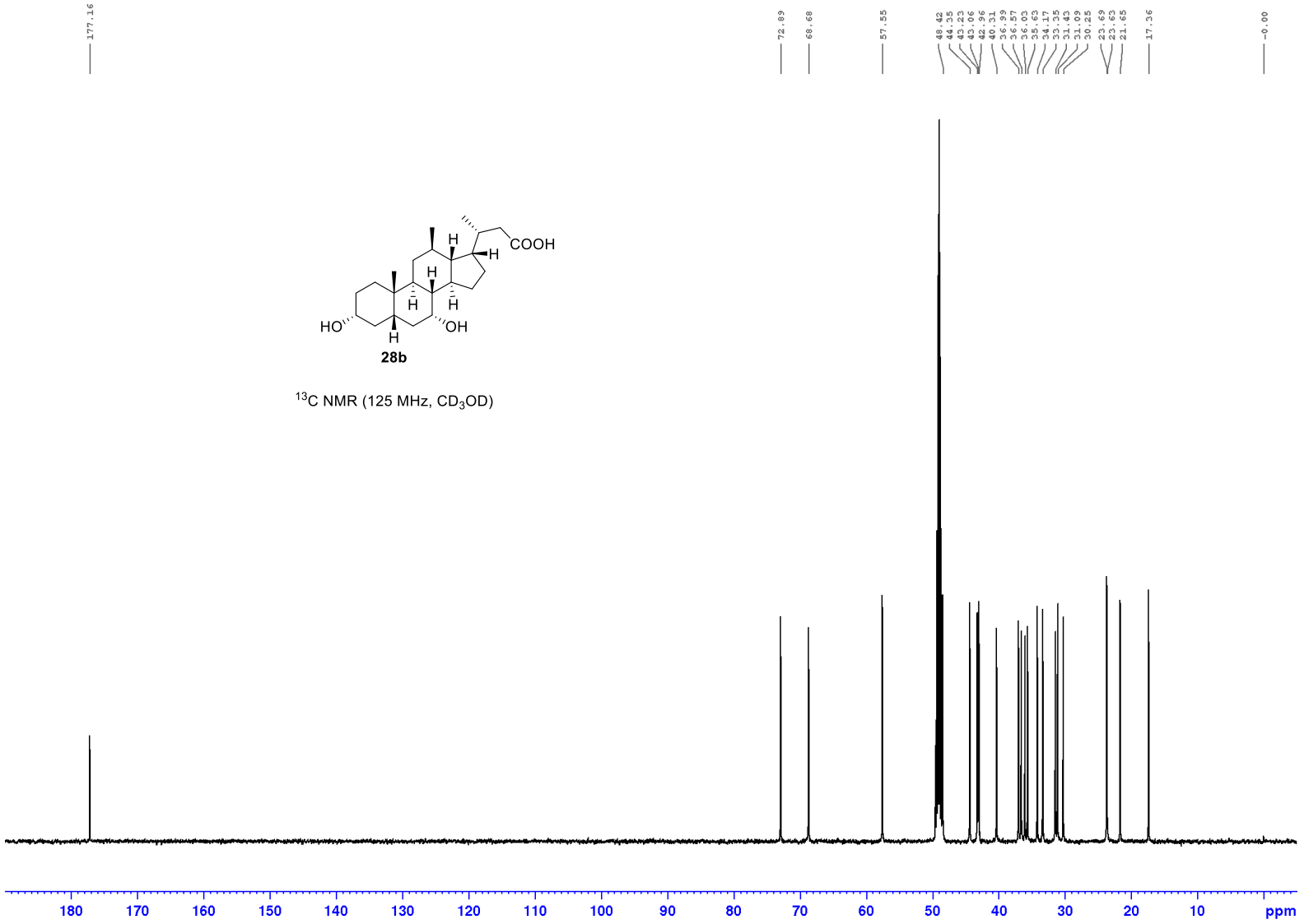

Figure S30. ^{13}C NMR spectrum of **28b**.

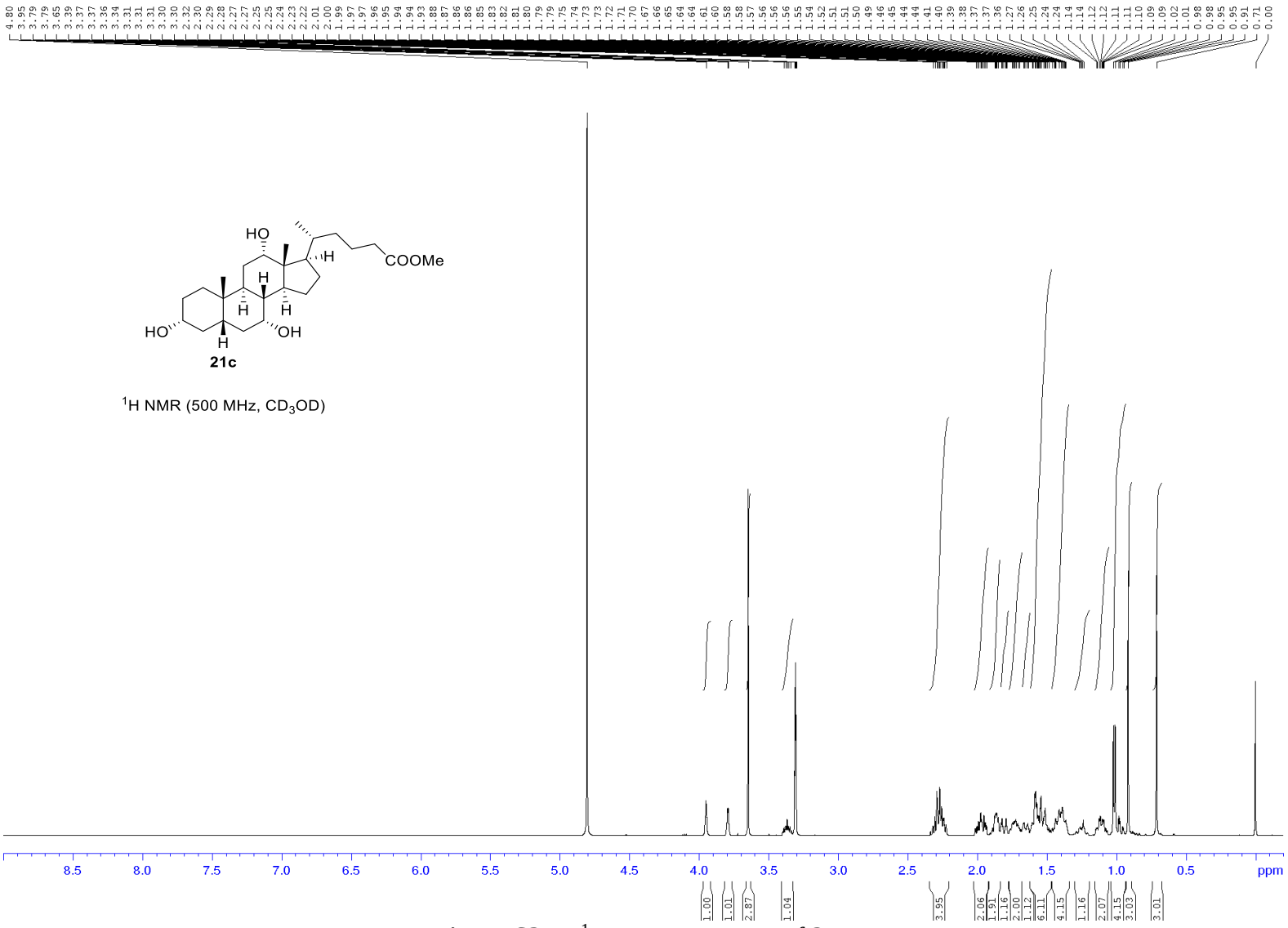

Figure S31a. ^{1}H NMR spectrum of **21c**.

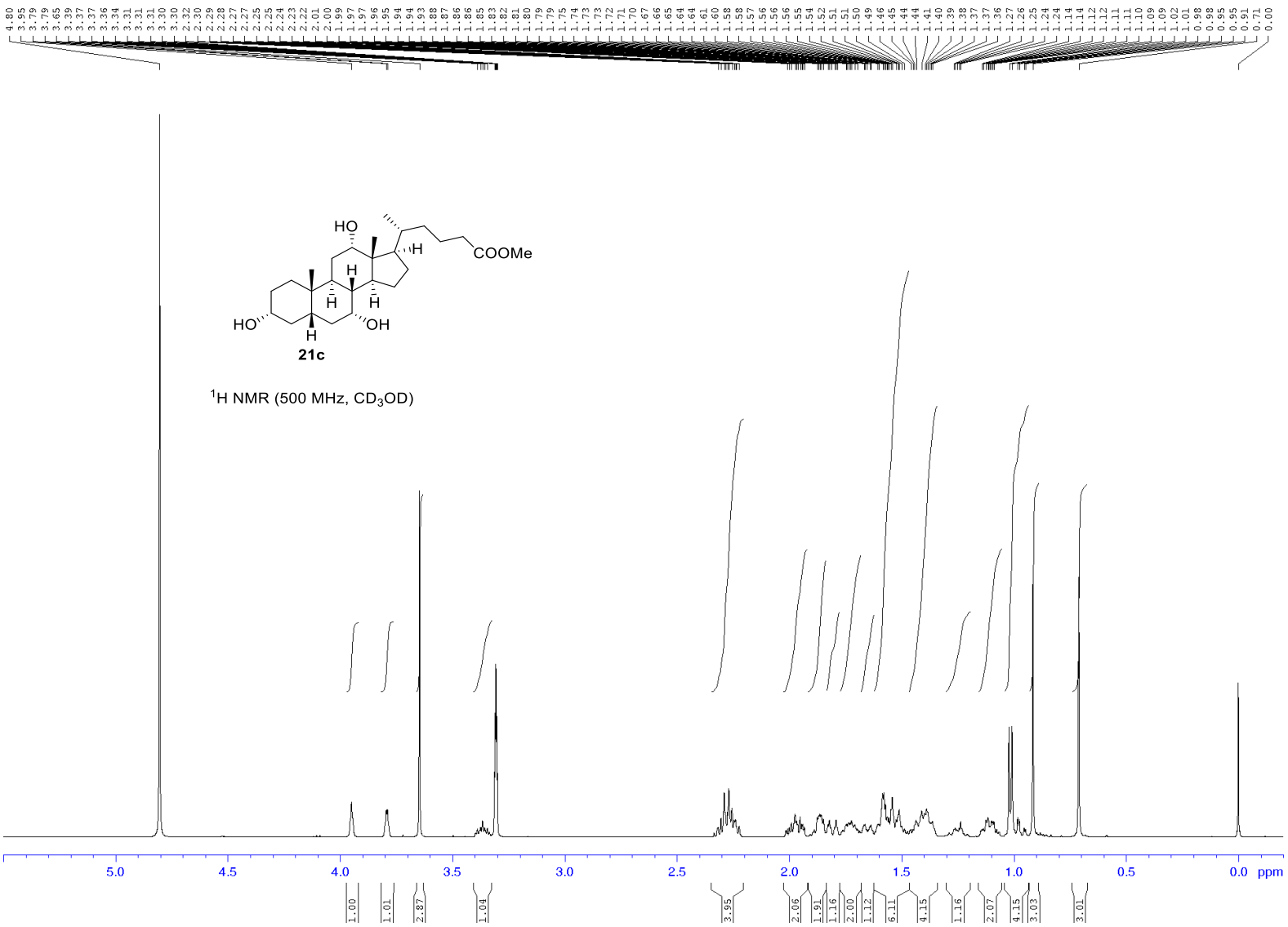

Figure S31b. ^{1}H NMR spectrum of **21c**.

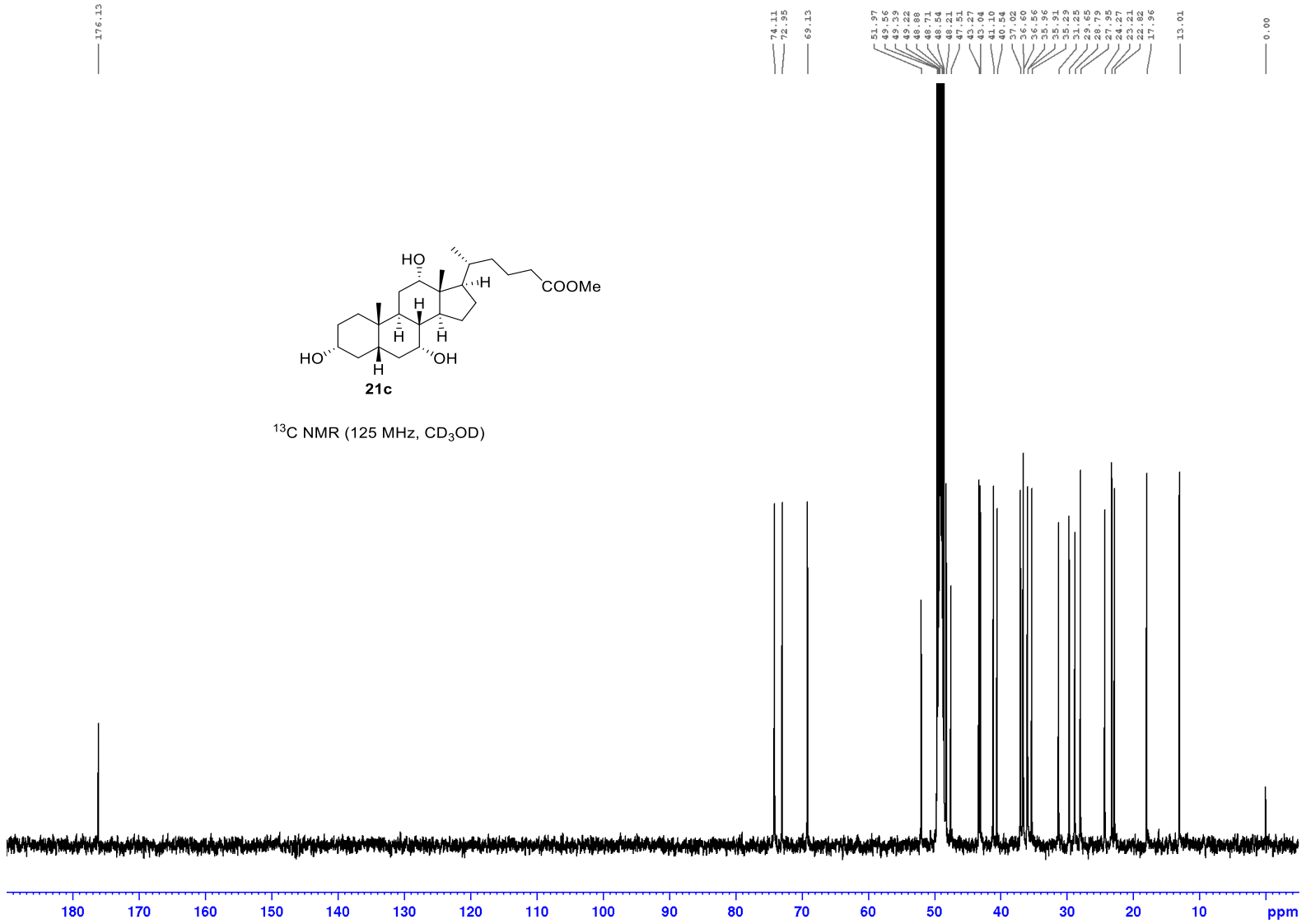

Figure S32. ^{13}C NMR spectrum of **21c**.

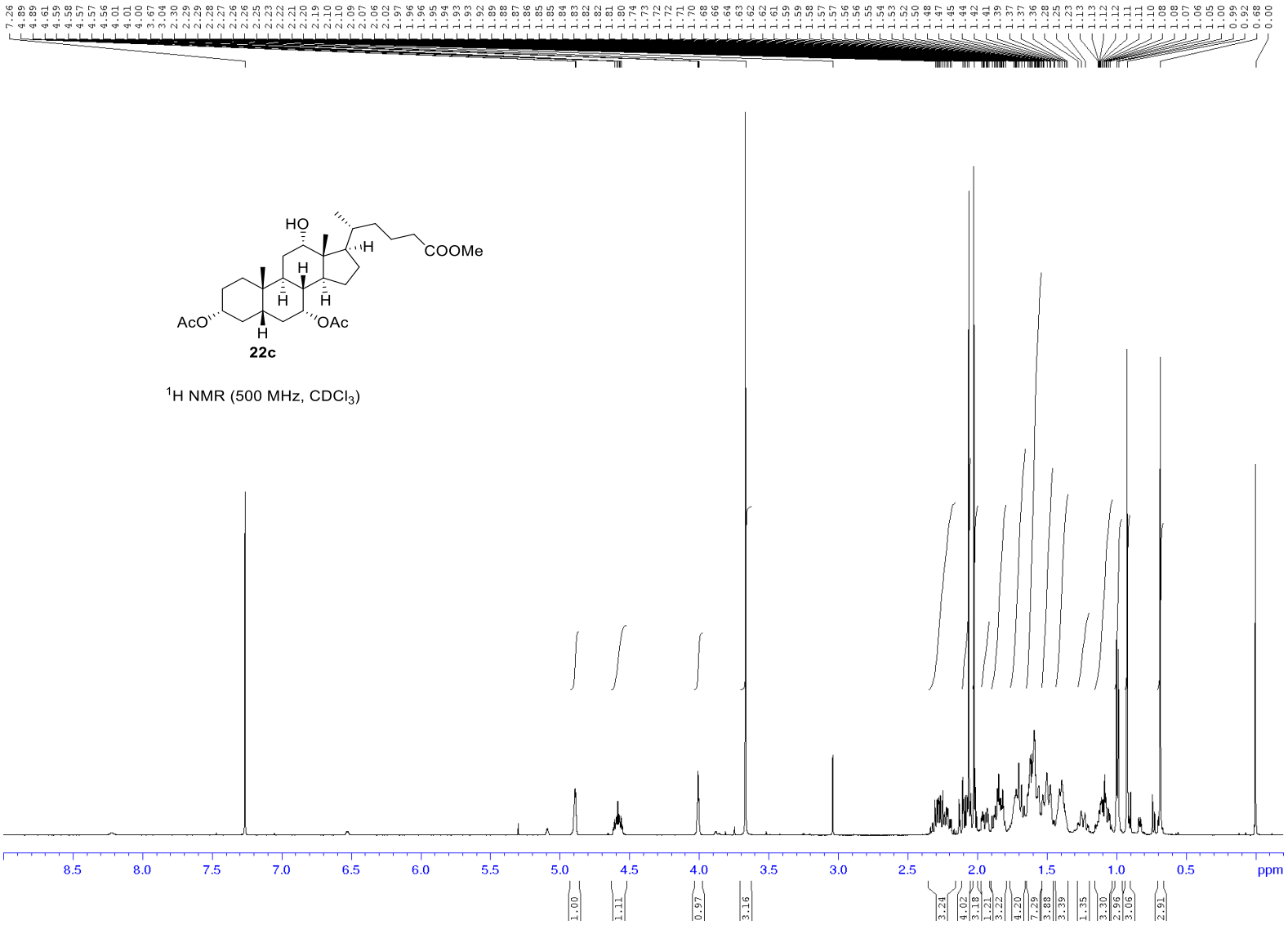

Figure S33a ^{1}H NMR spectrum of **22c**.

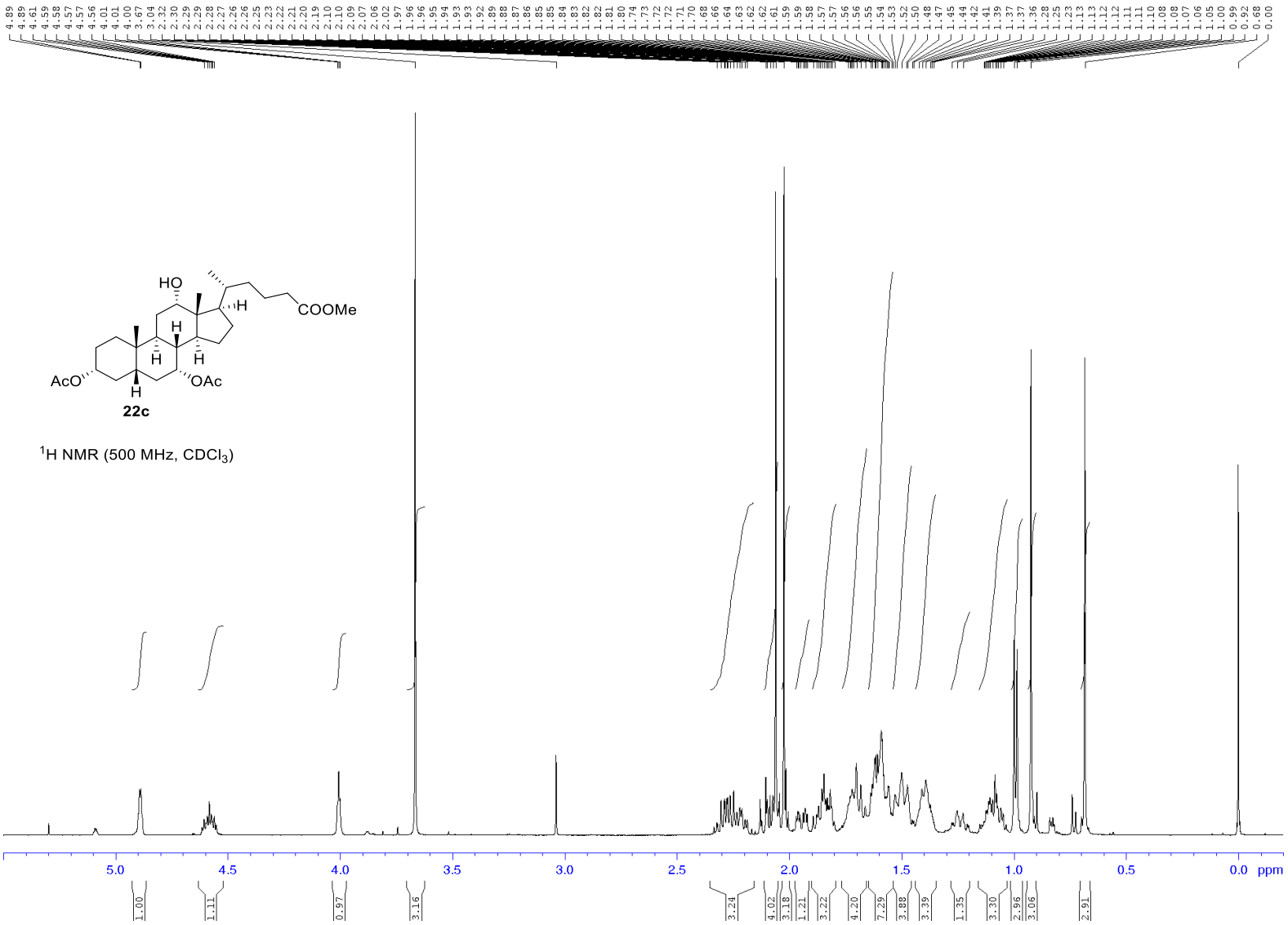

Figure S33b. ^{1}H NMR spectrum of **22c**.

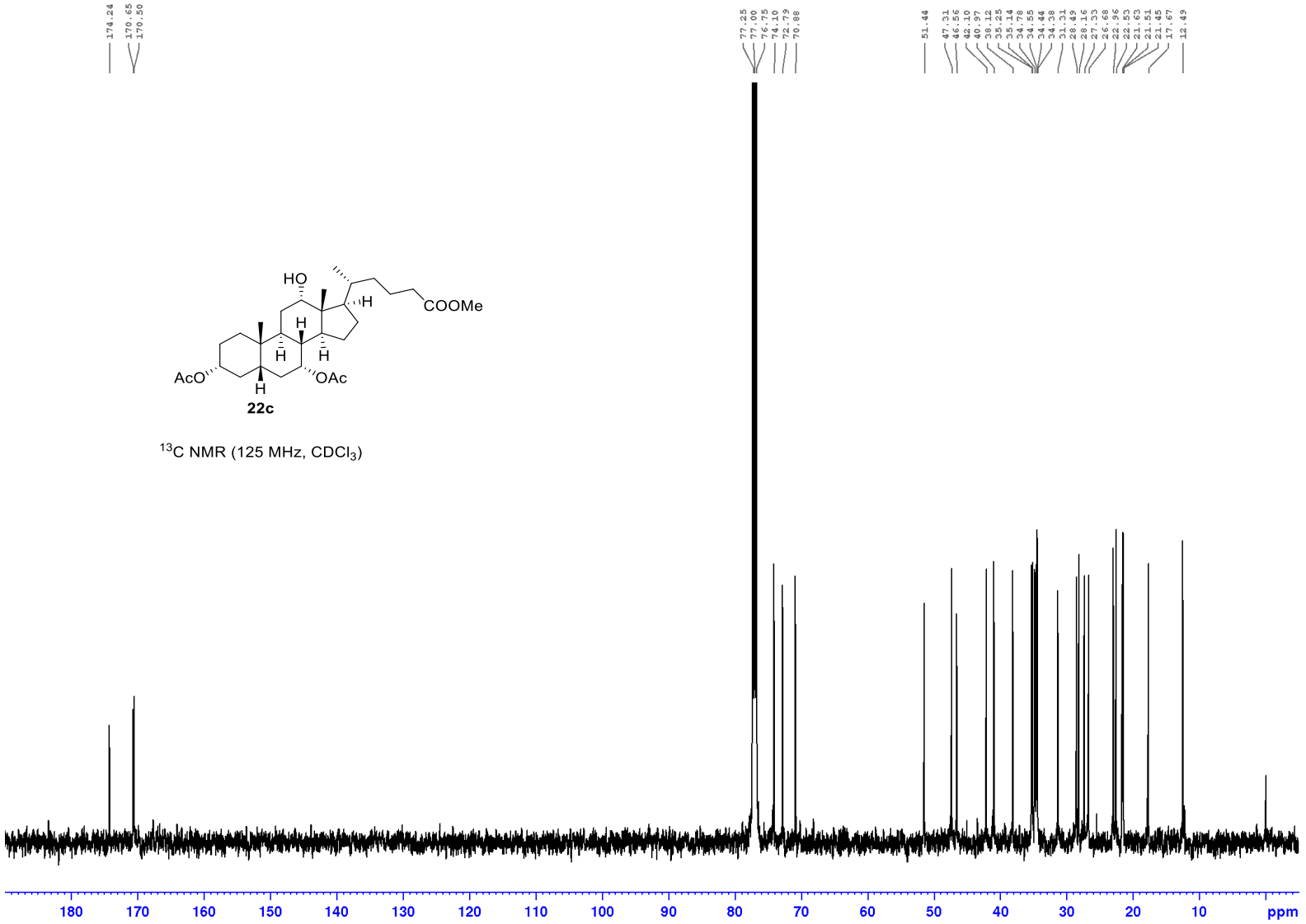

Figure S34. ^{13}C NMR spectrum of **22c**.

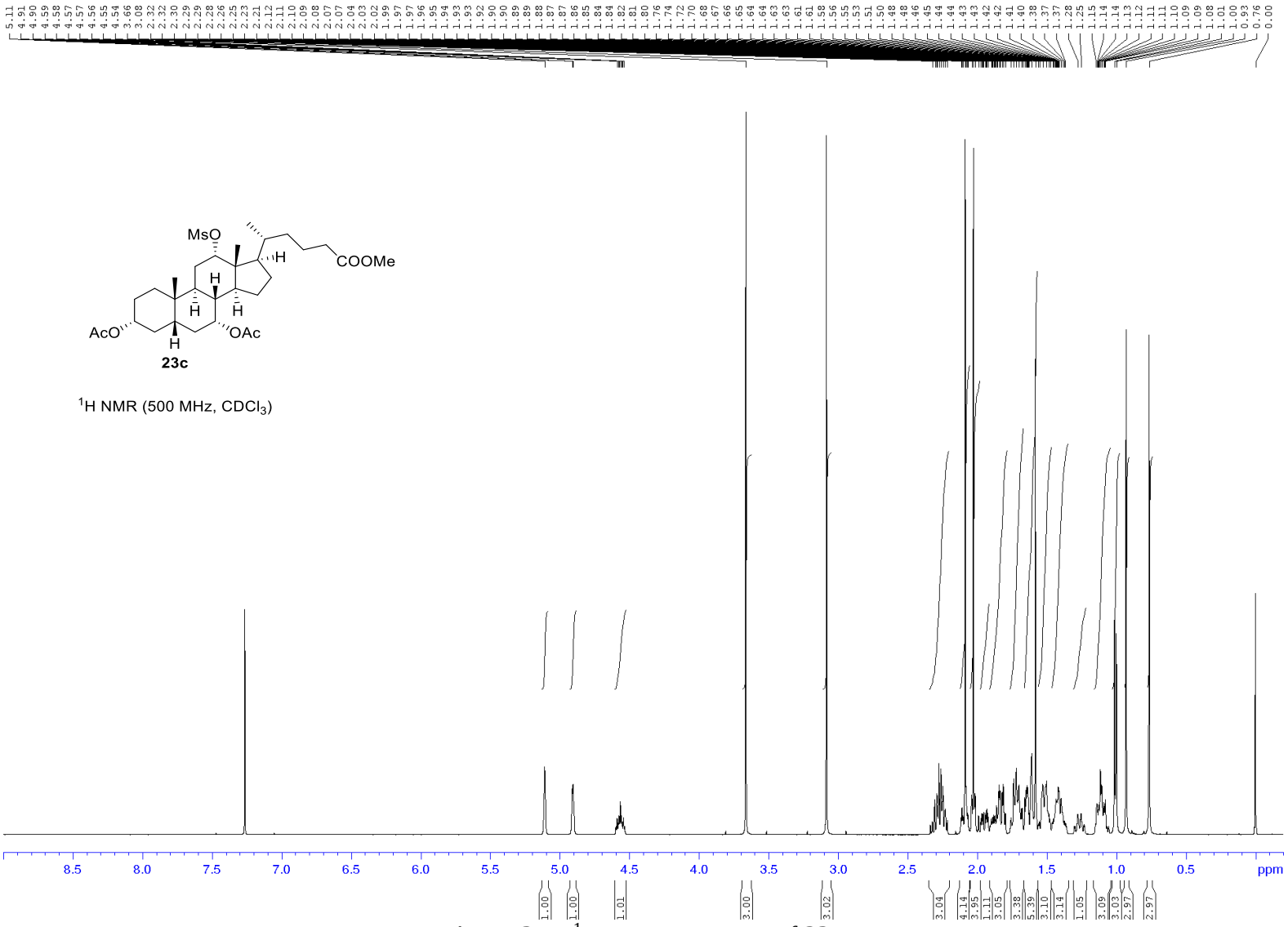

Figure 35a. ^{1}H NMR spectrum of **23c**.

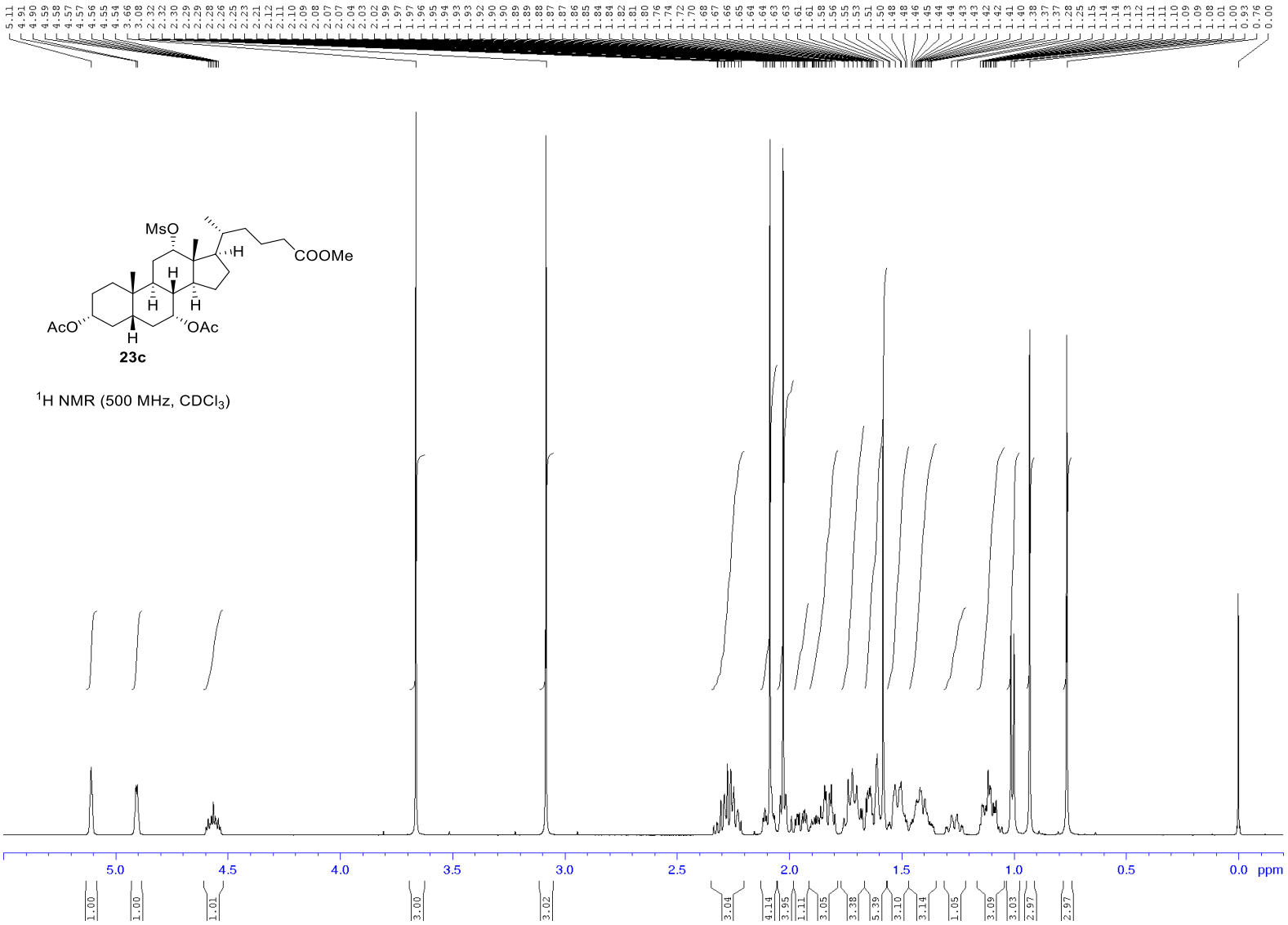

Figure S35b. ^{1}H NMR spectrum of **23c**.

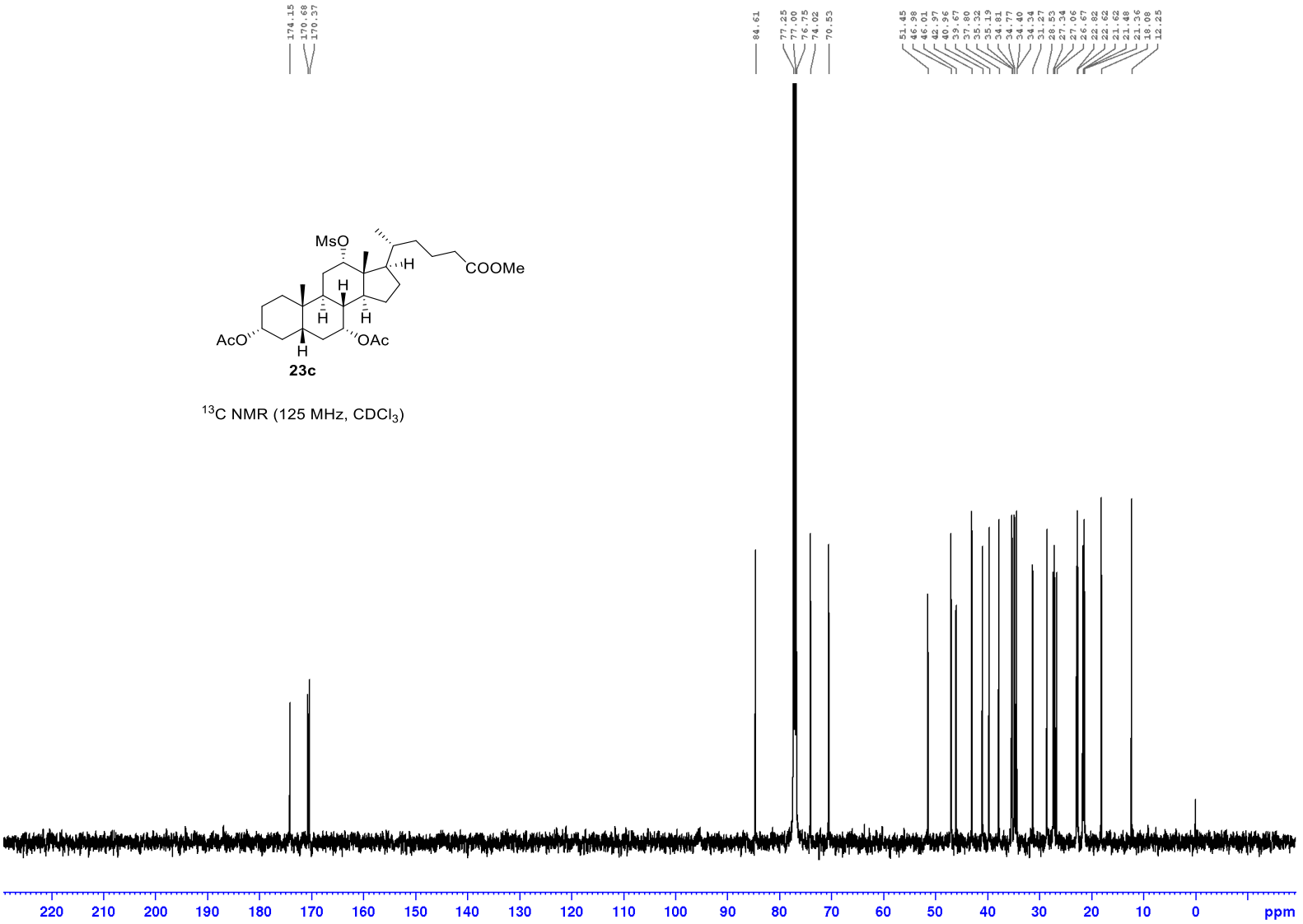

Figure S36. ^{13}C NMR spectrum of **23c**.

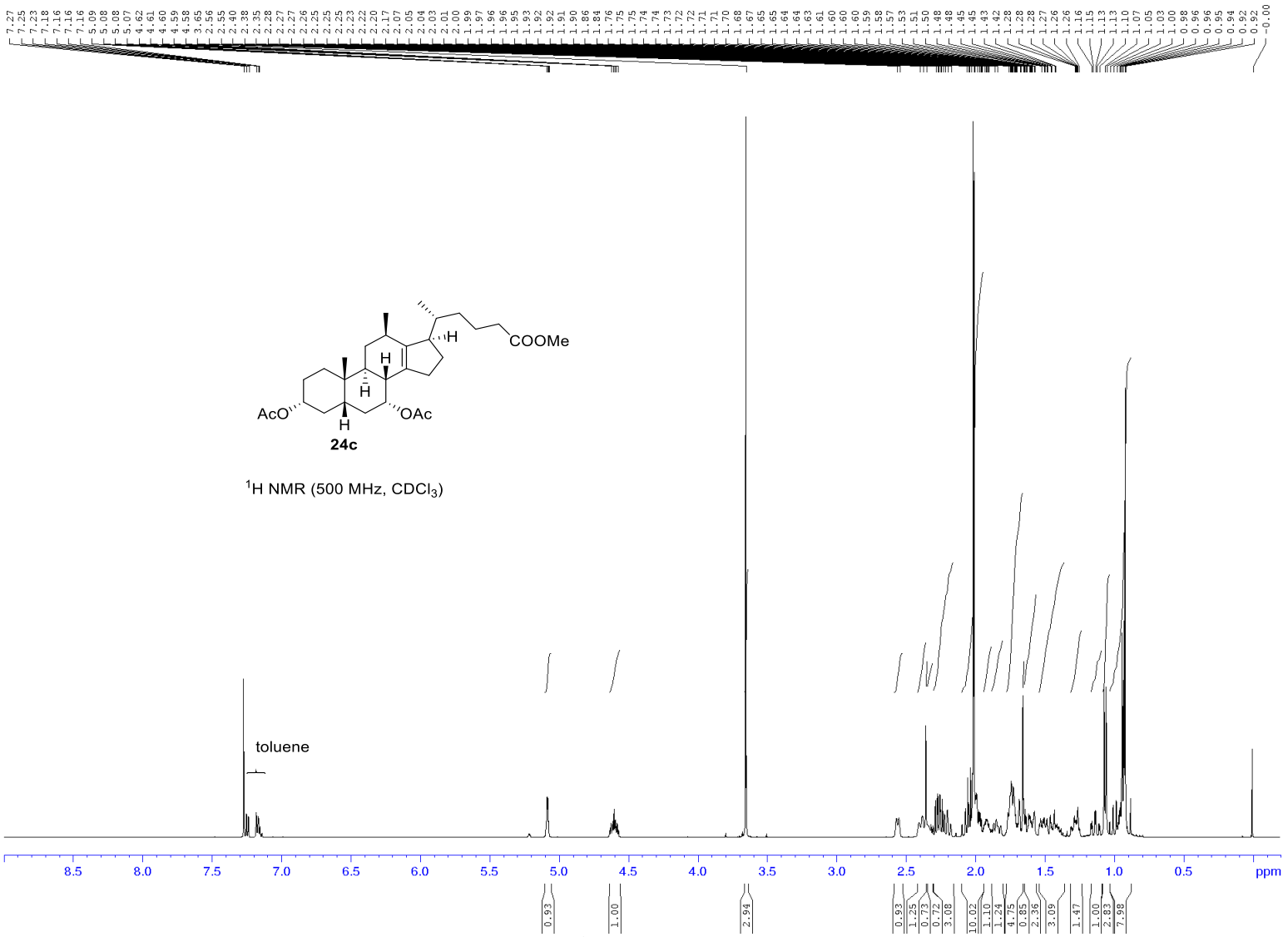

Figure S37a. ^{1}H NMR spectrum of **24c**.

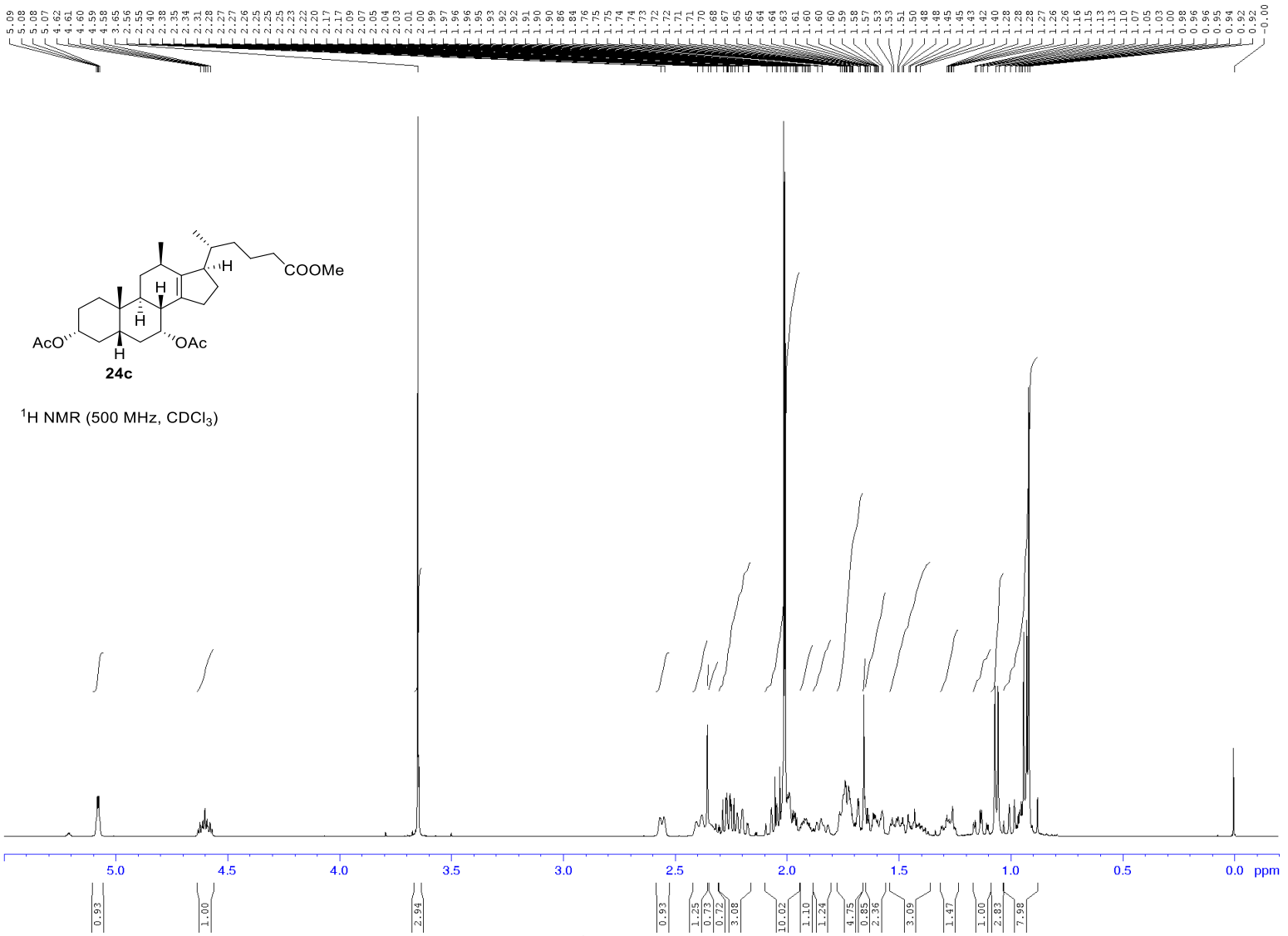

Figure S37b. ^{1}H NMR spectrum of **24c**.

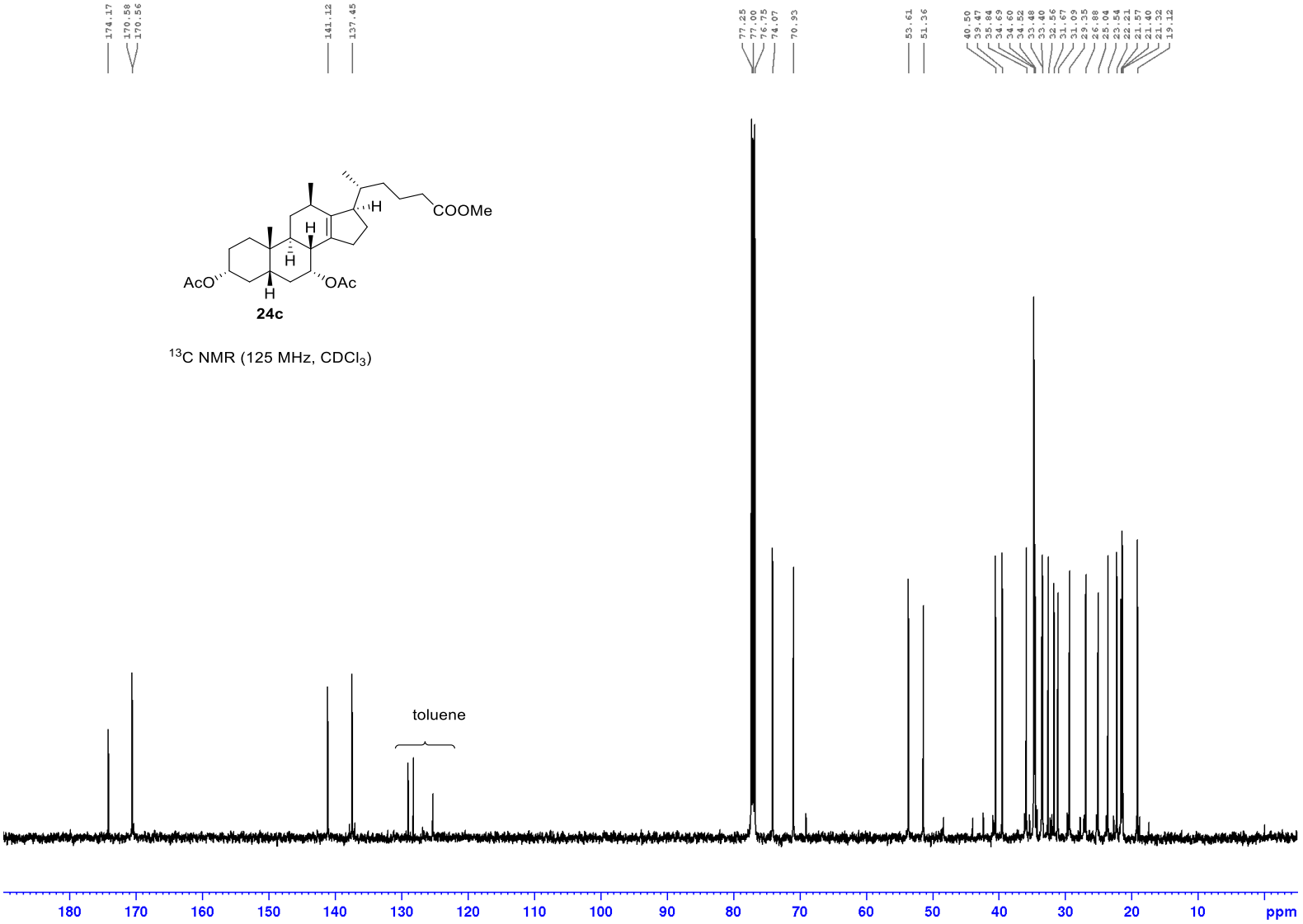

Figure S38. ^{13}C NMR spectrum of **24c**.

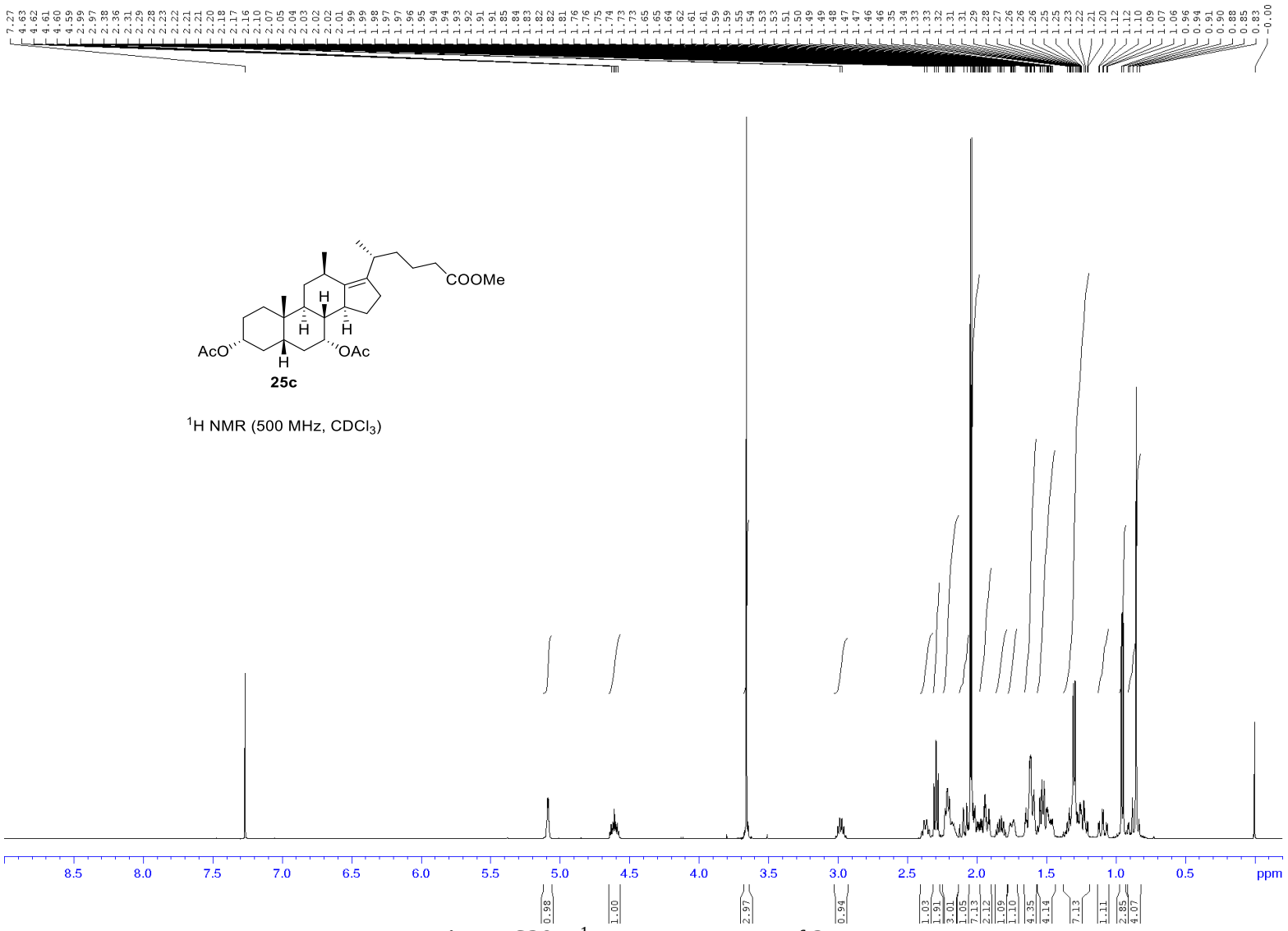

Figure S39a. ^{1}H NMR spectrum of **25c**.

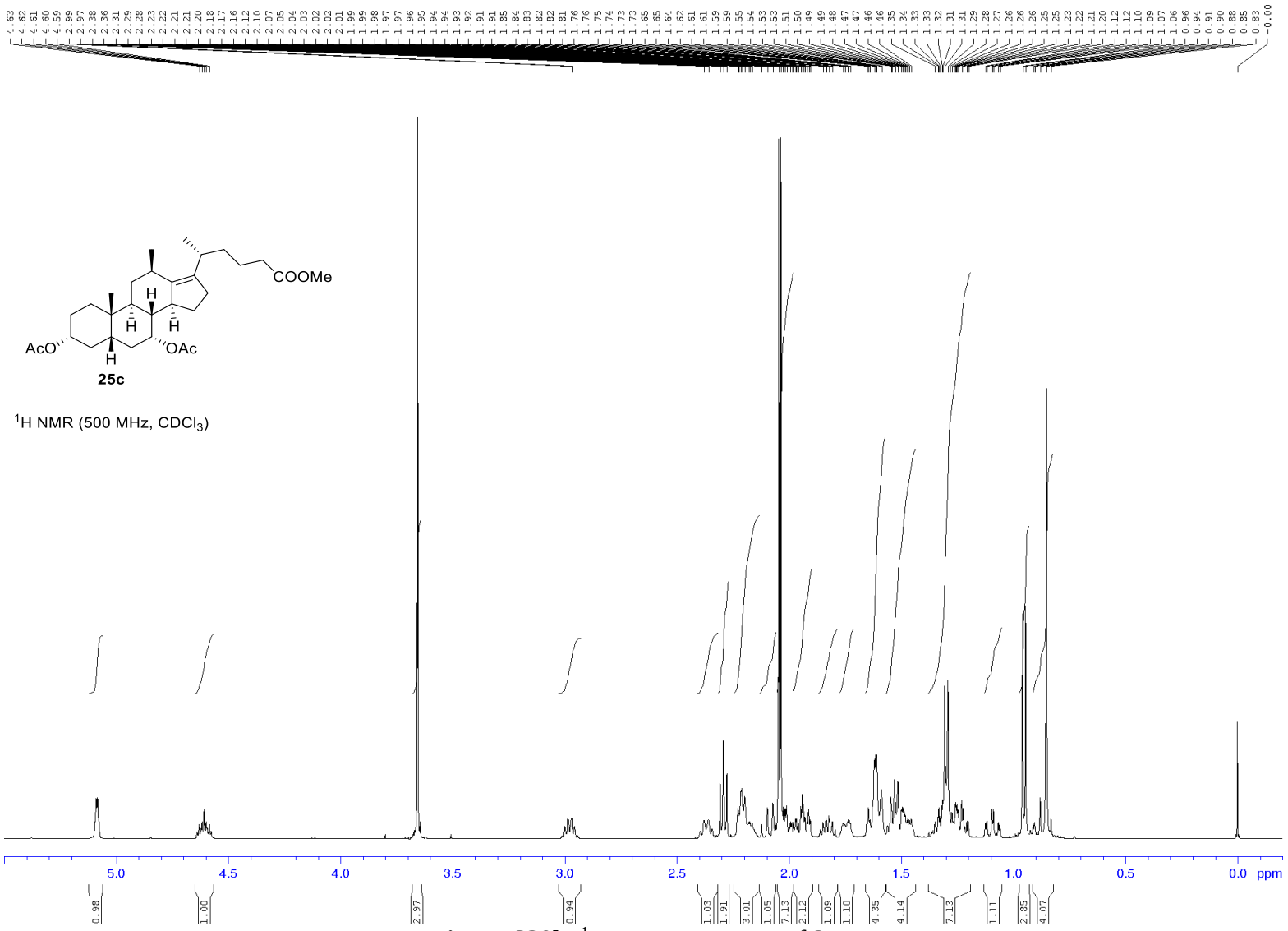

Figure S39b. ^{1}H NMR spectrum of **25c**.

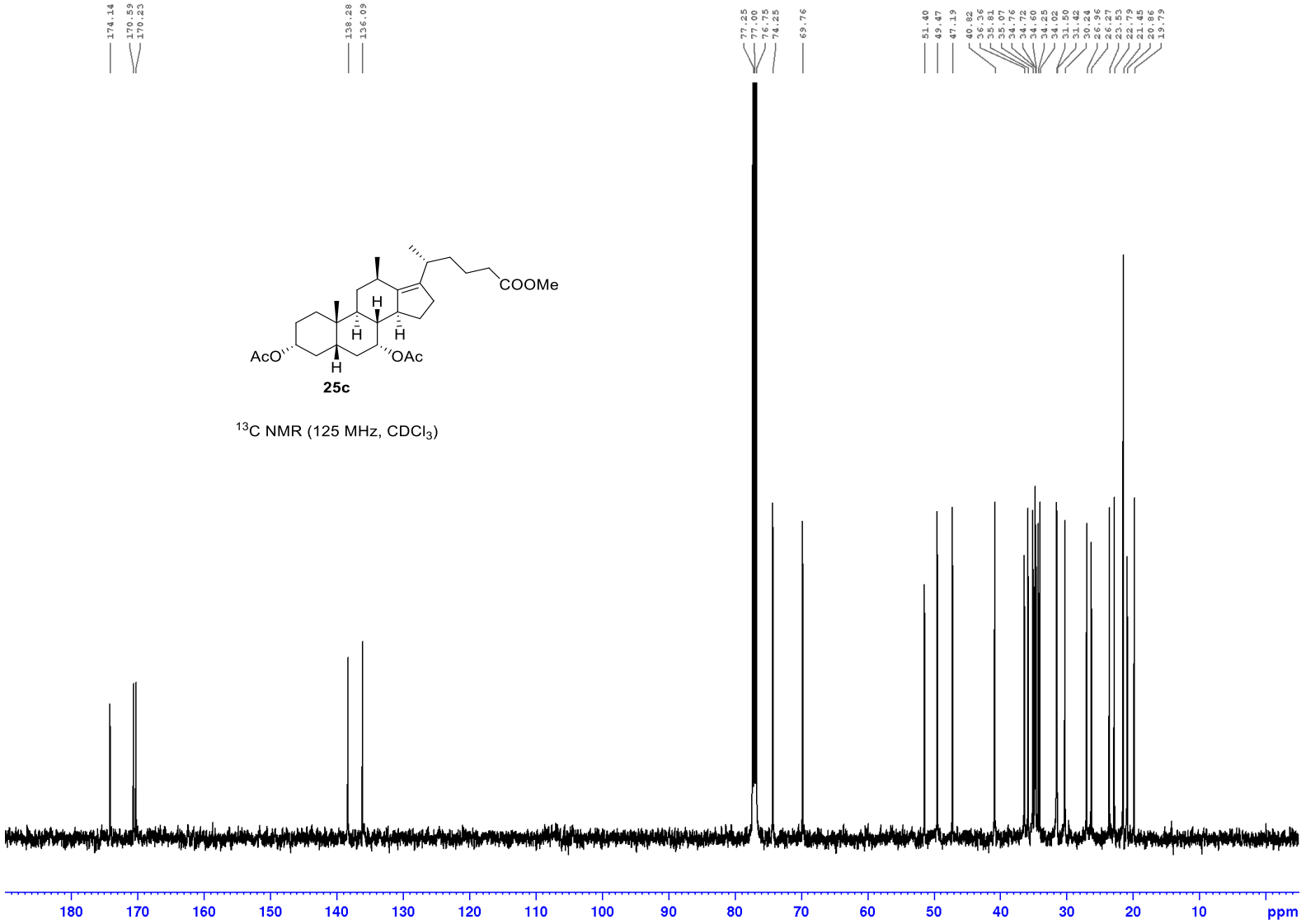

Figure S40. ^{13}C NMR spectrum of **25c**.

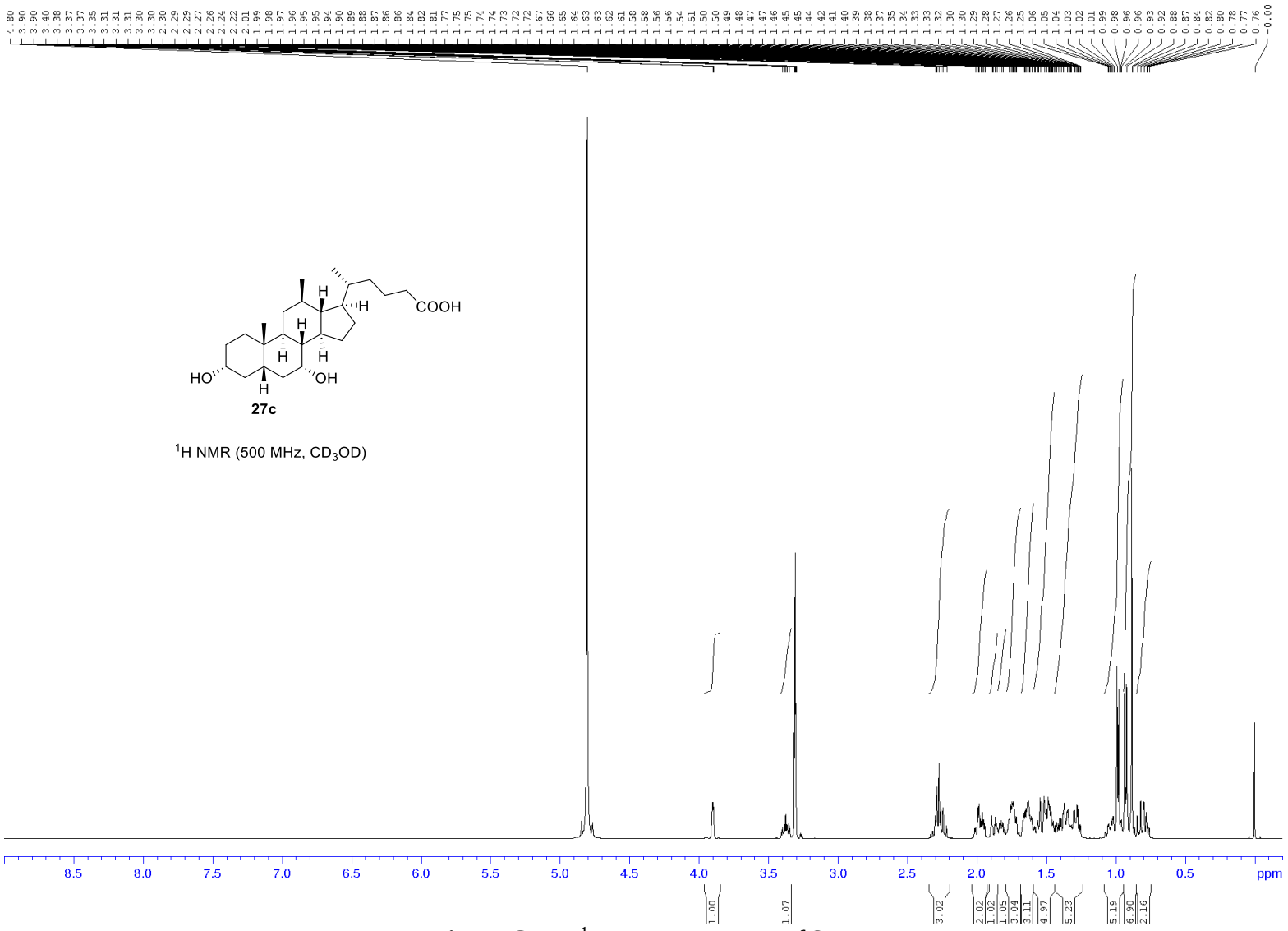

Figure S41a. ^{1}H NMR spectrum of **27c**.

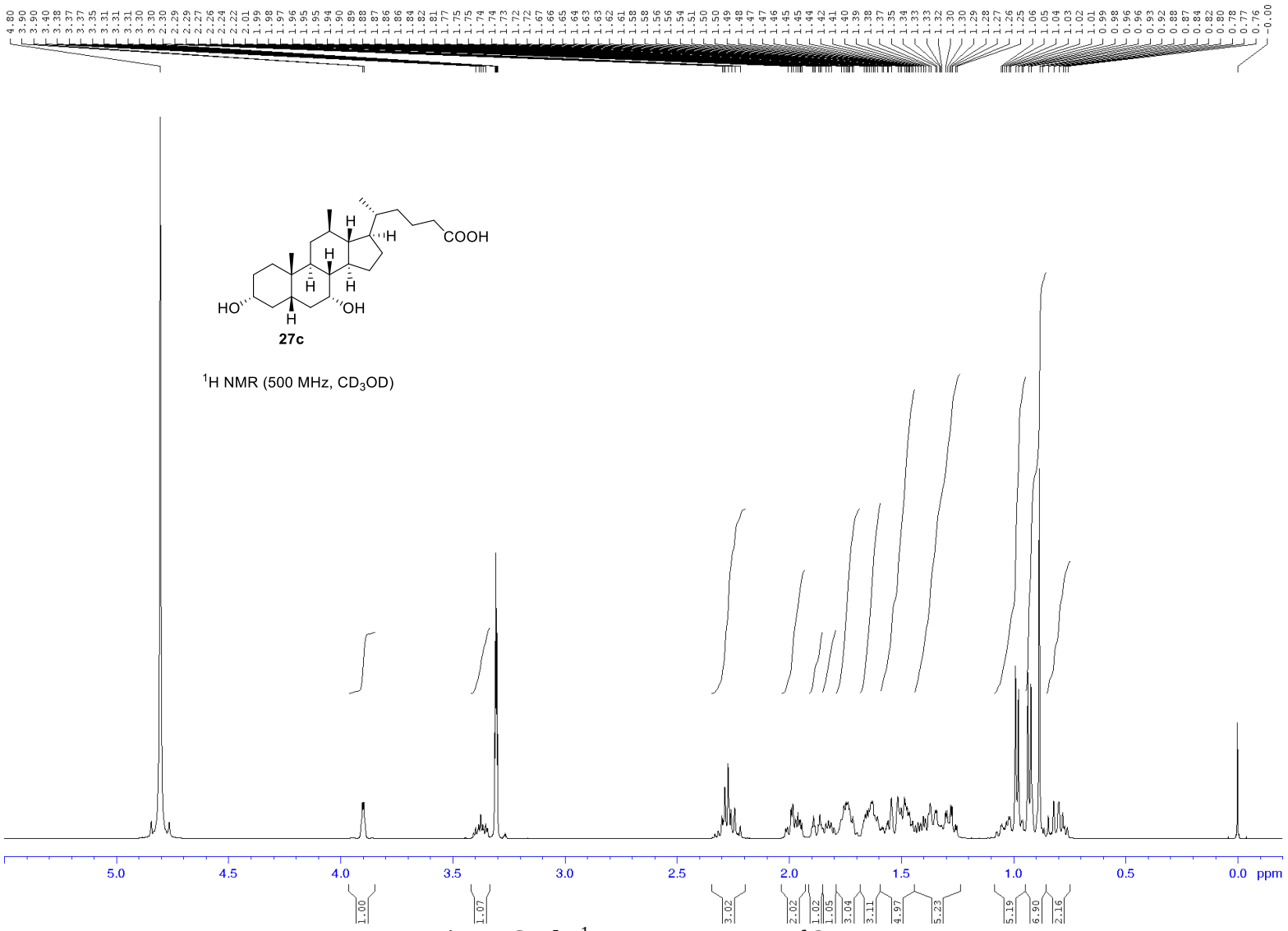

Figure S41b. ^{1}H NMR spectrum of **27c**.

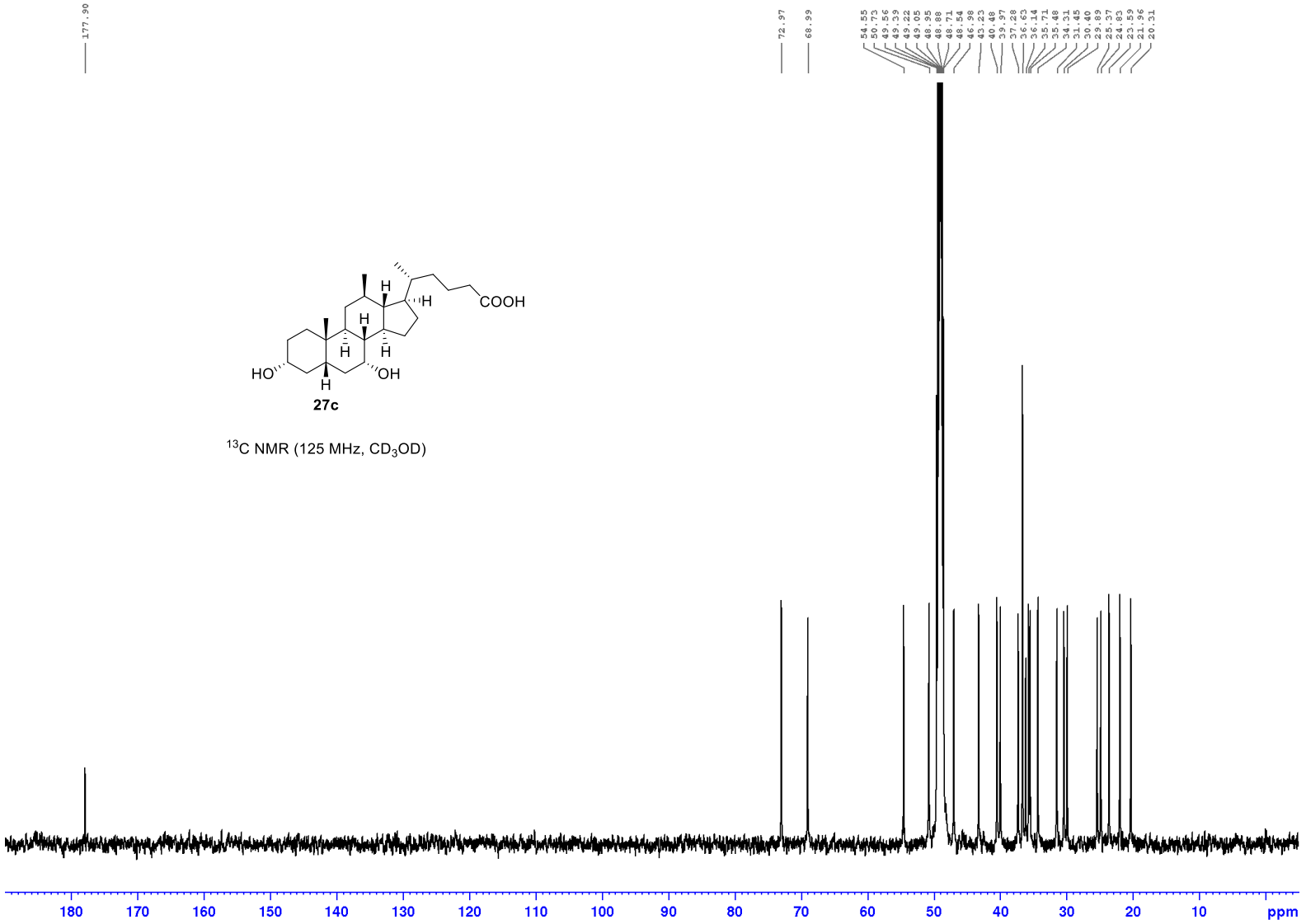

Figure S42. ^{13}C NMR spectrum of **27c**.

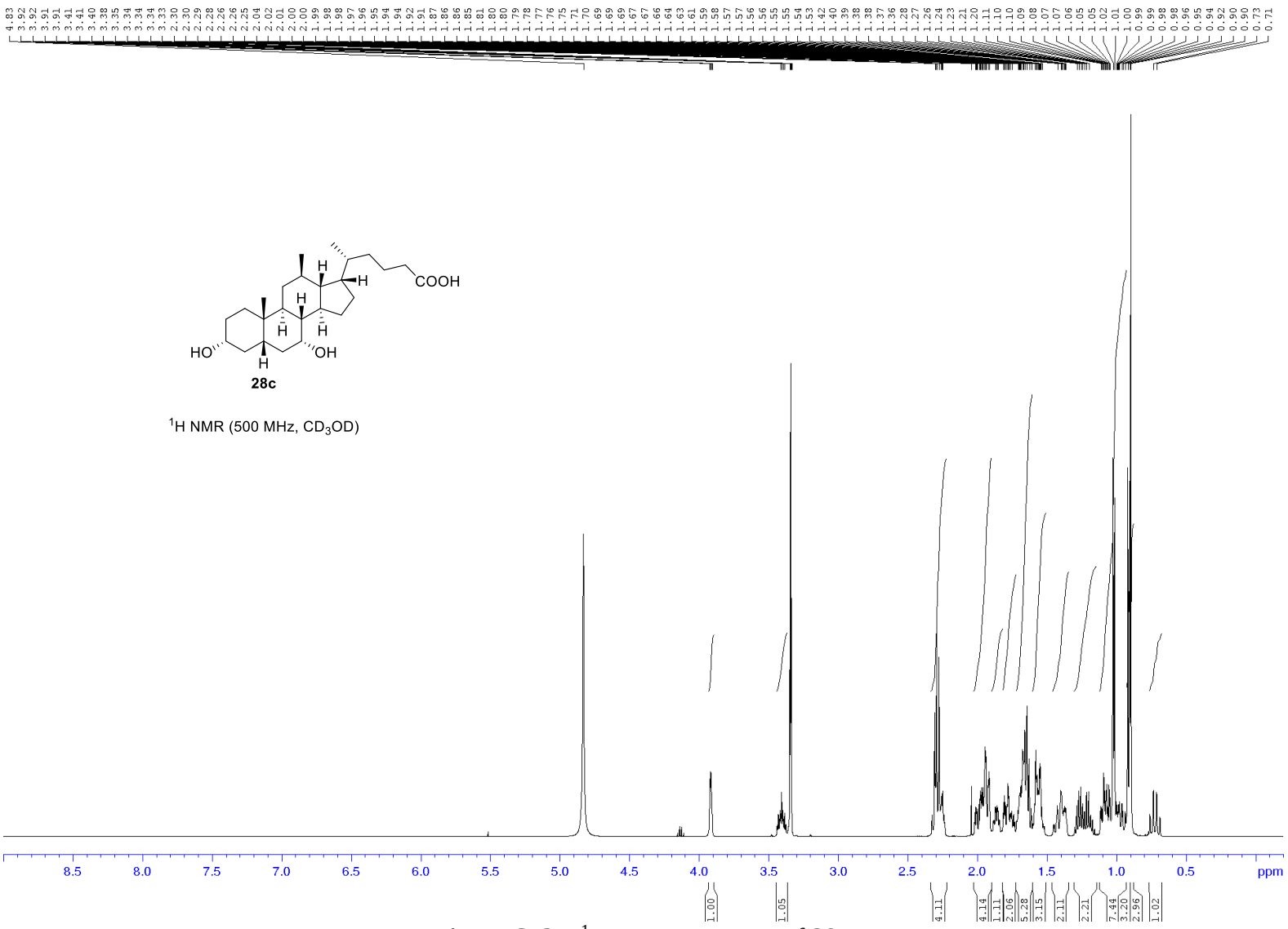

Figure S43a. ^{1}H NMR spectrum of **28c**.

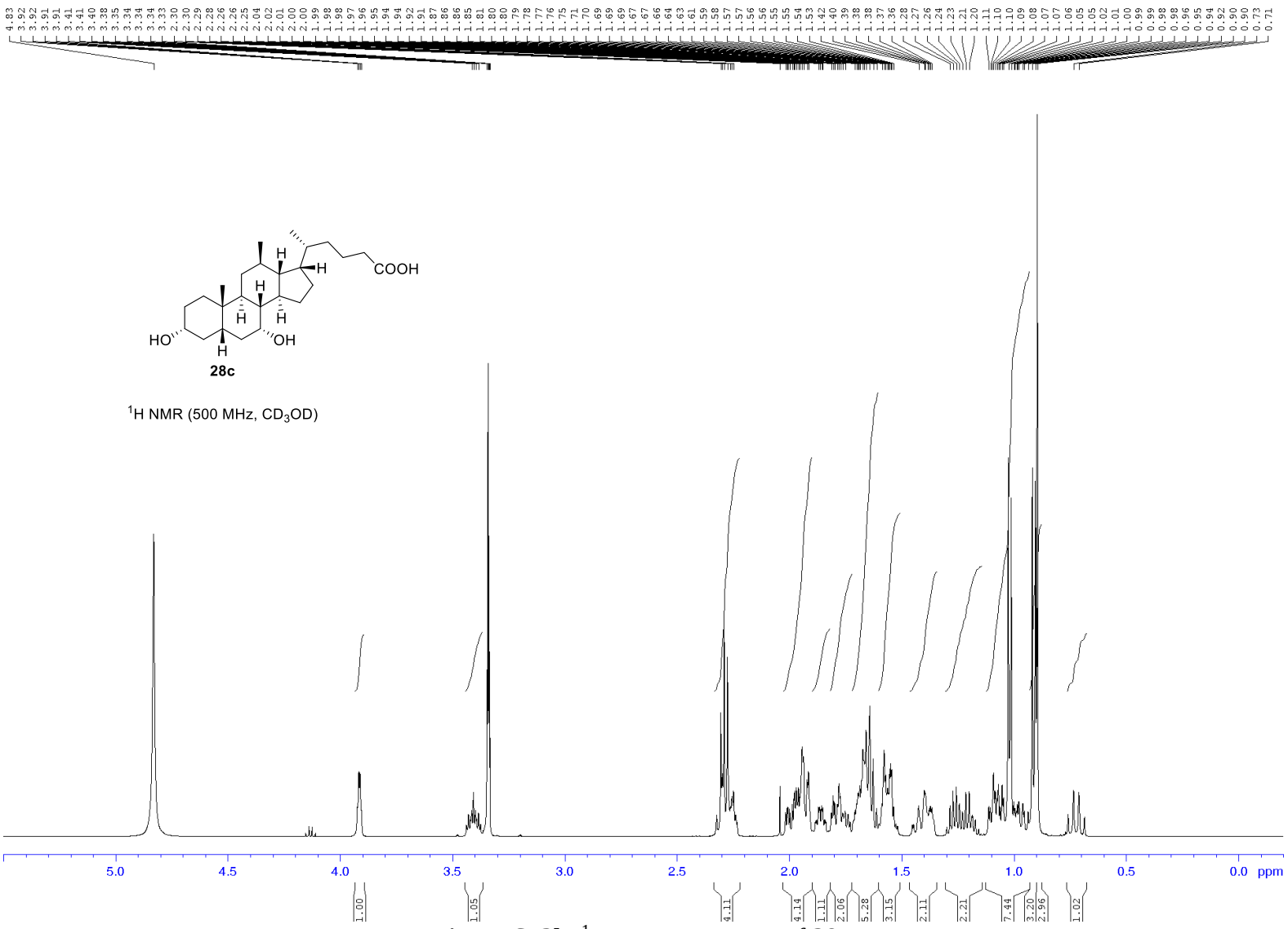

Figure S43b. ^{1}H NMR spectrum of **28c**.

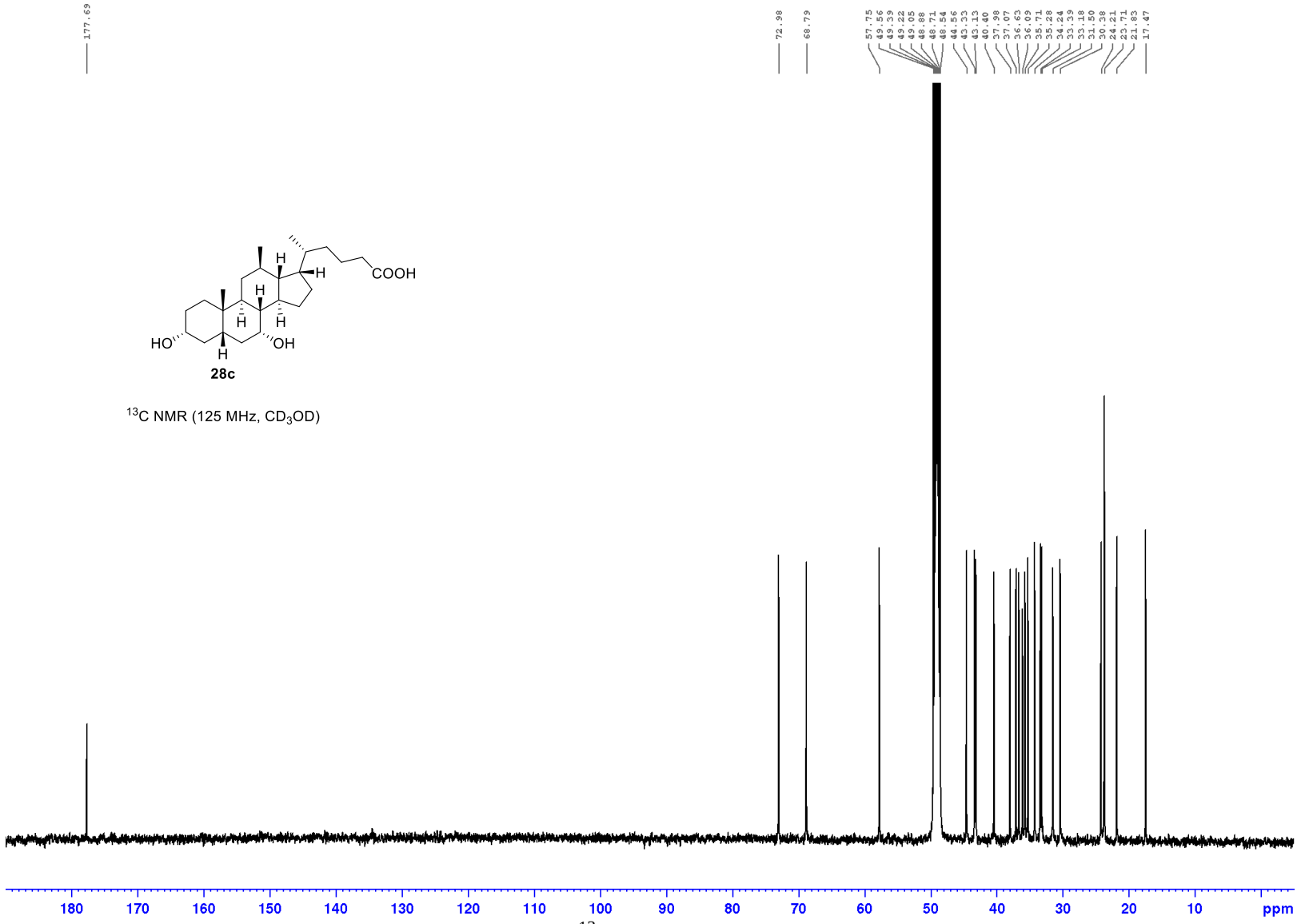

Figure S44. ^{13}C NMR spectrum of **28c**.

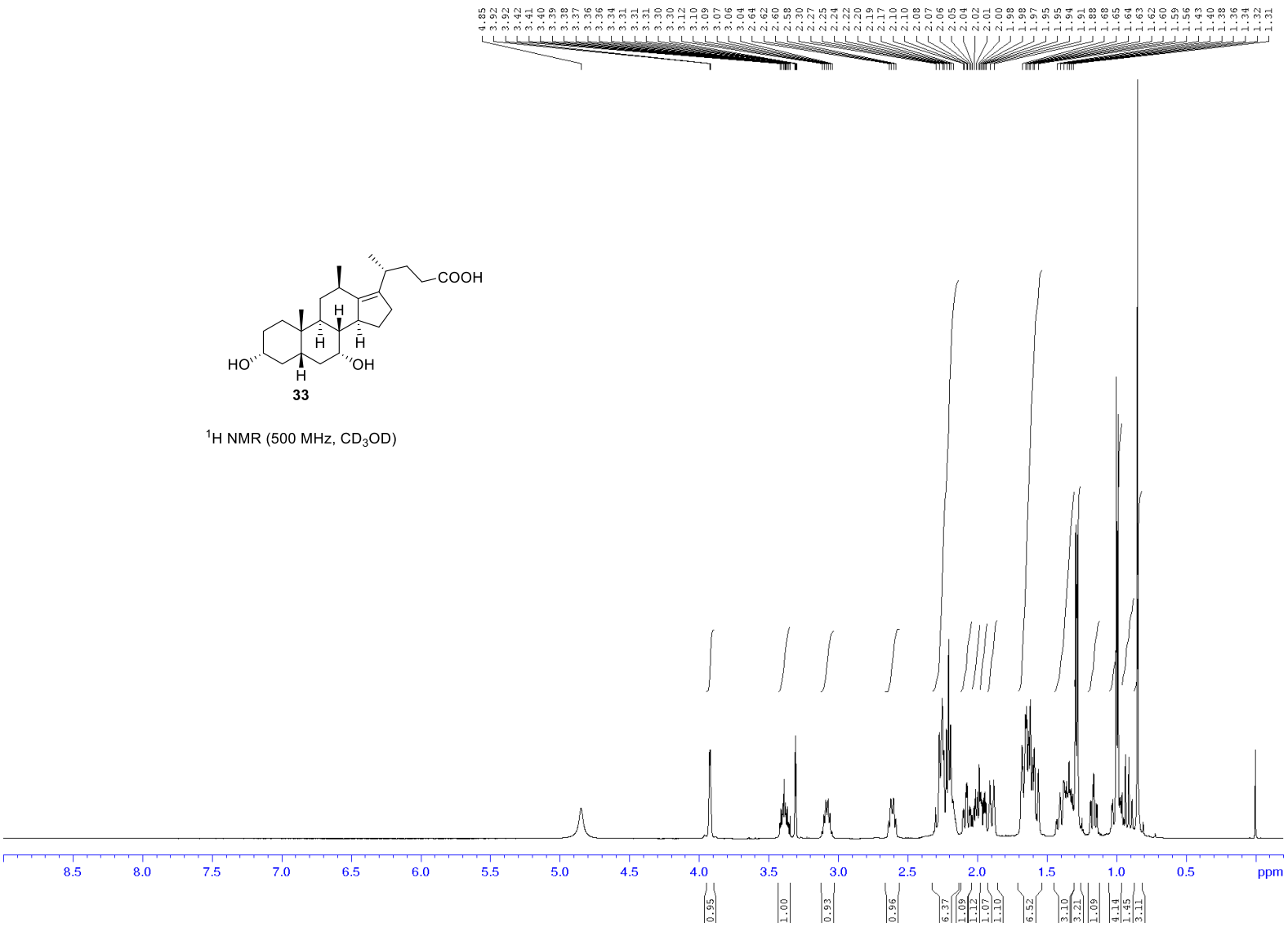

Figure S45a. ^{1}H NMR spectrum of **33**.

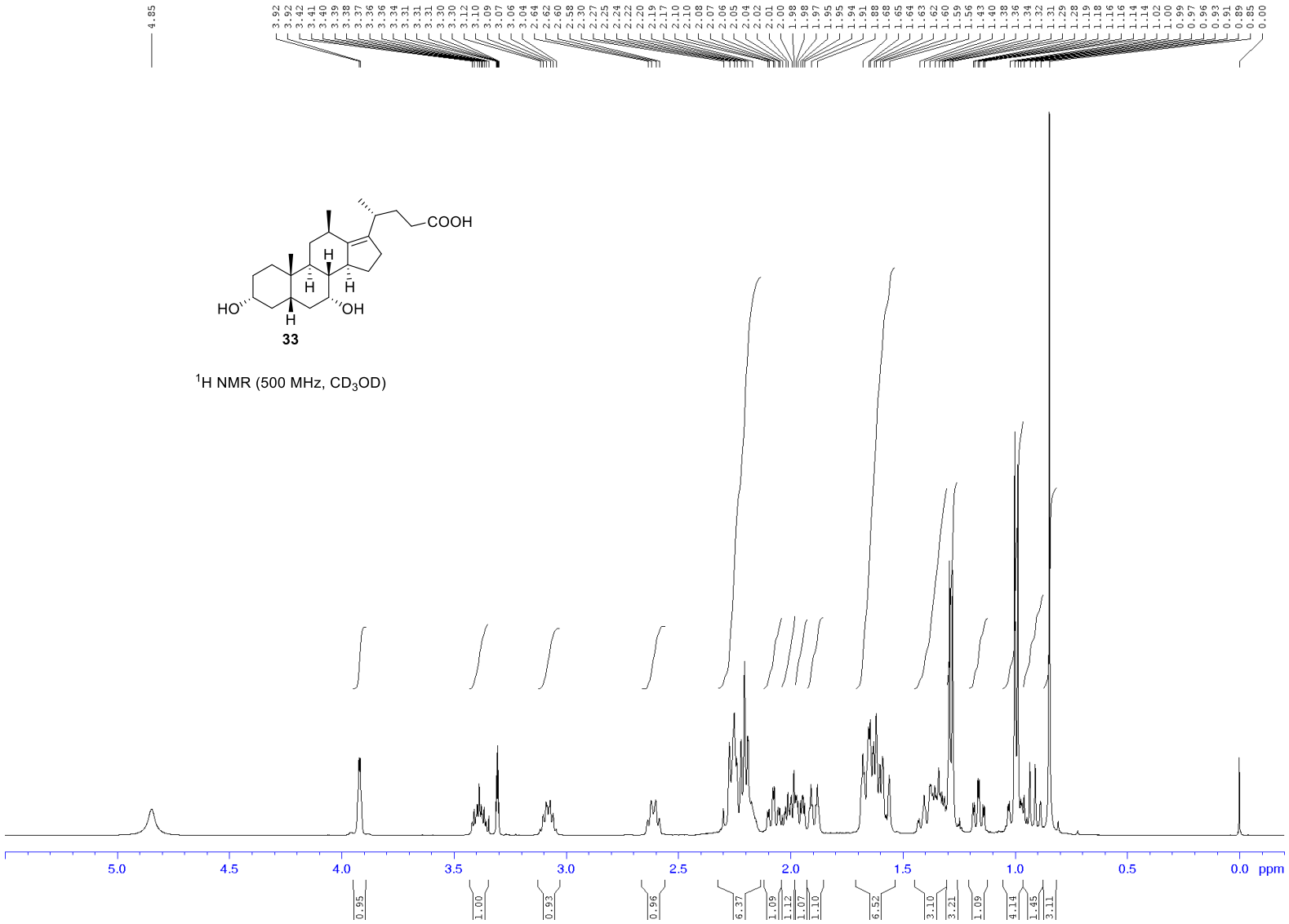

Figure S45b. ^{1}H NMR spectrum of **33**.

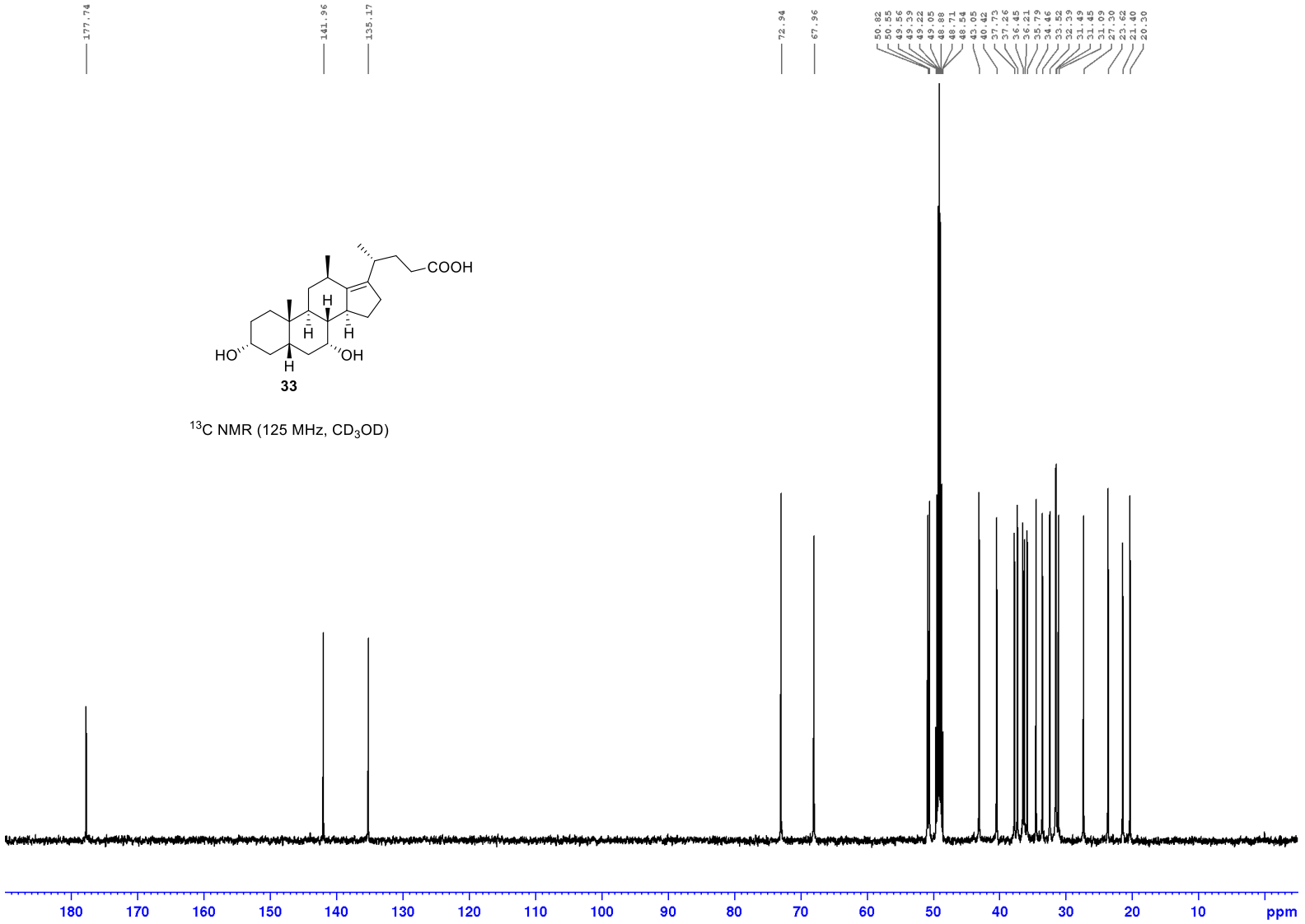

Figure S46. ^{13}C NMR spectrum of **33**.

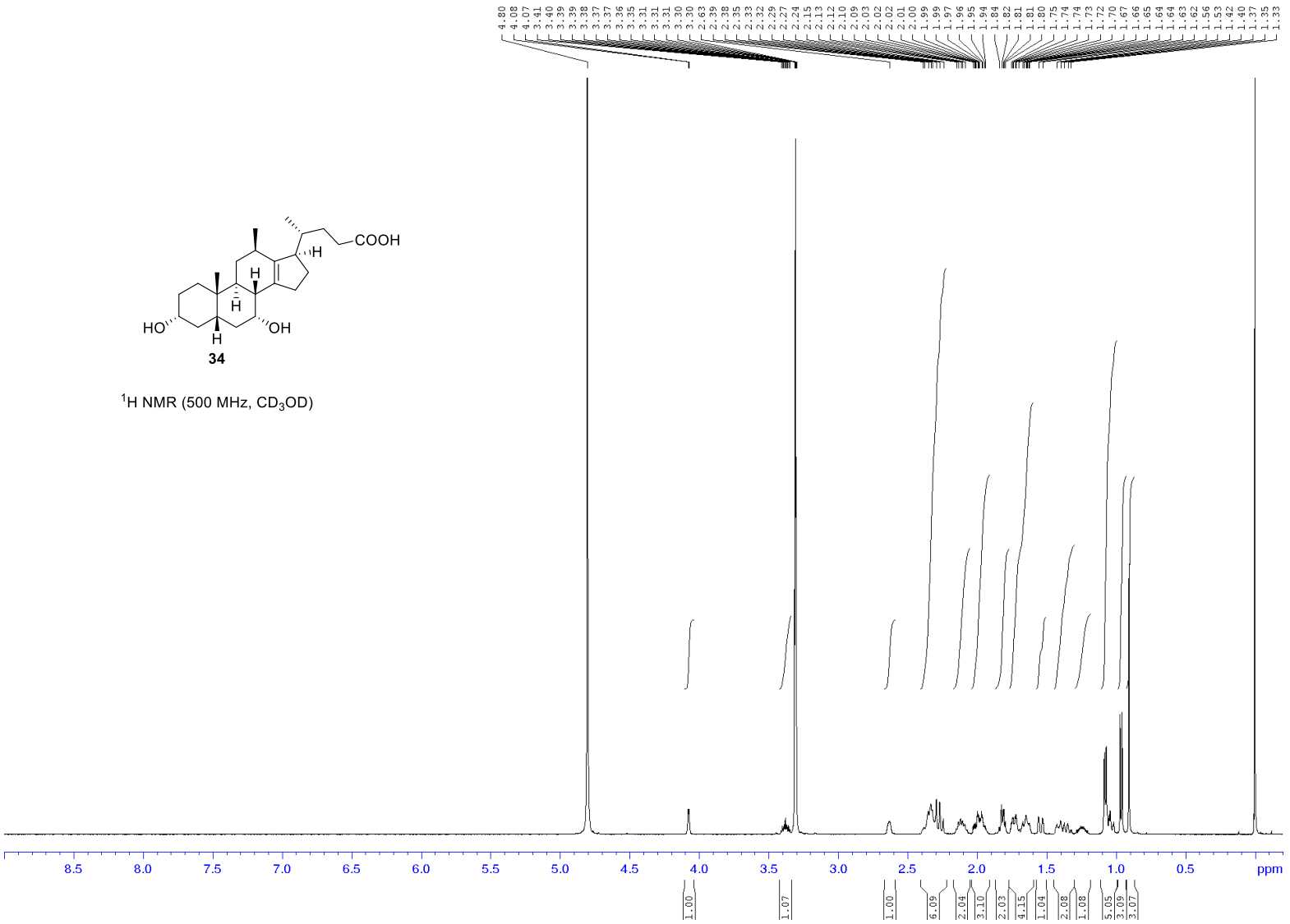

Figure S47a. ^{1}H NMR spectrum of **34**.

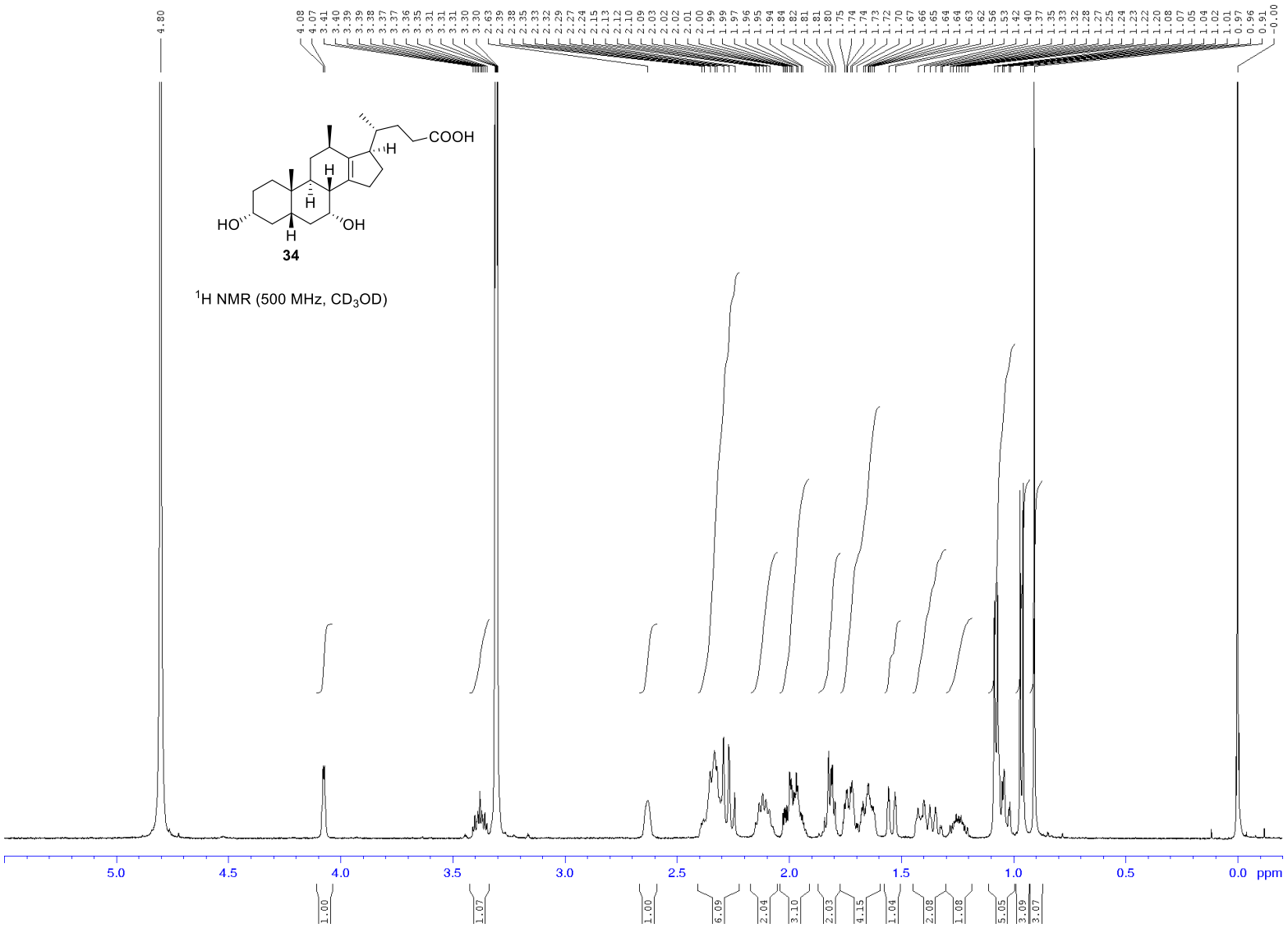

Figure S47b. ^{1}H NMR spectrum of **34**.

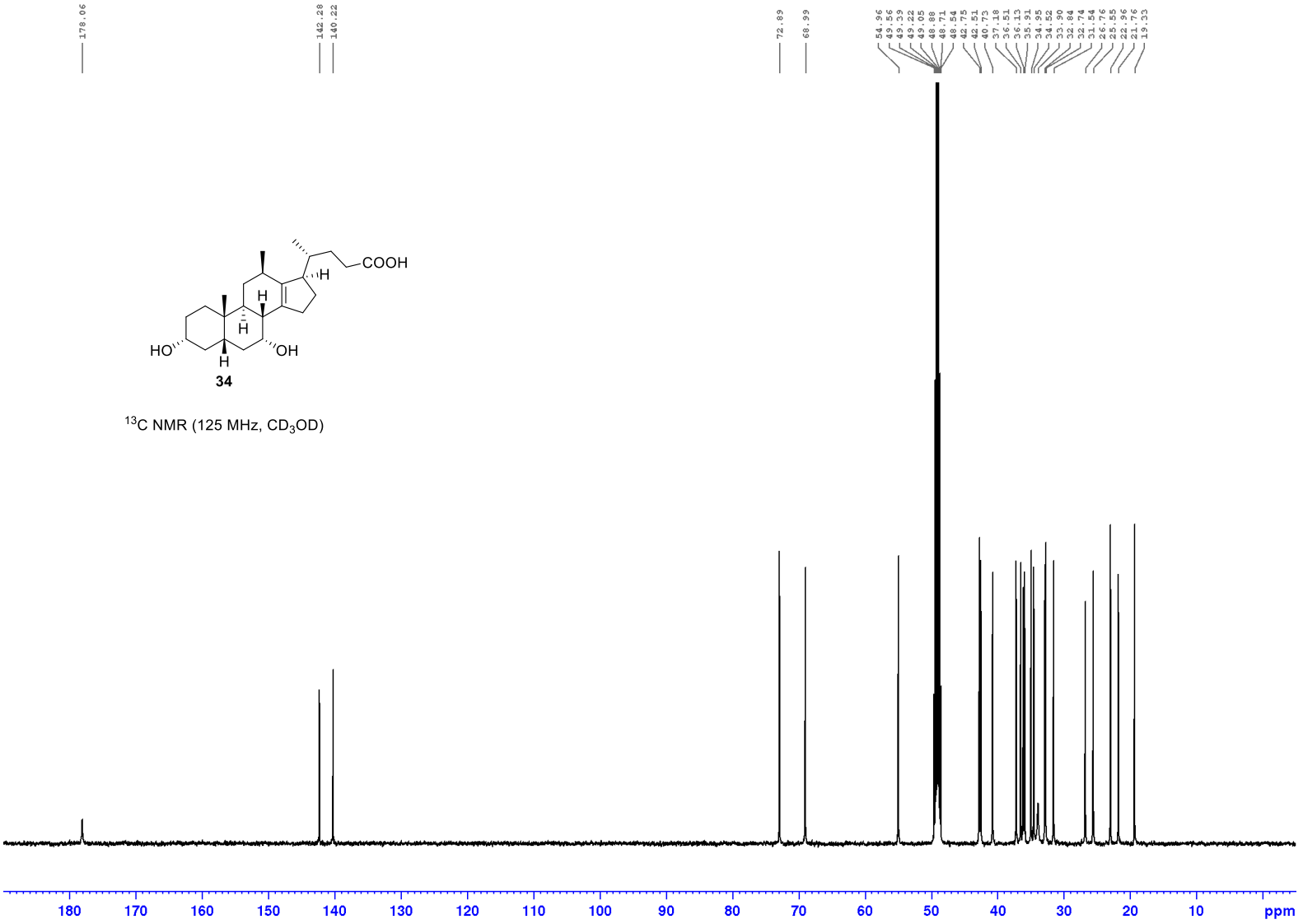

Figure S48. ^{13}C NMR spectrum of **34**.

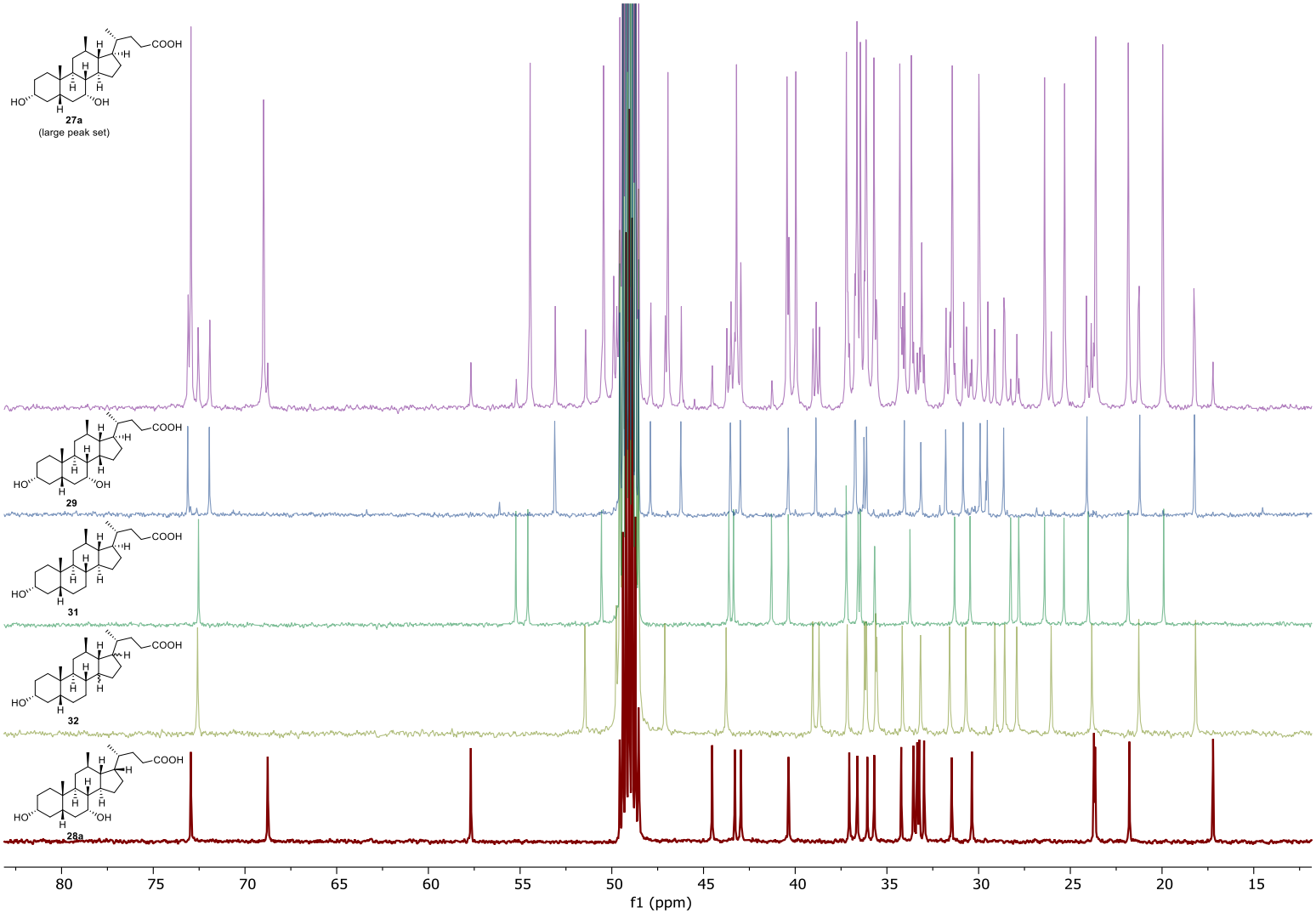

Figure S49. H-Cube hydrogenation of substrate **34**; Identification of reaction products from the ^{13}C NMR spectrum of the crude reaction product.

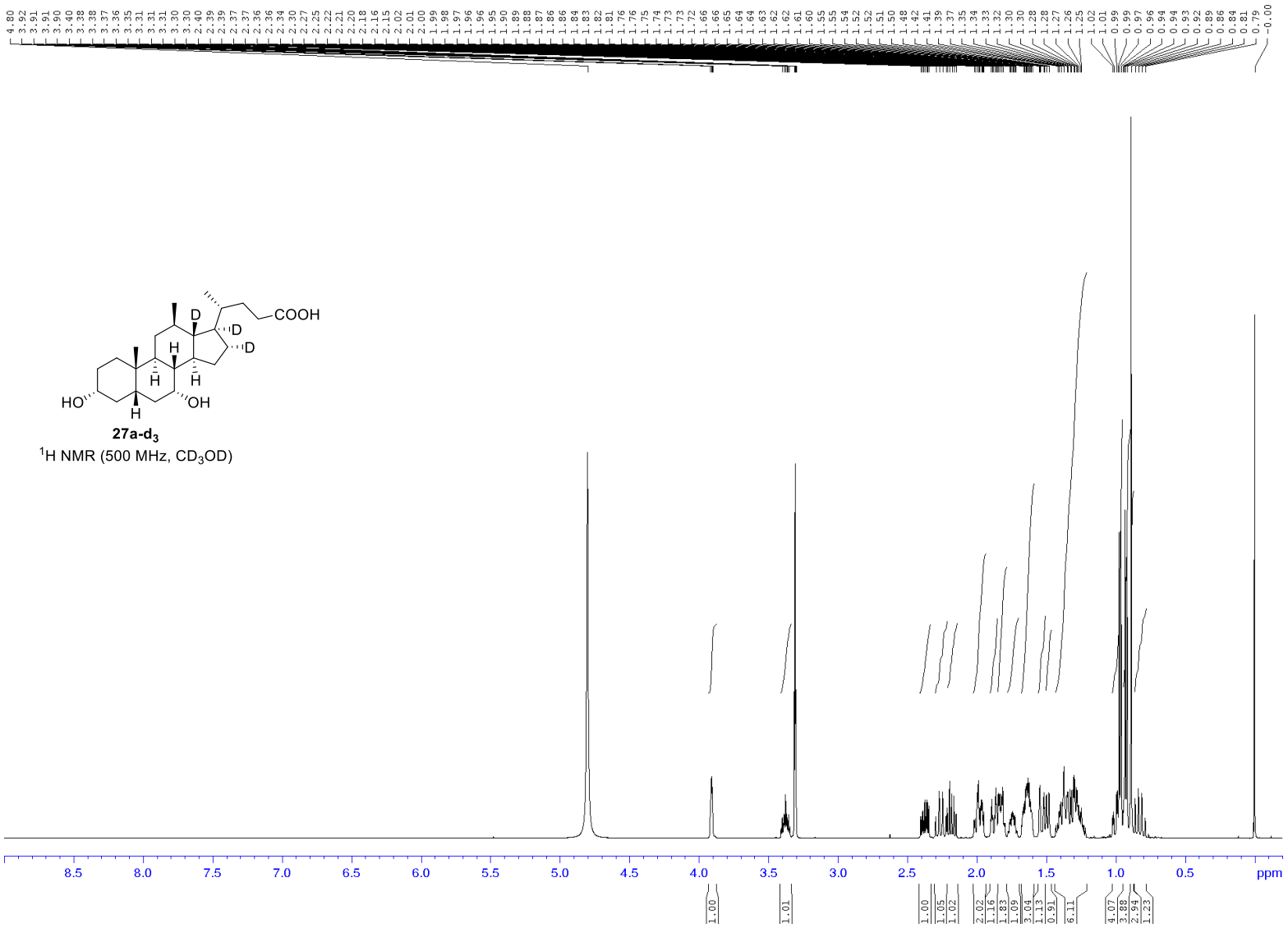

Figure S50a. ^{1}H NMR spectrum of **27a-d$_3$**.

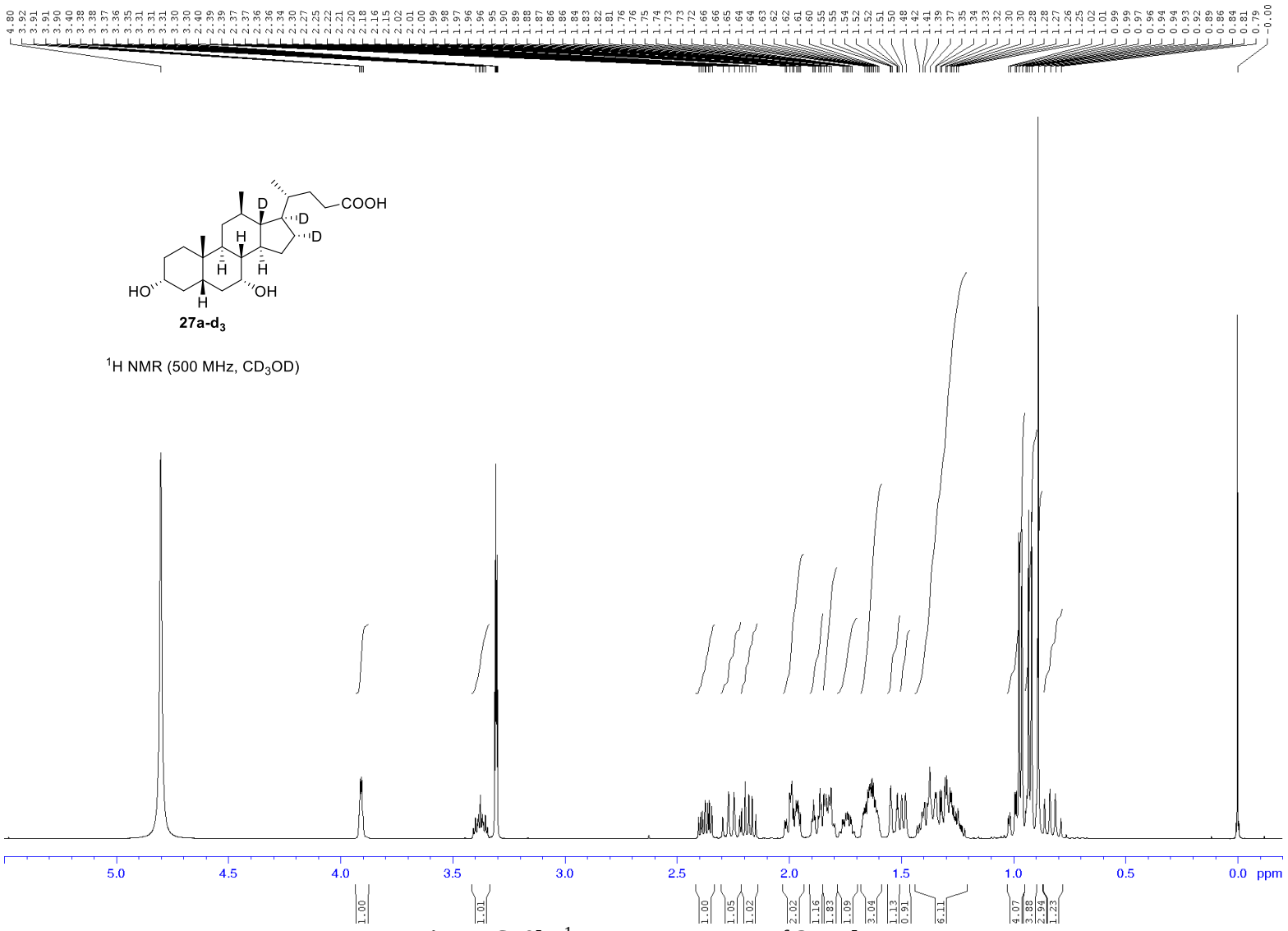

Figure S50b. ^{1}H NMR spectrum of **27a-d$_3$**.

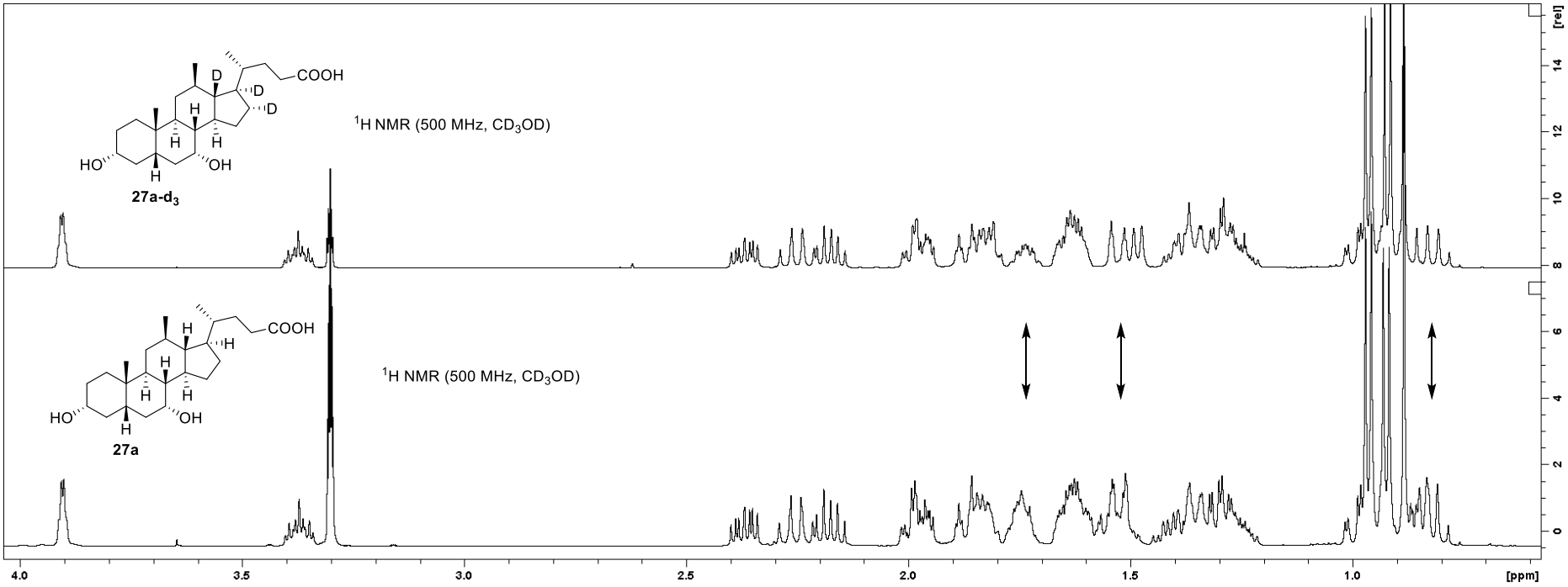

Figure S51. Comparison of proton NMR spectra of the deuterated 12β-methyl-18-*nor*-chenodeoxycholic acid (**27a-d3**) *vs.* the non-deuterated compound (**27a**).

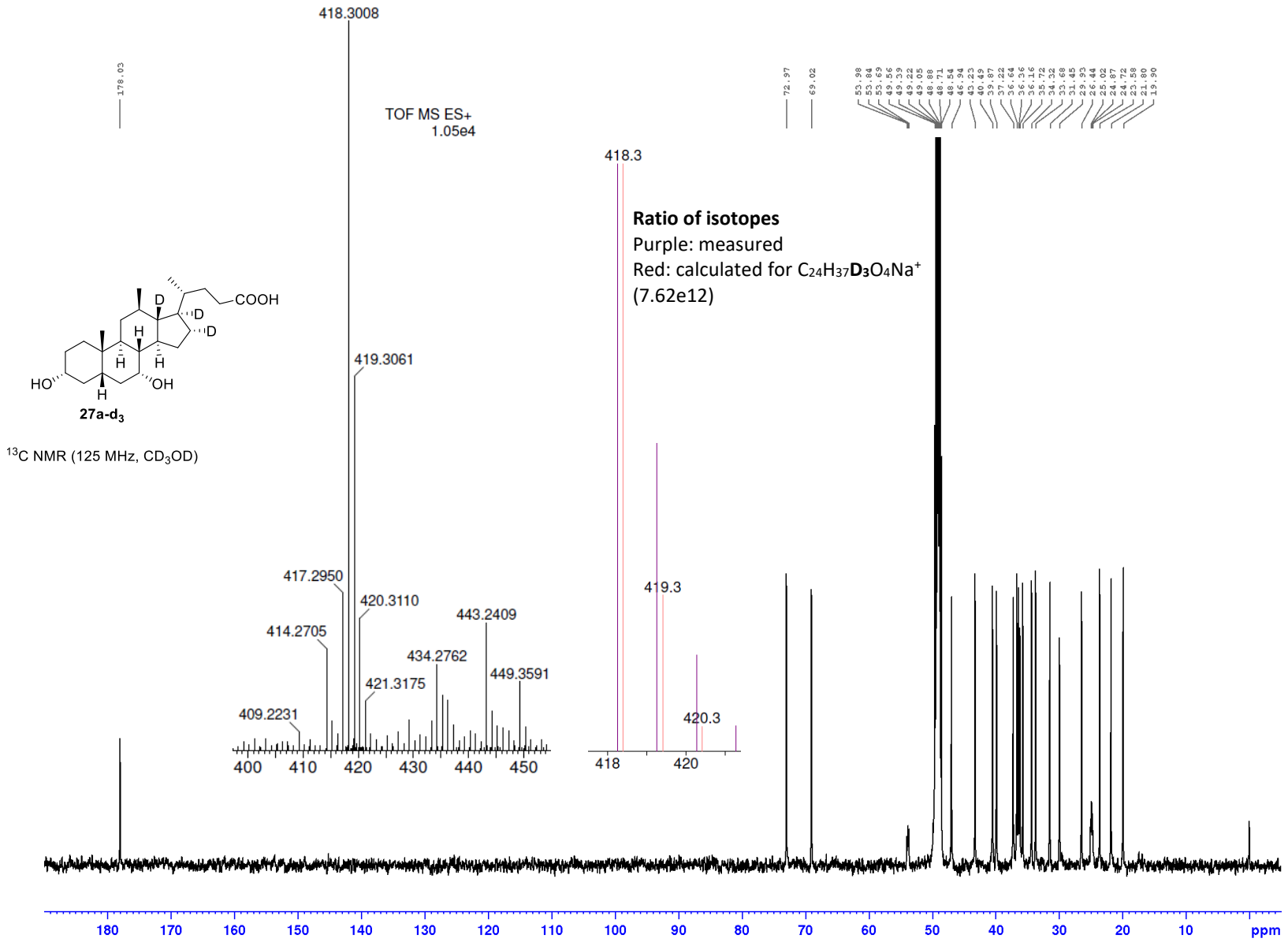

Figure S52. ^{13}C NMR spectrum of **27a-d$_3$** and assessment of the MS isotopdistribution.

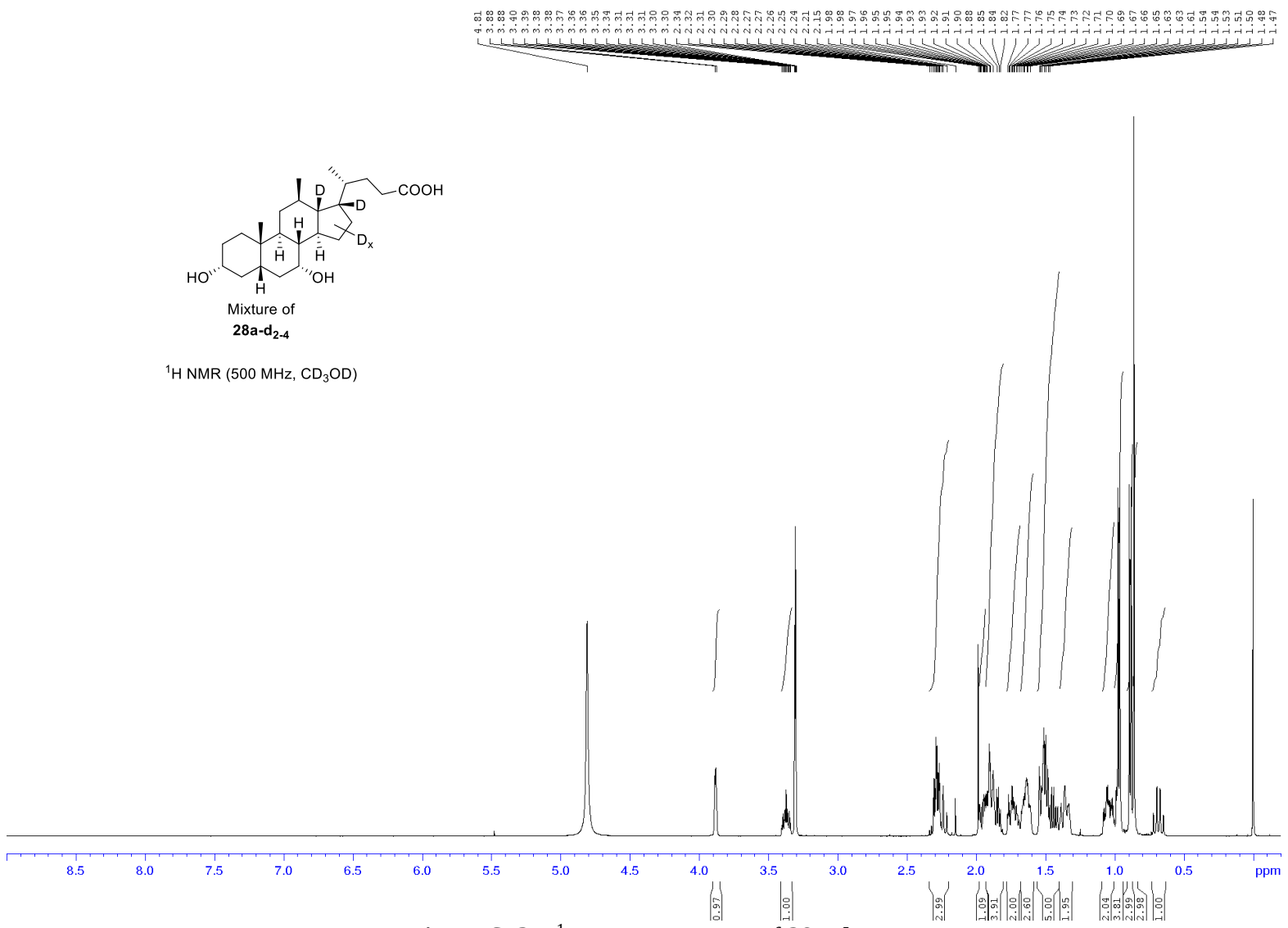

Figure S53a. ^{1}H NMR spectrum of **28a-d$_{2-4}$**.

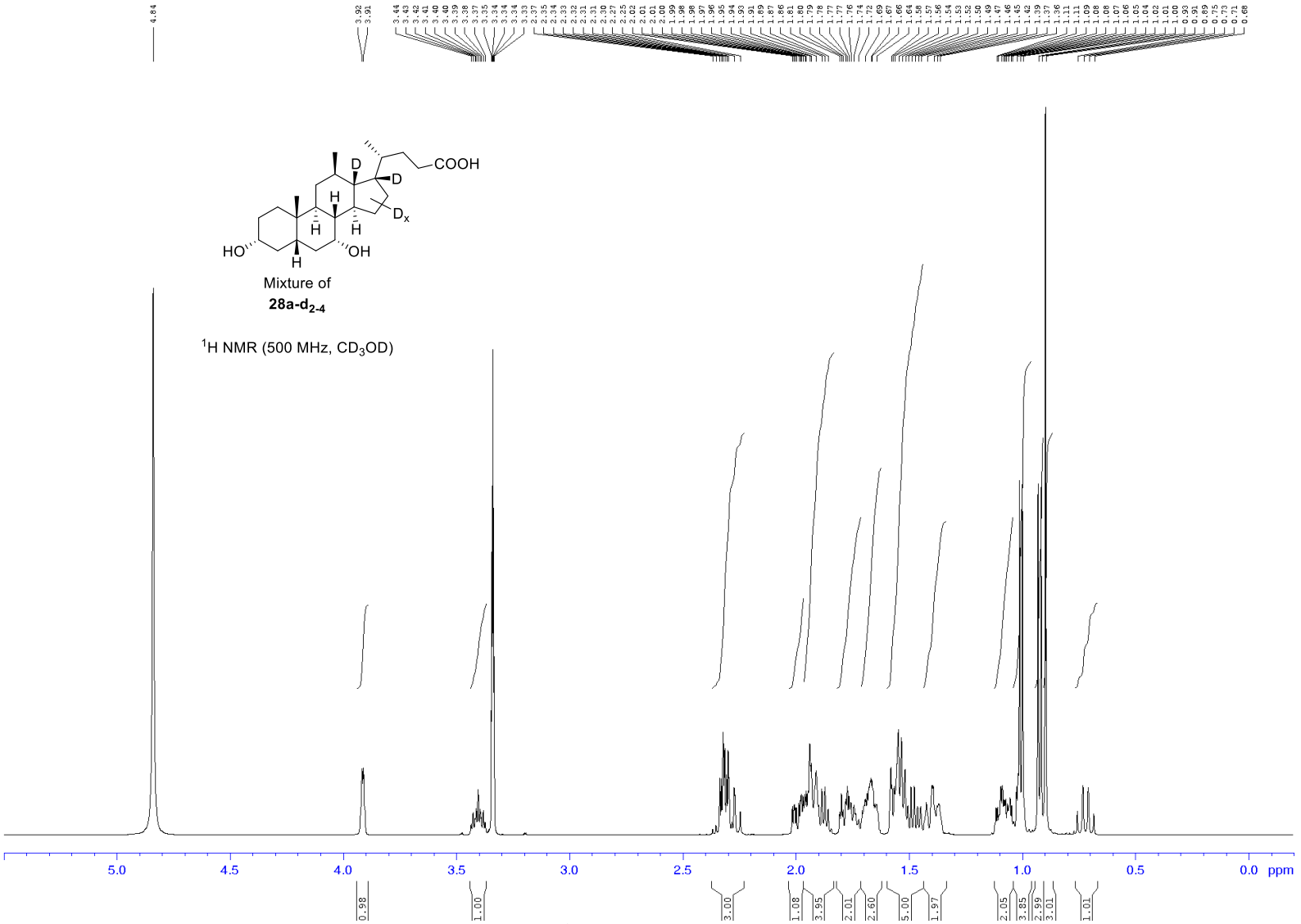

Figure S53b. ^{1}H NMR spectrum of **28a-d$_{2\text{-}4}$.**

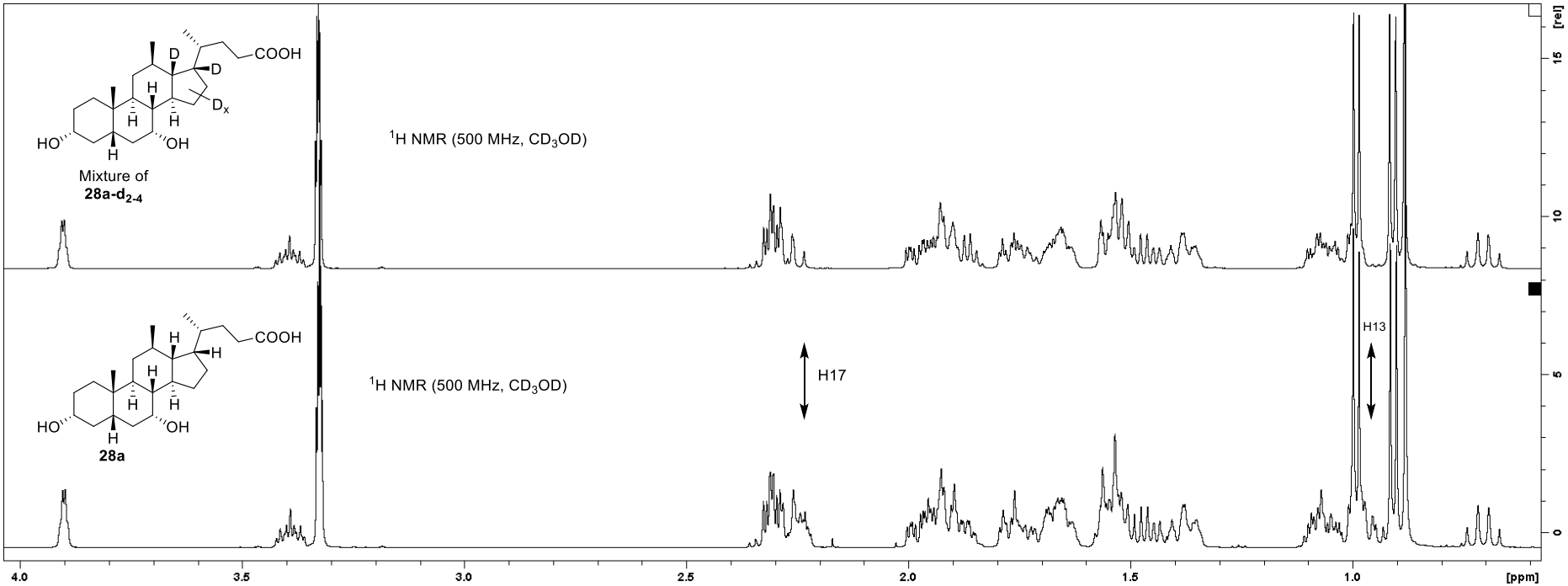

Figure S54. Comparison of proton NMR spectra of the mixture of deuterated 17-*epi*-12β-methyl-18-*nor*-chenodeoxycholic acid (**28a-d$_{2-4}$**) *vs.* the non-deuterated 17-*epi*-analog (**28a**).

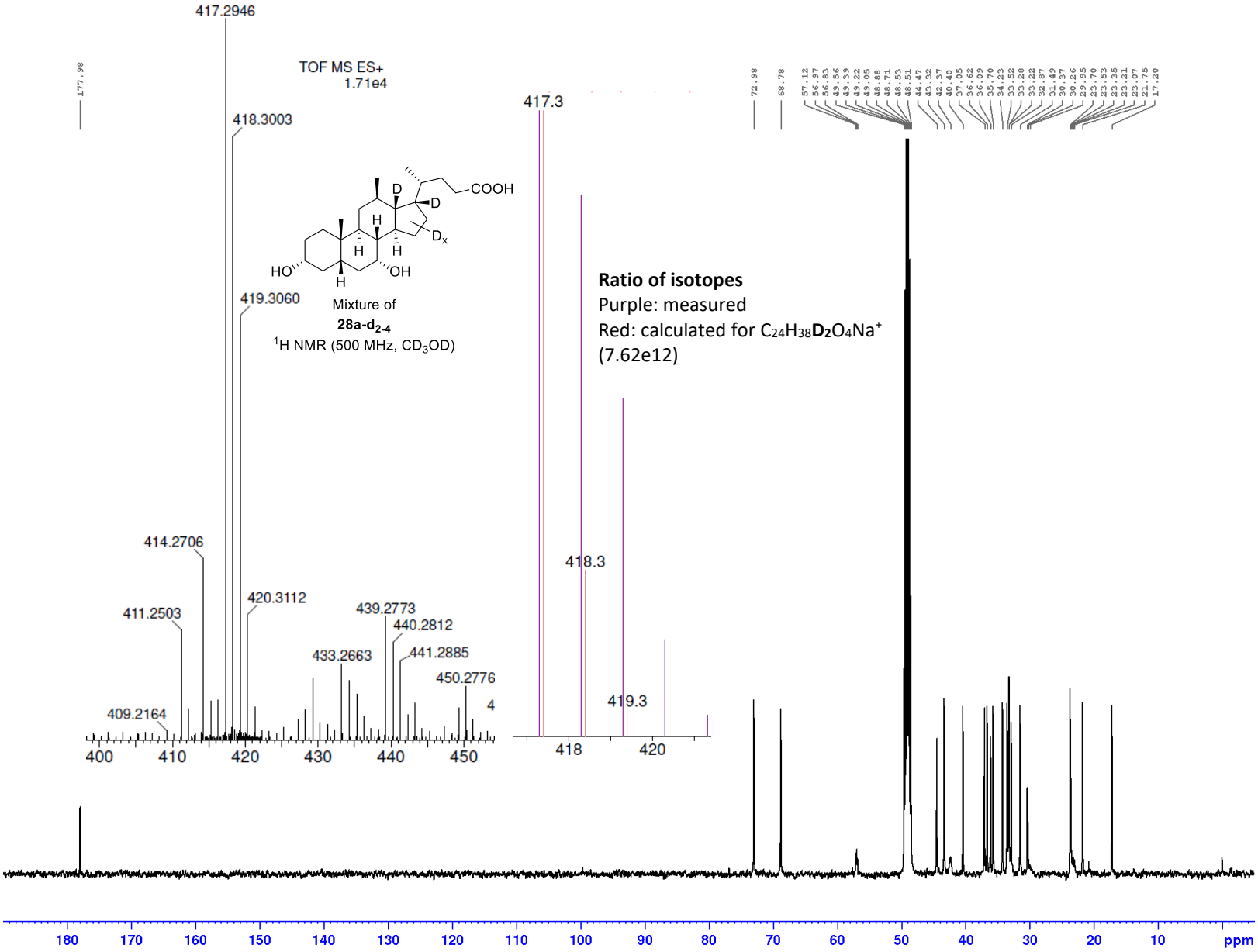

Figure S55. ^{13}C NMR spectrum of **28a-d$_{2\text{-}4}$** and assessment of the MS isotopdistribution.

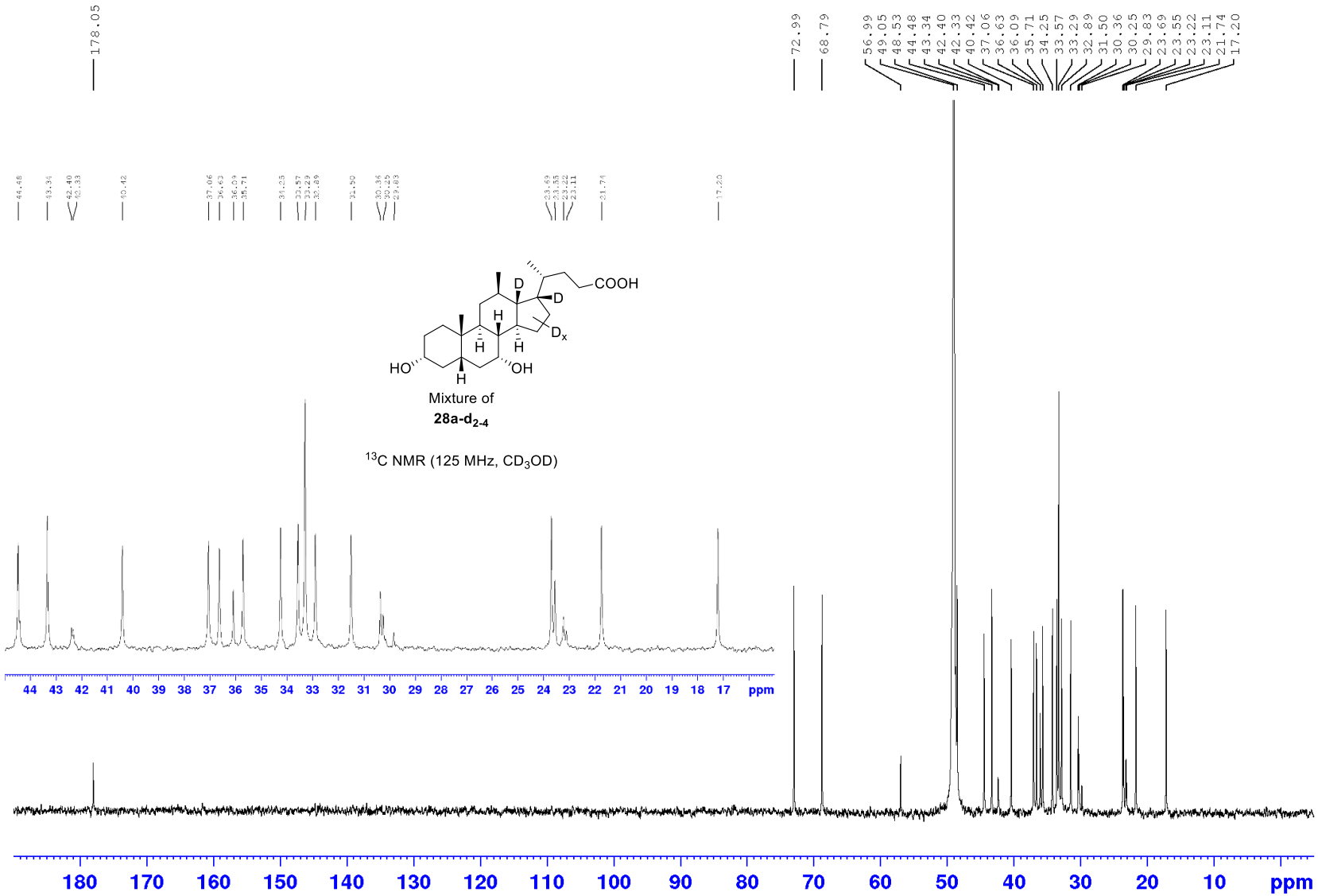

Figure S56. Semi-quantitative ^{13}C NMR spectrum of the mixture of **28a-d$_{2-4}$** (inverse gated, ^{1}H- and ^{2}H-decoupled; NS 9600).

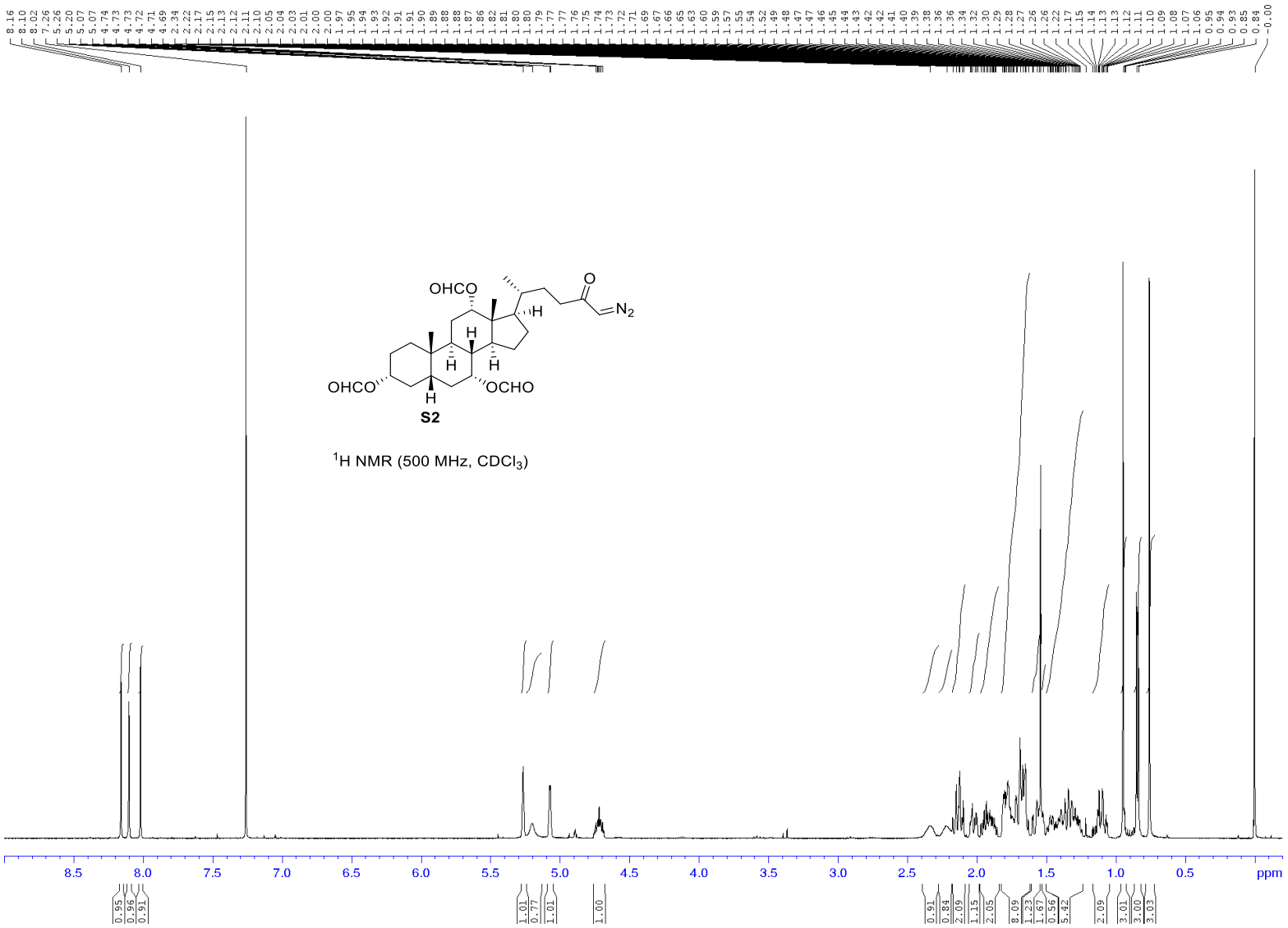

Figure S57. ^{1}H NMR spectrum of **S2**.

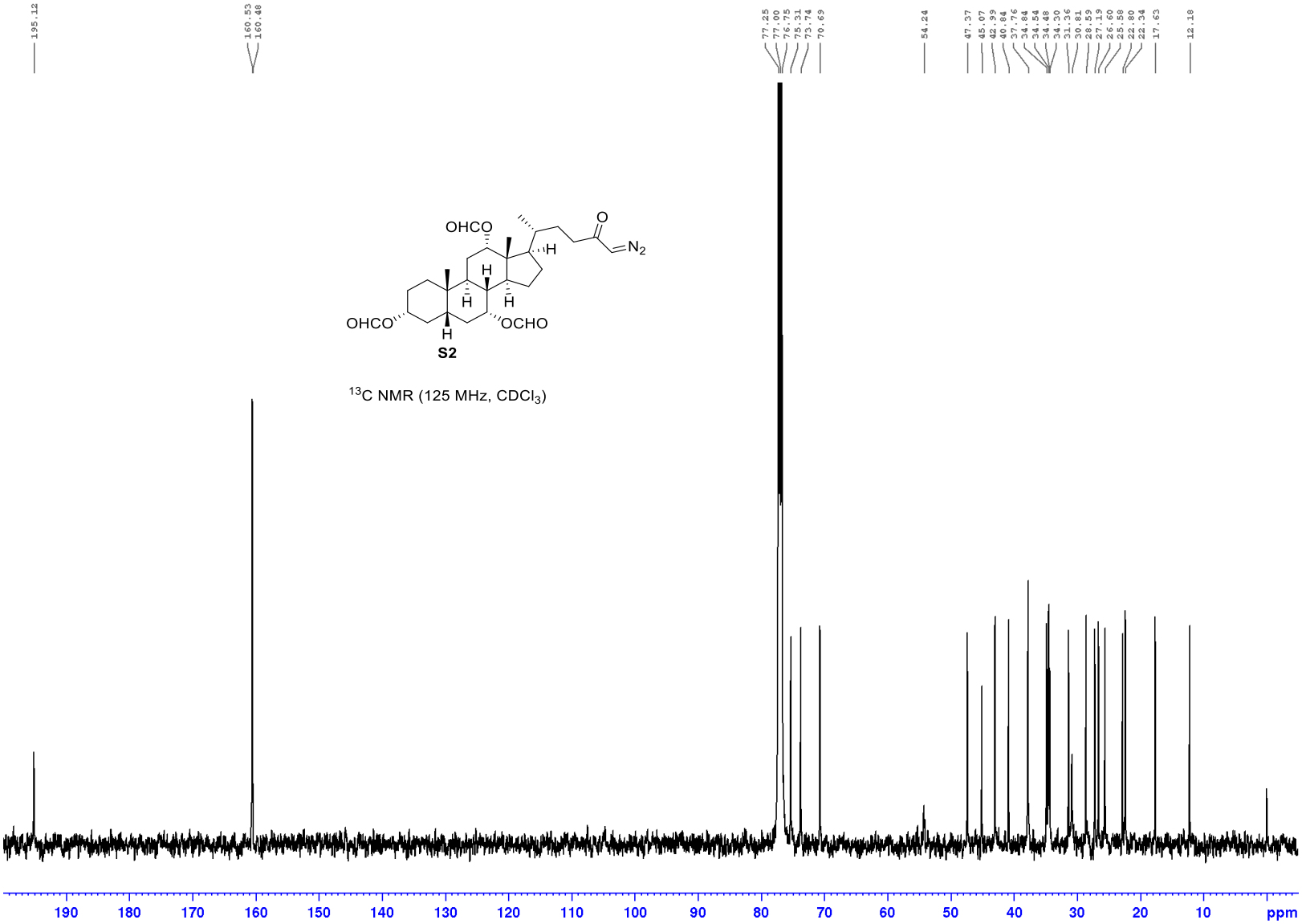

Figure S58. ^{13}C NMR spectrum of **S2**.

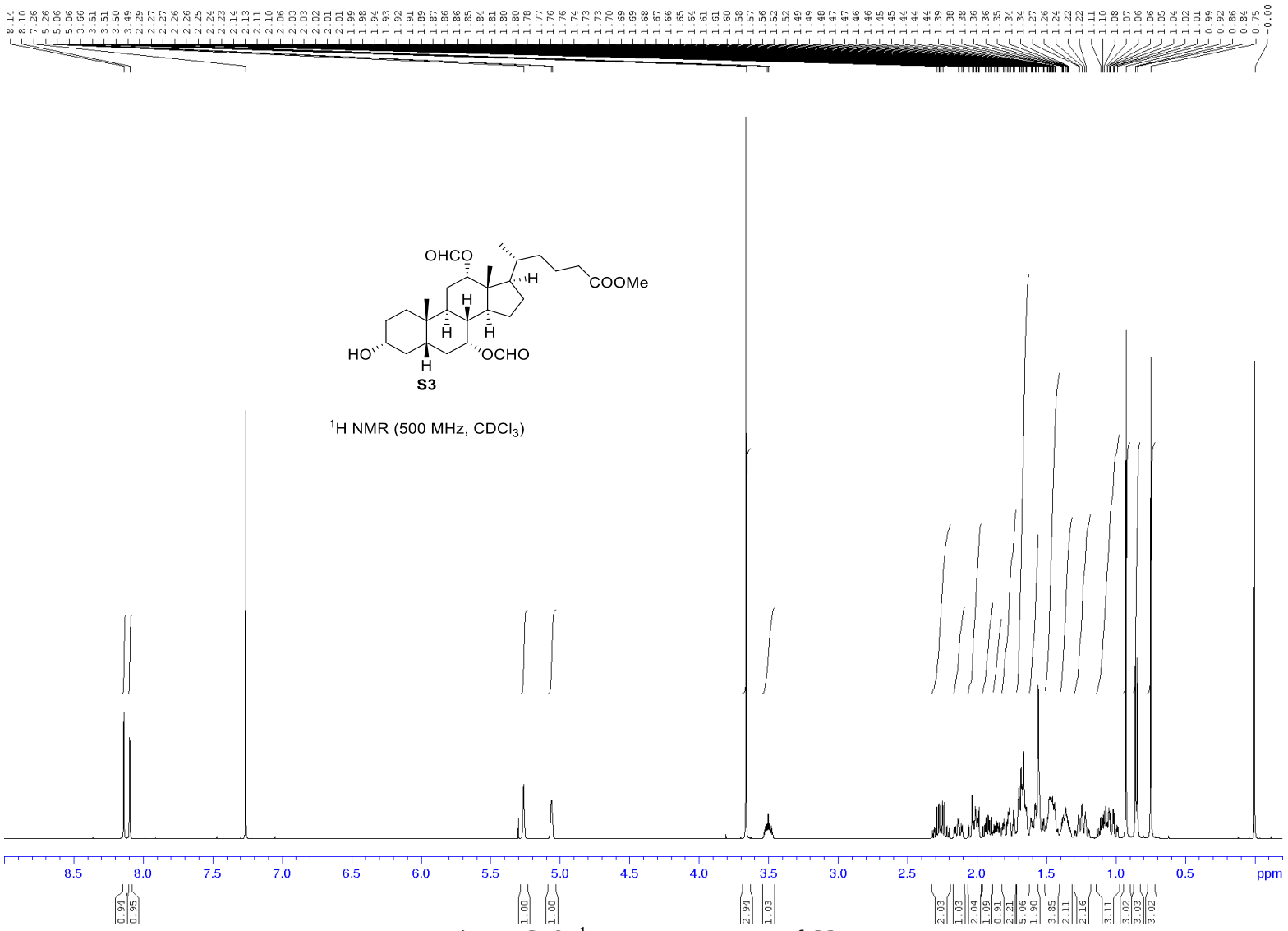

Figure S59. ^{1}H NMR spectrum of **S3**.

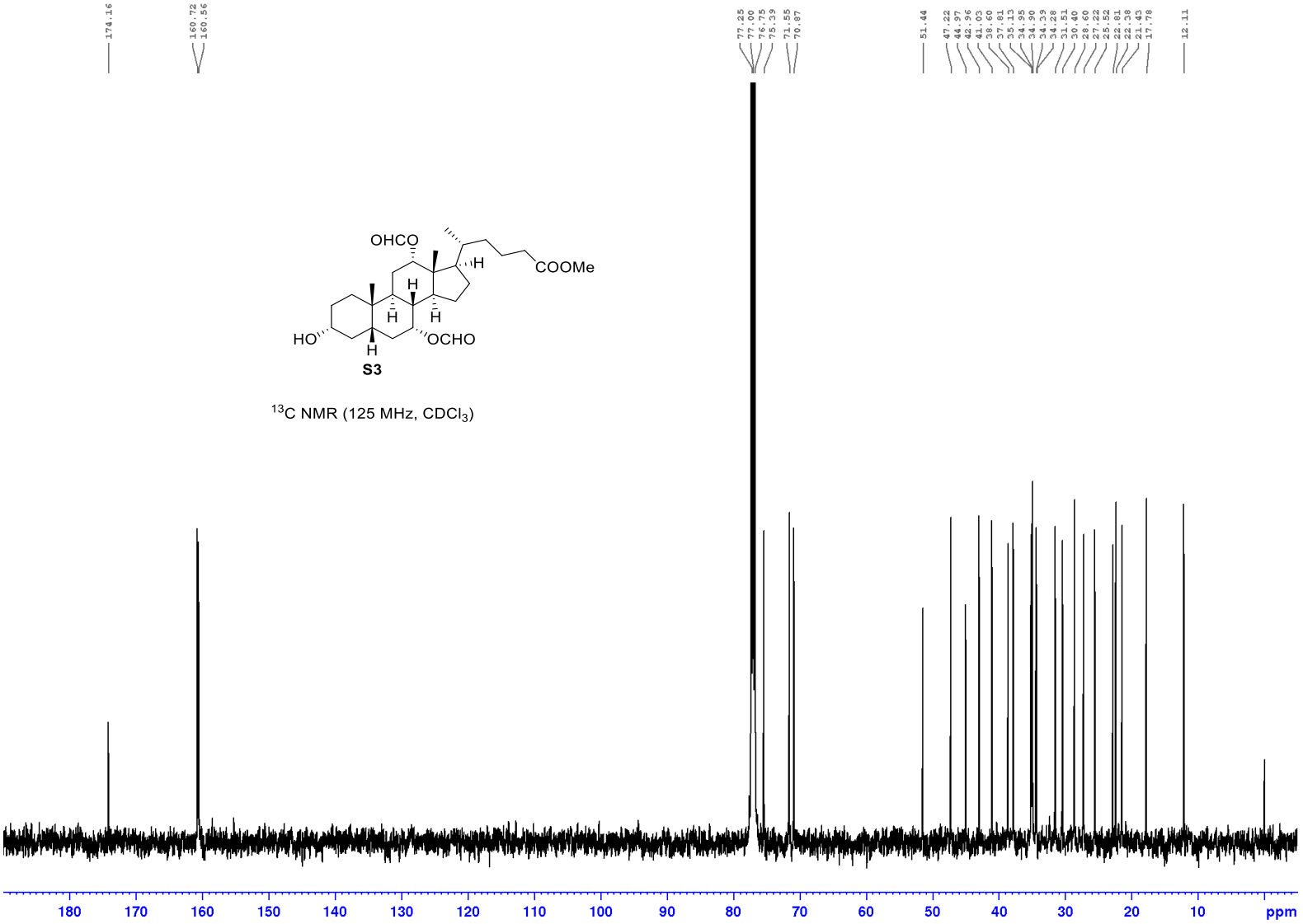

Figure S60. ^{13}C NMR spectrum of **S3**.

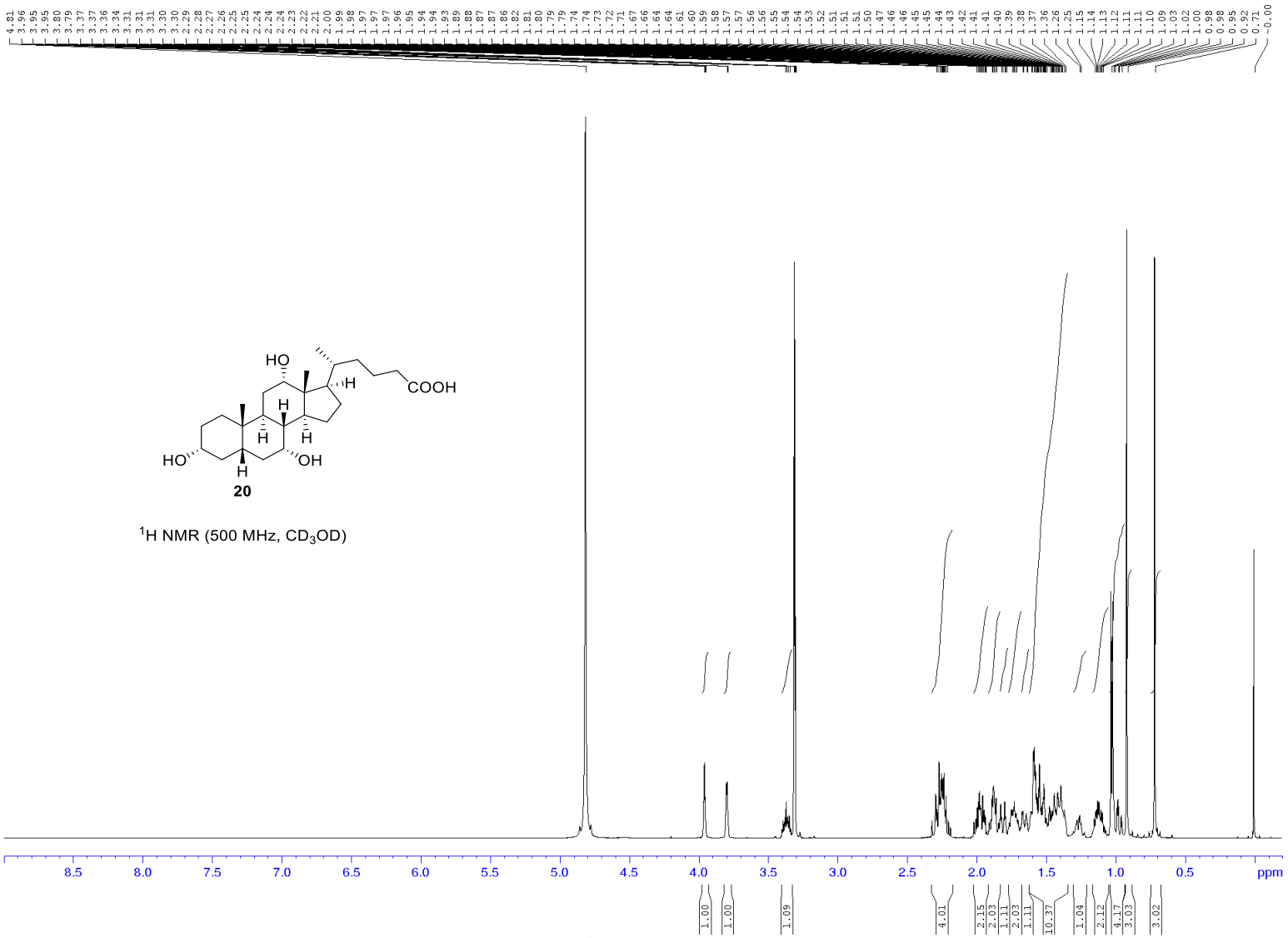

Figure S61a. ^{1}H NMR spectrum of **20**.

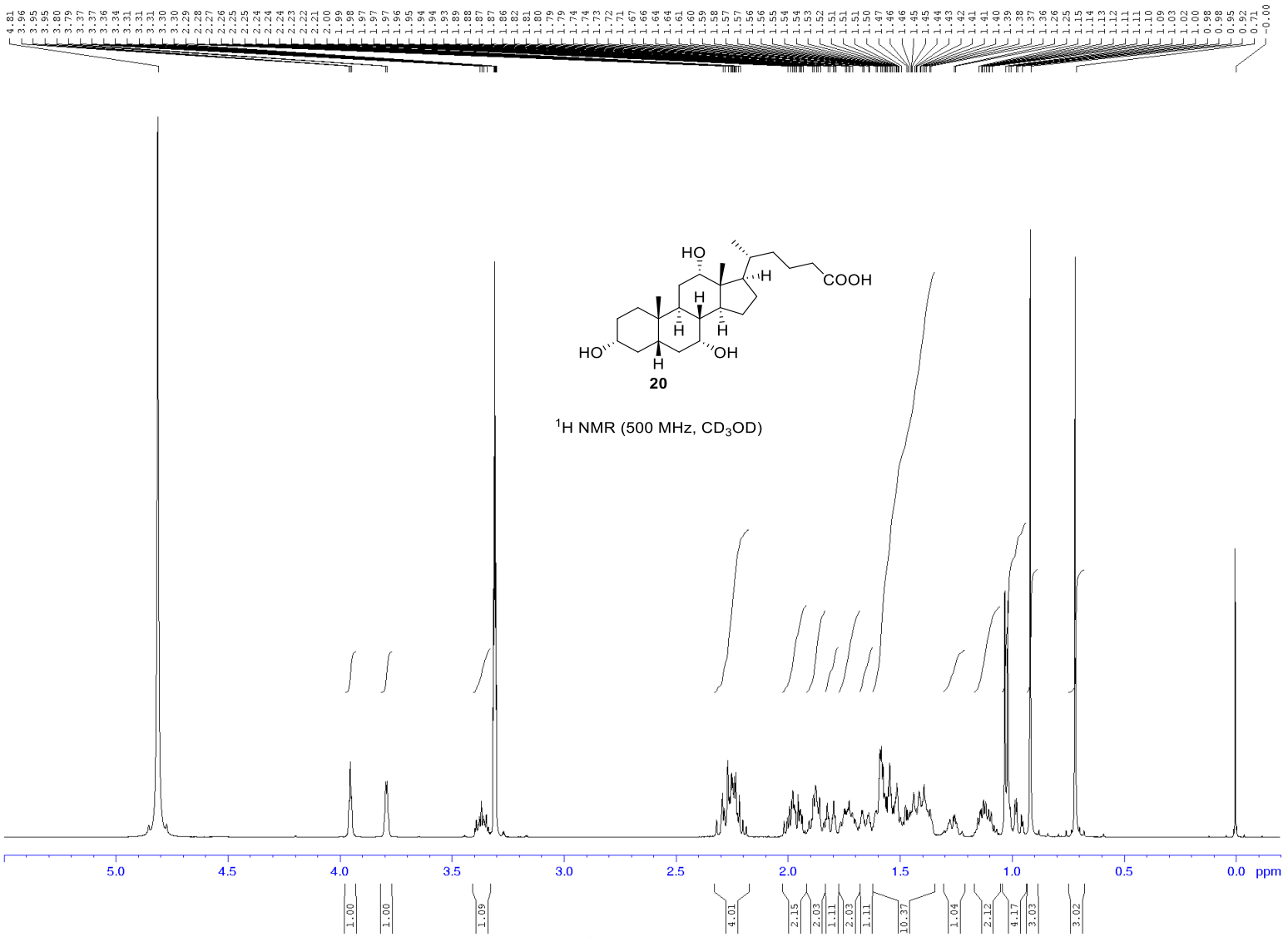

Figure S61b. ^{1}H NMR spectrum of **20**.

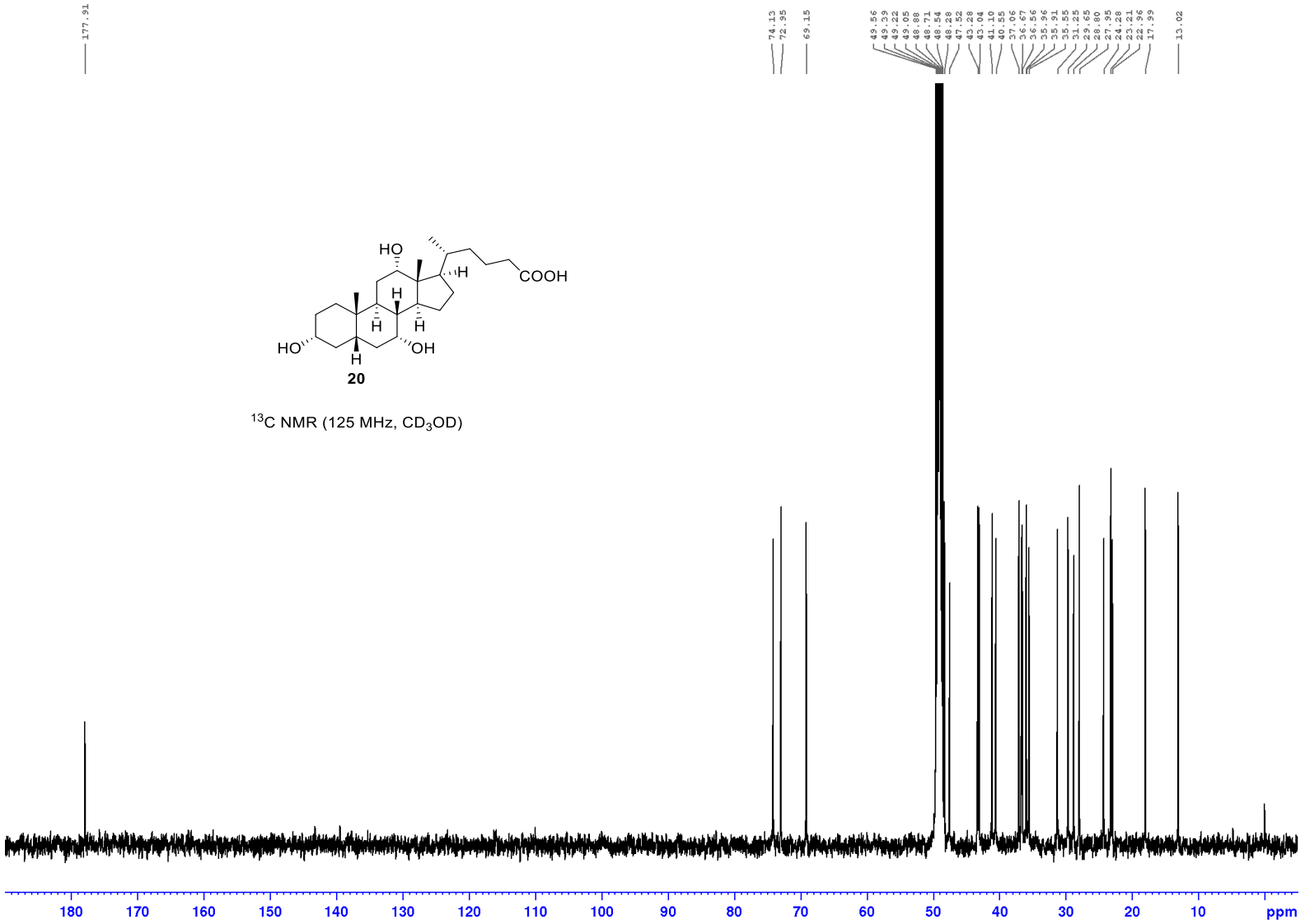

Figure S62. ^{13}C NMR spectrum of **20**.

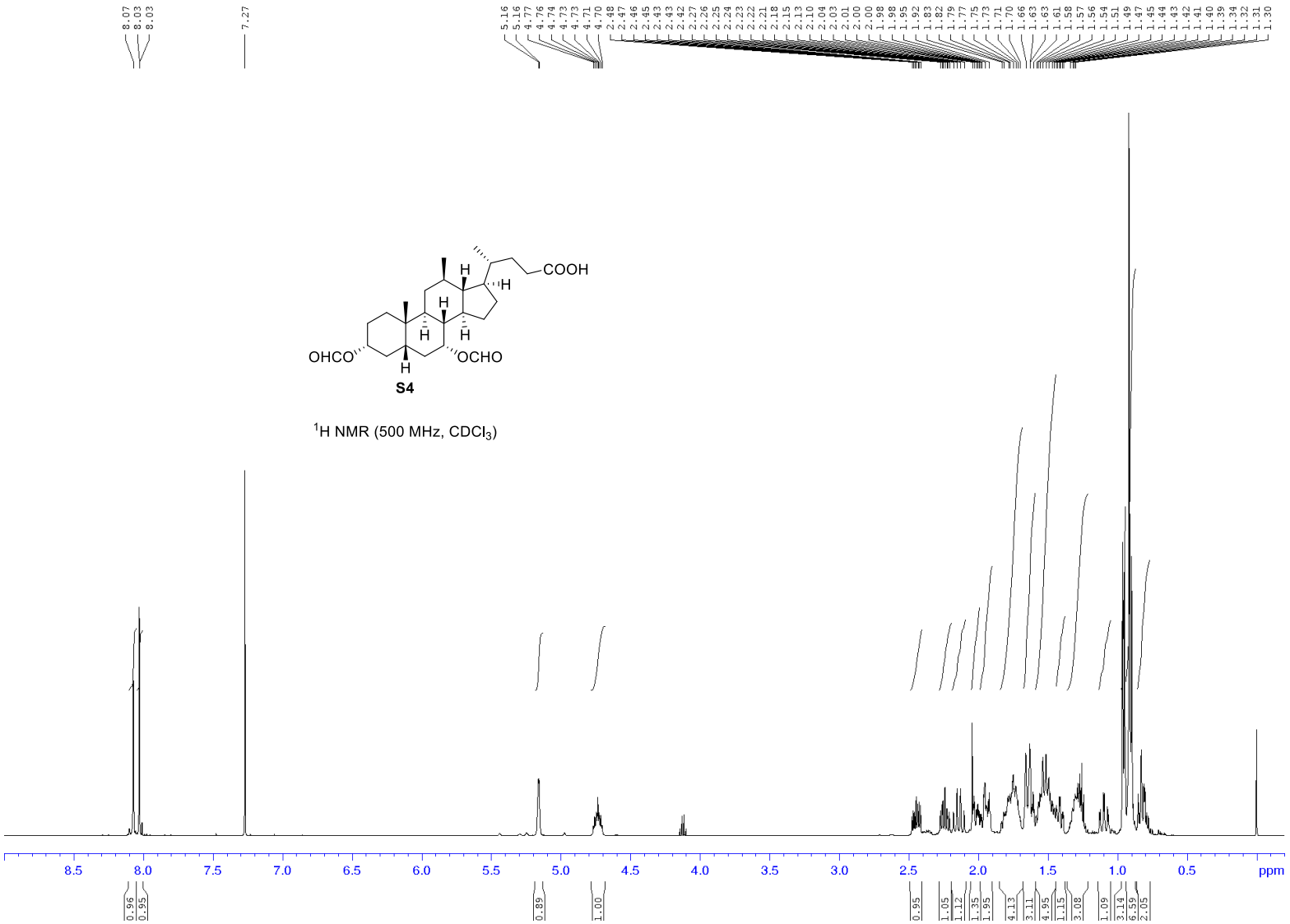

Figure S63a. ^{1}H NMR spectrum of **S4**.

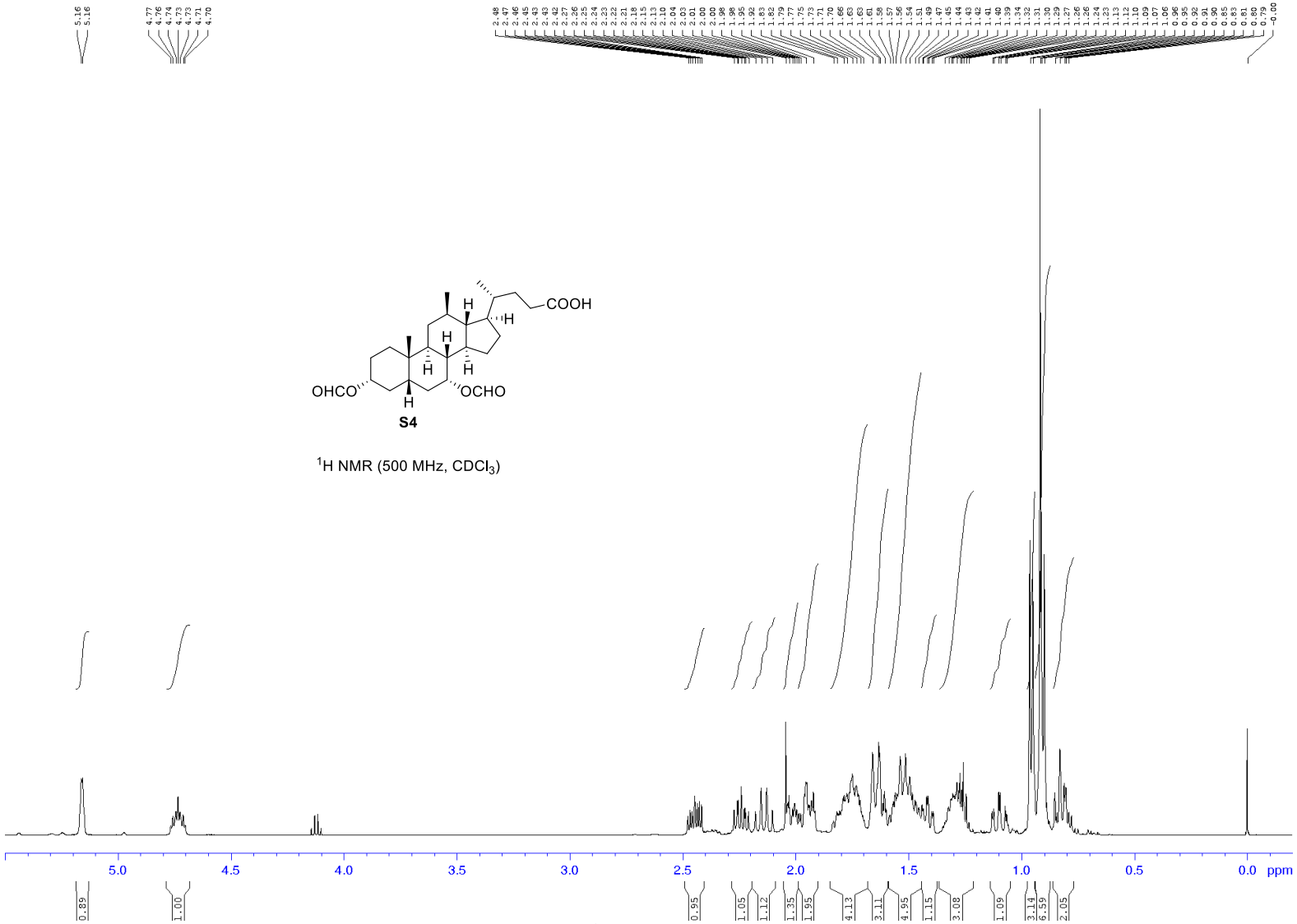

Figure S63b. ^{1}H NMR spectrum of **S4**.

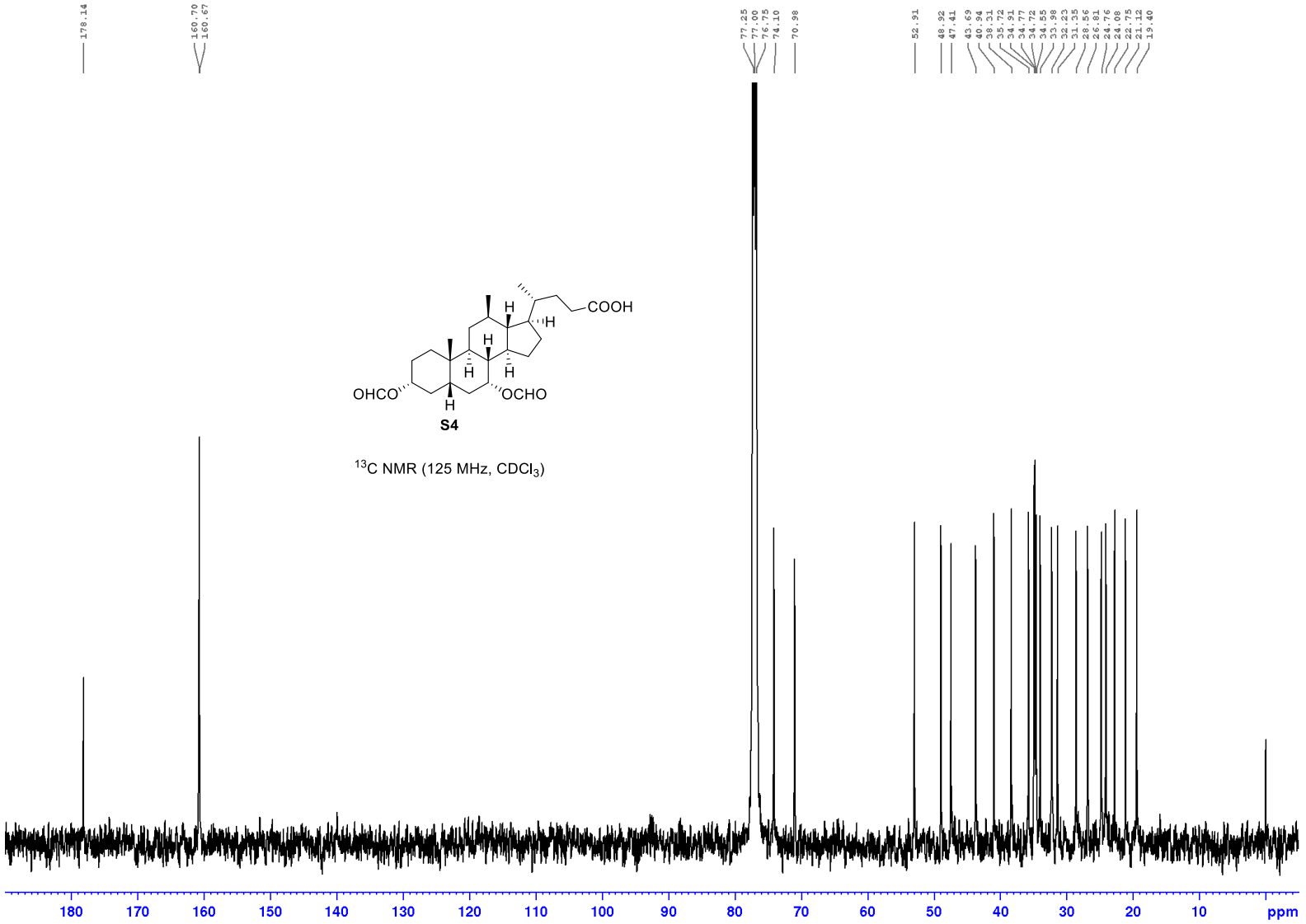

Figure S64. ^{13}C NMR spectrum of **S4**.

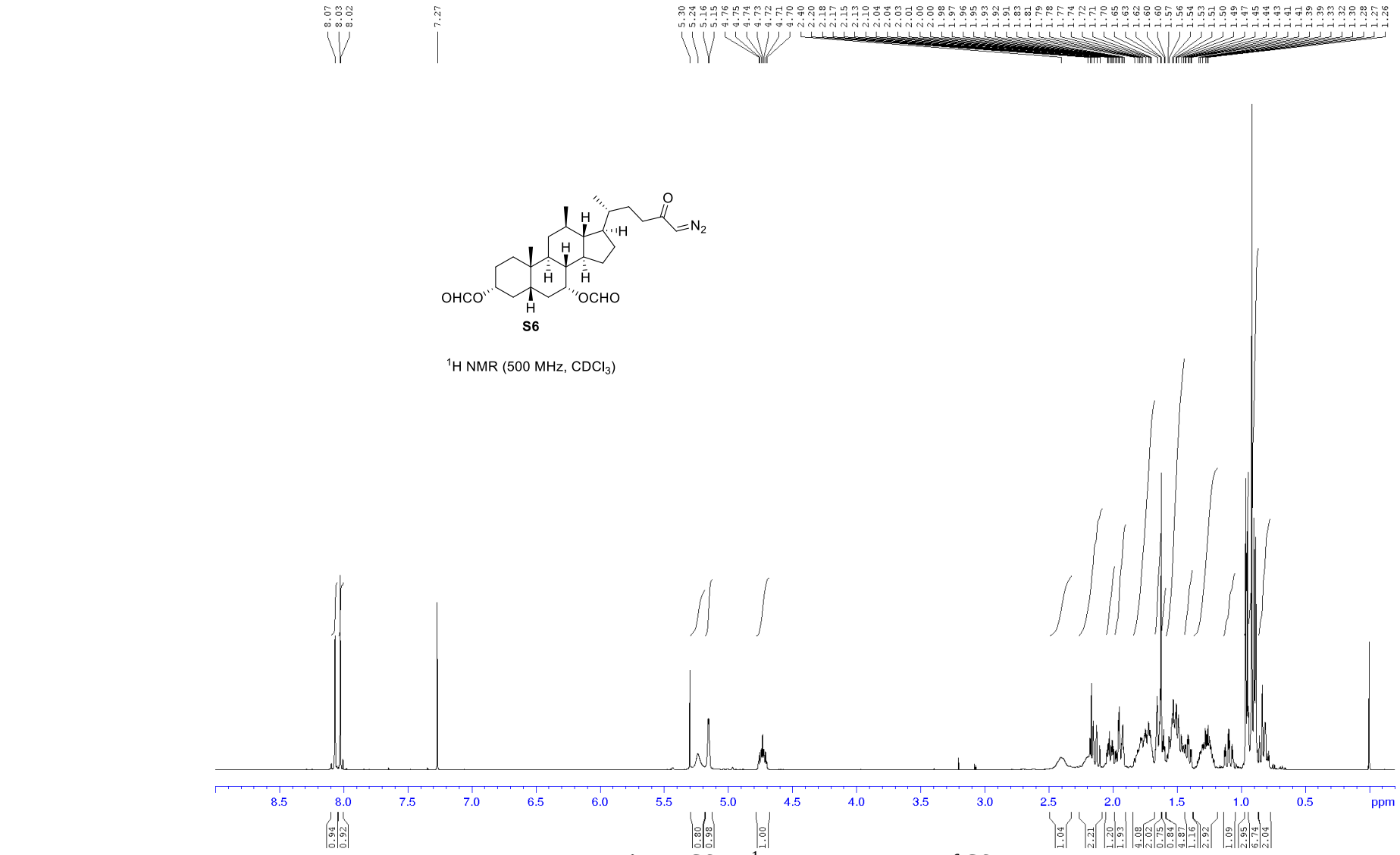

Figure S65a. ^{1}H NMR spectrum of **S6**.

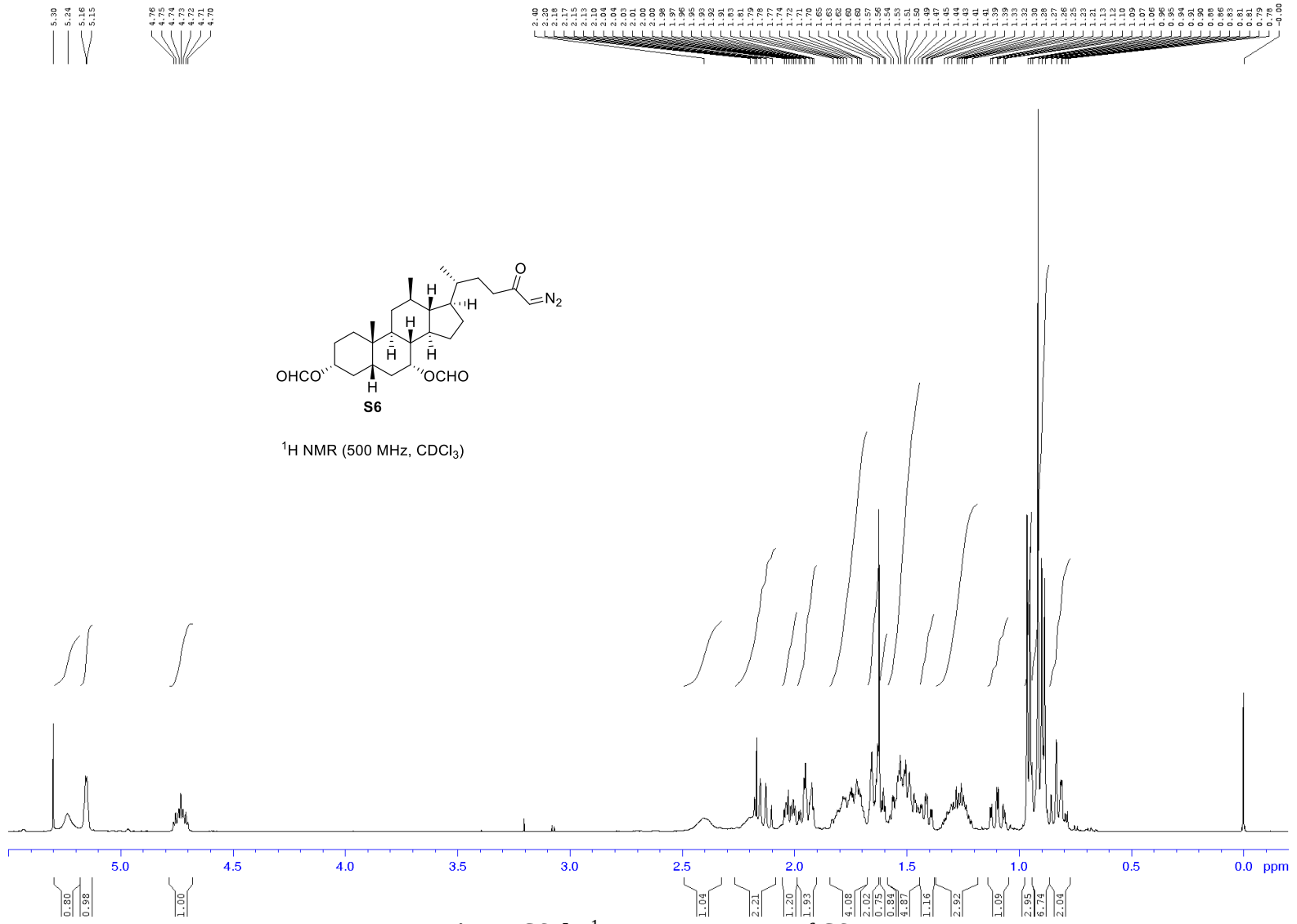

Figure S65b. ^{1}H NMR spectrum of **S6**.

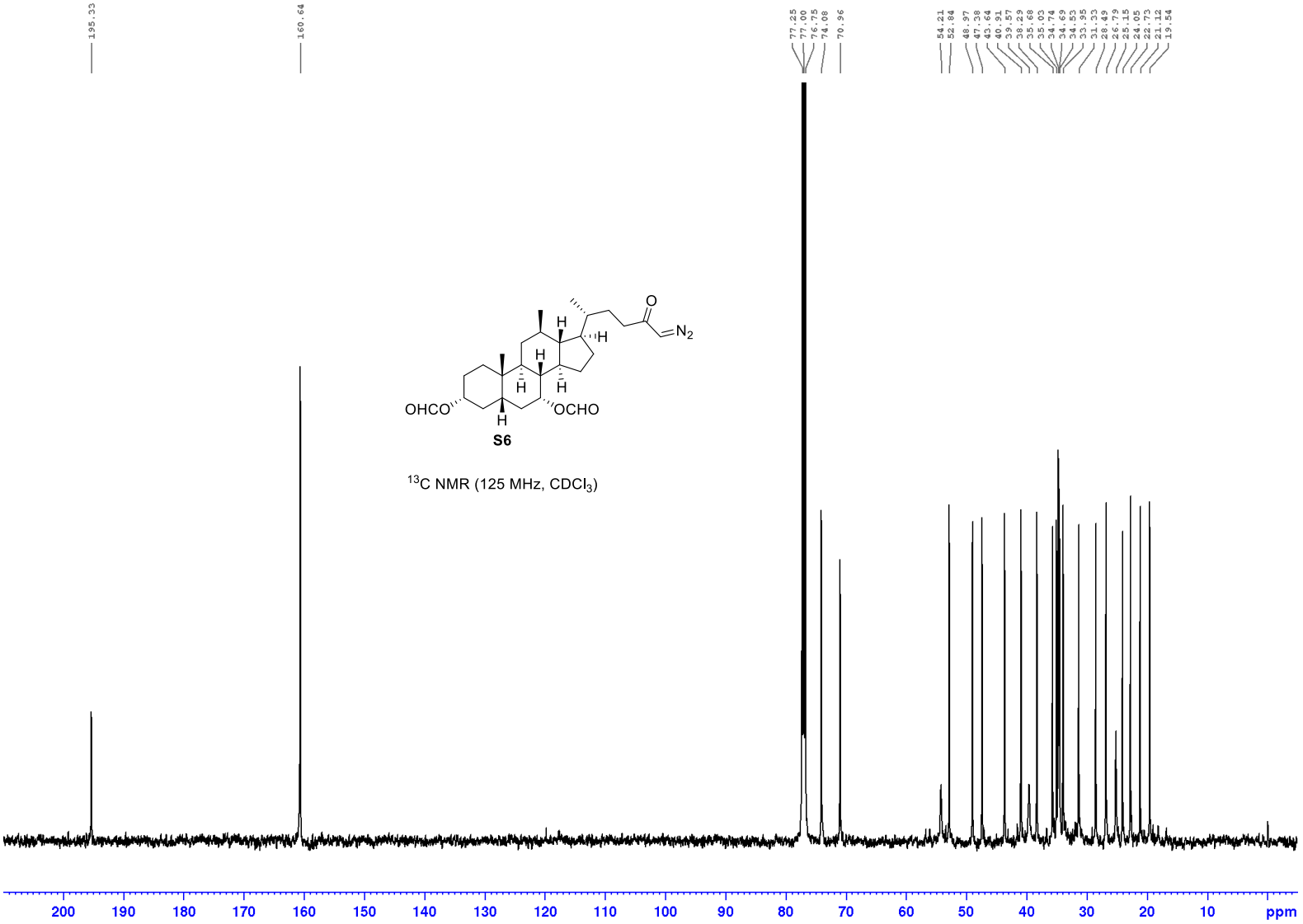

Figure S66. ^{13}C NMR spectrum of **S6**.

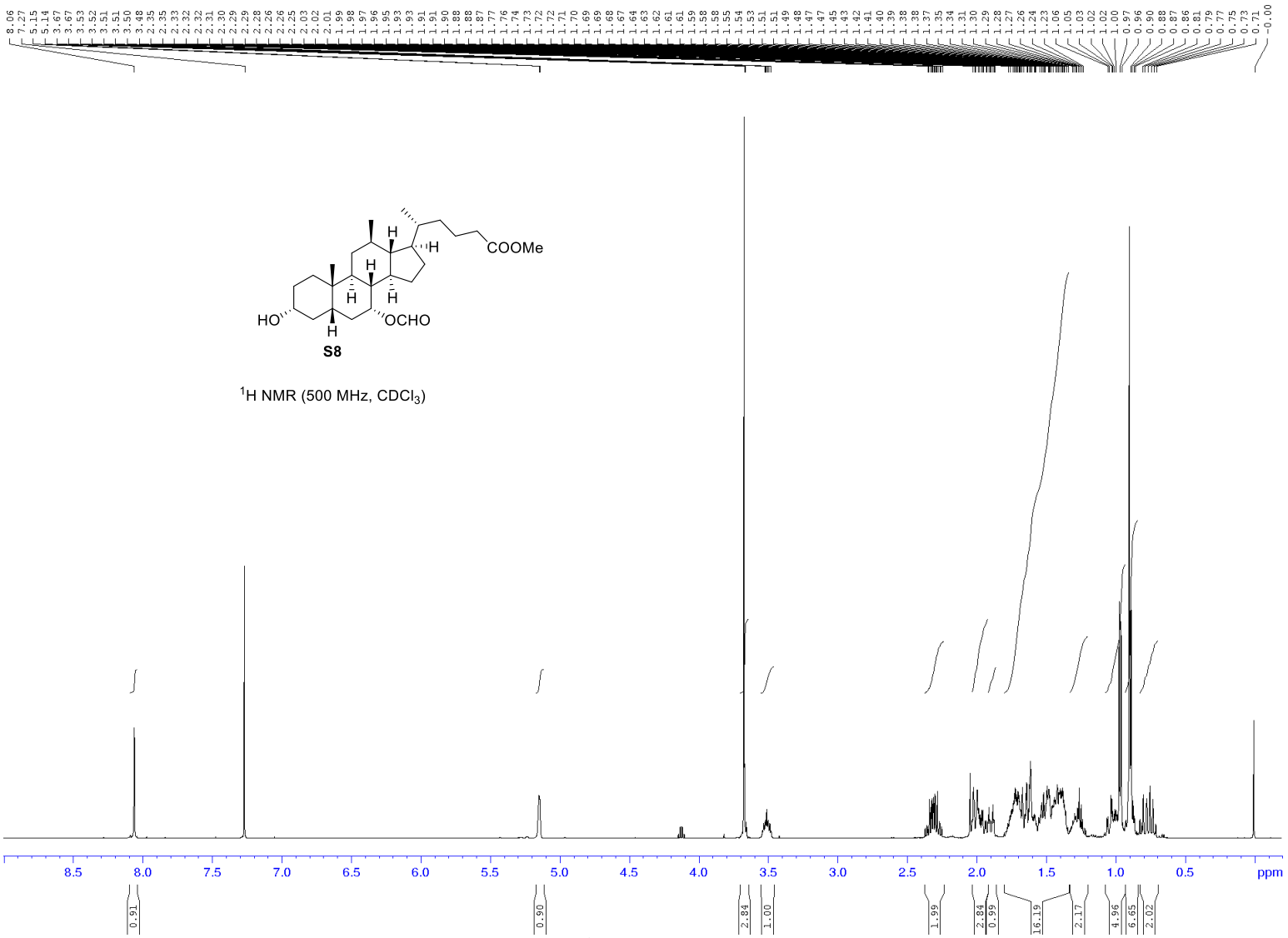

Figure S67a. ^{1}H NMR spectrum of **S8**.

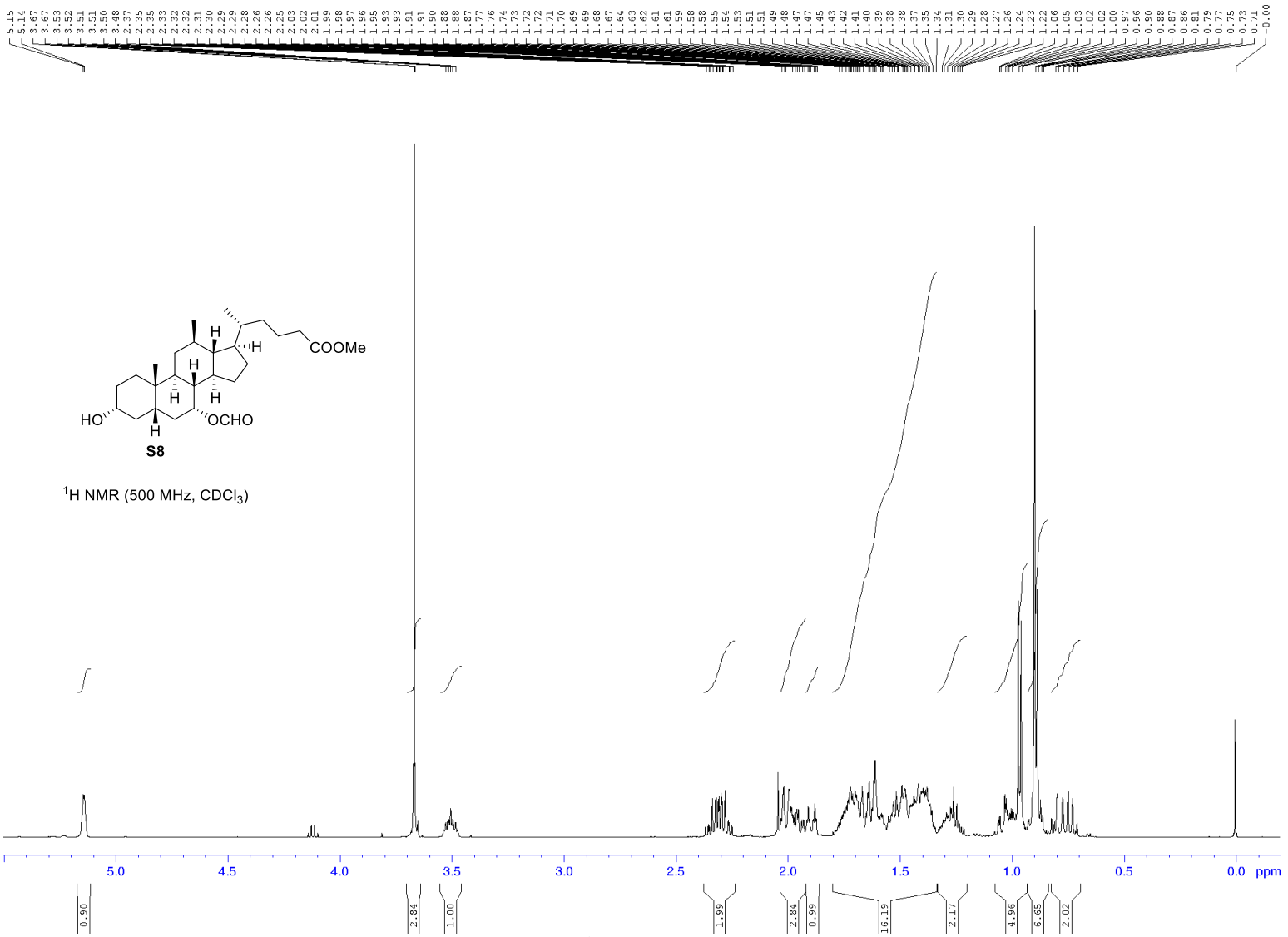

Figure S67b. ^{1}H NMR spectrum of **S8**.

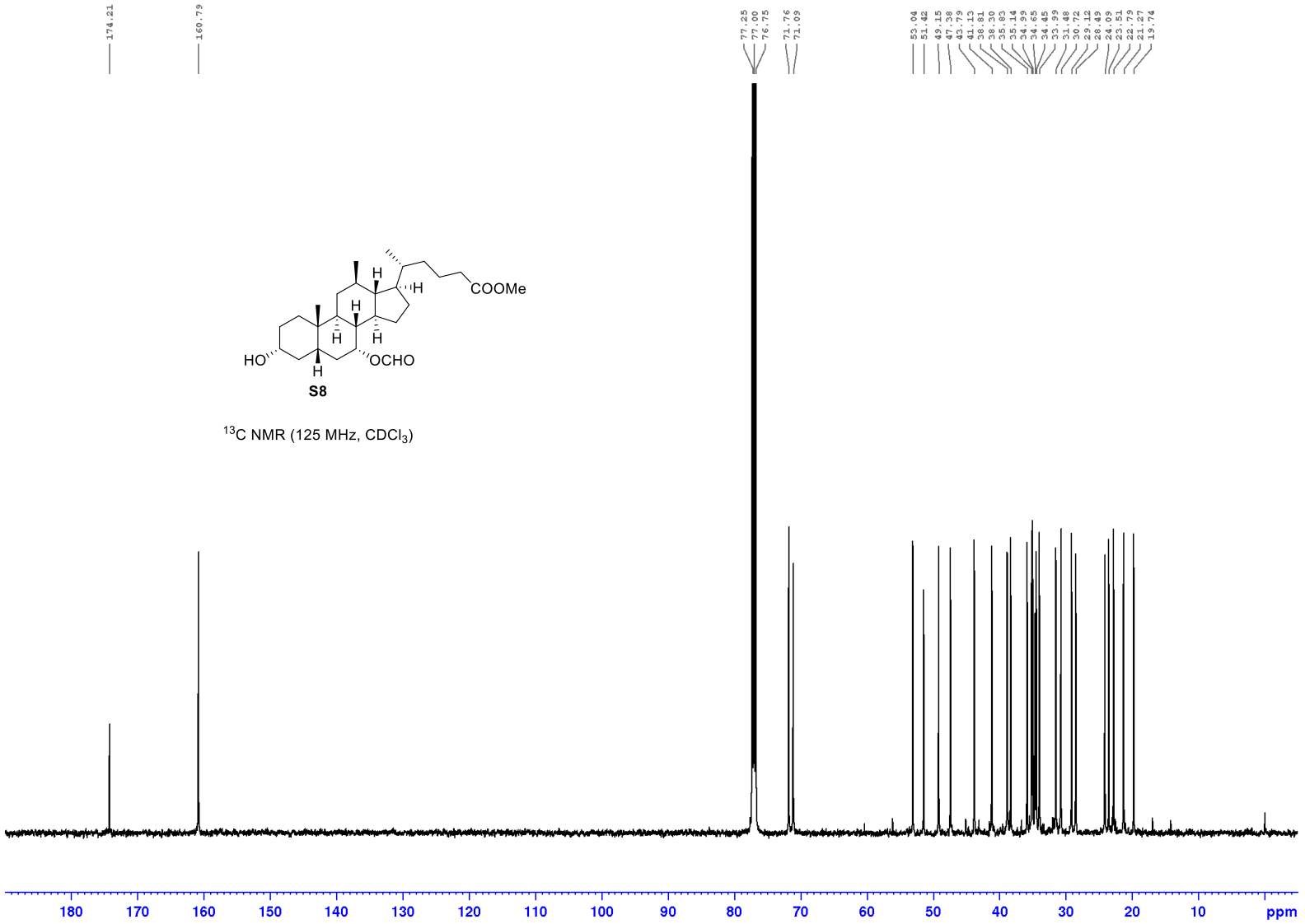

Figure S68. ^{13}C NMR spectrum of **S8**.

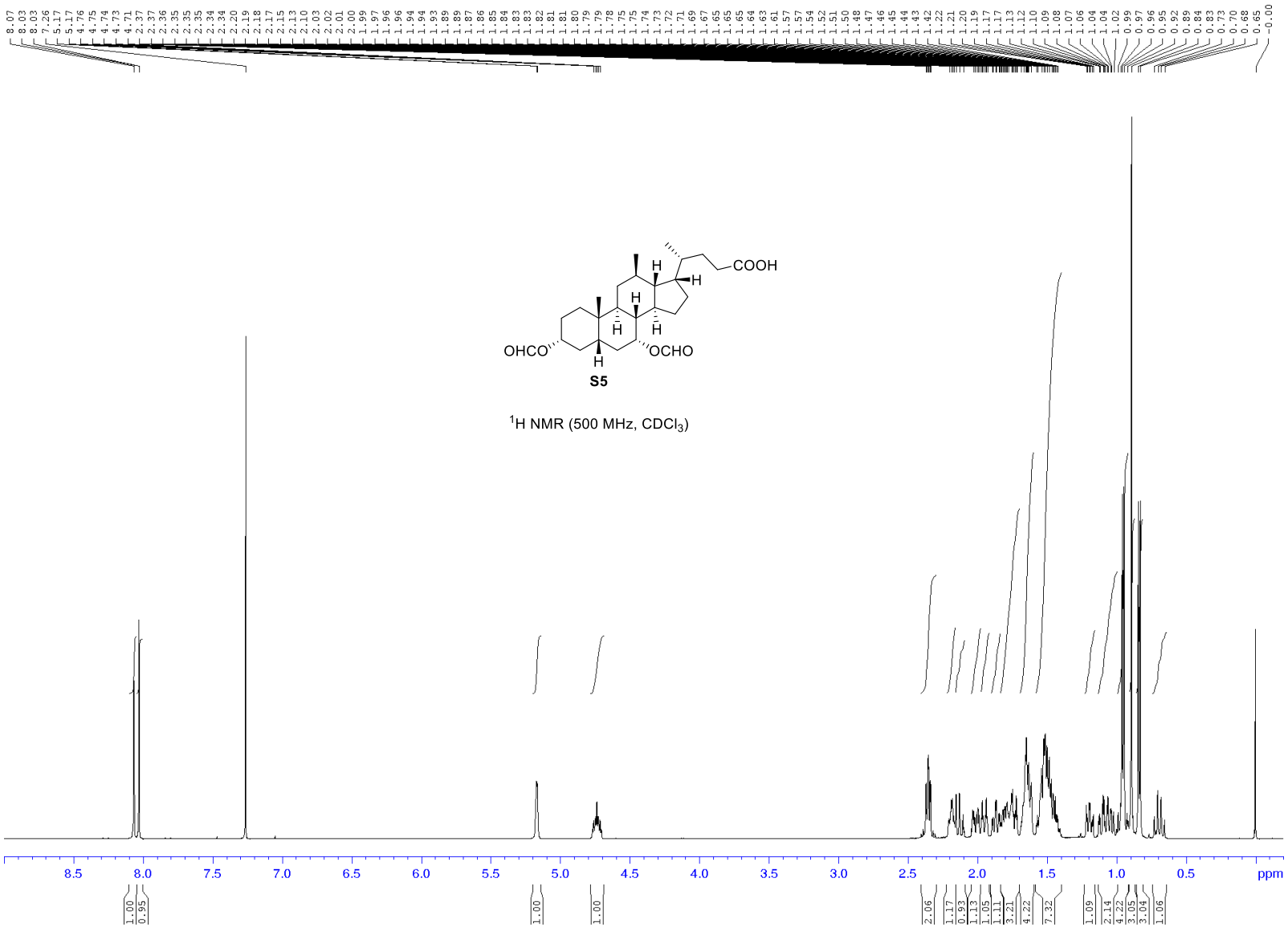

Figure S69a. ^{1}H NMR spectrum of **S5**.

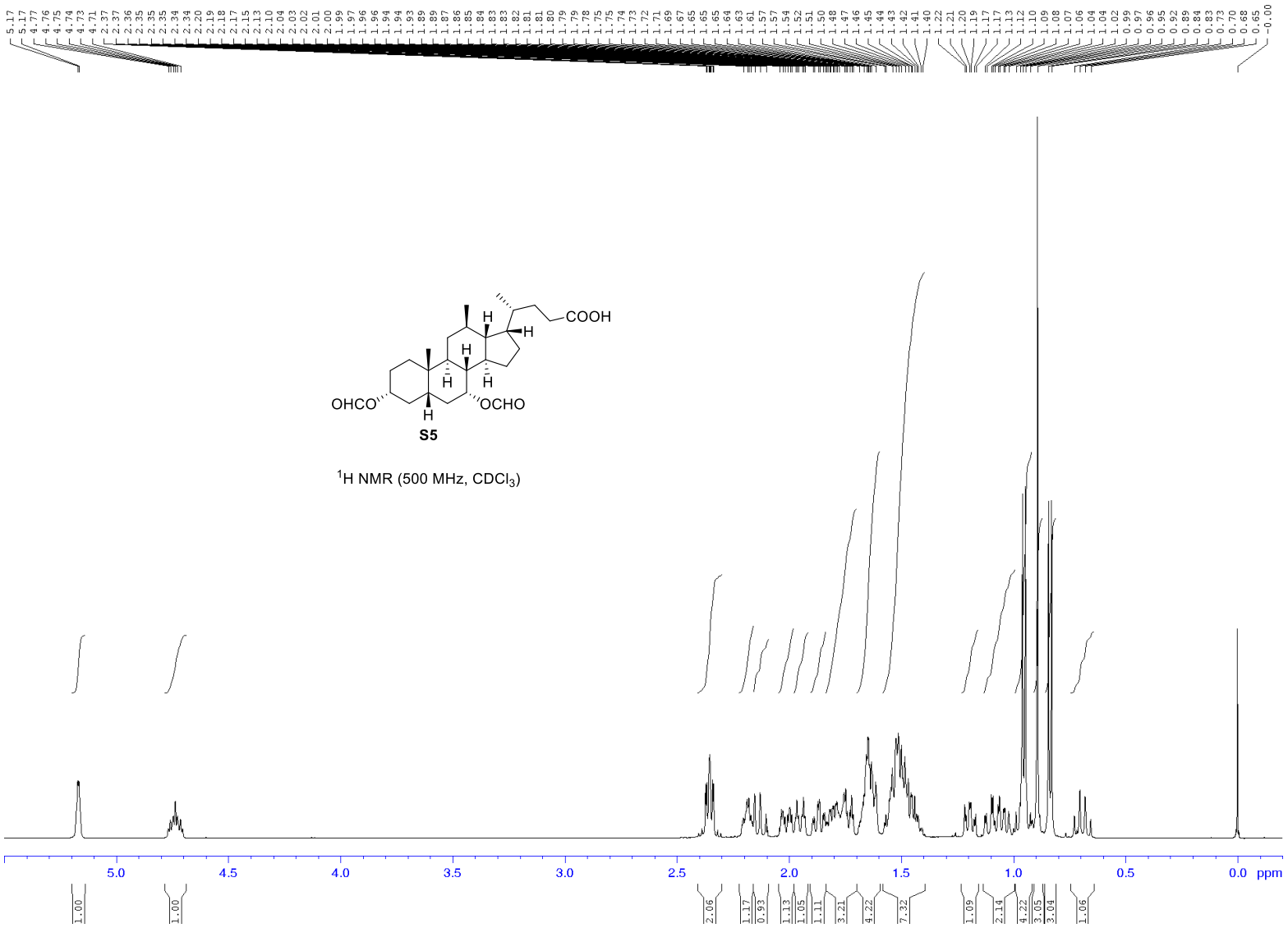

Figure S69b. ^{1}H NMR spectrum of **S5**.

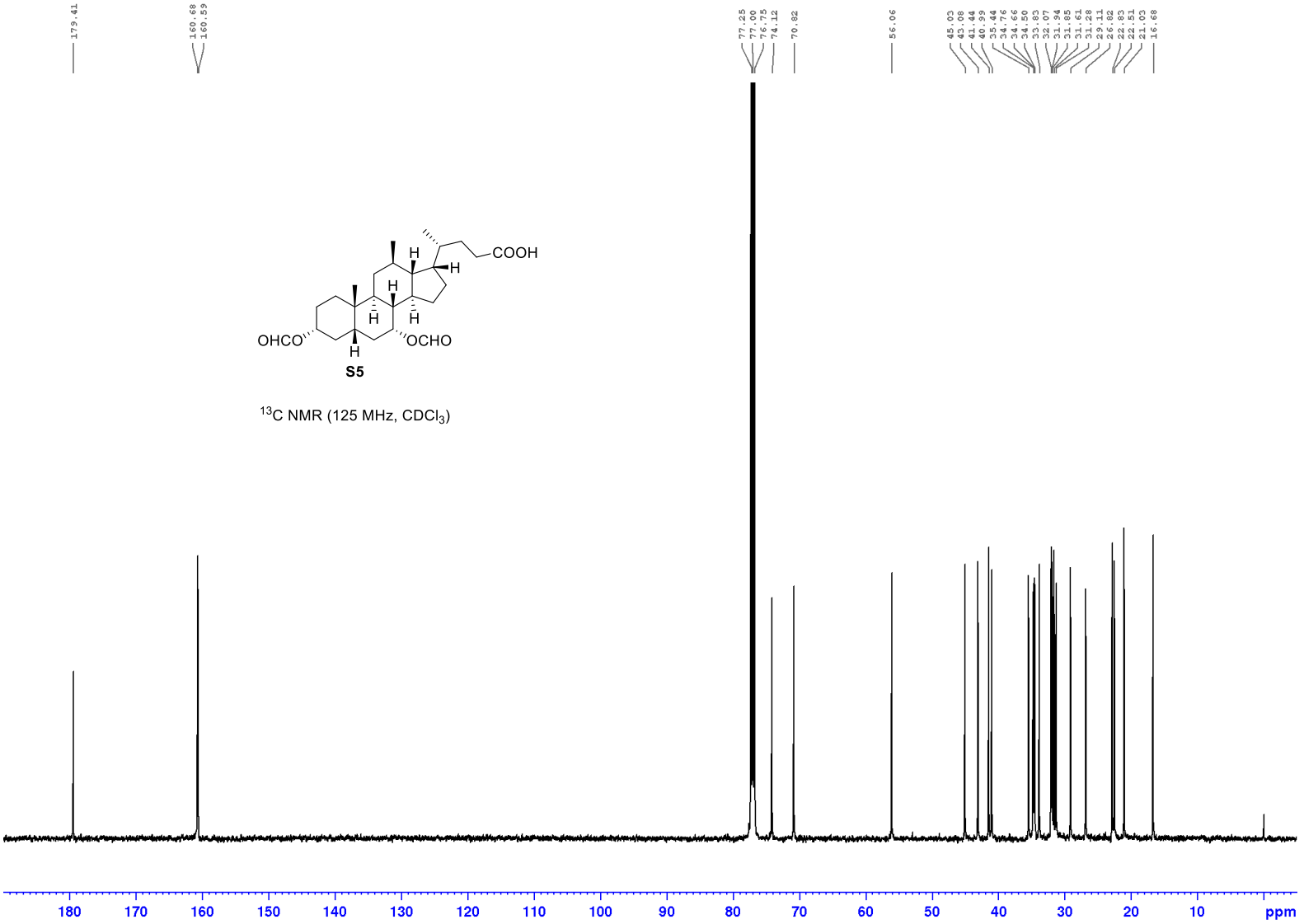

Figure S70. ^{13}C NMR spectrum of **S5**.

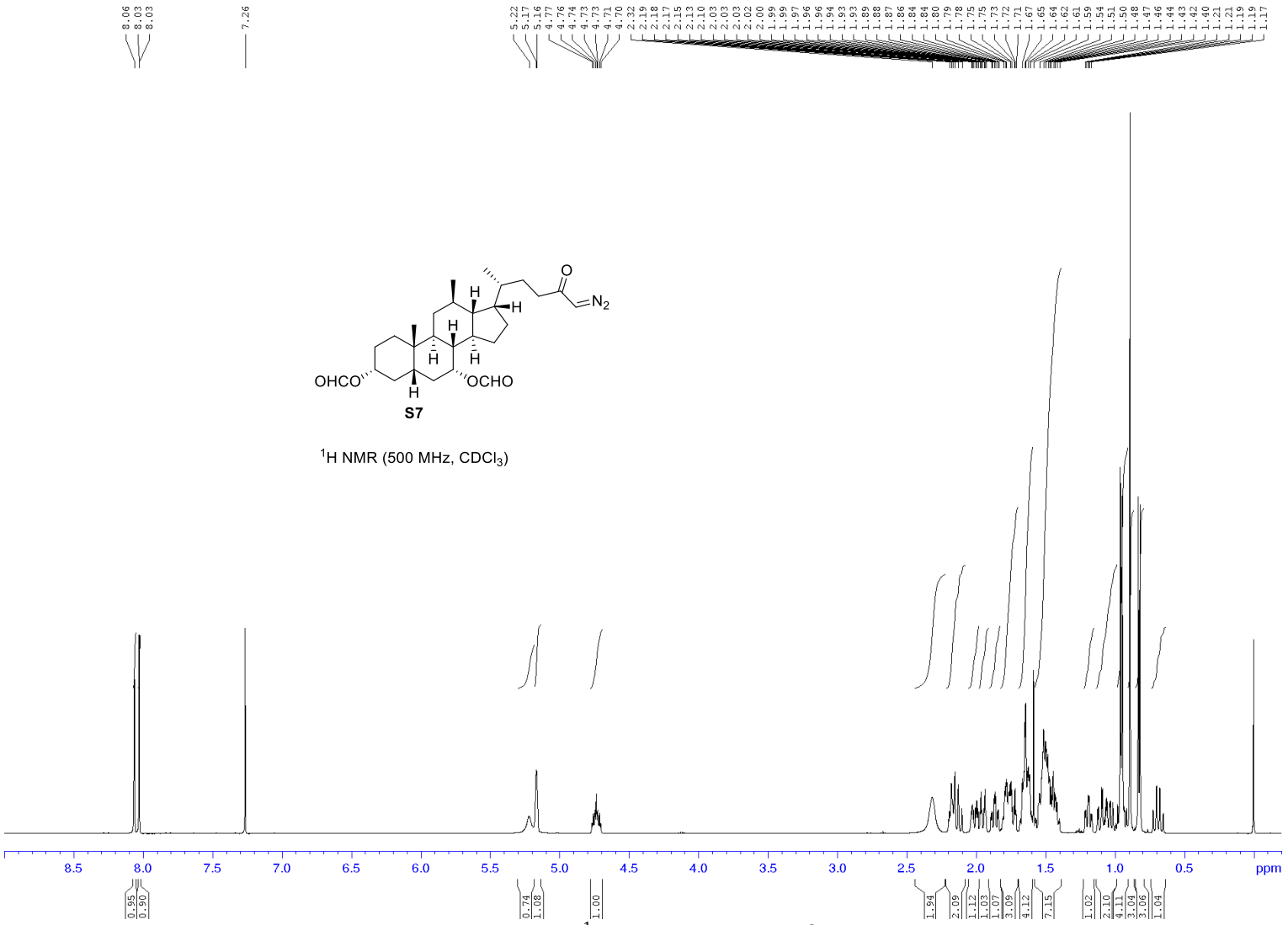

Figure S71a. ^{1}H NMR spectrum of **S7**.

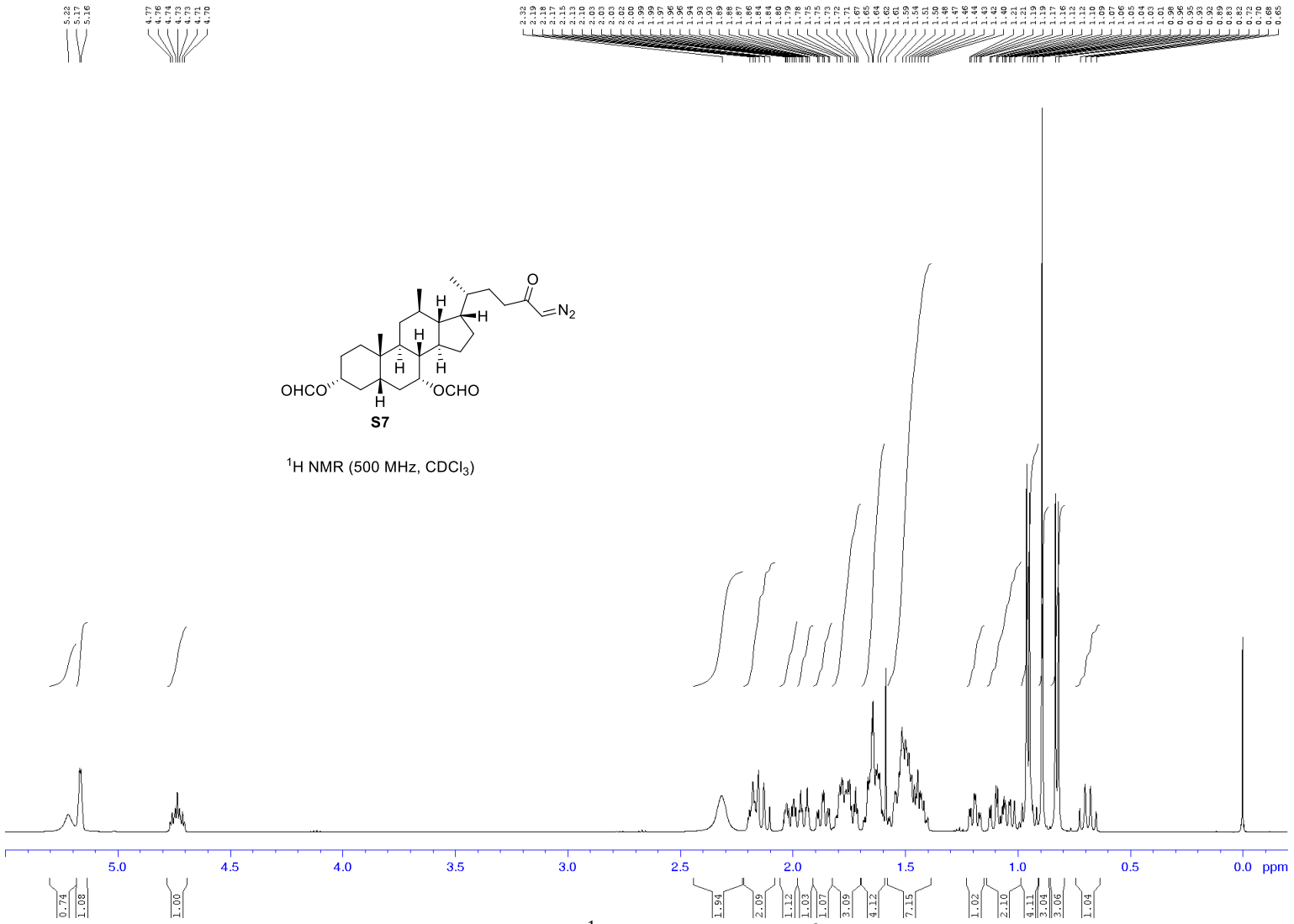

Figure S71b. ^{1}H NMR spectrum of **S7**.

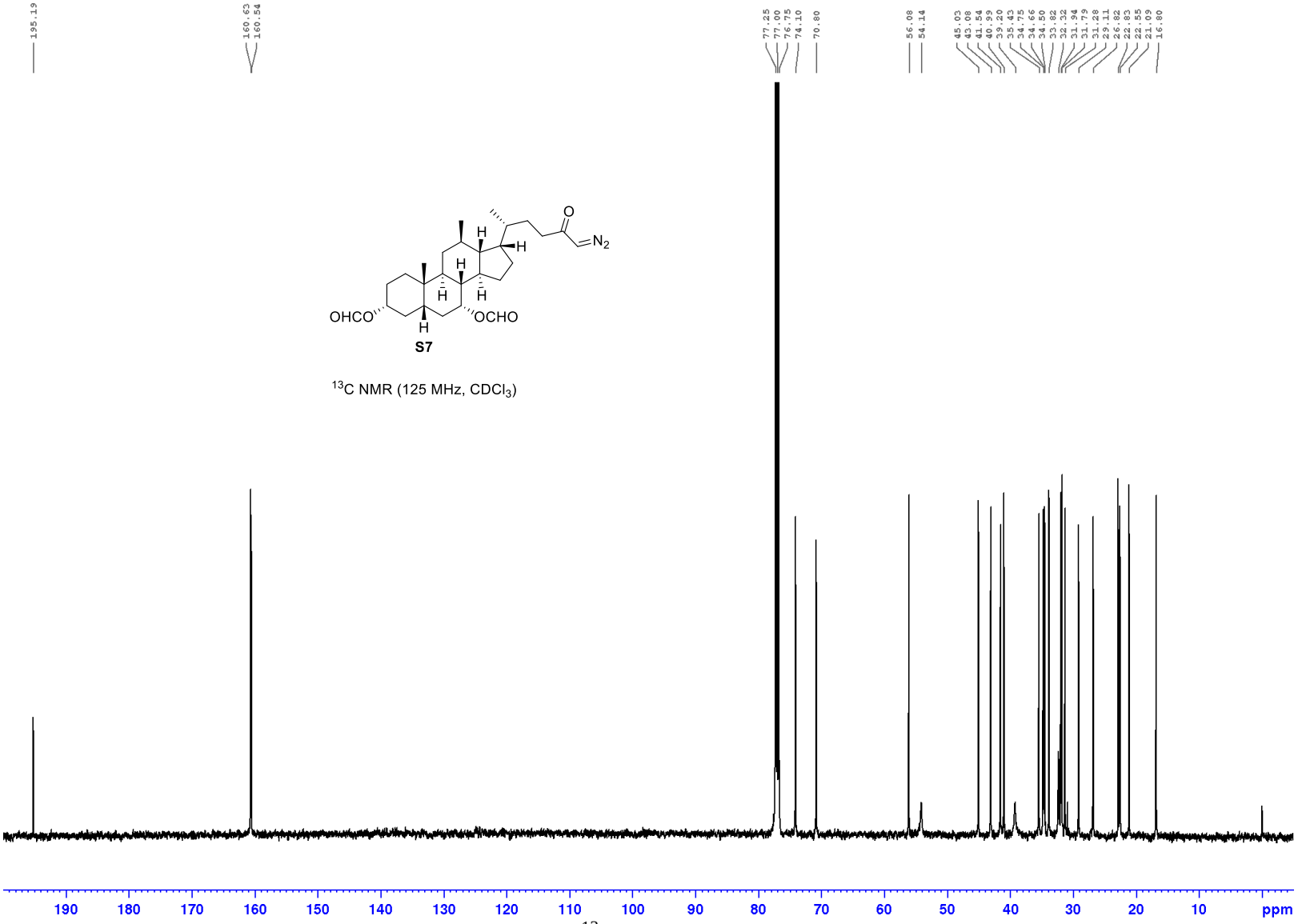

Figure S72. ^{13}C NMR spectrum of **S7**.

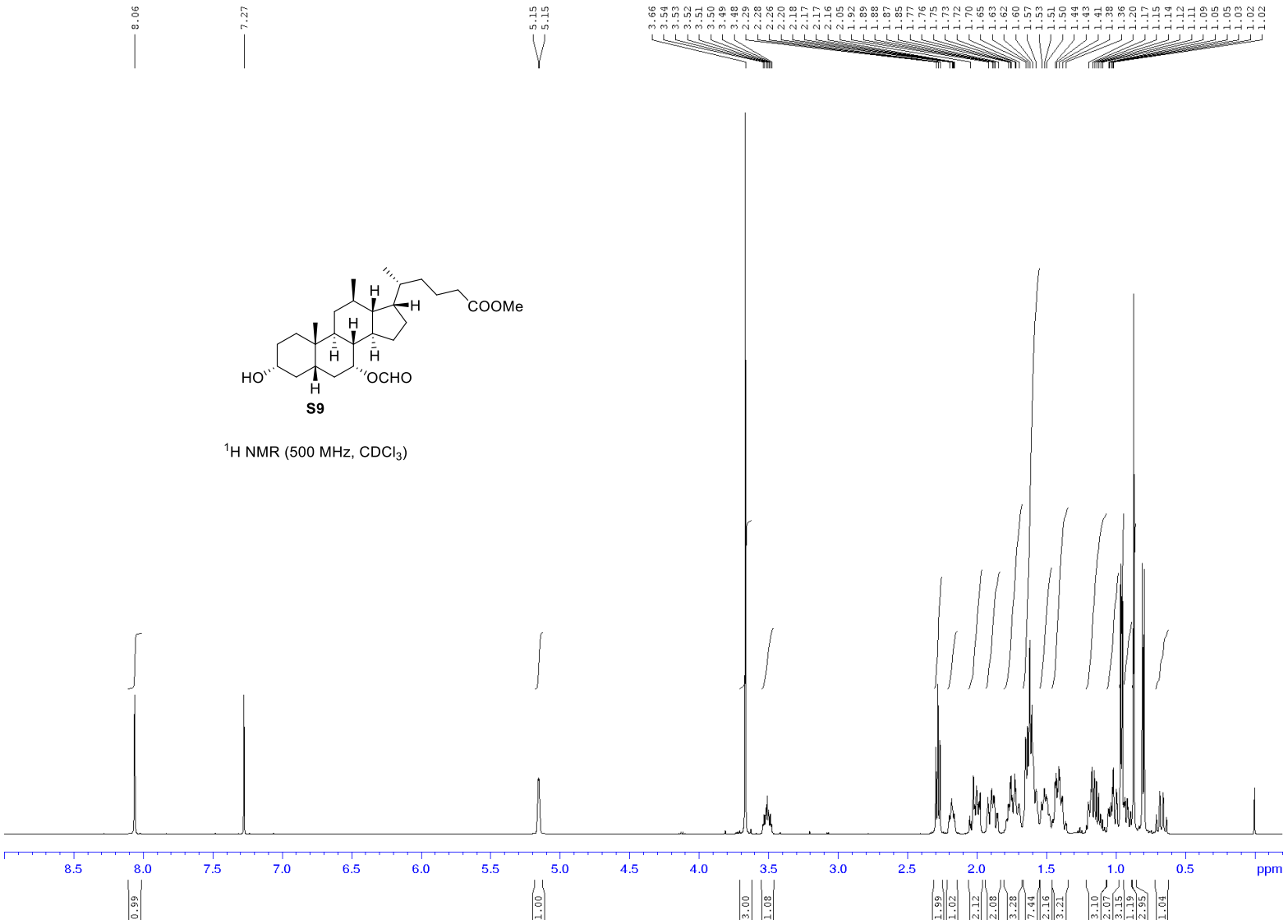

Figure S73a. ^{1}H NMR spectrum of **S9**.

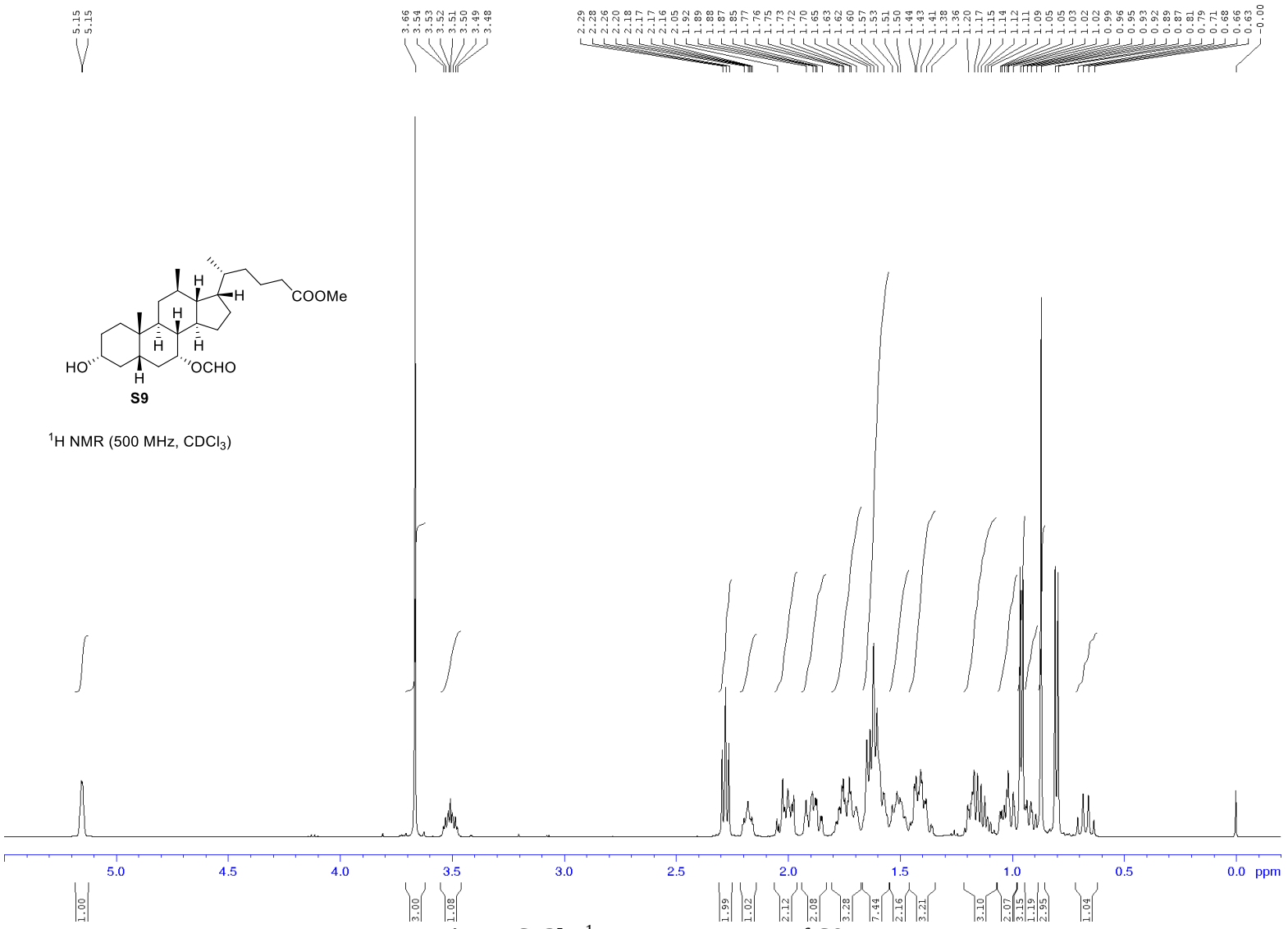

Figure S73b. ^{1}H NMR spectrum of **S9**.

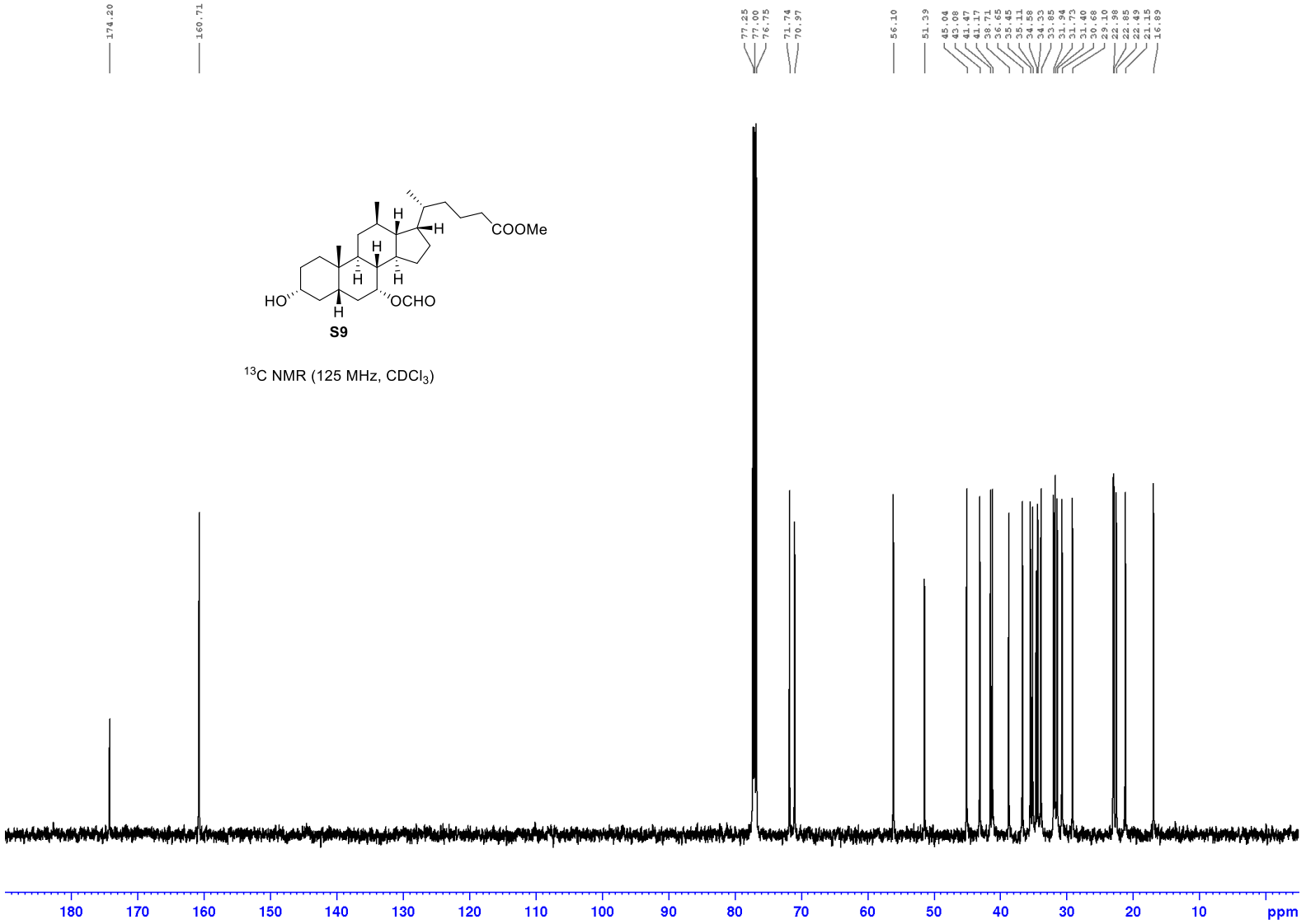

Figure S74. ^{13}C NMR spectrum of **S9**.

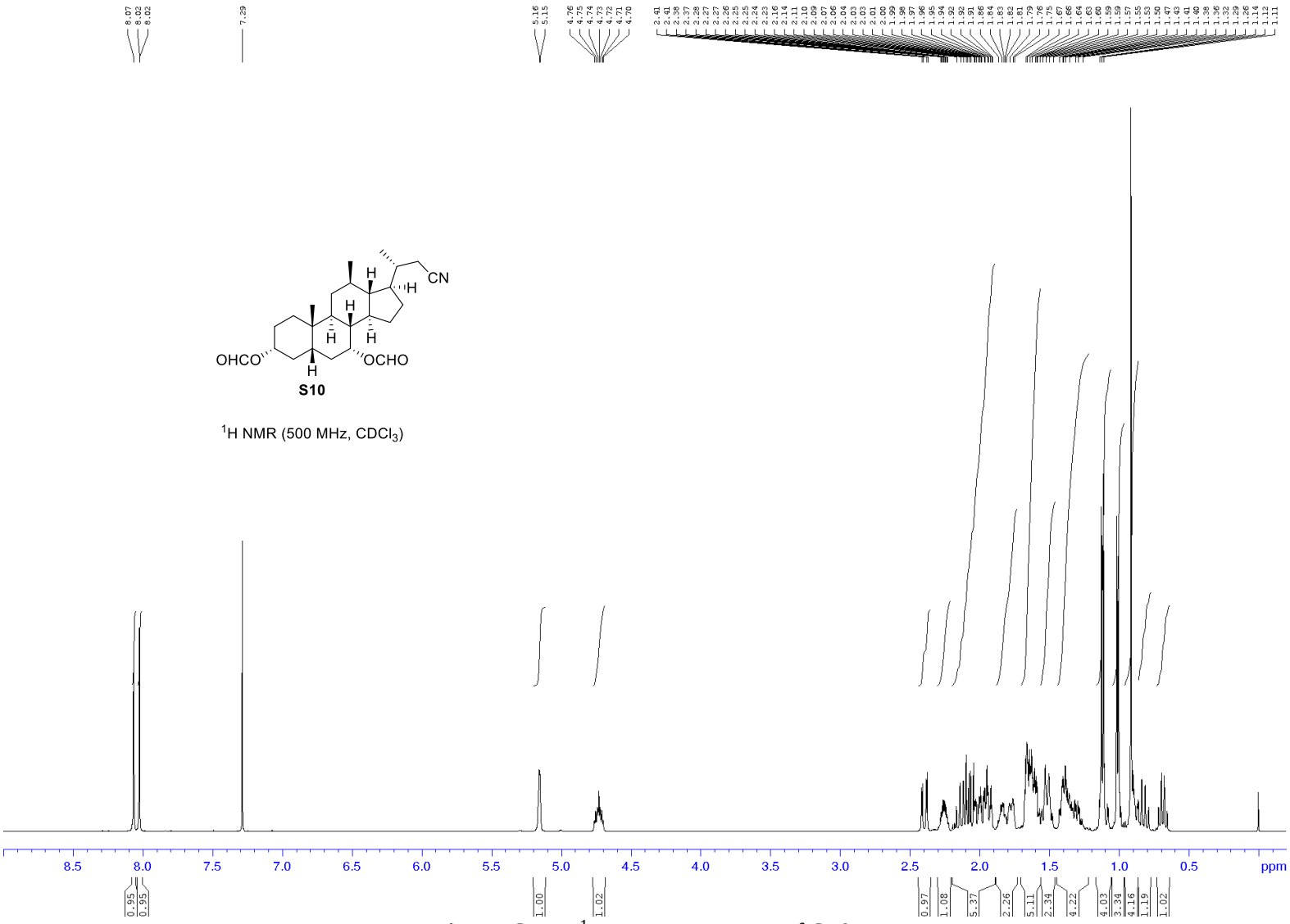

Figure S75a. ^{1}H NMR spectrum of **S10**.

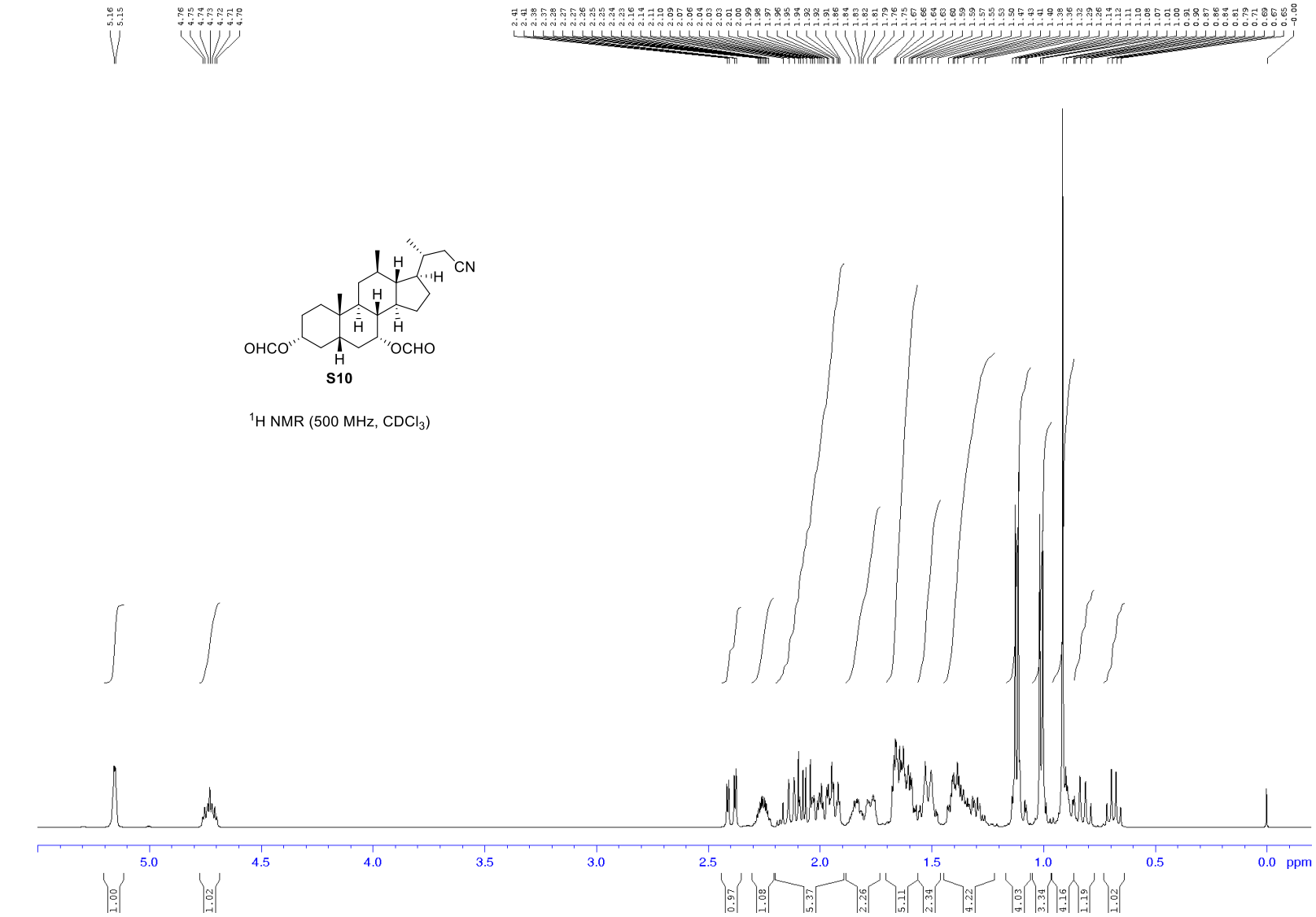

Figure S75b. ^{1}H NMR spectrum of **S10**.

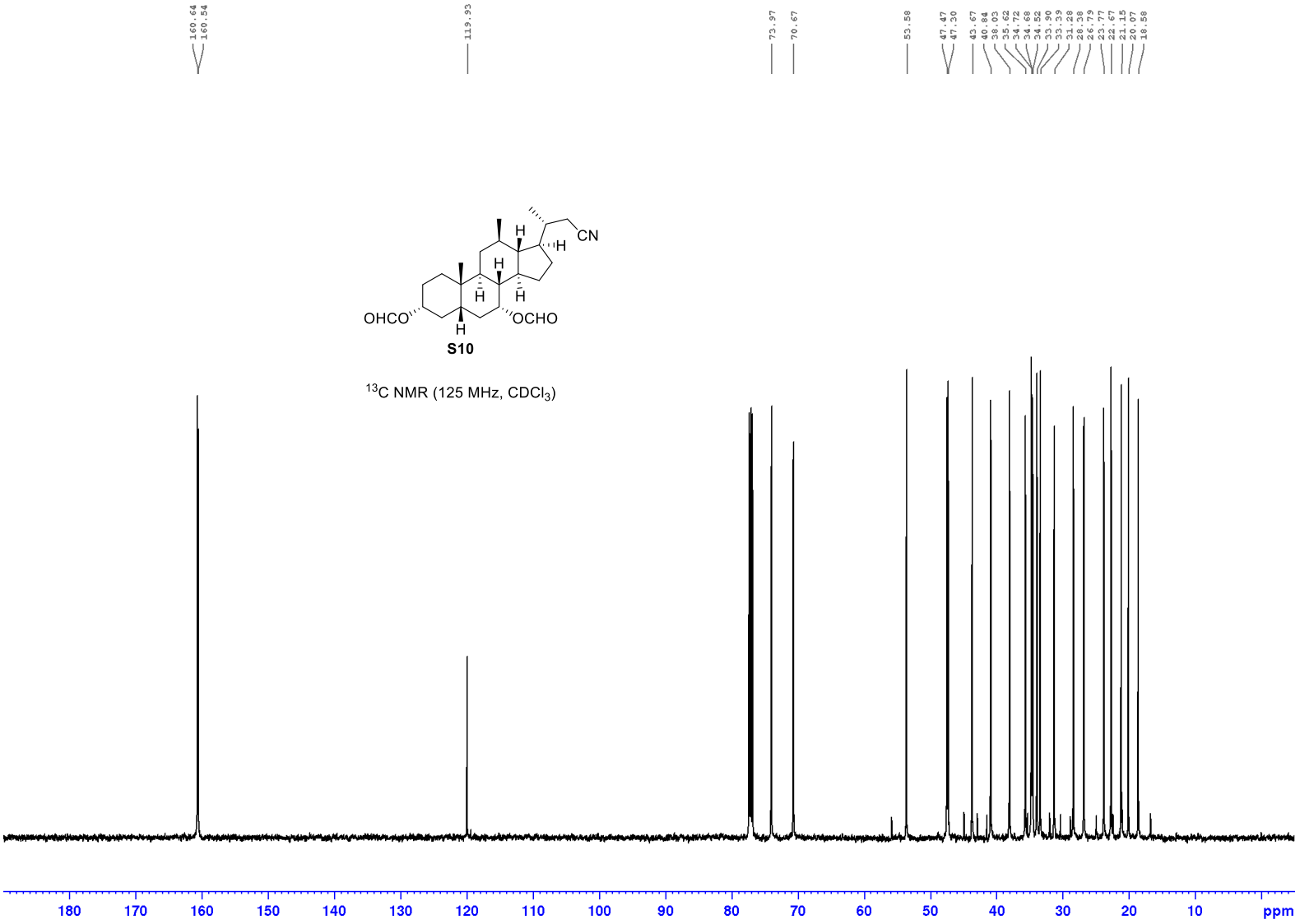

Figure S76. ^{13}C NMR spectrum of **S10**.

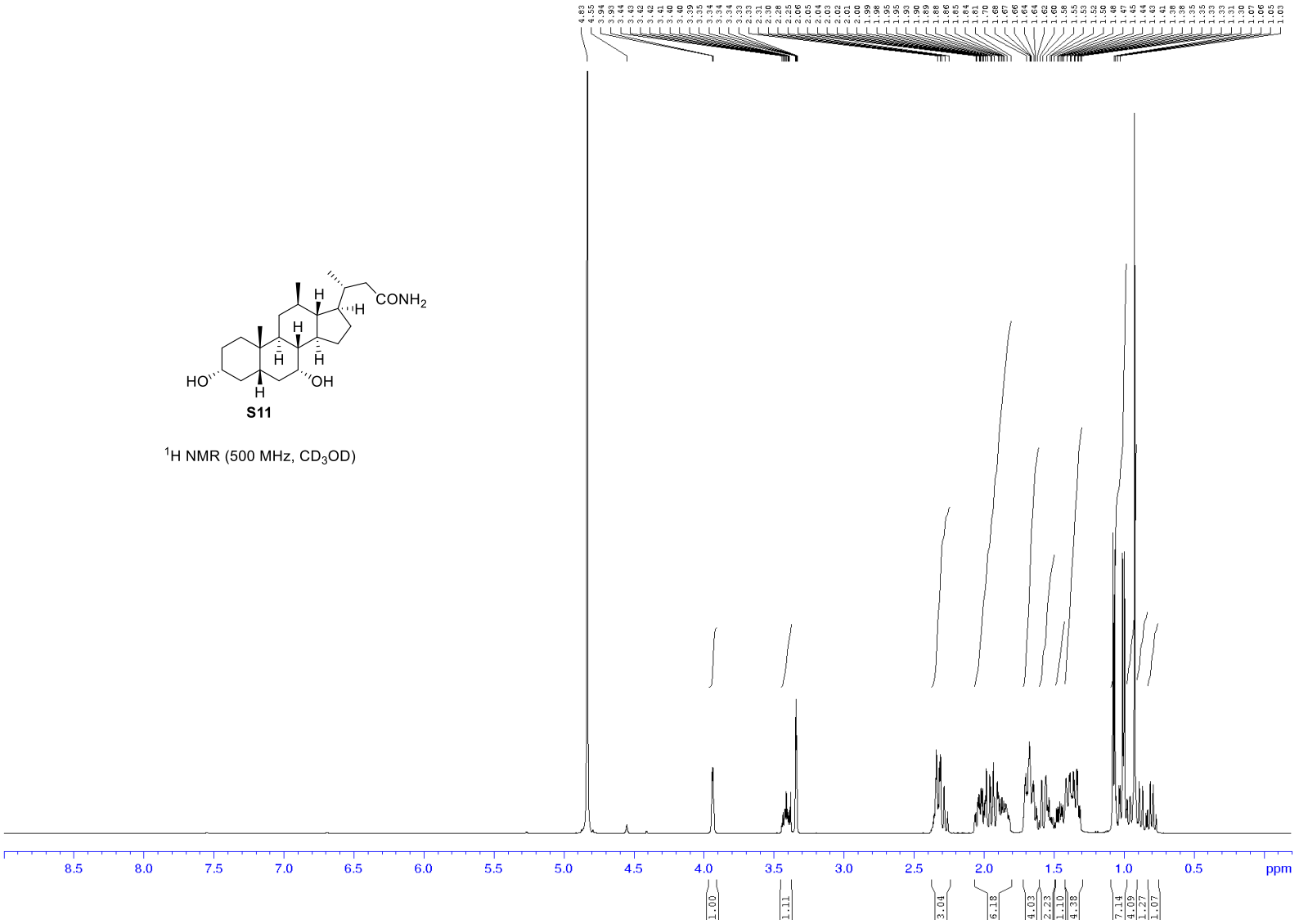

Figure S77a. ^{1}H NMR spectrum of **S11**.

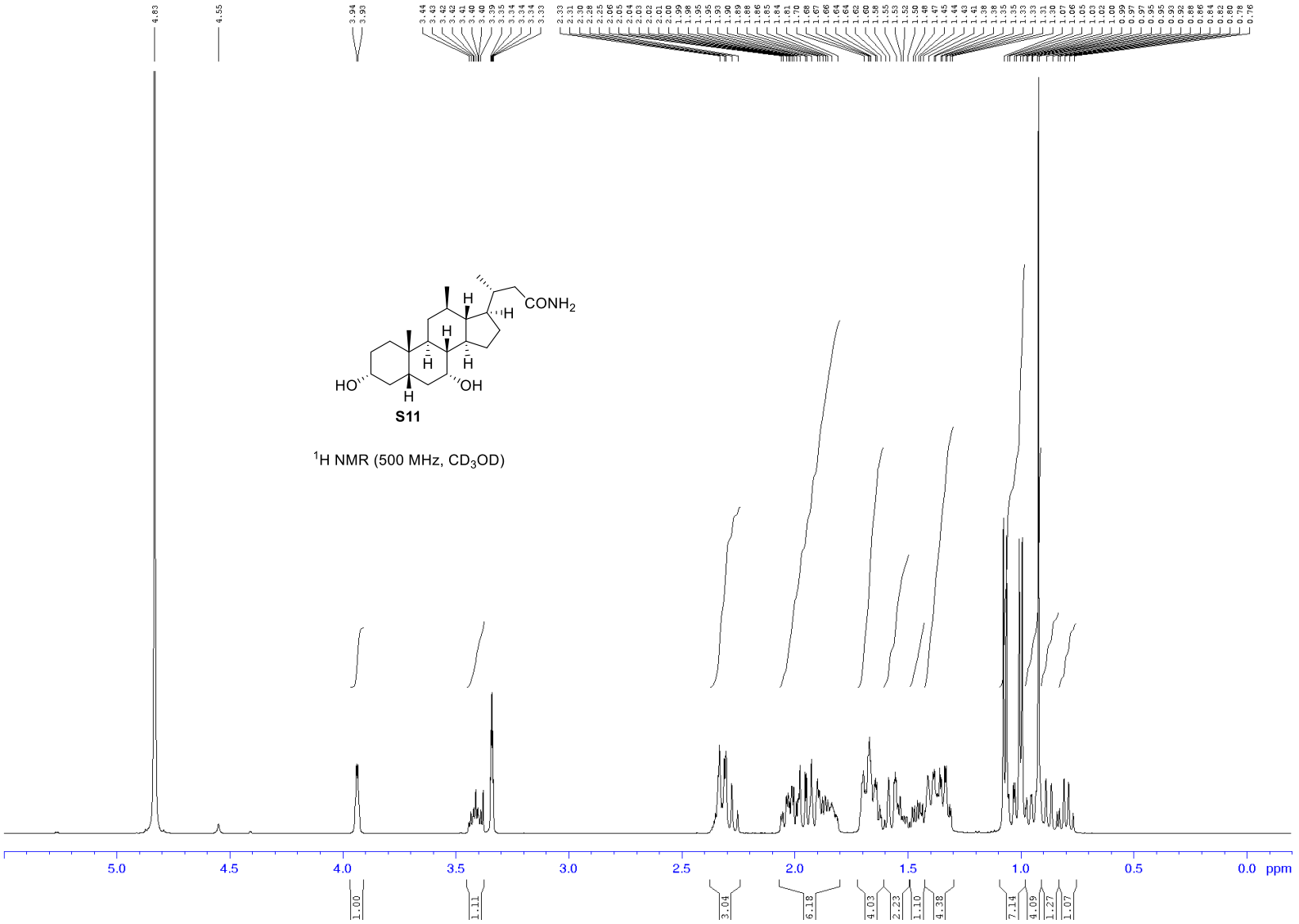

Figure S77b. ^{1}H NMR spectrum of **S11**.

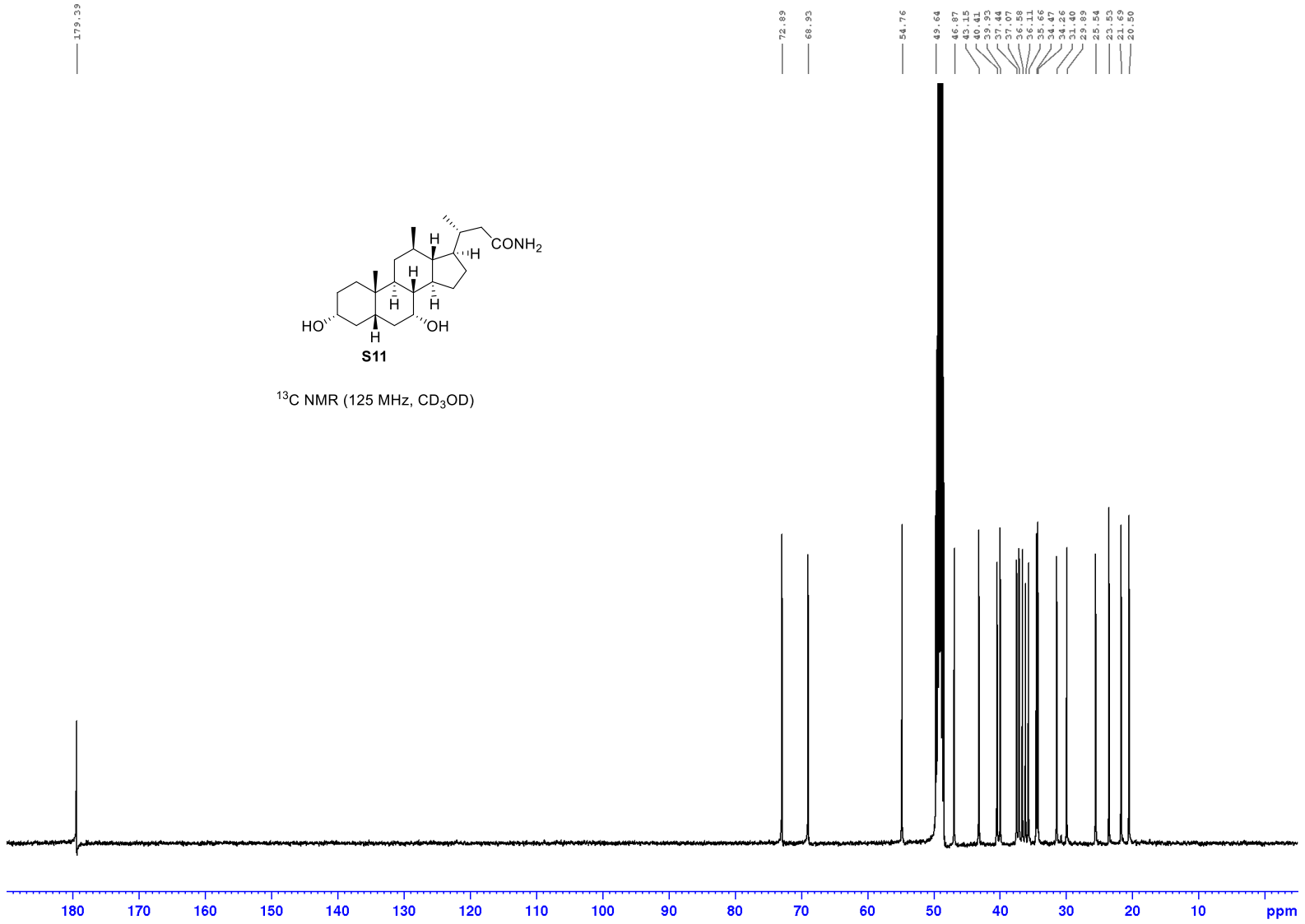

Figure S78. ^{13}C NMR spectrum of **S11**.

5. Pulse sequences used to acquire ^{13}C NMR spectra

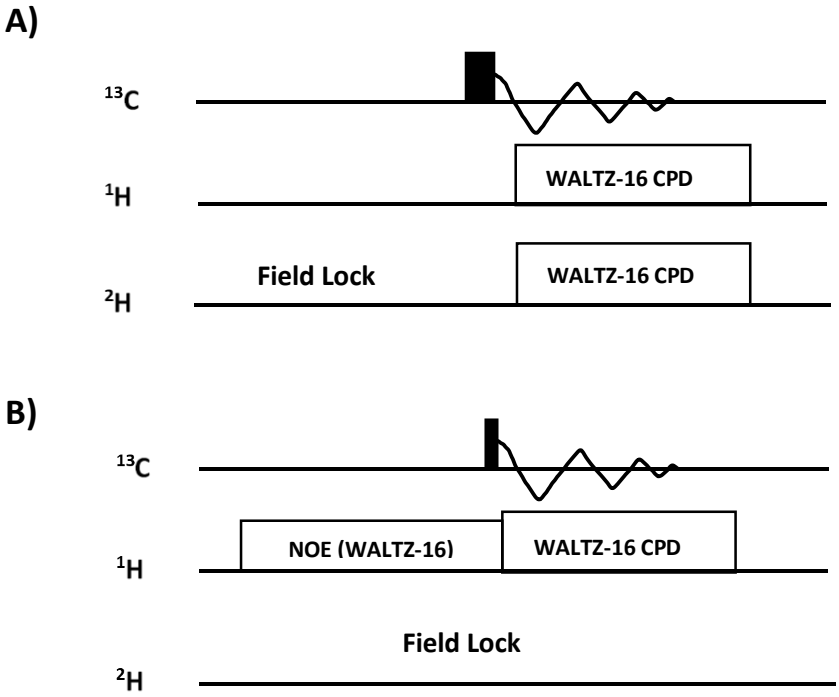

Figure S79. Pulse sequences used to acquire ^{13}C NMR spectra. **A**) ^{13}C with simultaneous inverse-gated ^{1}H and ^{2}H WALTZ-16 composite pulse decoupling during acquisition of FID, ^{2}H field lock only applied during recycle delay (zgig1h2hf3.arl); **B**) ^{13}C with power-gated ^{1}H WALTZ-16 composite pulse decoupling to build-up NOE and decouple ^{1}H during acquisition of FID, ^{2}H field lock applied continuously (standard zgpg30 pulse sequence).

```
;zgig1h2hf3.arl
;A. Lewis Callaghan Innovation, Rainer Kuemmerle Bruker Oct 1 2019
;1D 13C sequence with simultaneous inverse-gated 1H and 2H
decoupling
;avance-version for Bruker Topspin 2.x, 3.x
;using 2H lockswitch unit or BSMS 2H-TX board
;$CLASS=HighRes
;$DIM=1D
;$TYPE=
;$SUBTYPE=
;$COMMENT=
;$OWNER=Administrator
#include <Avance.incl>

"acqt0=-p1*2/3.1416"
"d11=30m"
"d12=20u"

1 ze
```

```
  d11 pl12:f2 pl17:f3
  50u LOCKDEC_ON
  50u LOCKH_ON
  d11 H2_PULSE

2 d11 do:f2 do:f3
  d11 H2_LOCK
  d12 LOCKH_OFF
  d1
  50u LOCKH_ON
  d12 H2_PULSE
  p1 ph1
  go=2 ph31 cpd2:f2 cpd3:f3
  d11 do:f2 do:f3 mc #0 to 2 F0(zd)
  d11 H2_LOCK
  d11 LOCKH_OFF
  d11 LOCKDEC_OFF
exit

ph1=0 2 2 0 1 3 3 1
ph31=0 2 2 0 1 3 3 1


;pl1 : f1 channel - power level for pulse (default)
;pl12: f2 channel - power level for CPD/BB decoupling
;pl17: f3 channel - power level for CPD/BB decoupling
;p1 : f1 channel -  high power pulse
;d1 : relaxation delay; 1-5 * T1
;d11: delay for disk I/O                             [30 msec]
;d12: delay for power switching                      [20 usec]
;cpd3: decoupling according to sequence defined by cpdprg3
;pcpd3: f3 channel - 90 degree pulse for decoupling sequence
;after locking run lock.3 macro
```

6. HPLC traces

6.1. HPLC analysis of crude rearrangement mixture 24a/25a

Scheme S4.

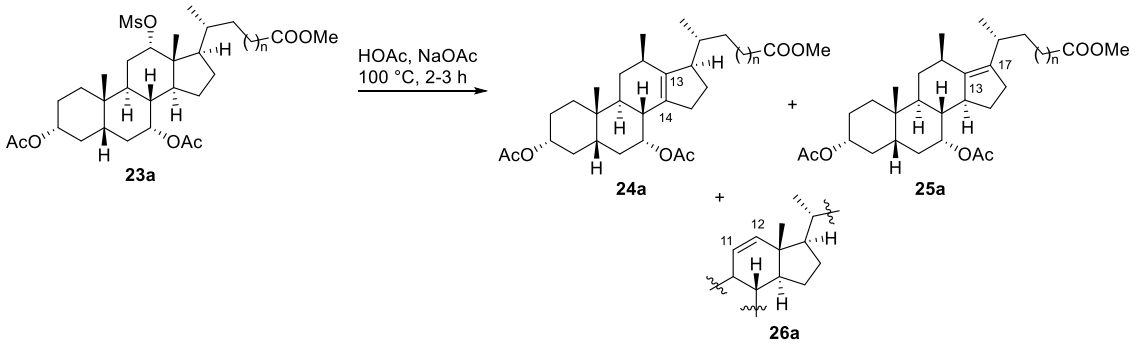

Method conditions:

Column:	Phenomenex Kinetex 2.6 µM C-18, pore size = 100 Å, 50 x 30 mm
Mobile Phase:	**A**: Water + 0.1% Formic Acid, **B**: Methanol
Gradient:	%B: T0=72, T6=72, T7=100, T9=100, T10=72, T12=72
Flow Rate:	1 mL/min
Sample Solvent:	Methanol
Detection:	Agilent 1290 Infinity II ELSD
Column Temp:	40 °C
Injection volume:	2.0 µL

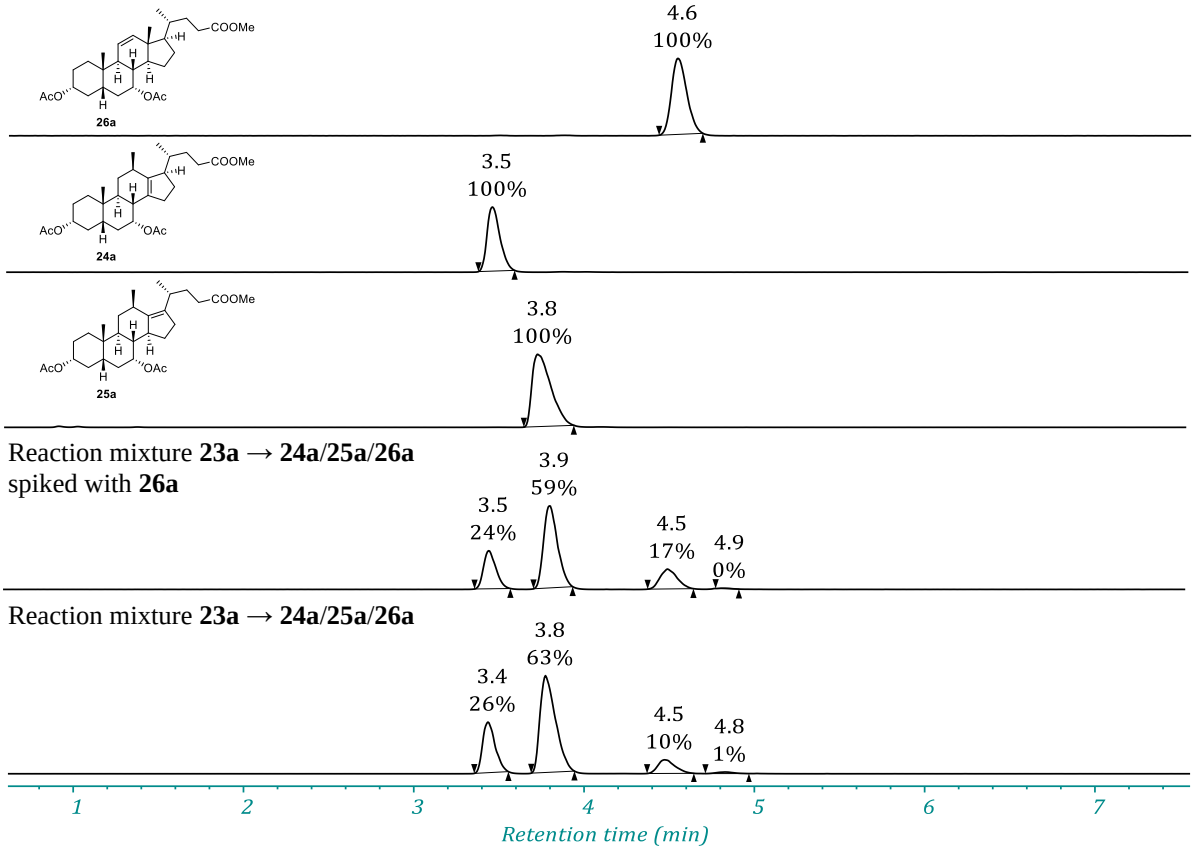

Figure S80.

6.2. HPLC analysis of crude mixture of 12β-methyl-18-*nor*-bile acids: 27a/28a/29/30/31/32

Method conditions:

Column: Phenomenex Kinetex 2.6 µM C-18, pore size = 100 Å, 50 x 30 mm
Mobile Phase: **A**: Water + 0.1% Formic Acid, **B**: Methanol
Gradient: %B: T0=60, T10=70, T11=100, T12=100, T14=60, T16
Flow Rate: 1 mL/min
Sample Solvent: Methanol
Detection: Agilent 1290 Infinity II ELSD
Column Temp: 40 °C
Injection volume: 2.0 µL

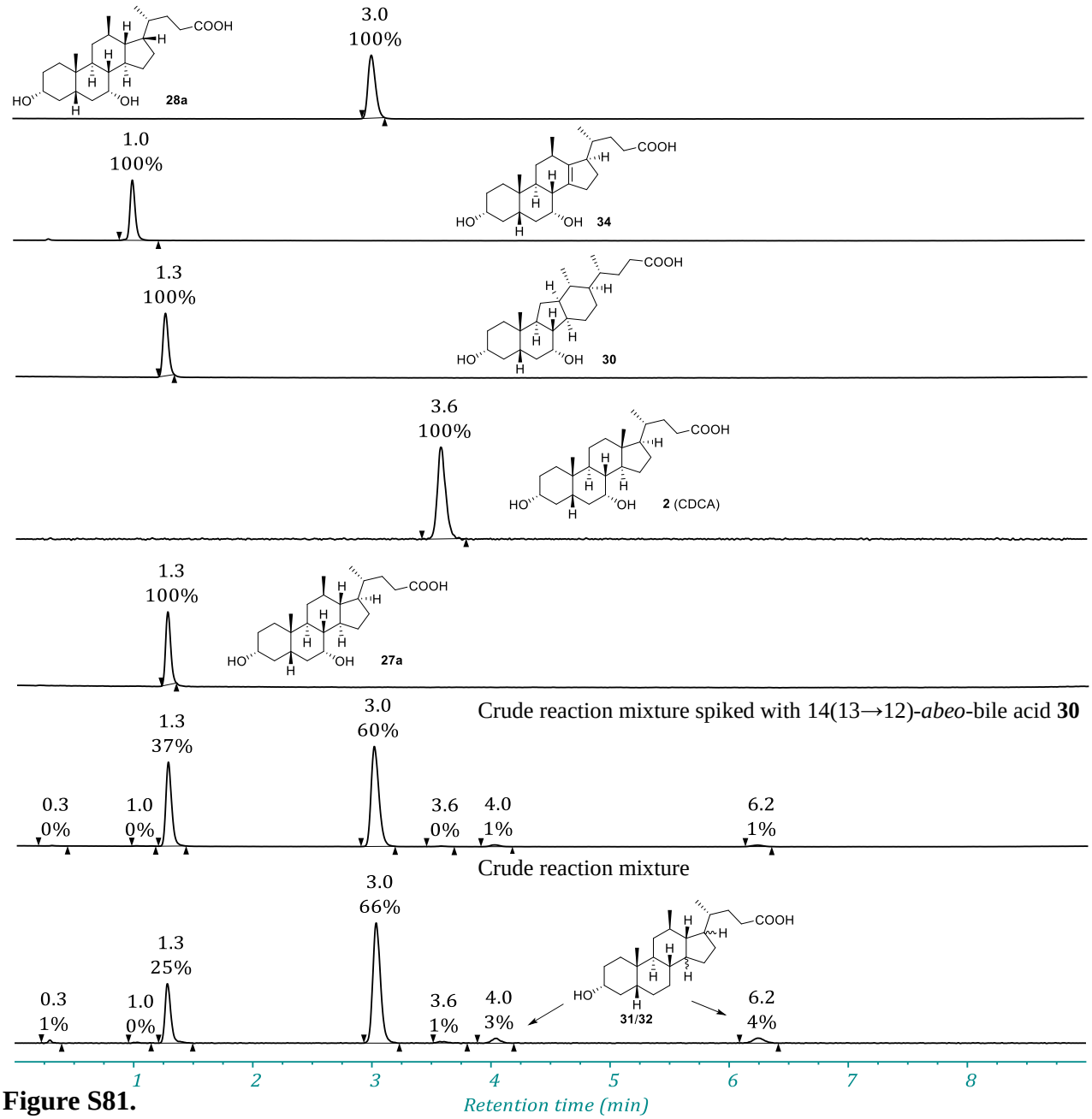

Figure S81.

6.3. HPLC traces of initially isolated samples of 27a, 28a, 29 and 30

Method conditions:

Column:	Phenomenex Luna C18(2) 5 mm 250x4.6 mm
Guard:	Phenomenex Security Guard C18 RP 4x3 mm
Mobile Phase:	20:80:0.05 Water/Methanol/Trifluoroacetic acid
Gradient:	Isocratic
Flow Rate:	1.0 mL/min
Sample Solvent:	Methanol
Detection:	*Refractive index*
Column Temp:	20 °C
Injection volume:	20 µL

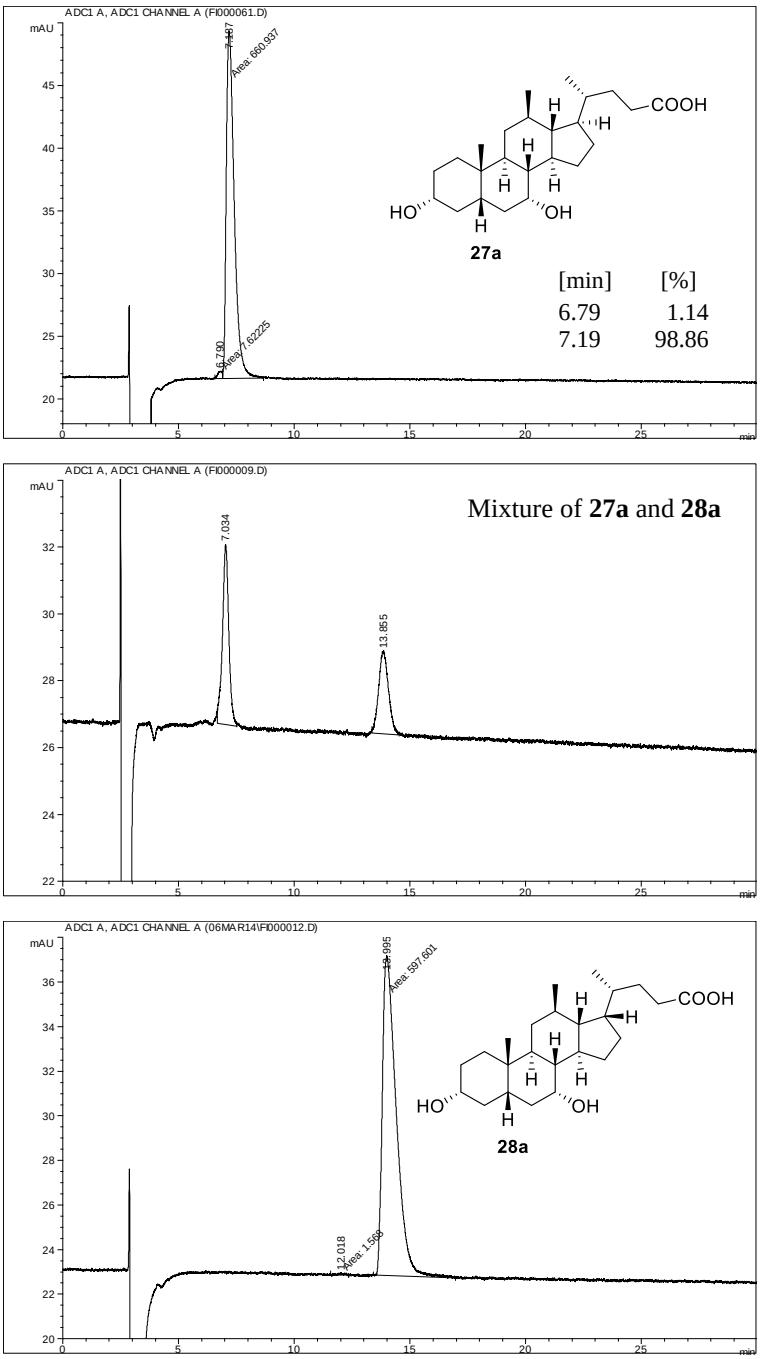

Figure S82a. HPLC traces of **27a** and **28a**.

Method conditions:

Column:	Phenomenex Luna C18(2) 5 mm 250x4.6 mm
Guard:	Phenomenex Security Guard C18 RP 4x3 mm
Mobile Phase:	30:70:0.05 Water/Methanol/Trifluoroacetic acid
Gradient:	Isocratic
Flow Rate:	1 mL/min
Sample Solvent:	Methanol
Detection:	*Refractive index*
Column Temp:	20 °C
Injection volume:	30 µL

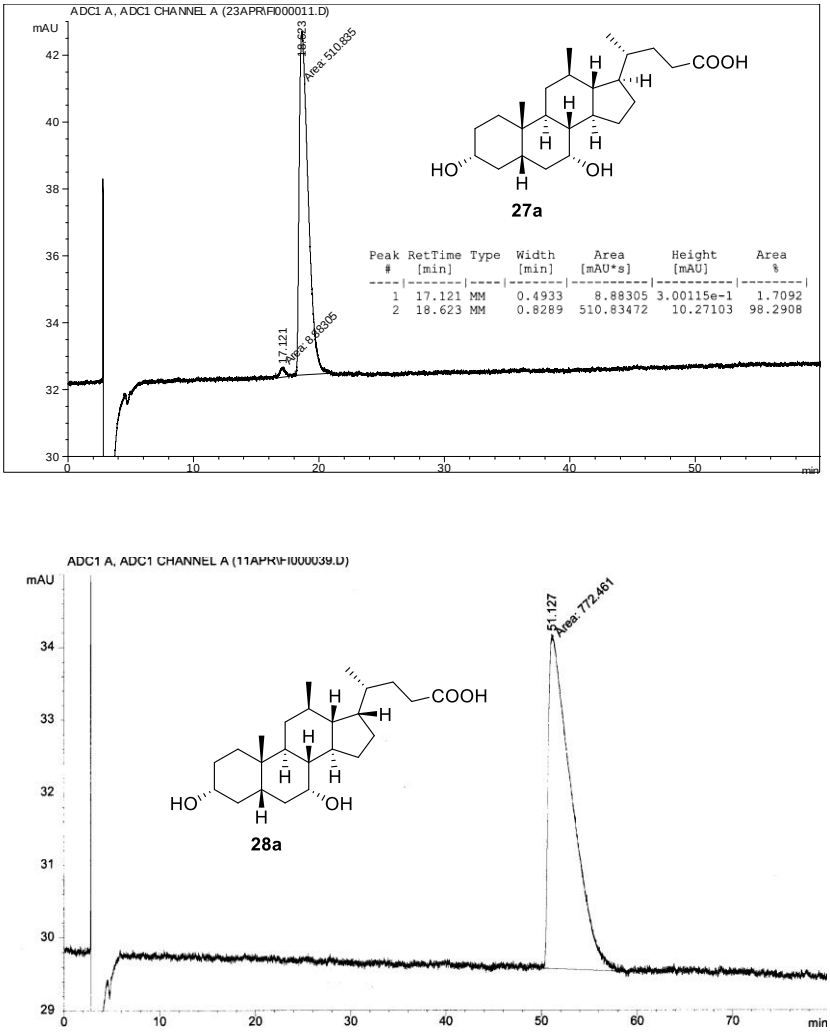

Figure S82b. HPLC traces of **27a** and **28a**.

Method conditions:

Column:	Phenomenex Luna C18(2) 5 mm 250x4.6 mm
Guard:	Phenomenex Security Guard C18 RP 4x3 mm
Mobile Phase:	20:80:0.05 Water/Methanol/Trifluoroacetic acid
Gradient:	Isocratic
Flow Rate:	1 mL/min
Sample Solvent:	Methanol
Detection:	*Refractive index*
Column Temp:	20 °C
Injection volume:	30 µL

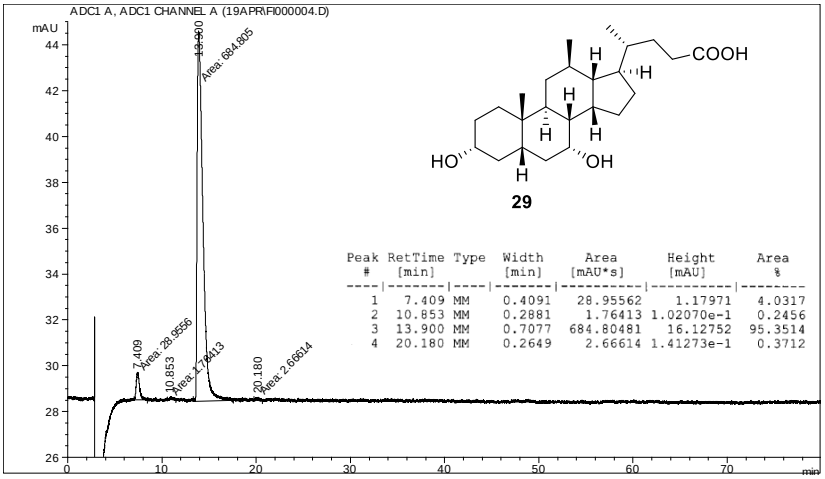

Figure S83. HPLC trace of **29**.

Method conditions:

Column:	Phenomenex Luna C18(2) 5 mm 250x4.6 mm
Guard:	Phenomenex Security Guard C18 RP 4x3 mm
Mobile Phase:	30:70:0.05 Water/Methanol/Trifluoroacetic acid
Gradient:	Isocratic
Flow Rate:	1 mL/min
Sample Solvent:	Methanol
Detection:	*Refractive index*
Column Temp:	20 °C
Injection volume:	30 mL

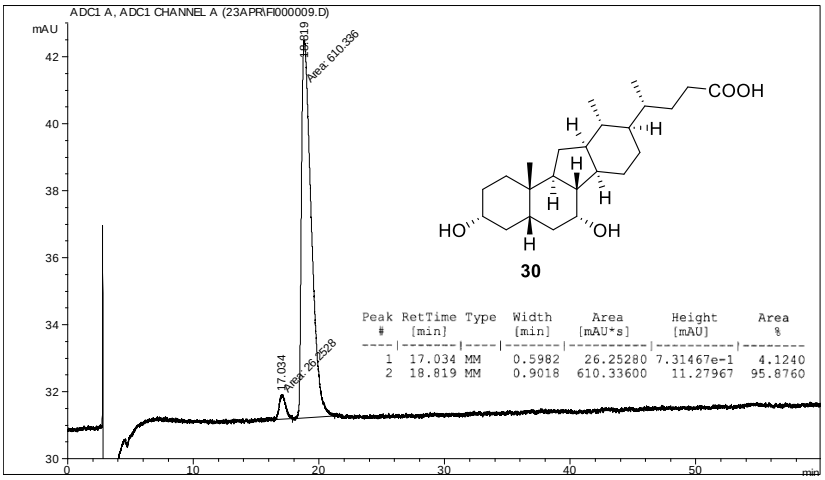

Figure S84. HPLC trace of **30**.

6.4. HPLC analysis of partially purified mixture of 12β-methyl-18,24-*bisnor*-alkene rearrangement products: 24b/25b

Method conditions:

Column: Phenomenex Luna C18(2) 5 µM, 250 x 4.6 mm
Guard: Phenomenex Security Guard C18 RP 4 x 3 mm
Mobile Phase: 20:80:0.05 Water : Methanol : Trifluoroacetic acid
Flow Rate: 1.0 mL/min
Sample Solvent: Methanol
Detection: UV at 220 nm
Column Temp: 20 °C
Injection volume: 20 µL

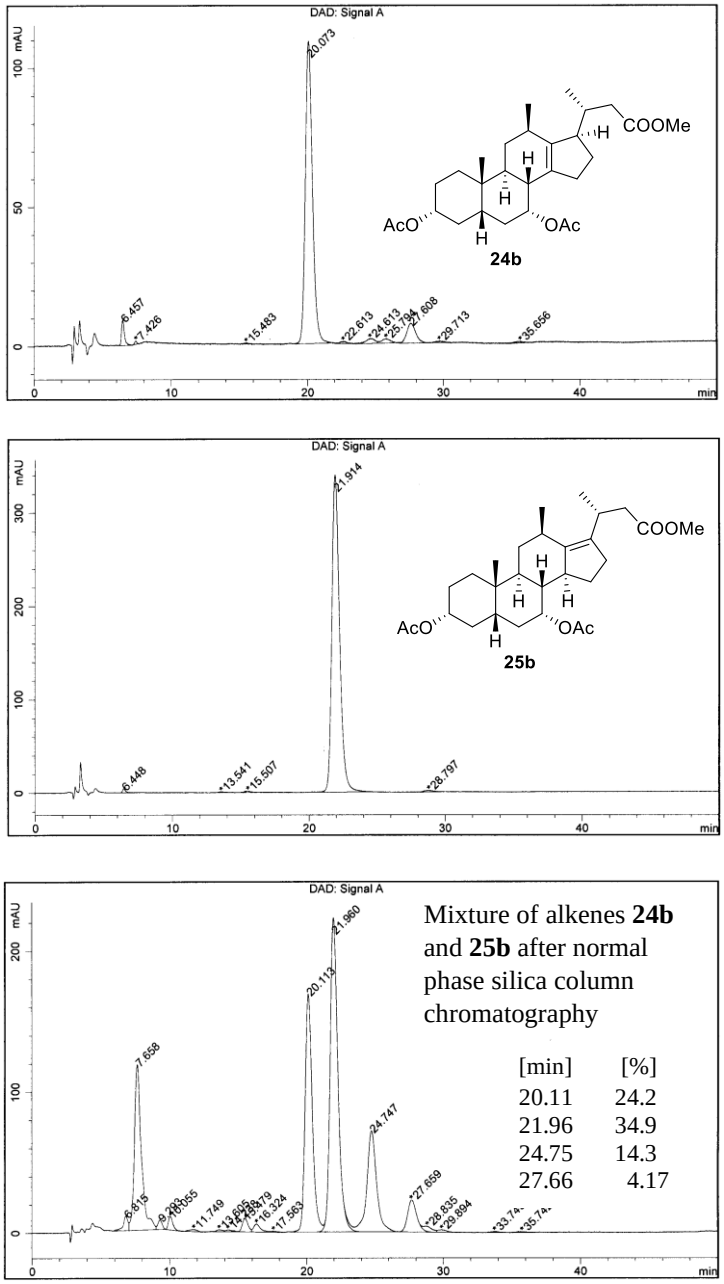

Figure S85. HPLC traces of **24b**, **25b** and mixture of 24-*nor*-alkenes after rearrangement reaction and chromatographic purification.

6.5. HPLC traces of the 12β-methyl-18,24-*bisnor*-bile acids 27b and 28b

Method conditions:

Column: Phenomenex Luna C18(2) 5 µM, 250 x 4.6 mm
Guard: Phenomenex Security Guard C18 RP 4 x 3 mm
Mobile Phase: 25:75:0.05 Water : Methanol : Trifluoroacetic acid
Flow Rate: 1.0 mL/min
Sample Solvent: Methanol
Detection: *Refractive index*
Column Temp: 20 °C
Injection volume: 20 µL

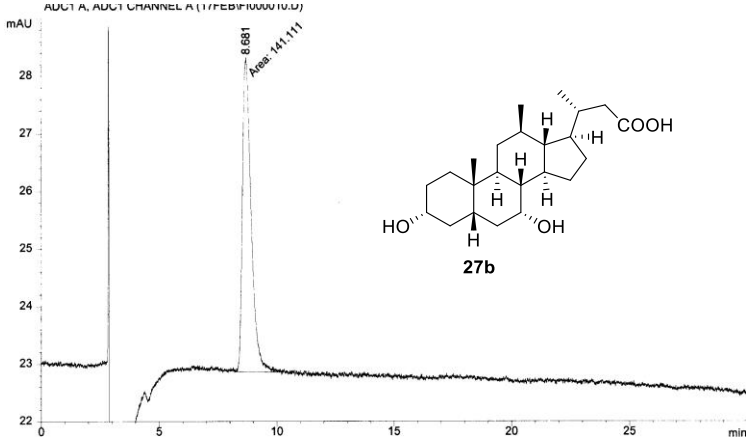

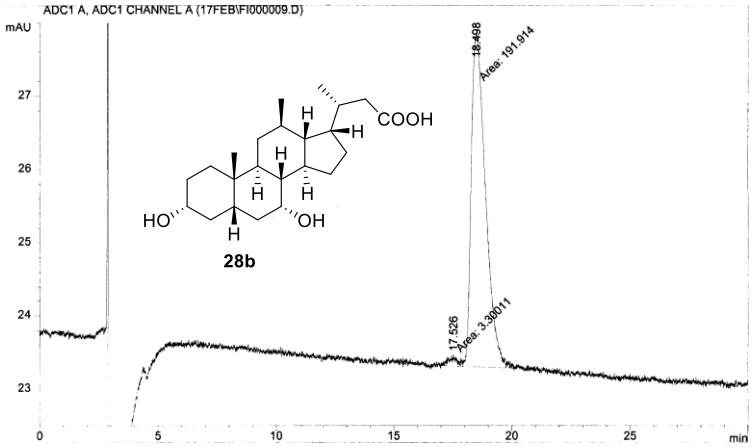

Peak #	RetTime [min]	Type	Width [min]	Area [mAU*s]	Height [mAU]	Area %
1	17.526	MF	0.3389	3.30011	1.62305e-1	1.6905
2	18.498	FM	0.7035	191.91399	4.54647	98.3095

Figure S86. HPLC traces of **27b** and **28b**.

6.6. HPLC traces of the 12β-methyl-25-*homo*-18-*nor*-bile acids 27c and 28c

Method conditions:

Column:	Phenomenex Luna C18(2) 5 mm 250x4.6 mm
Guard:	Phenomenex Security Guard C18 RP 4x3 mm
Mobile Phase:	20:80:0.05 Water/Methanol/Trifluoroacetic acid
Gradient:	Isocratic
Flow Rate:	1.0 mL/min
Sample Solvent:	Methanol
Detection:	*Refractive index*
Column Temp:	20 °C
Injection volume:	20 µL

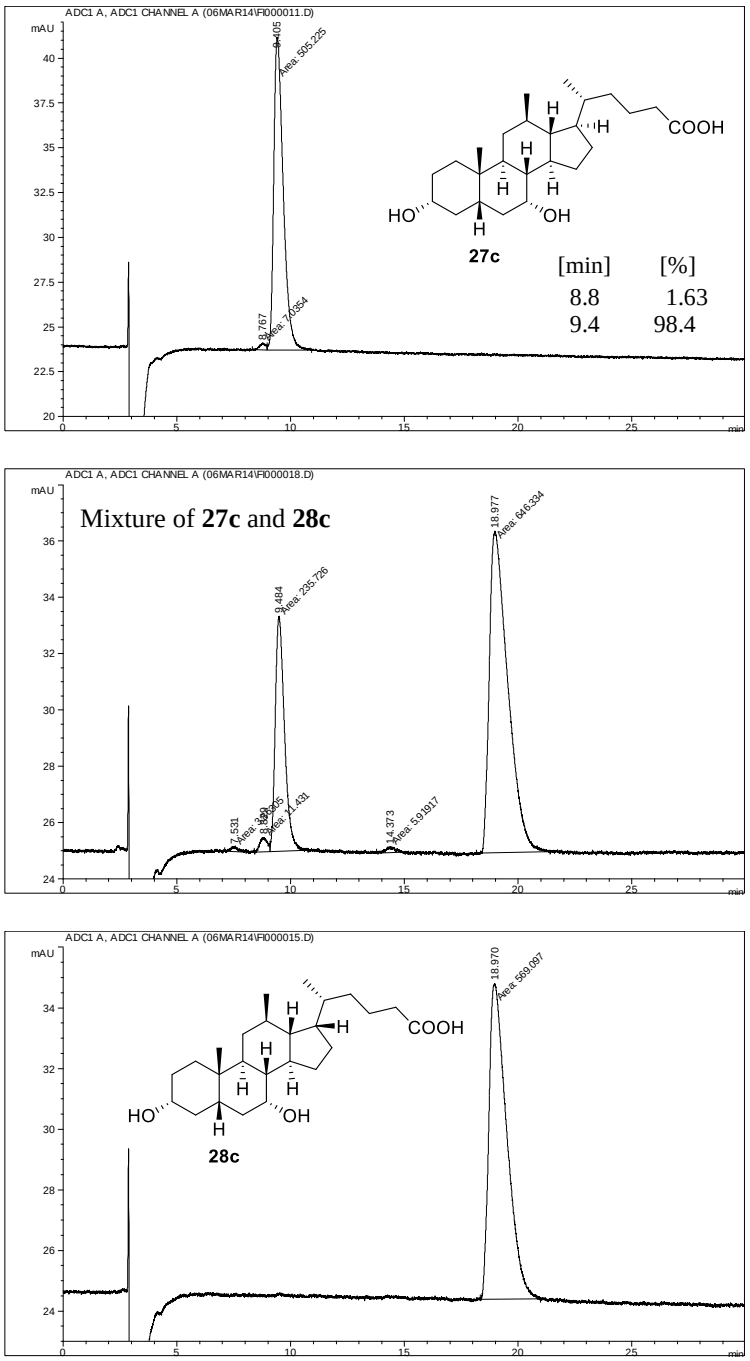

Figure S87. HPLC traces of **27c** and **28c**.

6.7. HPLC traces of 33 and 34 obtained from large scale synthesis (500 g campaign)

Method conditions:

Column: Phenomenex Luna C18(2) 5 µM, 250 x 4.6 mm
Guard: Phenomenex Security Guard C18 RP 4 x 3 mm
Mobile Phase: 30:70:0.05 Water : Methanol : Trifluoroacetic acid
Flow Rate: 1.0 mL/min
Sample Solvent: Methanol (10 mg/mL)
Detection: *Refractive index*
Column Temp: 20 °C
Injection volume: 20 µL

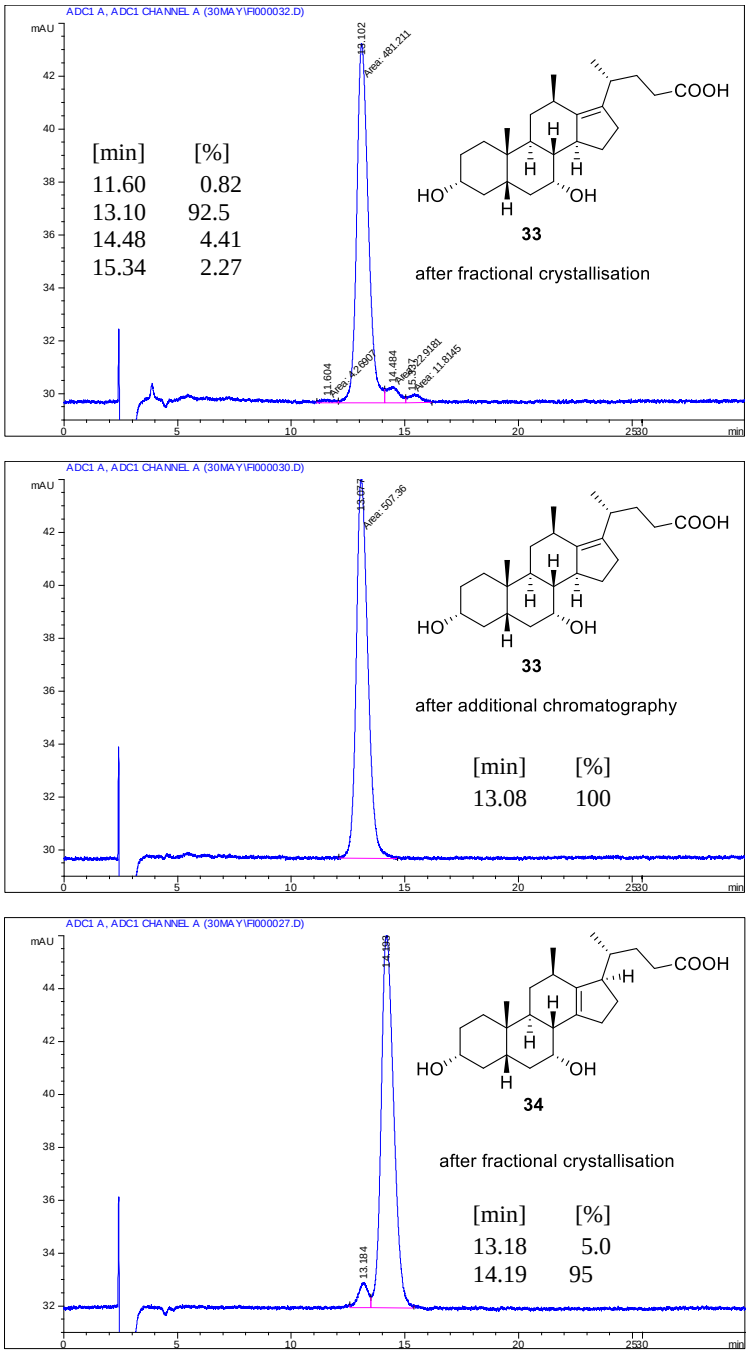

Figure S88. HPLC traces of **33** and **34**.

7. X-Ray Diffraction Data

All datasets were collected on an Agilent SuperNova diffractometer fitted with an EOS S2 detector at 120 K and using CuKα radiation (λ = 1.54184 Å). All ORTEP plots are with 30% probability ellipsoids. Minor disordered components and/or solvent molecules have been omitted for clarity.

Crystal structure data and structure refinement

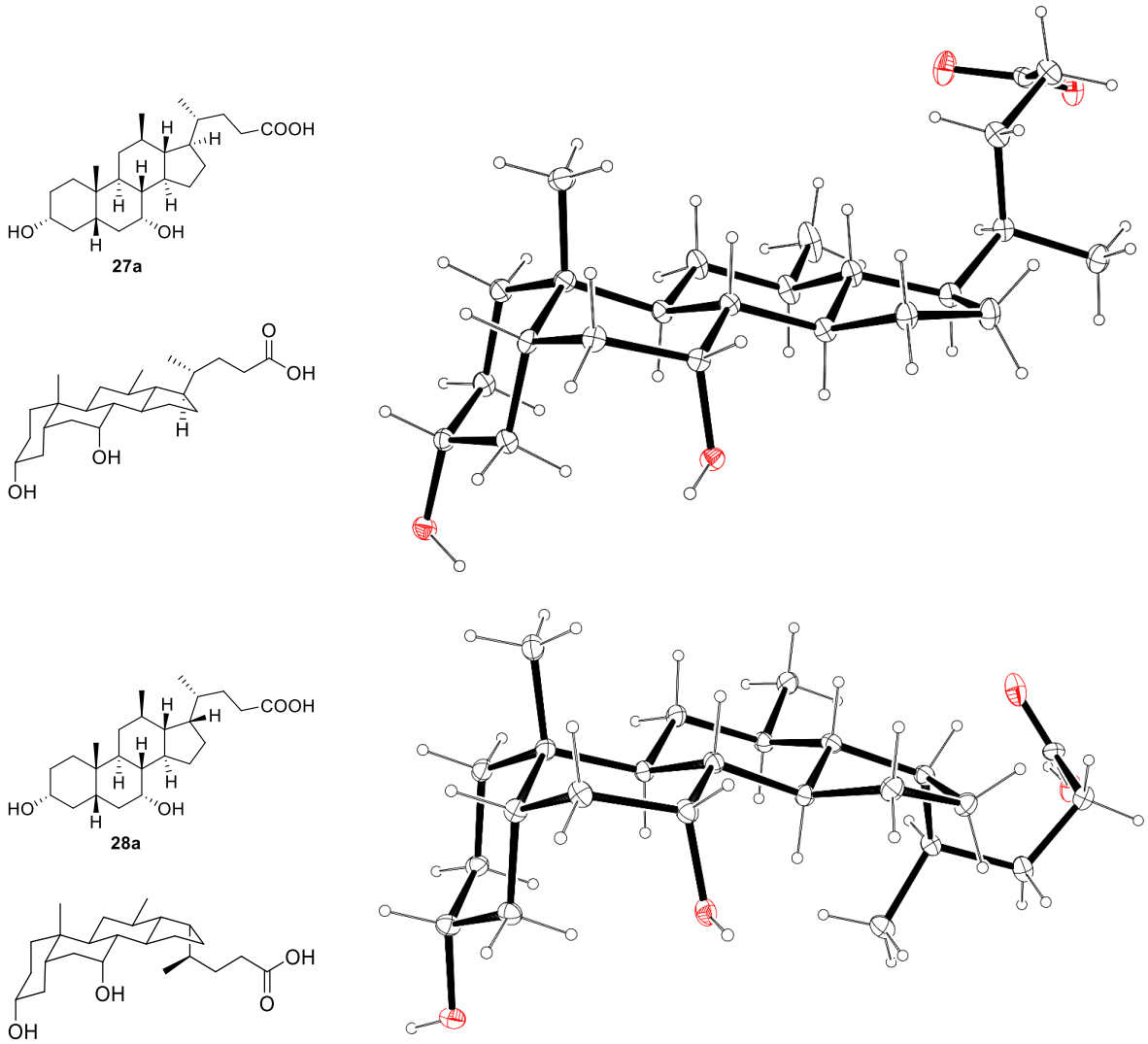

Figure S89. ORTEP representations of **27a** and **28a**.

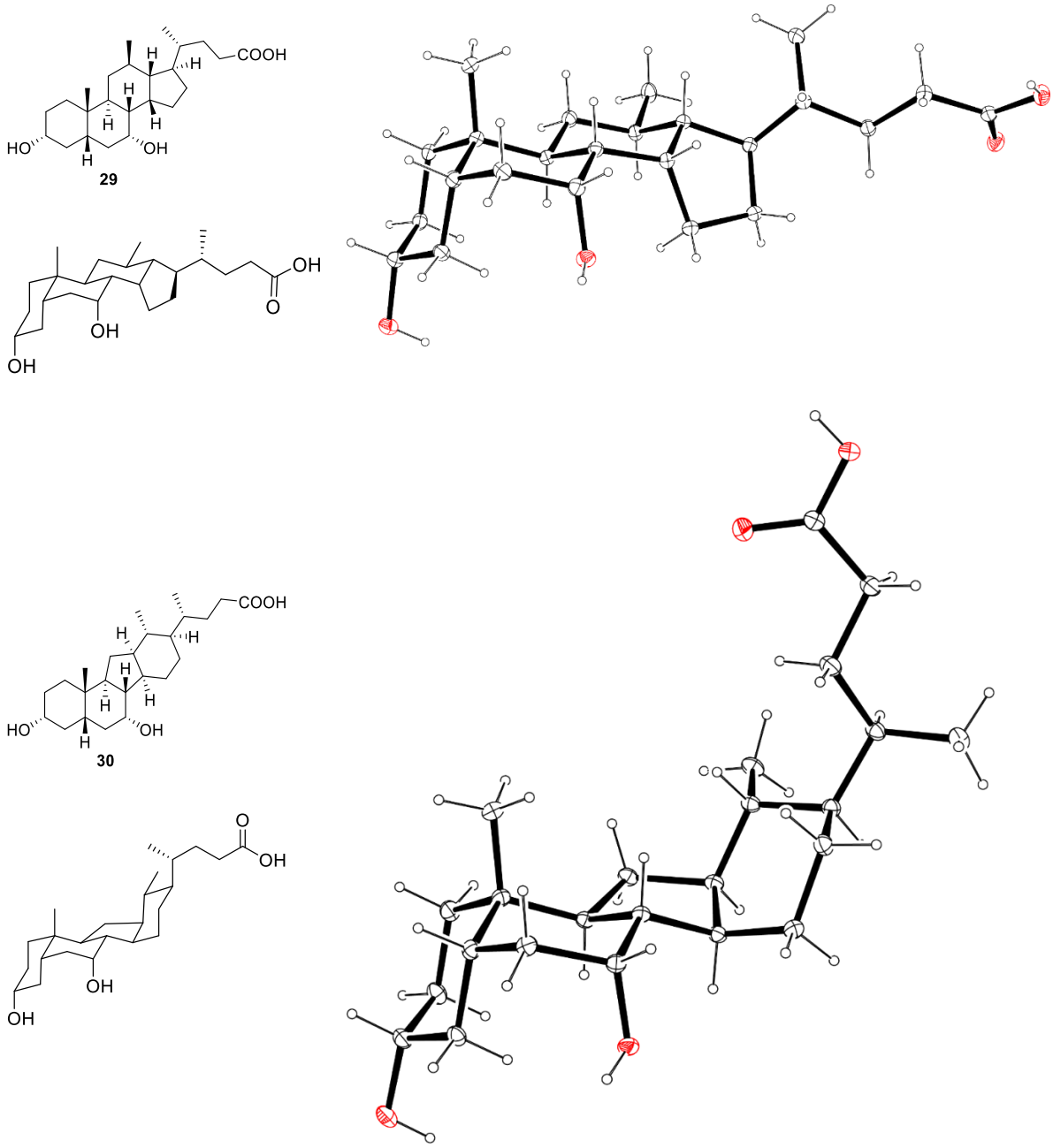

Figure S90. ORTEP representations of **29** and **30**.

Table S1. Crystal data and structure refinement for **27a**, **28a**, **29** and **30**.

Identification code	**27a**	**28a**	**29**	**30**
CCDC identifier	2094562	2094569	2094566	2094563
Empirical formula	$C_{24}H_{40}O_4 \cdot 2H_2O$	$C_{24}H_{40}O_4$	$C_{24}H_{40}O_4 \cdot H_2O$	$C_{24}H_{40}O_4 \cdot MeOH$
Formula weight (g/mol)	428.59	392.56	410.57	424.60
Crystal system	Orthorhombic	Monoclinic	Monoclinic	Orthorhombic
Space group	$P2_12_12_1$	$P2_1$	$P2_1$	$P2_12_12_1$
Unit cell dimensions				
a (Å)	8.29360(11)	10.1780(3)	10.3766(2)	9.48010(10)
b (Å)	9.96963(15)	9.8144(2)	7.67840(10)	11.64990(10)
c (Å)	28.1140(4)	10.7308(3)	14.0100(3)	21.8433(3)
α (°)	90	90	90	90
β (°)	90	94.553(2)	92.077(2)	90
γ (°)	90	90	90	90
Volume ($Å^3$)	2324.58(6)	1068.53(5)	1115.52(4)	2412.42(5)
Z	4	2	2	4
Calculated density (Mg/m^3)	1.225	1.220	1.222	1.169
Absorption coefficient (mm^{-1})	0.690	0.636	0.664	0.629
F (000)	944	432	452	936
Crystal size (mm^3)	0.675 × 0.101 × 0.033	0.172 × 0.111 × 0.087	0.496 × 0.049 × 0.043	0.490 × 0.100 × 0.058
Theta range for data collection	3.144 to 71.736°	4.133 to 71.618°	3.156 to 76.626°	4.301 to 71.715°
Index ranges	$-8 \le h \le 10$ $-12 \le k \le 12$ $-33 \le l \le 34$	$-12 \le h \le 12$ $-11 \le k \le 11$ $-13 \le l \le 13$	$-13 \le h \le 13$ $-9 \le k \le 9$ $-17 \le l \le 16$	$-11 \le h \le 11$ $-14 \le k \le 12$ $-25 \le l \le 26$
Reflections collected	15985	13478	22185	14596
Independent reflections	4497 [R(int) = 0.0269]	4087 [R(int) = 0.0250]	4644 [R(int) = 0.0583]	4715 [R(int) = 0.0289]
Completeness to theta	99.9% to 67.684°	99.9% to 67.684°	100.0% to 67.684°	99.9% to 67.684°
Data / restraints / parameters	4497 / 0 / 293	4087 / 1 / 259	4644 / 1 / 274	4715 / 0 / 290
Goodness-of-fit on F^2	1.072	1.063	1.045	1.027
Final R indices [I>2sigma(I)]	R1 = 0.0301 wR2 = 0.0807	R1 = 0.0264 wR2 = 0.0679	R1 = 0.0353 wR2 = 0.0911	R1 = 0.0336 wR2 = 0.0843
R indices (all data)	R1 = 0.0308 wR2 = 0.0816	R1 = 0.0271 wR2 = 0.0697	R1 = 0.0396 wR2 = 0.0946	R1 = 0.0350 wR2 = 0.0855
Absolute structure parameter	0.02(6)	-0.02(6)	-0.10(10)	0.12(8)
Largest diff. peak and hole ($e.Å^{-3}$)	0.314 and -0.188	0.179 and -0.143	0.208 and -0.182	0.336 and -0.206

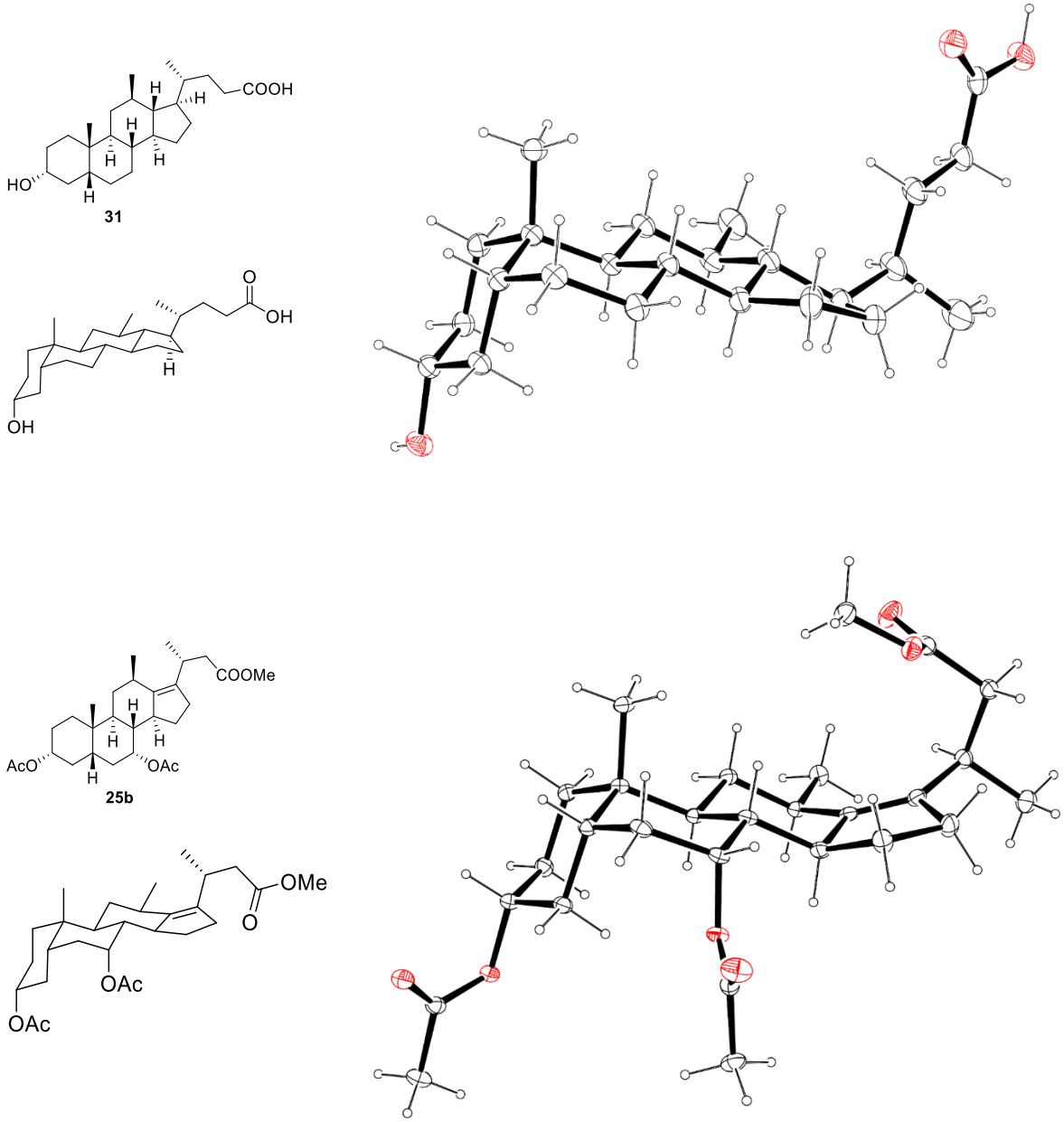

Figure S91. ORTEP representations for **31** and **25b**.

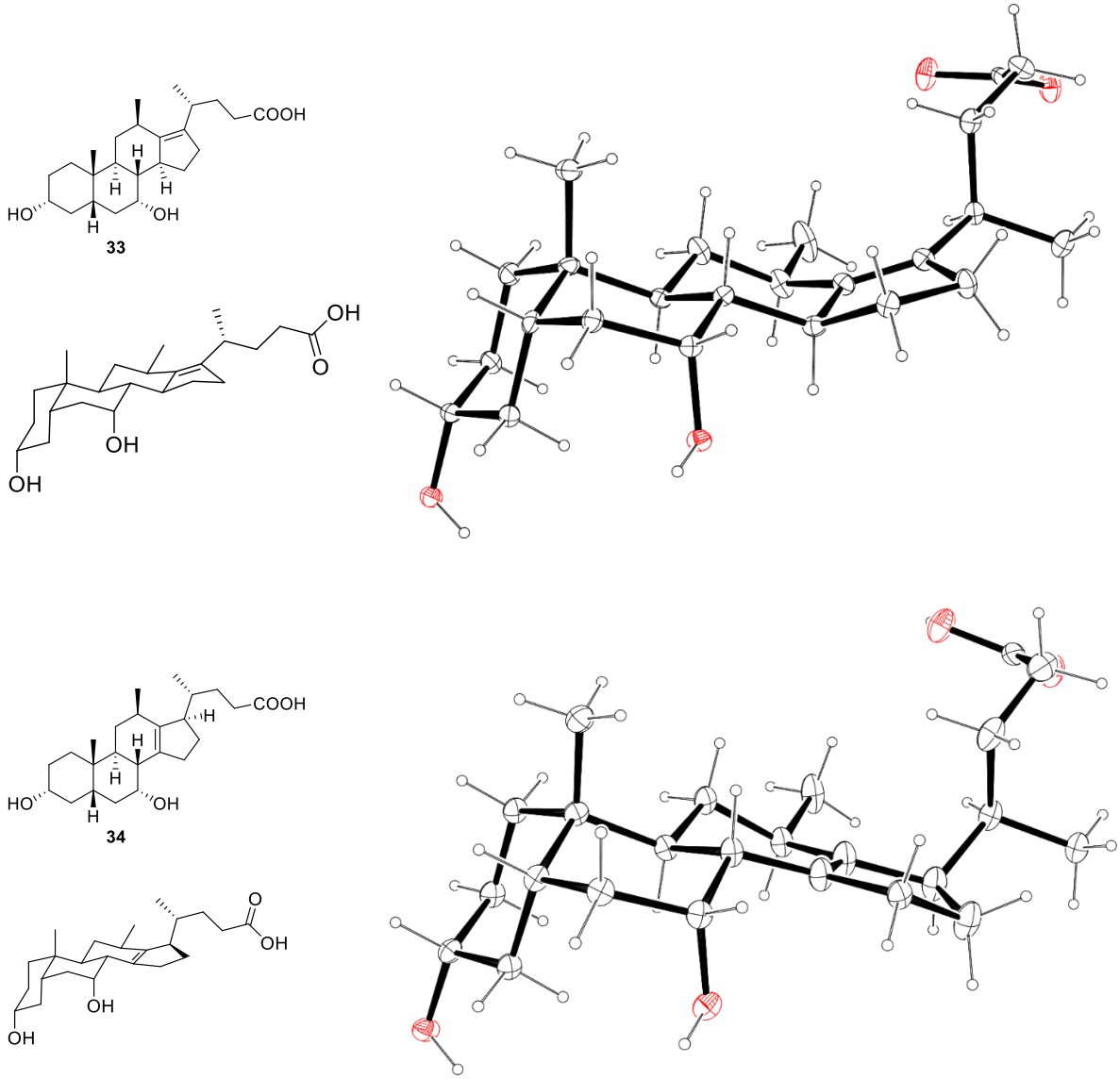

Table S92. ORTEP representations of **33** and **34**.

Table S2. Crystal data and structure refinement for **31**, **25b**, **33** and **34**.

Identification code	**31**	**25b**	**33**	**34**
CCDC identifier	2094564	2094561	2094567	2094565
Empirical formula	$C_{24}H_{40}O_3$	$C_{28}H_{42}O_6$	$C_{24}H_{38}O_4 \cdot 2H_2O$	$C_{24}H_{38}O_4 \cdot 2H_2O$
Formula weight (g/mol)	376.56	474.61	426.57	426.57
Crystal system	Tetragonal	Orthorhombic	Orthorhombic	Orthorhombic
Space group	*I*4	$P2_12_12_1$	$P2_12_12_1$	$P2_12_12_1$
Unit cell dimensions				
a (Å)	26.3766(4)	9.7271(2)	8.3063(3)	8.2311(3)
b (Å)	26.3766(4)	13.2670(3)	9.8640(3)	10.3667(6)
c (Å)	7.01614(15)	20.4560(5)	28.3674(10)	26.8026(15)
α (°)	90	90	90	90
β (°)	90	90	90	90
γ (°)	90	90	90	90
Volume (Å^3)	4881.29(17)	2639.84(10)	2324.24(14)	2287.1(2)
Z	8	4	4	4
Calculated density (Mg/m^3)	1.025	1.194	1.219	1.239
Absorption coefficient (mm^{-1})	0.507	0.662	0.690	0.087
F(000)	1664	1032	936	936
Crystal size (mm^3)	0.411 × 0.068 × 0.065	0.407 × 0.289 × 0.199	0.218 × 0.069 × 0.017	0.869 × 0.371 × 0.054
Theta range for data collection	4.742 to 73.494°	3.971 to 74.035°	4.746 to 68.244°	3.010 to 25.024°
Index ranges	$-32 \le h \le 30$ $-27 \le k \le 32$ $-8 \le l \le 8$	$-11 \le h \le 11$ $-10 \le k \le 16$ $-24 \le l \le 25$	$-10 \le h \le 6$ $-9 \le k \le 11$ $-33 \le l \le 32$	$-9 \le h \le 9$ $-11 \le k \le 12$ $-31 \le l \le 31$
Reflections collected	21887	10590	9136	11079
Independent reflections	4880 [R(int) = 0.0281]	5097 [R(int) = 0.0283]	4133 [R(int) = 0.0572]	4034 [R(int) = 0.0571]
Completeness to theta	99.9% to 67.684°	99.9% to 67.684°	98.4% to 67.684°	99.5% to 25.024°
Data / restraints / parameters	4880 / 1 / 255	5097 / 0 / 314	4133 / 8 / 288	4034 / 8 / 290
Goodness-of-fit on F^2	1.059	1.028	1.109	1.058
Final R indices [I>2sigma(I)]	R1 = 0.0301 wR2 = 0.0765	R1 = 0.0317 wR2 = 0.0773	R1 = 0.0538 wR2 = 0.1459	R1 = 0.0485 wR2 = 0.1137
R indices (all data)	R1 = 0.0315 wR2 = 0.0773	R1 = 0.0352 wR2 = 0.0803	R1 = 0.0816 wR2 = 0.1581	R1 = 0.0548 wR2 = 0.1181
Absolute structure parameter	0.11(8)	-0.07(9)	0.2(4)	0.1(10)
Largest diff. peak and hole (e.Å^{-3})	0.099 and -0.125	0.165 and -0.165	0.269 and -0.257	0.323 and -0.199

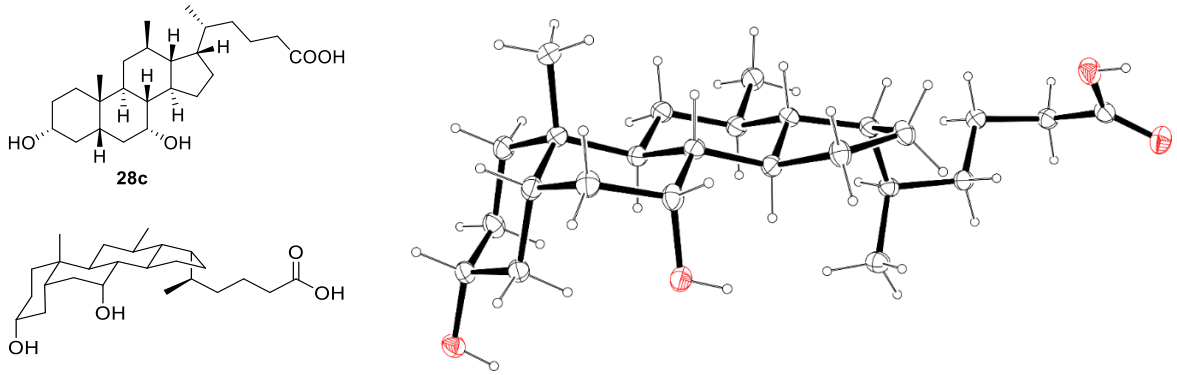

Figure S93. ORTEP representation of **28c**.

Table S3. Crystal data and structure refinement for **28c**.

Identification code	**28c**
CCDC identifier	2094568
Empirical formula	$C_{25}H_{42}O_4$
Formula weight (g/mol)	406.58
Crystal system	Orthorhombic
Space group	$P2_12_12_1$
Unit cell dimensions	
a (Å) b (Å) c (Å) α (°) β (°) γ (°)	7.0751(2) 14.6727(4) 22.0802(7) 90 90 90
Volume ($Å^3$)	2292.16(12)
Z	4
Calculated density (Mg/m^3)	1.178
Absorption coefficient (mm^{-1})	0.609
F (000)	896
Crystal size (mm^3)	0.232 × 0.142 × 0.082
Theta range for data collection	3.617 to 74.015°
Index ranges	$-8 \le h \le 4$ $-18 \le k \le 18$ $-25 \le l \le 27$
Reflections collected	9092
Independent reflections	4435 [R(int) = 0.0396]
Completeness to theta	99.9% to 67.684°
Data / restraints / parameters	4435 / 0 / 268
Goodness-of-fit on F^2	1.045
Final R indices [I>2sigma(I)]	R1 = 0.0441 wR2 = 0.1073
R indices (all data)	R1 = 0.0541 wR2 = 0.1151
Absolute structure parameter	0.39(19)‡
Largest diff. peak and hole ($e.Å^{-3}$)	0.178 and -0.161

‡ absolute structure known from unchanging (and known) steroid configuration.

8. Neutron diffraction data and structure refinement for 28a-$d_{2\text{-}4}$

Single-crystal neutron Laue diffraction data sets were collected from two roughly 1 × 1 × 1 mm diameter crystals of the mixture of **28a-$d_{2\text{-}4}$** on the instrument Koala[S1] at the OPAL research reactor, Australian Centre for Neutron Scattering, ANSTO, Australia. Koala uses a 'white' thermal-neutron beam (0.8 Å ≤ λ ≤ 5.2 Å) and a cylindrical image-plate detector in a vertical orientation. The crystals were mounted on aluminum pins for data collection. For each crystal, neutron Laue patterns were collected at room temperature in 21 exposures of 2 h each, separated by 9° rotations of the vertical φ-axis (perpendicular to the neutron beam), providing good data redundancy and near optimal completeness for Laue diffraction data. Reflections were indexed, integrated, and normalized to the wavelength distribution of the neutron beam using the LaueG[S2] software suite. Note that the dimensions of the unit cell cannot be unambiguously determined from white-beam Laue data, therefore the values determined from conventional monochromatic X-ray data for **28a** were used for subsequent crystallographic analysis.

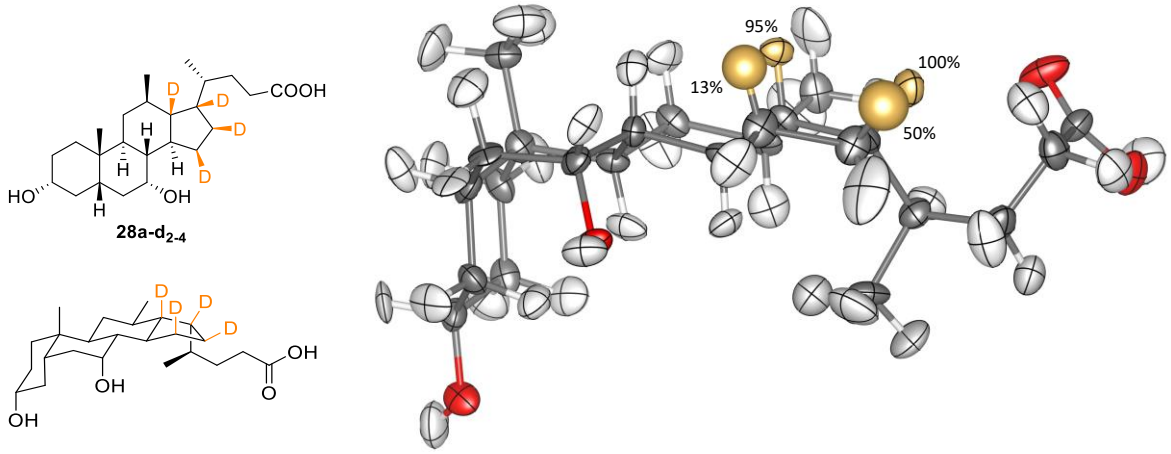

Figure S94. Structure of **28a-$d_{2\text{-}4}$** refined against room-temperature neutron Laue diffraction data. Carbon sites are grey, oxygen sites are red, hydrogen sites are white, and deuterated hydrogen sites are yellow (labelled with their refined deuterium percentage). Atomic displacement parameters are drawn as 30% probability ellipsoids with principal axes shown.

Structure refinements were carried out in the Jana2006[S3] program. To improve completeness, data from both crystals were used (scaled together) for the refinement. The structure model determined from X-ray diffraction data for **28a** was initially refined with all H sites fixed in position but free to vary their atomic displacement parameters (ADPs). The ADPs diverged to unreasonably large values on a subset of the H sites, which were subsequently split into mixed H/D sites. Refinement of the H/D ratios (constrained to 100% total occupancy in each case) substantially improved the quality of the fit to experimental data. Iterative refinement cycles revealed that only four sites deuterate to statistically significant extents, at 100% (within error, and subsequently fixed at that value), 95%, 50%, and 13%. The standard deviations on all these values were 2%. For the final refinement cycles, all structural parameters could be refined

freely including anisotropic ADPs on all sites except the 50% and 13% deuterated sites, for which isotropic ADPs had to be applied. This is a consequence of the opposite sign of neutron scattering lengths for H and D (b = –3.739 and 6.671 fm respectively[S4]), which substantially reduce the average contributions of these mixed sites to neutron diffraction data.

Experimental and refinement details are presented in Table S4, with the refined structure details presented in the deposited CIF and drawn in Figure S94 using the program VESTA.[S5]

Table S4. Data collection and refinement details for the neutron Laue diffraction experiment on **28a-d$_{2\text{-}4}$**.

Identification code	**28a-d$_{2\text{-}4}$**
CCDC identifier	2094996
Empirical formula	$C_{24}H_{37.42}D_{2.58}O_4$
Formula weight (g/mol)	395.20
Crystal system	Monoclinic
Space group	$P2_1$
Unit cell dimensions*	
a (Å)	10.1780
b (Å)	9.8144
c (Å)	10.7308
α (°)	90
β (°)	94.553
γ (°)	90
Volume (Å^3)	1068.53
Z	2
Calculated density (Mg/m^3)	1.228
Absorption coefficient (mm^{-1})	0.001
F_{000}	120
Crystal size (mm^3)	1 × 1 × 1
Q range for data collection	0.62 – 7.42 Å^{-1}
Wavelength range for data collection	0.85 – 1.80 Å
Index ranges	-11 ≤ h ≤ 11 -11 ≤ k ≤ 11 -12 ≤ l ≤ 12
Reflections collected	32202
Independent reflections	1583
Completeness to Q	80% to 7.42 Å^{-1}
Data / restraints / parameters	1583 / 0 / 607
Goodness-of-fit on F2	1.08
Final R indices [I>2σ(I)]	R1 = 0.0448 wR2 = 0.0239
R indices (all data)	R1 = 0.1565 wR2 = 0.0323

* Taken from the monochromatic X-ray experiment on **28a**; unit cell dimensions cannot be unambiguously refined against white-beam Laue data.

9. References

S1 Edwards, A. J. Neutron Diffraction - Recent Applications to Chemical Structure Determination. *Aust. J. Chem.* **2011**, *64*, 869-872.

S2 Piltz, R. O. Accurate data processing for neutron Laue diffractometers. *J. Appl. Cryst.* **2018**, *51*, 635-645.

S3 Petříček, V.; Dušek, M.; Palatinus, L. Crystallographic Computing System JANA2006: General features. Z. Kristallogr. **2014**, *229*, 345-352.

S4 Sears, V. F. Neutron scattering lengths and cross sections. *Neutron News* **1992**, *3*, 26-37.

S5 Momma, K.; Izumi, F. VESTA: a three-dimensional visualization system forelectronic and structural analysis. *J. Appl. Cryst.* **2008**, *41*, 653-658.